THE EXCHANGE EXCITATION OF HELIUM AND THE HYDROGEN MOLECULE BY LOW ENERGY ELECTRONS

Thesis by
David Chapman Cartwright

In Partial Fulfillment of the Requirements

For the Degree of
Doctor of Philosophy

California Institute of Technology
Pasadena, California
1968
(Submitted June 23, 1967)

ACKNOWLEDGMENTS

I would like to express my gratitude to Professor A. Kuppermann for his assistance in the selection and investigation of my research problem. I also want to thank Professor Kuppermann and the Atomic Energy Commission for partial support, the California Institute of Technology for teaching assistantships during 1962 and 1964, and the NSF for a summer fellowship in 1964.

Special thanks go to Professors W. A. Goddard and R. M. Pitzer for numerous fruitful discussions concerning aspects of my work. Their advice and assistance was instrumental in the completion of this research.

Mrs. Bertha Marston, the Physics Librarian, and Mr. Dana Roth, the Chemistry Librarian were very cooperative and I acknowledge their help.

A good many enjoyable discussions were shared with the members of the Kuppermann research group. Especially helpful were those with Mr. Don Truhlar and Mr. Merle Riley. Thanks also go to Mr. Chris Parr for his help during the early stages of the numerical work.

Last, but certainly not least, I want to thank my wife, Carole, for her enthusiasm and steady encouragement during the course of this work.

ABSTRACT

The theory of rearrangement collisions involving composite particles is reviewed and the "post", "prior" discrepancy discussed. Two recent improvements to the Born-Oppenheimer approximation, the Ochkur (O), and Ochkur-Rudge (OR) approximations are reviewed. These approximations are then used to calculate the total cross section for the electronic excitation, of molecular hydrogen by low energy electrons. Excitations from the ground ($X^1\Sigma_g^+$) state to the first ($b^3\Sigma_u^+$) and second ($a^3\Sigma_g^+$) triplet states are treated. All nuclear motions are taken into account. It is found that the first triplet cross section is sensitive to the choice of the ground state wave function whereas the second is not. The former is also sensitive to the quality of excited state wave function used. The results using the (O) approximation are significantly larger than those of the (OR) approximation, and the maximum cross section occurs at a somewhat lower energy. Use of the separated atom approximation produces results significantly lower than those obtained by including all the multicenter terms in the scattering amplitude. The calculations are carried out using the zeta function expansion method and are quite lengthy. The sum of the first and second (OR) triplet cross sections agrees well with a recent approximate experimental determination of the cross section for electron impact dissociation of H_2 into 2H.

These approximations are also used to calculate the total cross sections for excitation of helium from the ground to the 2^3S and 2^3P states. These cross sections are sensitive to the ground and excited state wave functions used. The (OR) results agree well with the available experimental data for these excitations.

The differential cross sections for these excitations are also calculated. Since there is no experimental data for the H_2 processes or for the 2^3P excitation in He, the quality of these calculations cannot be evaluated. The calculated angular distributions for the 2^3S excitation in He agree well with one set of experimental data but disagree with the other.

The (OR) approximation is found to give quite good results for total cross sections but its value in predicting angular distributions cannot be evaluated until more experimental data are available.

TABLE OF CONTENTS

I. The Theory of Rearrangement Scattering

The formal scattering theory for collisions that involve rearrangement of particles will now be outlined. Because of the breadth (and depth) in the theory of collision processes, this discussion will be limited to those principles necessary for the understanding of rearrangement scattering. The finer details, including mathematical rigor, can be found in any of a number of well written texts on the subject of scattering.[1]

An understanding of the scattering processes involved in a collision between composite bodies is most easily obtained by first reviewing simple potential scattering. The operator formalism will be used here because it is quite useful in treating a complex collision process. After obtaining the quantities pertinent for the description of potential scattering, the corresponding quantities for the collision between composite bodies can be found by direct extension.

1. Potential Scattering[2]

In the following discussion, the interaction potentials of the scattering system will be assumed to fall off faster than $1/r$. This excludes, for instance, the scattering of a charged particle by an ion. This is not a real restriction since such Coulomb scattering can be dealt with by appropriate modification of the scattering waves,[3] and then the same formalism can be used.

Consider the scattering of a particle of mass (m) by a potential $V(\vec{r})$. The kinetic energy operator is denoted by K_0 and the Hamiltonian of the system by H:

$$H = K_o + V ; \quad K_o \equiv - \frac{\hbar^2}{2m} \nabla^2 \tag{1-1}$$

and the familiar Schroedinger equation for energy E is

$$H\Phi = E\Phi \ . \tag{1-2}$$

The scattering states are of primary interest here and the following notation will be used in this connection. Let $\vec{k}_a$ denote the wave vector of the incident particles corresponding to energy E_a ($\hbar^2 k_a^2/2m$). The subscript (a) serves to define the initial conditions of the incident particle such as energy (E_a) and direction (Ω_a). Similarly, let $\vec{k}_b$ denote the wave vector for the scattered particle corresponding to energy (E_b) and direction Ω_b. For potential scattering $E_a = E_b$ but of course the directions of $\vec{k}_a$ and $\vec{k}_b$ are in general different.

The symbols φ_a, φ_b are used to denote plane waves of energy $E = E_a = E_b$ in the directions Ω_a and Ω_b respectively. They are solutions of

$$K_o \varphi_i = E \varphi_i \ , \tag{1-3}$$

and are given by $\varphi_i = e^{i\vec{k}_i \cdot \vec{r}}$, (i = a, b). The stationary wave solutions of (1-2) are denoted by $\psi_a^{\pm}$. The ($\pm$) superscript is used to distinguish between the solutions of (1-2) corresponding to outgoing (+) or incoming (-) spherical waves at infinity. That is, $\psi_a^{\pm}$ satisfies

$$H\psi_a^{\pm} = E\psi_a^{\pm} \ , \tag{1-4}$$

with the boundary condition

$$\psi_a^{\pm} \underset{r \to \infty}{\sim} e^{i\vec{k}_a \cdot \vec{r}} + f_a^{\pm}(\Omega_b) \frac{e^{\pm ik_a r}}{r} \quad . \tag{1-5}$$

The subscript (b) on Ω_b in (1-5) is used to indicate the direction of the scattered particle associated with $\vec{k}_b$. The subscript (a or b) on ψ is used to denote the initial conditions of the incident particle; that is, the energy and direction as given by $\vec{k}_a$ or $\vec{k}_b$. There is an equation for $\psi_b^{\pm}$ similar to (1-5) with (a) and (b) interchanged. For a choice of one or the other boundary conditions (+ or -), the solution of (1-4) can be shown to be unique as long as the potential is sufficiently well behaved.[4] In practice, the potentials encountered satisfy this well-behaved condition.

As usual, the differential and total cross sections are determined from the quantity $f_a^+(\Omega_b)$ in (1-5). For elastic scattering the differential cross section is[5]

$$\frac{d\sigma}{d\Omega_b} = |f_a^+(\Omega_b)|^2 \quad . \tag{1-6}$$

As mentioned above, the subscripts (a) or (b) on Ω indicate the particle being scattered from direction (a) to direction (b). The total cross section is given by

$$\sigma = \int \frac{d\sigma}{d\Omega_b} \, d\Omega_b \quad . \tag{1-7}$$

Let us now consider two potentials U and $\hat{U}$ which satisfy the required condition of being well-behaved. Let ξ and $\hat{\xi}$ be the stationary eigenfunctions of the corresponding Hamiltonians. In particular, ξ_a^+ and $\hat{\xi}_b^-$ are the solutions of

$$(K_o + U)\xi_a^+ = E\,\xi_a^+ \tag{1-8}$$

$$(K_o + \hat{U})\hat{\xi}_b^- = E\,\hat{\xi}_b^- \tag{1-9}$$

satisfying the asymptotic conditions

$$\xi_a^+ \underset{r \to \infty}{\sim} e^{i\vec{k}_a \cdot \vec{r}} + f_a^+(\Omega_b)\frac{e^{ik_a r}}{r} \tag{1-10}$$

$$\hat{\xi}_b^- \underset{r \to \infty}{\sim} e^{i\vec{k}_b \cdot \vec{r}} + \hat{f}_b^-(\Omega_a)\frac{e^{-ik_b r}}{r}\,. \tag{1-11}$$

The functions ξ_a^+ and $\hat{\xi}_b^-$ represent therefore eigenfunctions of different Hamiltonians for the same energy E. From (1-8) - (1-11) the following very useful property of the scattering amplitudes can be derived:[6]

$$\langle \hat{\xi}_b^- | U - \hat{U} | \xi_a^+ \rangle = -\frac{2\pi\hbar^2}{m} f_a^+(\Omega_b) + \frac{2\pi\hbar^2}{m} \hat{f}_b^{-*}(-\Omega_a) \tag{1-12}$$

where by definition, $(-\Omega)$ is the direction opposite to (Ω). Equation (1-12) is very general requiring only that the potentials be real and fall off faster than $1/r$.

As an example of the use of (1-12), let $U = V$ and $\hat{U} = 0$. Then, using (1-3) and (1-4), one finds that (1-12) becomes

$$\langle \varphi_b \mid V \mid \psi_a^+ \rangle = \frac{-2\pi\hbar^2}{m} f_a^+(\Omega_b) . \tag{1-13}$$

Note that $\hat{f}_b^- \equiv 0$ because in for this choice of $\hat{U}$ in (1-9), the particle is free and hence not scattered. If now one chooses $U = 0$ and $\hat{U} = V$, (1-12) becomes

$$\langle \psi_b^- \mid V \mid \varphi_a \rangle = \frac{-2\pi\hbar^2}{m} \hat{f}_b^-(-\Omega_a) \tag{1-14}$$

since for this choice $f_a^+ \equiv 0$. Finally, if the choice $U = \hat{U}$ is made, (1-12) becomes

$$f_a^+(\Omega_b) = \hat{f}_b^{-*}(-\Omega_a) \tag{1-15}$$

which, as a result of (1-13) and (1-14), implies that

$$\langle \psi_b^- \mid V \mid \varphi_a \rangle = \langle \varphi_b \mid V \mid \psi_a^+ \rangle . \tag{1-16}$$

Equations (1-13) and (1-14) relate the transition amplitude to the scattering amplitude. The last equation, (1-16), is important because it represents the reversibility of the scattering process. Physically, this means the scattering process is the same running forward or backward in time. As will be discussed in section (I-3), an expression analogous to (1-16) for the case of complex collisions has led to the "post", "prior" paradox of rearrangement scattering.

For simplicity in dealing with more complex collision processes, it is convenient to define an operator which can be related to the familiar scattering amplitude (1-13) or (1-14). This operator (T) (called the transition matrix, or scattering matrix or T-operator) is defined such that its plane wave matrix representation elements are equal to the scattering amplitudes:

$$T_{a,b} \equiv \langle \varphi_b | T | \varphi_a \rangle = \langle \varphi_b | V | \psi_a^+ \rangle = \langle \psi_b^- | V | \varphi_a \rangle \, . \qquad (1\text{-}17)$$

The quantity $T_{a,b}$ is called the transition amplitude and is unique for a given potential scattering process. A more complete definition of the operator T is reserved for a later section.

The Schrödinger equation for the scattering, (1-4), together with the boundary condition (1-5) can be replaced by an integral equation. This is particularly useful since it is a convenient starting point for an approximate iteration scheme. It also leads to the Green's function operators which form the basis of a powerful theoretical approach for the treatment of scattering processes. The integral equation and associated Green's function operator are obtained as follows.

Equation (1-4) is rearranged to the form

$$(E - K_o)\psi_a^{\pm} = V\psi_a^{\pm} \qquad (1\text{-}18)$$

and the free particle Green's function for energy E is defined as the solution of

$$(E - K_o)\mathcal{G}_o^+(\vec{r}, \vec{r}') = \delta(\vec{r} - \vec{r}') \qquad (1\text{-}19)$$

with outgoing asymptotic behavior,

$$\mathcal{G}_o^+(\vec{r}, \vec{r}') \underset{r \to \infty}{\sim} - \frac{m}{2\pi\hbar^2} \frac{e^{ikr}}{r} e^{-i\vec{k} \cdot \vec{r}'} .$$

The solution to (1-19) with incoming asymptotic behavior $\mathcal{G}_o^-$ is also useful; it is found to be the complex conjugate of $\mathcal{G}_o^+(\vec{r}_1, \vec{r}')$.[7] For potential scattering, these Green's functions are[8]:

$$\mathcal{G}_o^+(\vec{r}, \vec{r}') = - \frac{m}{2\pi\hbar^2} \frac{e^{ik|\vec{r} - \vec{r}'|}}{|\vec{r} - \vec{r}'|} ; \mathcal{G}_o^-(\vec{r}, \vec{r}') = \mathcal{G}_o^{+*}(\vec{r}, \vec{r}') . \quad (1\text{-}20)$$

From the theory of inhomogeneous partial differential equations, the general solution to (1-18) can be written as the sum of the homogeneous solution and a particular solution.[9] Using the Green's functions defined above, the integral equation solutions to (1-4) and (1-5) are:

$$\psi_a^{\pm} = \varphi_a - \frac{m}{2\pi\hbar^2} \int \frac{e^{\pm ik|\vec{r} - \vec{r}'|}}{|\vec{r} - \vec{r}'|} V(\vec{r}') \psi_a^{\pm}(\vec{r}') d\vec{r}' . \quad (1\text{-}21)$$

The Green's function operator G_o is defined such that its coordinate matrix representation gives the $\mathcal{G}_o(\vec{r}, \vec{r}')$ functions of (1-20). That is,

$$\langle \vec{r} | G_o^+ | \vec{r}' \rangle \equiv \mathcal{G}_o^+(\vec{r}, \vec{r}') ; \quad \langle \vec{r} | G_o^- | \vec{r}' \rangle \equiv \mathcal{G}_o^-(\vec{r}, \vec{r}') . \quad (1\text{-}22)$$

The meaning of this operator can be seen from the effect of it operating on a state vector $|u\rangle$ of finite norm. The spatial wave function $u(\vec{r})$ is the coordinate representation of the state vector:

$$u(\vec{r}) \equiv \langle \vec{r} | u \rangle \ . \tag{1-23}$$

Thus, the effect of G_o^+ operating on the state vector $|u\rangle$ in the coordinate representation is

$$\langle \vec{r} | G_o^+ | u \rangle = \int \langle \vec{r} | G_o^+ | \vec{r}' \rangle \langle \vec{r}' | u \rangle d\vec{r}' = \int \mathcal{G}_o^+(\vec{r}, \vec{r}') u(\vec{r}') d\vec{r}' \ . \tag{1-24}$$

However, the definition above is not sufficient to be generally useful because of its singular behavior. This can be seen by examining the asymptotic form of (1-24):

$$\langle \vec{r} | G_o^+ | u \rangle \underset{r \to \infty}{\sim} -\frac{m}{2\pi\hbar^2} \frac{e^{ikr}}{r} \int e^{-i\vec{k} \cdot \vec{r}'} u(\vec{r}') d\vec{r}' \ . \tag{1-25}$$

As (1-25) shows, G_o^+ operating on a vector of finite norm ($|u\rangle$) produces a function which is not in general square-integrable. To eliminate this singular property, the $G_o^\pm$ operators are defined in terms of a limit of well-behaved operators:

$$G_o^\pm = \lim_{\epsilon \to 0^+} \frac{1}{E - K_o \pm i\epsilon} \ , \quad (\epsilon > 0) \ . \tag{1-26}$$

These $G_o^\pm$ operators, when operating on vectors of finite norm, produce functions which are square-integrable. As defined in (1-26)

the $G_o^{\pm}$ operators are well-behaved and bounded everywhere except for $\epsilon = 0$. As $\epsilon \to 0$ from the upper half-plane, the right hand side of (1-26) approaches G_o^+; and as it approaches zero from the lower half-plane it becomes G_o^-.

For the remainder of this discussion, the limiting process in (1-26) will not be written explicitly but just assumed. Fortunately, for purposes of manipulation of these operators, such details of rigor can be ignored - as they will from now on.

Utilizing this formalism, the integral equations (1-21) can be written in the operator notation as

$$\psi_a^{\pm} = \varphi_a + G_o^{\pm} V \psi_a^{\pm} \tag{1-27}$$

$$= \varphi_a + \frac{1}{E - K_o \pm i\epsilon} V \psi_a^{\pm} . \tag{1-28}$$

Note that iteration of (1-27) results in the Born expansion for the scattering process which in this operator notation is written as:

$$\psi_a^{\pm} = \left[1 + \sum_{n=1}^{\infty} (G_o^{\pm} V)^n \right] \varphi_a \quad . \tag{1-29}$$

As will be seen, it is very often quite convenient to assume that the potential (V) can be written as the sum of two parts, one of which admits to an exact solution. That is, write

$$V = U_1 + W_1 \tag{1-30}$$

$$H = K_o + U_1 + W_1 = H_1 + W_1 \ . \tag{1-31}$$

Assume that the stationary wave scattering solutions are known:

$$H_1 \chi_a^{\pm} = E \chi_a^{\pm} \ , \tag{1-32}$$

$$\chi_a^{\pm} \underset{r \to \infty}{\sim} \varphi_a + g_a^{\pm}(\Omega_b) \frac{e^{\pm ikr}}{r} \tag{1-33}$$

where the notation used is consistent with that introduced above.

In analogy with (1-17), a transition matrix (T') for collisions at energy E, governed by the Hamiltonian H_1 can be defined as

$$T'_{a,b} \equiv \langle \varphi_b | T' | \varphi_a \rangle = \langle \varphi_b | U_1 | \chi_a^+ \rangle = \langle \chi_b^- | U_1 | \varphi_a \rangle \tag{1-34}$$

and the analog of (1-15) is

$$g_a^+(\Omega_b) = g_b^{-*}(-\Omega_a) = -\frac{m}{2\pi\hbar^2} T'_{a,b} \ . \tag{1-35}$$

The transition amplitude ($T_{a,b}$) for the complete Hamiltonian (1-31) is given by (1-17). By using (1-12) with $U \equiv V$ and $\hat{U} \equiv U_1$ one finds

$$\langle \chi_b^- | W_1 | \psi_a^+ \rangle = -\frac{2\pi\hbar^2}{m} f_a^+(\Omega_b) + \frac{2\pi\hbar^2}{m} g_b^{-*}(-\Omega_a)$$

$$\text{(using (1-35))} = -\frac{2\pi\hbar^2}{m} [f_a^+(\Omega_b) - g_a^+(\Omega_b)]$$

$$(\text{by (1-34), (1-17)}) = T_{a,b} - T'_{a,b} \ . \tag{1-36}$$

Thus the transition amplitude for the two potential scattering can be written as

$$T_{a,b} = T'_{a,b} + \langle \chi_b^- | W_1 | \psi_a^+ \rangle \tag{1-37}$$

$$= T'_{a,b} + \langle \psi_b^- | W_1 | \chi_a^+ \rangle \ . \tag{1-38}$$

Equation (1-38) was obtained by interchanging the definitions of U and $\hat{U}$. From (1-37), (1-38) it is evident that

$$\langle \chi_b^- | W_1 | \psi_a^+ \rangle = \langle \psi_b^- | W_1 | \chi_a^+ \rangle \ . \tag{1-39}$$

As was done for the total Hamiltonian H, Green's functions and Green's function operators can be defined for H_1. That is, for H_1, $\mathcal{G}_1^{\pm}$ is the solution of

$$(E - H_1)\, \mathcal{G}_1^{\pm}(\vec{r}, \vec{r}') = \delta(\vec{r} - \vec{r}') \tag{1-40}$$

with the appropriate outgoing (+) or incoming (-) asymptotic boundary condition. This Green's function can be used to solve the equation

$$(E - H_1)\psi_a^{\pm} = W_1 \psi_a^{\pm} \tag{1-41}$$

in the form

$$\psi_a^{\pm} = \chi_a^{\pm} + \int \mathcal{G}_1^{\pm}(\vec{r}, \vec{r}')W_1(\vec{r}')d\vec{r}' \quad . \tag{1-42}$$

In the operator notation, the Green's function operators corresponding to H_1 and H for energy E are defined as

$$G_1^{\pm} \equiv \frac{1}{E - H_1 \pm i\epsilon} \tag{1-43}$$

$$G^{\pm} \equiv \frac{1}{E - H \pm i\epsilon} \tag{1-44}$$

where as above the limiting process $\epsilon \to 0^+$ is assumed but not written explicitly.

By using the definition of these operators, the following very useful identities can be derived (see Appendix A): $(H_o \equiv K_o)$

$$(E - H_1)G_1^{\pm} = 1, \quad G_1^{\pm}(E - H_1) = 1 \tag{1-45}$$

$$(E - H)G^{\pm} = 1, \quad G^{\pm}(E - H) = 1 \tag{1-46}$$

$$\frac{1}{E - H \pm i\epsilon} - \frac{1}{E - H_o \pm i\epsilon} = \frac{1}{E - H_o \pm i\epsilon} V \frac{1}{E - H \pm i\epsilon} \tag{1-47}$$

$$= \frac{1}{E - H \pm i\epsilon} V \frac{1}{E - H_o \pm i\epsilon} \tag{1-48}$$

$$(1 + G^{\pm}V)(1 - G_o^{\pm}V) = 1 \tag{1-49}$$

$$(1 - G_o^{\pm}V)(1 + G^{\pm}V) = 1 \quad . \tag{1-50}$$

In each of the above equations, there are analogous identities with H_1 and U_1 in place of H and V; and also with H_1 and W_1 in place of H_o and V.

The complete solution of the two-potential Hamiltonian H at energy E can be written in this operator notation as

$$\psi_a^{\pm} = \chi_a^{\pm} + G_1^{\pm} W_1 \psi_a^{\pm} \ . \tag{1-51}$$

Note that (1-51) can be written in a number of equivalent forms by using the above operator identities. For instance, by rearranging (1-51) to

$$(1 - G_1^{\pm} W_1)\psi_a^{\pm} = \chi_a^{\pm} \ , \tag{1-52}$$

left-multiplying by $(1 + G^{\pm} W_1)$ and using the identity (1-49) with $G_o^{\pm}$, V replaced by $G_1^{\pm}$, W_1 (1-52) becomes

$$\psi_a^{\pm} = (1 + G^{\pm} W_1)\chi_a^{\pm} \ . \tag{1-53}$$

Or, by writing the Schrödinger equation in the form

$$(E - H_o)\psi_a^{\pm} = (U_1 + W_1)\psi_a^{\pm} = V\psi_a^{\pm} \ , \tag{1-54}$$

the formal solution

$$\psi_a^{\pm} = \varphi_a + G_o^{\pm} V \psi_a^{\pm} \tag{1-55}$$

can be rearranged to the form

$$(1 - G_o^{\pm} V)\,\psi_a^{\pm} = \varphi_a \ . \tag{1-56}$$

Left-multiplying by $(1 + G^{\pm}V)$ and using identity (1-49) yields another alternate expression

$$\psi_a^{\pm} = (1 + G^{\pm}V)\varphi_a \tag{1-57}$$

which can be compared with (1-51) and (1-53). The physical significance of the terms in these three equations will be discussed in a later section. (Of course the equation for $\chi_a^{\pm}$, (1-33), can be similarly manipulated.)

From the equations derived above, a formal definition of the T operator can be given. By (1-17), the transition matrix is given by

$$T_{a,b} \equiv \langle \varphi_b | T | \varphi_a \rangle = \langle \varphi_b | V | \psi_a^{+} \rangle \ . \tag{1-58}$$

From (1-57) it can be written as

$$T_{a,b} = \langle \varphi_b | V + VG^{+}V | \varphi_a \rangle \tag{1-59}$$

which serves to define the T operator as

$$T = V + V \frac{1}{E - H + i\varepsilon} V \ . \tag{1-60}$$

As mentioned earlier, in the case of potential scattering this operator is unique for a given H and E.

2. Treatment of Collisions Between Complex Systems

The preceeding discussion has been limited to potential scattering in order to understand how the operator formalism is developed. In this section, the concepts presented in section 1 are generalized to allow consideration of inelastic processes between composite bodies.

2.1 General considerations[2]

In the analysis of collision processes between complex systems it is useful to introduce the concept of a channel. A channel is defined[11] as any possible configuration of a system of particles as a result of a collision between them. In the discussion that follows, a channel will be denoted by a Greek subscript. In a collision process written symbolically as

$$A + X \rightarrow B + Y \quad , \tag{2-1}$$

the entrance channel (α) is composed of particles A and X. If the collision is elastic (no change in the internal energy of the particles) the exit channel (β) is identical with the entrance channel. For the sake of this discussion, exchange elastic scattering is included as an elastic collision. If the internal energy of the colliding particles changes, the collision is termed inelastic and the exit channel (β) differs from the entrance channel (α). In the following discussion, all channels will be assumed to be composed of two particles which may be complex, i. e. have internal structure. Thus consideration of processes such as ionization is being excluded; but this is no serious restriction.[12]

In any collision process in which the interactions between the particles of the system depend only on the relative positions of the particles, the center-of-mass motion can be separated from the relative motion of the two particles.[13] Consequently, for any channel ($\gamma = \alpha, \beta$) consisting of two-composite particles C and Z, a reduced mass

$$M_\gamma = \frac{M_C M_Z}{M_C + M_Z} \tag{2-2}$$

and a relative kinetic energy

$$E_{kE}^{rel} = \frac{p_\gamma^2}{2M_\gamma} \; ; \; \vec{p}_\gamma = \frac{(M_Z \vec{p}_C - M_C \vec{p}_Z)}{(M_C + M_Z)} \tag{2-3}$$

can be defined. This is called the relative center-of-mass coordinate system.

Although the theoretical description of the collision process is most easily carried out in the center-of-mass system of coordinates, the experiment is performed in the laboratory system of coordinates. The relation between the angles in the center-of-mass system (Θ, Φ) and those in the laboratory system (θ, φ) is given by[14] (for the process (2-1), assuming particle X to be at rest)

$$\tan\theta = \frac{\sin\Theta}{\cos\Theta + \tau} \; ; \; \tau = \left[\frac{M_A M_B}{M_X M_Y} \frac{E_\alpha}{E_\beta}\right]^{1/2}, \tag{2-4}$$

where E_α and E_β denote the kinetic energy in the entrance (α) and exit (β) channels, and the masses of the particles involved have the appropriate subscripts.

Consider an inelastic collision process of the type symbolically indicated by (2-1). In a given channel (γ), the wave function which describes the internal quantum state of the two particles (non-interacting) can be written in the product form

$$\eta_\gamma = \xi_c \xi_z \ . \tag{2-5}$$

That is, if h_c and h_z are the Hamiltonians describing the internal motions of the sub-particles composing C and Z, then

$$h_c \xi_c = e_c \xi_c \ ; \ h_z \xi_z = e_z \xi_z \tag{2-6}$$

$$e_\gamma = e_c + e_z$$

where e_γ is the total internal energy of the particles in channel (γ). If V_γ represents the interaction between the sub-particles composing C and those composing Z, the total Hamiltonian of the system in channel (γ) is

$$H = H_\gamma + V_\gamma \tag{2-7}$$

$$= h_c + h_z + p_\gamma^2/2M_\gamma + V_\gamma \ . \tag{2-8}$$

The total energy state of a channel (γ) will be denoted by a lower case subscript, say $g \equiv (\gamma, \vec{k}_g)$ where $\vec{k}_g$ denotes the wave number of the relative kinetic energy in channel (γ). In any channel (γ), the total energy (E) is the sum of the internal energies of the particles in the channel and their relative kinetic energy. Since the total energy (E) of the system is conserved in the collision process, the total energy in the entrance (α) and exit (β) channels is the same:

$$E = e_\alpha + \frac{\hbar^2 k_a^2}{2M_\alpha} = e_\beta + \frac{\hbar^2 k_b^2}{2M_\beta} \quad . \tag{2-9}$$

From the above equation, the necessary condition for the exit channel (β) to be open is

$$E - e_\beta \geq 0 \quad . \tag{2-10}$$

For given initial conditions of the system $a \equiv (\alpha, \vec{k}_a)$, three stationary waves are important; the plane wave Φ_a and the two waves $\psi_a^{\pm}$. The plane wave satisfies

$$H_\alpha \Phi_a = E \Phi_a \tag{2-11}$$

$$\Phi_a = \eta_\alpha \varphi_a \; ; \quad \varphi_a \equiv e^{i\vec{k}_a \cdot \vec{r}_\alpha} \quad , \tag{2-12}$$

where η is defined in (2-5) and $\vec{r}_\alpha$ denotes the vector distance between the center of masses of the two colliding particles in channel (α). The stationary waves ($\psi_a^{\pm}$) are solutions of the complete H with energy E whose asymptotic form corresponds to: the plane

wave Φ_a and outgoing (+) and incoming (-) spherical waves in the entrance channel (α); just outgoing (+) or incoming (-) spherical waves in all other exit channels (β). That is,

$$H\psi_a^{\pm} = E\psi_a^{\pm} \tag{2-13}$$

$$\psi_a^{\pm} \underset{r_\alpha \to \infty}{\sim} \eta_\alpha \left[\varphi_a + f_{a\alpha}^{\pm}(\Omega_a) \frac{e^{\pm i k_a r_\alpha}}{r_\alpha} \right] \tag{2-14}$$

$$\underset{r_\beta \to \infty}{\sim} \eta_\beta f_{a\beta}^{\pm}(\Omega_b) \frac{e^{\pm i k_b r_\beta}}{r_\beta} \quad (\beta \pm \alpha) \ . \tag{2-15}$$

From these equations, the collision process (2-1) in which particle B is emitted in the direction Ω_b with kinetic energy $\hbar^2 k_b^2 / 2M_\beta$ is given by[15]

$$\frac{d\sigma_{a,b}}{d\Omega_b} = \frac{v_b}{v_a} \left| f_{a\beta}^{+}(\Omega_b) \right|^2 \ . \tag{2-16}$$

In the case of elastic scattering $\beta = \alpha$ but $b \neq a$ since in general $\vec{k}_b \neq \vec{k}_a$ even though $k_b = k_a$.

A transition matrix $T_{a,b}$ for the collision process (2-1) can be defined in a manner analogous to the definitions made in Section (I-1). An operator T, governed by the Hamiltonian (2-8) at energy E is defined such that

$$T_{a,b} \equiv \langle \Phi_b | T | \Phi_a \rangle = - \frac{2\pi\hbar^2}{M_\beta} f^+_{a\beta}(\Omega_b) \quad . \tag{2-17}$$

The above definition of the operator T is consistent with the definition of Section I, (I - 1 - 17), in that the matrix is formed between vectors of the same total energy. However, (2-17) is not the usual definition of the matrix representation of an operator because the state vectors in (2-17) are not always orthogonal.[16] Nonetheless, it is possible to write the transition amplitude for the scattering process ($\alpha \to \beta$) in terms of a certain operator $T_{a\beta}$ defined for the specific entrance and exit channels.[16] This generalization will not be discussed here.

In passing, it is worth mentioning that in some cases, such as collisions involving three or more particles, the approximate solutions of the integral equations may not be unique.[17] However, when the solutions obtained are first order in the interaction potentials, as in the calculations performed here, uniqueness is assured.[17b]

2.2 Green's function operators and integral equations for collisions between complex systems

The Green's function operators and integral equations are obtained in a manner analogous to that used in the treatment of potential scattering. By a slight extension of the notation, Green's function operators $[E - H \pm i\epsilon]^{-1}$ and $[E - H_\gamma \pm i\epsilon]^{-1}$ can be associated with the Hamiltonians H and H_γ respectively of (2-7). Identities among these operators analogous to (1-45) through (1-50) can be derived by direct extension of the potential scattering results. By use of these identities, integral equations for the scattering processes can be derived.

For instance, assume that the complete Hamiltonian can be written as

$$H = H_\alpha + U_\alpha + W_\alpha \tag{2-18}$$

$$= \hat{H} + W_\alpha \ . \tag{2-19}$$

That is, assume that the interaction potential in channel α, (V_α), can be written as the sum of two potentials U_α and W_α. In addition, assume that the stationary scattering solutions, $\zeta_a^\pm$, of $\hat{H}$ for energy E exist;

$$\hat{H}\zeta_a^\pm = (H_\alpha + U_\alpha)\zeta_a^\pm = E\zeta_a^\pm \ , \tag{2-20}$$

$$\zeta_a^\pm \underset{r_\alpha \to \infty}{\sim} \eta_\alpha \left[e^{i\vec{k}_a \cdot \vec{r}_\alpha} + g_{a\alpha}^\pm(\Omega_a) \frac{e^{\pm ik_a r_\alpha}}{r_\alpha} \right]$$

$$\underset{r_\beta \to \infty}{\sim} \eta_\beta \, g_{a\beta}^\pm(\Omega_b) \frac{e^{\pm ik_b r_\beta}}{r_\beta} \ . \tag{2-21}$$

(Of course, one can also talk about solutions of $\hat{H}$ where $\alpha \longrightarrow \beta$ and $a \longrightarrow b$. The above merely serves as an illustration.) The above solutions can also be written in integral equation form:

$$\zeta_a^\pm = \Phi_a + \frac{1}{E - H_\alpha \pm i\varepsilon} U_\alpha \zeta_a^\pm \ . \tag{2-22}$$

Using the identity (analogous to (I-1-49))

$$(1 + \frac{1}{E - H_\alpha - U_\alpha \pm i\varepsilon} U_\alpha)(1 - \frac{1}{E - H_\alpha \pm i\varepsilon} U_\alpha) = 1 \qquad (2\text{-}23)$$

(2-22) can be rewritten as

$$\zeta_a^\pm = [1 + \frac{1}{E - \hat{H} \pm i\alpha} U_\alpha] \Phi_a \ . \qquad (2\text{-}24)$$

In a similar fashion, the scattering solutions $\psi_a^\pm$ to the complete Hamiltonian (2-18) at energy E can be written as

$$\psi_a^\pm = \zeta_a^\pm + \frac{1}{E - H \pm i\varepsilon} W_\alpha \psi_a^\pm \qquad (2\text{-}25)$$

$$= [1 + \frac{1}{E - H \pm i\varepsilon} W_\alpha] \zeta_a^\pm \ . \qquad (2\text{-}26)$$

3. Rearrangement Collisions

The treatment of complex collision processes outlined above will now be specialized to that of rearrangement collisions.

Let H and $\hat{H}$ be two possible Hamiltonians describing the given quantum system. Specifically, assume that they have the same kinetic energy but may have different potential energies. At energy E, denote their stationary scattering solutions by ψ and $\hat{\psi}$ respectively. Because of the possible difference in their potentials,

some channels may be open for collisions governed by H that are not open for collisions governed by $\hat{H}$, and vice-versa. If channel (β) is open for $\hat{H}$, then one of the stationary solutions of $\hat{H}$ corresponding to $b \equiv (\beta, \vec{k}_b)$ is $\hat{\psi}_b^-$. The subscript (b) denotes the initial conditions for this wave and hence (β) can be considered as the entrance channel for $\hat{\psi}_b^-$. If channel (δ) is also open to collisions governed by $\hat{H}$ (also at energy E), then $\hat{\psi}_b^-$ will have the asymptotic form:

$$\hat{\psi}_b^- \underset{r_\beta \to \infty}{\sim} \eta_\beta \left[e^{i\vec{k}_b \cdot \vec{r}_\beta} + \hat{f}_{b\beta}^-(\Omega_b) \frac{e^{-ik_b r_\beta}}{r_\beta} \right] \tag{3-1}$$

$$\underset{r_\delta \to \infty}{\sim} \eta_\delta \hat{f}_{b\delta}^-(\Omega_d) \frac{e^{-ik_d r_\delta}}{r_\delta} \quad (\delta \neq \beta) \ . \tag{3-2}$$

[There is, of course, a $\hat{\psi}_b^+$ solution to $\hat{H}$ but as will be shown, only one of the two solutions need be considered; $\hat{\psi}_b^-$ is used here.] Let ψ_a^+ be a similar solution of H for the (same) energy E corresponding to the initial conditions (a). Then the following powerful relation can be derived:[18]

$$\langle \hat{\psi}_b^- | H - \hat{H} | \psi_a^+ \rangle = - \frac{2\pi\hbar^2}{M_\beta} f_{a\beta}^+(\Omega_b) + \frac{2\pi\hbar^2}{M_\alpha} \hat{f}_{b\alpha}^{-*}(-\Omega_a) \ . \tag{3-3}$$

It should be emphasized that f^+ and $\hat{f}^-$ will not in general exist for all α and β, since H and $\hat{H}$ will not usually have the same sets of open channels.

Equation (3-3) can be manipulated into a form containing the transition matrices for the collision processes governed by H and $\hat{H}$ as follows. When $H \equiv \hat{H}$, (3-3) reduces to

$$\frac{2\pi\hbar}{M_\beta}^2 f^{+}_{a\beta}(\Omega_b) = \frac{2\pi\hbar}{M_\alpha}^2 f^{-*}_{b\alpha}(-\Omega_a) \tag{3-4}$$

where the ($\wedge$) superscript has been dropped. Note that (3-4) means that (2-17) can equally well be written as

$$T_{a,b} \equiv \langle \Phi_b | T | \Phi_a \rangle = - \frac{2\pi\hbar}{M_\alpha}^2 f^{-*}_{b\alpha}(-\Omega_a) \, . \tag{3-5}$$

In a similar fashion, a transition matrix can be defined for collisions governed by $\hat{H}$ at energy E. In analogy with (II-2-17)

$$\hat{T}_{a,b} \equiv \langle \Phi_b | \hat{T} | \Phi_a \rangle = - \frac{2\pi\hbar}{M_\alpha}^2 \hat{f}^{-*}_{b\alpha}(-\Omega_a) \tag{3-6}$$

$$= - \frac{2\pi\hbar}{M_\beta}^2 \hat{f}^{+}_{a\beta}(\Omega_b) \, . \tag{3-7}$$

Using these definitions allows (3-3) to be written in the form

$$\langle \Phi_b | T | \Phi_a \rangle = \langle \Phi_b | \hat{T} | \Phi_a \rangle + \langle \hat{\psi}^{-}_b | H - \hat{H} | \psi^{+}_a \rangle \, . \tag{3-8}$$

As will be shown immediately, (3-8) is a quite general and powerful relation between the Hamiltonians H, $\hat{H}$ and their respective transition matrices.

The rearrangement collision is indicated schematically by

$$A + BX \rightarrow AX + B \tag{3-9}$$

where A, B are the particles undergoing the exchange. Without loss of generality, the target particle X (hereafter called the "core") is assumed to be infinitely heavy.[19] Channel (α) will be used to denote a channel in which A is free and B is bound to the core, and channel (β) one in which B is free and A is bound.

To clarify the description of the rearrangement process, the Hamiltonian is written in two equivalent forms:

$$H = H_\alpha + V_\alpha = (K_A + K_B + U_B) + (U_A + W_{AB}) \tag{3-10}$$

$$= H_\beta + V_\beta = (K_B + K_A + U_A) + (U_B + W_{AB}); \tag{3-11}$$

where K_A, K_B denote the kinetic energies of particles A, B; U_A, U_B represent the interaction of particles A, B with the core; and W_{AB} is the interaction between particles A, B. The total Hamiltonian has been written in the two forms (3-10), (3-11) to emphasize the "prior" and "post" forms (respectively) of the collision process. As written in (3-9), the rearrangement collision is assumed to proceed from left to right and the terms "prior", "post" have evolved in the literature to describe which particle is free, A or B. The origin of this terminology will become apparent a little later.

The wave functions for particles A, B as free particles are denoted by the plane waves φ_A, φ_B. They are solutions of

$$(E_A - K_A)\varphi_A = 0 \; ; \quad (E_B - K_B)\varphi_B = 0 \, . \tag{3-12}$$

The wave functions describing the particles A, B bound to the core are written as η_A, η_B. They satisfy

$$(W_A - K_A - U_A)\eta_A = 0; \; (W_B - K_B - U_B)\eta_B = 0 \, . \tag{3-13}$$

Let $\chi_A^{\pm}$, $\chi_B^{\pm}$ be the stationary scattering waves of energy E_A, E_B satisfying

$$(E_A - K_A - U_A)\chi_A^{\pm} = 0; \; (E_B - K_B - U_B)\chi_B^{\pm} = 0 \tag{3-14}$$

with the asymptotic behavior as indicated by the (±) superscripts. [It is worth noting here that for some cases (3-14) may represent scattering involving Coulomb potentials. In such cases, the formalism is still applicable as long as the appropriate boundary conditions are enforced. See ref. 3.]

Because it will prove useful later, (3-14) is also written in its equivalent integral equation form:

$$\chi_A^{\pm} = \varphi_A + \frac{1}{E_A - K_A - U_A \pm i\varepsilon} U_A \varphi_A; \; \chi_B^{\pm} = \varphi_B + \frac{1}{E_B - K_B - U_B \pm i\varepsilon} U_B \varphi_B. \tag{3-15}$$

The scattering wave solution to the total Hamiltonian, subject to the appropriate (±) asymptotic boundary condition, satisfies

$$\left\{E - [(K_A + K_B + U_B) + (U_A + W_{AB})]\right\} \psi_i^{\pm} = 0 \tag{3-16}$$

$$\left\{E - \left[(K_B + K_A + U_A) + (U_B + W_{AB}) \right] \right\} \psi_f^{\pm} = 0 \,. \qquad (3\text{-}17)$$

In (3-16), the terms are grouped to indicate the "prior" form in which A is free. The subscript (i) on the wave function is used to denote this "prior" solution. Similarly, (3-17) represents the "post" form in which B is free, and the subscript (f) denotes this case. [The case when A and B are identical particles is discussed at the end of this section.]

The "prior" and "post" relationship of $\psi_i^{\pm}$ and $\psi_f^{\pm}$ with respect to the incident and scattered particle is perhaps seen more clearly when (3-16) and (3-17) are written in their integral form:

$$\psi_i^{\pm} = \chi_A^{\pm} \eta_B + \frac{1}{E - K_A - K_B - U_A - U_B \pm i\epsilon} W_{AB} \psi_i^{\pm} \qquad (3\text{-}18)$$

$$= \left[1 + \frac{1}{E - K_A - K_B - U_A - U_B - W_{AB} \pm i\epsilon} W_{AB}\right] \chi_A^{\pm} \eta_B \qquad (3\text{-}19)$$

$$\psi_f^{\pm} = \chi_B^{\pm} \eta_A + \frac{1}{E - K_A - K_B - U_A - U_B \pm i\epsilon} W_{AB} \psi_f^{\pm} \qquad (3\text{-}20)$$

$$= \left[1 + \frac{1}{E - K_A - K_B - U_A - U_B - W_{AB} \pm i\epsilon} W_{AB}\right] \chi_B^{\pm} \eta_A \,. \qquad (3\text{-}21)$$

The above integral equations were obtained by the same techniques used to find (II-2-24) and (II-2-26).

Equations (3-16) through (3-21) might seem a little artificial at first since it may appear as if trickery is being used to generate two solutions to the same Hamiltonian. Keep in mind that the two solutions $\psi_i^{\pm}$ and $\psi_f^{\pm}$ represent two physically different

scattering states in which A and B respectively is the free particle.

Energy conservation requires that

$$E = E_A + W_B = E_B + W_A. \tag{3-22}$$

As indicated above, E_j and W_j represent the kinetic energy and binding energy to the core respectively of particle j. The term "core" is used to describe the composite particle X in (3-9).

The transition amplitude for the rearrangement collision process $T_{a,b}$ can be derived using either of two equivalent approaches - the "prior" (3-16) or the "post" (3-17) interaction forms. The "prior" form will be used here and the equivalence with the "post" form will be demonstrated.

As indicated in (3-8), two matrix elements must be formed in order to calculate the transition amplitude. The second term on the right-hand side of (3-8) can be found as follows. Choose H and $\hat{H}$ respectively as

$$H = K_A + U_A + K_B + U_B \tag{3-23}$$

$$\hat{H} = K_A + U_A + K_B + U_B + W_{AB}. \tag{3-24}$$

This choice is dictated by the decision to use the "prior" form. The solution of (3-23) for energy E,

$$(E_A + W_B - K_A - U_A - K_B - U_B)\psi_a^+ = 0 . \tag{3-25}$$

corresponding to the initial conditions [$a \equiv (\alpha, \vec{k}_a)$] and outgoing (asymptotic) spherical waves can be written using (3-13) and (3-14) as

$$\psi_a^+ = \chi_A^+ \eta_B \,. \tag{3-26}$$

$\hat{\psi}_b^-$ is the corresponding solution of $\hat{H}$ at energy E for the "initial" conditions [$b \equiv (\beta, \vec{k}_b)$] and incoming (asymptotic) spherical waves. The additional matrix element necessary to characterize the scattering as governed by $\hat{H}$ is according to (3-8)

$$\hat{T} = \langle \Phi_b | T | \Phi_a \rangle \,. \tag{3-27}$$

This term represents a rearrangement scattering at energy E as governed by H (3-23). An expression for it in terms of the pertinent wave functions can also be found by applying (3-8) to

$$H' = K_A + K_B + U_B \tag{3-28}$$

$$\hat{H}' = K_A + U_A + K_B + U_B \,. \tag{3-29}$$

This specific choice of Hamiltonians is again dictated by the decision to use a "prior" interaction. The solution of $\hat{H}'$ (3-29) at energy E for the "initial" conditions (b') and incoming (asymptotic) spherical waves

$$(E_B + W_A - K_A - U_A - K_B - U_B)\,\hat{\psi}_{b'}^- = 0 \tag{3-30}$$

can be written in a factored form by using (3-14), (3-15) as

$$\hat{\psi}^{-}_{b'} = \eta_A \chi^{-}_B \ . \tag{3-31}$$

(The primes are introduced here just to avoid confusion with (3-23), (3-24) and their solutions.) Similarly, the solution of H' (3-28) at energy E for the initial conditions (a') can be written as

$$\psi^{+}_{a'} = \varphi_A \eta_B \ . \tag{3-32}$$

By inspection of H' (3-28), one sees that particle A is completely free, experiencing no interaction with the core or particle B. Consequently, A is not scattered and the T' operator associated with H' is identically zero. Using this fact, along with (3-28) through (3-32), one finds that (3-8) takes the form

$$\langle \Phi_{b'} | \hat{T}' | \Phi_{a'} \rangle = \langle \eta_A \chi^{-}_B | U_A | \varphi_A \eta_B \rangle . \tag{3-33}$$

The total transition amplitude for the rearrangement of (3-9) is found by using (3-23) through (3-26) in (3-8), along with (3-33). One finds for this "prior" form that

$$T^{\text{prior}}_{a,b} \equiv \langle \Phi_b | T_{ab} | \Phi_a \rangle$$

$$= \langle \eta_A \chi^{-}_B | U_A | \varphi_A \eta_B \rangle + \langle \hat{\psi}^{-}_b | W_{AB} | \chi^{+}_A \eta_B \rangle \ , \tag{3-34}$$

where the subscripts a, b denote the channels for the process (3-9). Note that an immediate simplification to (3-34) can be made. In the first term on the right hand side, the wave functions χ_B^- and η_B are independent of the coordinates of particle A and consequently an integration can be performed over the coordinates of particle B. Since χ_B^- and η_B are eigenfunctions of the same hermitian operator but with different eigenvalues, these functions are orthogonal and thus the first term in (3-34) vanishes identically. The transition amplitude for the rearrangement process (3-9) thus reduces to

$$T_{a,b}^{prior} = \langle \hat{\psi}_b^- | W_{AB} | \chi_A^+ \eta_B \rangle \ . \qquad (3\text{-}35)$$

This result shows that the core does not contribute to rearrangement scattering; a result which is quite logical on physical grounds.

The equivalence of the "prior" and "post" forms of the transition amplitude will now be demonstrated. To obtain the "post" form, the role of H and $\hat{H}$ are reversed in (3-23) and (3-24), and one chooses

$$H' = K_A + U_A + K_B + U_B \qquad (3\text{-}36)$$

$$\hat{H}' = K_A + U_A + K_B \ . \qquad (3\text{-}36)$$

[Note in passing that $\hat{H}'$ equal to (3-28) is not permissible on physical grounds since $\hat{H}'$ admits no solution which will satisfy the boundary conditions [$b \equiv (\beta, \vec{k}_b)$], A bound.] Then the "post" forms equivalent to (3-34) and (3-35) are found to be

$$T^{post}_{a,b} \equiv \langle \Phi_b | T_{ab} | \Phi_a \rangle$$

$$= \langle \eta_A \varphi_B | U_B | \chi^+_A \eta_B \rangle + \langle \eta_A \chi^-_B | W_{AB} | \psi^+_a \rangle \,, \tag{3-37}$$

and

$$T^{post}_{a,b} = \langle \eta_A \chi^-_B | W_{AB} | \psi^+_a \rangle \,. \tag{3-38}$$

The first term on the right hand side of (3-37) vanishes for the same reason the analogous term of (3-34) vanished.

Now, $\hat{\psi}^-_b$ is written in its integral equation form (3-21)

$$\hat{\psi}^-_b = [1 + \frac{1}{E - K_A - K_B - U_A - U_B - W_{AB} - i\epsilon} W_{AB}] \chi^-_B \eta_A \tag{3-39}$$

$$\equiv [1 + G^- W_{AB}] \chi^-_B \eta_A \,. \tag{3-40}$$

If W_{AB} is assumed to be hermitian and use is made of the fact that $(G^-)^\dagger = G^\dagger$, then

$$(G^- W_{AB})^\dagger = W^\dagger_{AB} G^{-\dagger} = W_{AB} G^+ \,, \tag{3-41}$$

and one can use (3-40) to write the "bra" $\langle \hat{\psi}^-_b |$ as

$$\langle \hat{\psi}^-_b | = \langle \chi^-_B \eta_A | (1 + W_{AB} G^+) \,. \tag{3-42}$$

Using (3-42), the "prior" form of the transition amplitude (3-35) can be written

$$
\begin{aligned}
T_{a,b}^{prior} &= \langle \hat{\psi}_b^- | W_{AB} | \chi_A^+ \eta_B \rangle \\
&= \langle \chi_B^- \eta_A | W_{AB} + W_{AB} G^+ W_{AB} | \chi_A^+ \eta_B \rangle \qquad (3\text{-}43) \\
&= \langle \chi_B^- \eta_A | W_{AB} (1 + G^+ W_{AB}) | \chi_A^+ \eta_B \rangle \\
&= \langle \chi_B^- \eta_A | W_{AB} | \psi_a^+ \rangle \qquad [\text{by (3-19)}] \\
&= T_{a,b}^{post} \quad .
\end{aligned}
$$

Thus, as expected on physical grounds, the "prior" and "post" forms of the transition amplitude for the process (3-9) are equivalent. In passing, it is worth mentioning that the operator appearing in (3-43) is often called the "effective interaction" or "t-matrix" for the scattering of A by B in the presence of the core.[20]

The above results, though exact, are the origin of what is known in the literature as the "prior", "post" paradox. The source of the paradox can be traced to the necessity of using approximate wave functions in actual calculations. For, when approximate wave functions are inserted into the first term on the right hand sides of (3-34) and (3-37), these matrix elements will not vanish in general. For example, if the Born approximation is applied to (3-34), in which χ_B^- is replaced by φ_B, φ_B is not formally orthogonal to η_B since they are eigenfunctions of different Hamiltonians. As a result of this fact, much effort has been expended in an effort to modify (3-34) and (3-37)

in such a manner that this discrepancy will disappear.[21] Recently, it has been pointed out that this paradox is a result of the inadequacies of perturbation theory,[19] and all approximations should be developed from the formally exact result (3-35) or (3-38). However, at present this view is not shared by all researchers in the field,[22] and in at least one instance, including the core gives improved agreement with experiment.[23]

In the preceeding discussion, the particles undergoing rearrangement have been treated as distinguishable. This is not a restriction because when the Hamiltonian for the collision process is spin independent, the effect of exchange (if the particles are indistinguishable) can be accounted for by the appropriate linear combination of exchange degenerate scattering amplitudes.[24] It is quite reasonable in atomic and molecular collision processes to assume the interactions are spin independent and this approximation is applied here. Consequently, detailed consideration of the exchange of identical particles can be reserved until the end of a calculation. This is discussed further in Appendix C.

4. Approximations to the Exact Scattering Amplitude

In this section, some of the commonly used approximations to the exact transition amplitude (3-35) or (3-38) will be briefly discussed. These approximations are most conveniently presented with the integral equations for the various scattering states in mind since the terms in these equations have some physical meaning.

4.1 Distorted wave approximation[25]

If the "prior" form is used to describe the rearrangement process, the exact transition amplitude is given by (3-35). In practice, since $\hat{\psi}_b^-$ cannot be found exactly (because $\hat{\psi}_b^-$ represents the solution to the scattering problem), some approximation has to be employed. One frequently used approximation is to neglect the second term on the right hand side of (3-40). Then (3-35) becomes

$$T_{a,b}^{DW} = \langle \eta_A \chi_B^- | W_{AB} | \chi_A^+ \eta_B \rangle \ . \qquad (4\text{-}1)$$

In (4-1), the interaction between A and B is treated to first order while the interactions of A and B with the core are treated exactly. The functions χ_B^- and χ_A^+ are called "distorted waves" because, as seen from (3-15), they represent the result of the distortion of the respective plane waves due to the interaction with the core. The second term on the right hand sides of (3-15) represents this distortion. This approximation is expected to give good results when the interaction between A and B is very small such that $\hat{\psi}_b^-$ deviates very little from $\eta_A \chi_B^-$.

4.2 Born approximation[26]

The Born approximation can be considered as an additional approximation to the "distorted-wave" scattering amplitude of (4-1). In this approximation, all the distortion effects are neglected and the scattered waves χ_B^- and χ_A^+ are replaced by their respective plane waves. With these approximations, (4-1) reduces to

$$T^{B}_{a,b} = \langle \eta_A \varphi_B | W_{AB} | \varphi_A \eta_B \rangle \ . \qquad (4\text{-}2)$$

The physical assumption that accompanies such an approximation is evident from (3-15). As seen from these equations, the Born approximation assumes that the core potentials are not effective in distorting the plane waves. This is certainly expected to be a valid assumption if the energy of the incident particle is sufficiently high, and numerous calculations have verified that it holds for such an energy range.[27] There is another condition for low incident energy for which (4-2) may be expected to give reliable results. The low energy criteria is determined by finding the condition under which the interaction is truly a perturbation. It is[28]

$$|W_{AB}| << \frac{\hbar^2}{ma^2}, (k_a \lesssim 1) \ , \qquad (4\text{-}3)$$

where (a) is the range of the interaction potential W_{AB}. The physical meaning of (4-3) can be found by noticing that the right hand side of (4-3) is the order of the kinetic energy of a particle bound in a box of dimension (a). Thus, if the interaction is too weak to form a bound state, (4-2) may describe the scattering process adequately. Note that (4-3) is a stronger criteria than the usual high energy requirement because it is valid for all energies ($\hbar/a \sim p = \hbar k$). It is also important to remember that both the high and low energy criteria stated above are necessary but not sufficient conditions for the validity of (4-2).

4.3 Close-coupling approximation[29]

There is another method of solving the rearrangement scattering problems which is worth mentioning. It is called the close-coupling approximation and was not treated here because it is most easily derived from the differential equations rather than the integral equation approach presented here.[29]

The basis of the method involves expanding the solution of the scattering problem in terms of the eigenfunctions of the bound systems (the composite particles in (3-9)). In practice, one limits the number of terms in the expansion to the ones that most effect the scattering process. When exchange is included, there results a set of coupled integro-differential equations. Since this method seems at present to be limited (on practical grounds) to spherically symmetric scatterers with a small number of particles, it will not be presented here. The results obtained using this approach will be briefly discussed in a later section.[30]

In closing this section, it is felt worthwhile to mention a few points concerning the use of the above mentioned approximations to the exact $T_{a,b}$. As a general rule, when performing a distorted wave calculation according to (4-2), unless the interactions with the "core" are spherically symmetric, the distorted waves are extremely difficult to obtain due to the mathematical complexities of the non-separable inhomogeneous partial differential equations. In addition, it has been found that for some processes, the Born approximation gives better agreement with experiment.[31] The apparent reason for this is that in some cases there is a partial cancellation of errors in the Born treatment which doesn't occur in the "distorted-wave" approach. Unfortunately, there is no method which allows one

to establish beforehand which approximation will describe a given collision process most accurately. This serves to warn that the "distorted-wave" approximation should not be considered as superior to the Born approximation for all collision processes.

The remainder of Section I will be devoted to the discussion of some of the recent improvements to the Born-Oppenheimer approximation.[26] As indicated above, a tractable model for the general rearrangement process is necessary if many of the interesting physical problems are going to be solved. As will be seen, these new modifications appear to provide a useful model which will enable calculations to be performed for processes that were previously inaccessible theoretically.

5. Improvements on the Born-Oppenheimer Approximation

In this section, and the remainder of this paper, the wave functions and scattering amplitudes will be written as functions of position only. That is, the spin dependence will not be written explicitly; and all the results will be written as if the particles undergoing exchange are distinguishable. As mentioned in Section 3, this technique is possible because the Hamiltonian describing the scattering process is assumed independent of spin. After the scattering amplitude for the given process has been found, the lack of distinguishability among the participating particles can be accounted for by the appropriate linear combination of the scattering amplitude. The necessary modifications are discussed in Appendix C for the case of electron scattering from a two electron bound system.

The Born-Oppenheimer approximation (BO), as applied to low energy electron-atom or electron-molecule (rearrangement)

collisions, has been less than successful.[32] In most calculations using the (BO) approximation, the cross section is found to be a factor of about 10 larger than experiment in the region near excitation threshold. The reason is (apparently) in part due to the retention of the core interaction in the expression for the transition amplitude. That is, the investigators apply the plane wave approximation to (3-34) rather than (3-35) and hence calculate according to ("prior" form)

$$T_{a,b} = \langle \eta_A \varphi_B | U_A | \varphi_A \eta_B \rangle + \langle \eta_A \varphi_B | W_{AB} | \varphi_A \eta_B \rangle . \quad (5\text{-}1)$$

Of course, the core term in (5-1) does not vanish now since φ_B and η_B are in general not orthogonal and, as discussed in Section 4, the "prior", "post" discrepancy appears. It is felt by this writer that a better approximation is to omit the core term in (5-1); i. e. the approximations should be applied to (3-35) or (3-38). This is the approach used in the discussion that follows.

For simplicity in the presentation of the recent modifications of the (BO) approximation [and because explicit calculations were carried out for such systems], the case of the electron impact excitation of a two electron system (atom or diatomic molecule) is used. Denote the ground and excited state wave functions for the bound system as

$$\psi_i(\vec{r}_1, \vec{r}_2) \text{ and } \psi_f(\vec{r}_1, \vec{r}_2) \quad (5\text{-}2)$$

[The subscripts (i, f) can be considered as equivalent to (α, β)] respectively, and let the incident electron ("prior" form) be denoted by the subscript 3. The wave functions (5-2) are assumed to have

the spatial symmetry consistent with the Pauli Principle. In some cases (when the bound system is a diatomic molecule) the bound state wave functions will contain other variables. However, without loss of flexibility, these other variables can be omitted and the wave functions written as (5-2). Then, according to (2-17) and (4-2), the scattering amplitude in the (BO) approximation is ("prior" form); (The letter $\mathcal{T}$ is used to denote scattering amplitude while T denotes the transition amplitude.).

$$\mathcal{T}_{fi}^{BO}(k, \theta, \varphi) \equiv - \frac{M_f}{2\pi\hbar^2} \langle \eta_A(\vec{r}_3, \vec{r}_2)\varphi_B(\vec{r}_1) | \frac{e^2}{r_{13}} | \varphi_A(\vec{r}_3)\eta_B(\vec{r}_1, \vec{r}_2) \rangle, \quad (5\text{-}3)$$

where electrons 1 and 3 have been assumed to undergo the rearrangement. According to (2-2), when one particle in channel ($f \equiv \beta$) is an electron and the other a massive particle, the reduced mass becomes

$$M_f \equiv \frac{m_e M_c}{m_e + M_c} = m_e \frac{1}{(1 + \frac{m_e}{M_c})} = m_e - 0\left(\frac{m_e}{M_c}\right), \quad (5\text{-}4)$$

where m_e, M_c are respectively the masses of the electron and the heavy core. Since $m_e/M_c \approx 10^{-3}$, (5-3) can be well approximated by

$$\mathcal{T}_{fi}^{BO}(k, \theta, \varphi) = - \frac{m_e e^2}{2\pi\hbar^2} \langle \eta_A(3, 2)\varphi_B(1) | \frac{1}{r_{13}}) | \varphi_A(3)\eta_B(1, 2) \rangle \quad (5\text{-}5)$$

where the coordinates are identified by the electron subscript. Transforming from Dirac to integral notation, (5-5) becomes

$$T_{fi}^{BO} = -\frac{m_e^2}{2\pi\hbar^2}\int\left(\frac{1}{r_{31}}\right)e^{i(\vec{k}_o\cdot\vec{r}_3 - \vec{k}'\cdot\vec{r}_1)}\psi_f^*(3,2)\psi_i(1,2)d\vec{r}_1 d\vec{r}_2 d\vec{r}_3, \qquad (5\text{-}6)$$

where $k_o \equiv k_i$ and $k' \equiv k_f$ are the electron wave numbers. Note that in (5-6) (the "prior" form), electrons (3) and (1) are (arbitrarily) assumed to be involved in the exchange. As mentioned earlier, this implies no loss of generality since the possibility of exchange between (3) and (2) can be accounted for by linear combinations of (5-6) containing appropriate coefficients (see Appendix C).

5.1 The Ochkur approximation

The first significant improvement of the (BO) approximation was made by Ochkur[33] in 1964. Ochkur exhibited shrewdness when he observed that the scattering amplitude in the (BO) approximation was not consistent with first order perturbation theory. Specifically, he noticed that the scattering amplitude contained more than just the leading term in an expansion of T_{fi}^{BO} (5-6) in inverse powers of the incident electron energy (the direct Born approximation does not contain such high order terms). This fact is contrary to first order perturbation theory because at high incident energy, where the scattering potential is certainly a perturbation, only the leading term in a power series of inverse incident energy should be present. Consequently, it is necessary to modify the (BO) approximation in such a way as to be consistent with these concepts.

In the case of two bound electrons, the appropriate modification of the exchange scattering amplitude T_{fi}^{BO} is found by expansion of (5-6) in inverse powers of the incident electron energy. If the term with the lowest power of inverse energy is the only one retained, T_{fi}^{BO} becomes (see Appendix D for the details)

$$T_{fi}^{O} = -\frac{2}{k_o^2} \int \psi_f^*(\vec{r}_2, \vec{r}_1)\psi_i(\vec{r}_1, \vec{r}_2) e^{i\vec{q}\cdot\vec{r}_1} \, d\vec{r}_1 d\vec{r}_2 \ . \qquad (5\text{-}7)$$

The Ochkur modification of the (BO) approximation does not suffer from the familiar "prior"-"post" discrepancy as can be seen from (5-7). Even if one considers the core terms necessary in the (BO) approximation, when the (BO) approximate scattering amplitude is expanded in inverse powers of the energy, these core terms are $O(k_o^{-6})$ and hence dropped in favor of (5-7).

However, since the presentation of the Ochkur results, several authors have pointed out that (5-7) is deficient with respect to some of the more subtle aspects of scattering theory. These corrections to the Ochkur modification are presented next.

5.2 The Rudge modification of the Ochkur result

Shortly after the publication of the Ochkur modification, Rudge pointed out[34] that the Ochkur result is not consistent with any trial function which satisfies the proper boundary conditions and is derivable from a variational expression.[35] By the manipulation of a variational expression, Rudge obtained an improvement on the Ochkur result which is (see Appendix E for a derivation of this result):

$$T_{fi}^{OR} = \frac{2a_o}{[a_o k' - (I_i/R)^{1/2}{}_i]^2} \int e^{i\vec{q}\cdot\vec{r}_1} \psi_f^*(\vec{r}_2, \vec{r}_1)\psi_i(\vec{r}_1, \vec{r}_2)d\vec{r}_1 d\vec{r}_2 , \tag{5-8}$$

where (I_i/R) is the ionization energy of the initial bound state measured in Rydbergs, and k' is the wave number of the scattered electron satisfying

$$k' = \left[k_o^2 - \frac{2m}{\hbar^2}(W_f - W_i)\right]^{1/2} . \tag{5-9}$$

Equation (5-9) represents energy conservation, where W_i, W_f are the energies of the initial and final states of the bound system. The Rudge expression (5-8) [which is labeled by the symbols (OR)] is also expected to be superior to the Ochkur result since the former is complex while the latter is not in general. This superiority derives from the fact that a complex scattering amplitude is a necessary condition if particle flux is to be conserved.[36]

However, a critical examination of the Rudge result, (5-8), indicates that it is in error for certain cases. This can be seen by rewriting (5-8) in the form

$$T_{fi}^{OR} = \frac{2a_o e^{2i\delta_{fi}}}{[a_o^2 k'^2 + (I_i/R)]} \int e^{i\vec{q}\cdot\vec{r}_1} \psi_f^*(\vec{r}_2, \vec{r}_1)\psi_i(\vec{r}_1, \vec{r}_2)d\vec{r}_1 d\vec{r}_2, \tag{5-10}$$

where

$$\delta_{fi} \equiv \tan^{-1} \frac{(I_i/R)^{1/2}}{a_o k'} . \tag{5-11}$$

Now the exact scattering amplitude for a collision process (general, not just exchange) satisfies what is called "microreversibility" or "detailed-balance".[37] This just corresponds to the collision process running in reverse and is expressed formally as[38]

$$|T_{fi}|^2 = |T_{if}|^2 \quad . \tag{5-12}$$

As a result of the form of (5-10), when the final state can be reached by both exchange and direct excitation, the total amplitude squared does not satisfy detailed balance. This is because in this situation, the amplitudes for the direct and exchange excitations are added, and from (5-10) the detailed balance won't hold since

$$\delta_{fi} \neq \delta_{if} = \tan^{-1} \frac{(I_f/R)^{1/2}}{a_o k_o} \quad . \tag{5-13}$$

However, in the case of pure exchange, (the case of interest here) there is no contribution from direct excitation and consequently the Rudge result satisfies the principle of detailed balance.

The remainder of this thesis will be devoted to the application of the Ochkur (O) and the Ochkur-Rudge (OR) approximation in the description of the electron excitation of helium and molecular hydrogen.

II. The Exchange Excitation of Molecular Hydrogen

1. Review of Previous Calculations

Because of the mathematical complexities associated with the non-central nature of the molecular field, there have been relatively few calculations of electron-molecule collision processes. Of those reported, a majority[39] have been for the hydrogen molecule because it is the simplest of the neutral molecules. A brief review of previous calculations for the exchange excitation of the hydrogen molecule is as follows.

The first such calculation was done by Massey and Mohr[40] who considered just the first triplet excitation process ($X\ ^1\Sigma_g^+ \rightarrow b\ ^3\Sigma_u^+$). By applying the Born-Oppenheimer (BO) approximation (I-5-1) to describe the excitation process and estimating the contribution from the multicenter terms which appear in the scattering amplitude, they obtained a total cross section which violated conservation of particle flux.[41] Their predicted maximum cross section exceeds recent experimental data[42] for the process by a factor of 7. Edelstein[43] applied variational techniques to obtain the cross section for the ($X\ ^1\Sigma_g^+ \rightarrow b\ ^3\Sigma_u^+$) process. However, no details appeared in his publication and the shape of the cross section he reported disagrees markedly with the experimental results. Khare and Moiseiwitsch (KM) have also calculated[44] the cross section for the process ($X\ ^1\Sigma_g^+ \rightarrow b\ ^3\Sigma_u^+$) employing the (BO), the Ochkur (O), and the first order exchange (E1) approximations. However, (KM) applied the separated atom (SA) approximation in order to evaluate the multicenter integrals that appeared. In addition, Khare (K) has completed a calculation[45] for the excitation of the ($b\ ^3\Sigma_u^+$), ($a\ ^3\Sigma_g^+$) and ($c\ ^3\Pi_u$) states from the ground

state ($X\ ^1\Sigma_g^+$) using one-center wave functions and the (O) approximation. These latter two calculations (which are the best to date), including the effect of the (SA) approximation, will be compared with the results reported in the present work and evaluated accordingly.

In this thesis, the (OR) theory is used for the calculation of the total cross sections for the exchange excitation of the first ($b\ ^3\Sigma_u^+$) and second ($a\ ^3\Sigma_g^+$) triplets from the ground state ($X\ ^1\Sigma_g^+$) of molecular hydrogen. Polarization and higher order effects are neglected. The effects of the nuclear motions are included and shown to be important. The results are seen to agree well with the available experimental data.[42] The calculations performed here were done using exponent-optimized minimum basis set two-center wave functions for the molecule and include all the multicenter terms which appear in the scattering amplitude. In addition, three different ground state wave functions and two different ($b\ ^3\Sigma_u^+$) wave functions were tried in these calculations in order to determine the effect on the total cross sections of using different approximate wave functions. The calculations were also done using the (O) approximation, and the (SA) version of the (OR) and (O) approximations. These latter two calculations, designated respectively by the symbols (ORSA) and (OSA), are compared with the (OR) results.

The second section of this chapter is devoted to the treatment of the additional complexities in the calculation of the electronic excitation cross section introduced by the motion of the nuclei. The third and fourth sections respectively treat the wave functions used and the methods employed to evaluate the multicenter integrals that appear in the scattering amplitude. The last two sections discuss the calculation of the cross sections and the quality of the results.

2. Treatment of Nuclear Motion

2.1 The complete excitation cross section

The electronic excitation of the hydrogen molecule can be treated as follows.

Let n, ν, J, and M be the electronic, vibrational, and rotational quantum numbers for the initial state of the hydrogen molecule and n', ν', J', M' the corresponding final state ones. The molecular wave function can be written as:[46]

$$\Phi(\vec{\zeta}_1, \vec{\zeta}_2; R, \chi, \phi) = \Psi(\vec{r}_1, \vec{r}_2; R, \chi, \phi) S(\vec{s}_1, \vec{s}_2)$$

$$\Psi(\vec{r}_1, \vec{r}_2; R, \chi, \phi) = \psi_n(\vec{r}_1, \vec{r}_2; R) \xi_{n\nu J}(R)\, Y_J^M(\chi, \phi). \qquad (2\text{-}1)$$

Here Ψ and S are the total space and electronic spin wave functions; ψ, ξ, and Y are the electronic-space, vibrational, and rotational (spherical harmonics) wave functions; $\vec{\zeta}_1 \equiv (\vec{r}_1, \vec{s}_1)$ and $\vec{\zeta}_2 \equiv (\vec{r}_2, \vec{s}_2)$ are the space and spin coordinate pairs for the bound electrons in a molecule-fixed coordinate system; R is the internuclear distance; and χ, ϕ are the spherical polar angles of the molecular axis with respect to some space-fixed axis. In the (BO) approximation, the differential cross section (per unit solid angle) for scattering of an electron into a given direction after the exchange excitation of the molecule from the initial state i(nνJM) to the final state f(n'ν'J'M') can be written as[47]

$$I_i^f(k_o, \theta, \varphi) = \frac{3}{(2\pi)^2 a_o^2} \frac{k'}{k_o} \left| \int e^{-i\vec{k}' \cdot \vec{r}_1} \Psi_f^*(\vec{r}_3, \vec{r}_2; R, \chi, \phi) \left(\frac{1}{r_{3\,1}}\right) \right.$$

$$e^{i\vec{k}_o \cdot \vec{r}_3} \Psi_i(\vec{r}_1, \vec{r}_2; \vec{R}, \chi, \phi)\, d\vec{R}\, d\vec{r}_1\, d\vec{r}_2\, d\vec{r}_3 \Big|^2 \qquad (2\text{-}2)$$

where $a_o = \hbar^2/me^2$ is the Bohr radius, $\vec{r}_3$ and $(\vec{r}_1, \vec{r}_2)$ denote the positions of the incident and bound electrons in a molecular-fixed coordinate system; $r_{3\,1}$ is the distance of the incident electron to the molecular electron (1); $d\vec{R}$, $d\vec{r}_j$ are the internuclear and j^{th} electron volume elements; $\vec{k}_o$, $\vec{k}'$ are the wave vectors for the incident and scattered electrons; θ, φ are the spherical polar angles which define the direction of the scattered electron in a laboratory-fixed system whose z-axis is in the direction of $\vec{k}_o$; and the subscripts i, f denote the initial and final state wave functions. As mentioned in Section I-5, it is assumed that the core should not contribute to the excitation process and hence this interaction is omitted in (2-2). In addition only the spatial dependence is written in (2-2); the factor of 3 results from having performed the spin integration [see Section I-3 and Appendix C].

It should be noted that k' is determined by k_o and the excitation energy according to

$$k'(k_o, i, f) = \left[k_o^2 - \frac{2m}{\hbar^2}(E_f - E_i)\right]^{1/2} \qquad (2\text{-}3)$$

where E_f, E_i are the final and initial energies of the molecule and (m) is the mass of the electron. Because of the energy degeneracy of the rotational levels with respect to M and M', k' (for a given electronic transition) is a function of k_o, n, ν, J, n', ν', and J' only.

Substitution of (2-1) into (2-2) gives

$$I_i^f(k_o, \theta, \varphi) =$$

$$3\frac{k'}{k_o} \left| \int \xi^*_{n'\nu'J'}(R)\, Y^{M'*}_{J'}(\chi, \phi)\, T_{fi}\, \xi_{n\nu J}(R)\, Y^{M}_{J}(\chi, \phi) R^2 d\, R d\, \Omega \right|^2, \tag{2-4}$$

where $d\Omega$ is the element of solid angle corresponding to χ, ϕ. T_{fi} is the electronic scattering amplitude which, in the (BO) approximation, is given by:

$$T_{fi}^{BO}(k_o, \theta, \varphi; R, \chi, \phi) \equiv$$

$$\frac{1}{2\pi a_o} \int e^{-i\vec{k}' \cdot \vec{r}_1} \psi^*_{n'}(\vec{r}_3, \vec{r}_2; R)\left(\frac{1}{r_{31}}\right) e^{i\vec{k}_o \cdot \vec{r}_3} \psi_n(\vec{r}_1, \vec{r}_2; R) d\vec{r}_1 d\vec{r}_2 d\vec{r}_3. \tag{2-5}$$

As discussed in Section (I-5), the (BO) approximation is not consistent with first order perturbation theory. It was shown there that a significant improvement might be expected if the (BO) expression is replaced by the (O) or (OR) approximations, which are (respectively):

$$T_{fi} = \frac{2}{a_o k_o^2} \int e^{i\vec{q} \cdot \vec{r}_1} \psi^*_{n'}(\vec{r}_1, \vec{r}_2; R) \psi_n(\vec{r}_1, \vec{r}_2; R)\, d\vec{r}_1\, d\vec{r}_2 \tag{2-6}$$

$$T_{fi} = \frac{2a_o}{\left[a_o k' - (I_n/\mathcal{R})^{1/2} i\right]^2} \int e^{i\vec{q} \cdot \vec{r}_1} \psi^*_{n'}(\vec{r}_1, \vec{r}_2; R) \psi_n(\vec{r}_1, \vec{r}_2; R) d\vec{r}_1 d\vec{r}_2 \tag{2-7}$$

where

$$\vec{q} \equiv \vec{k}_o - \vec{k}' \tag{2-8}$$

is the momentum transferred to the bound system; I_n is the ionization potential of state n, and R is one Rydberg. Note in passing that, as a result of the Born-Oppenheimer separation of nuclear and electronic motion, the electronic wave functions depend only parametrically on the nuclear coordinates.

Given the hydrogen molecule wave functions, and for a particular choice of T_{fi}, (2-4) represents the differential cross section for the excitation process $i(n\nu JM) \rightarrow f(n'\nu'J'M')$. However, since electronic excitation is the primary interest here, some of the nuclear motion will be averaged-over in (2-4).

2.2 Rotationally averaged cross section

Under most experimental conditions, the target molecules are not all in the same quantum state. For the case of molecular hydrogen at temperature T (around room temperature) essentially all of the molecules are in the ground electronic and vibrational states, but many rotational states are represented, their relative populations being determined by the Boltzmann distribution for this temperature. Furthermore, as a result of electron impact on a molecule in a given initial rotational state, several rotational states of the electronically excited molecule can be produced. These various rotational states can be accounted for as follows. Define the rotationally averaged cross section as

$$I_{n\nu}^{n'\nu'}(k_o, \theta, \varphi; T) \equiv \langle I_{n\nu JM}^{n'\nu'}(k_o, \theta, \varphi) \rangle_T \qquad (2\text{-}9)$$

where

$$I_{n\nu JM}^{n'\nu'}(k_o, \theta, \varphi) = \sum_{J'=0}^{J'_{max}} \sum_{M'=-J'}^{J'} I_i^f(k_o, \theta, \varphi) \ . \qquad (2\text{-}10)$$

The averaging indicated by the angular brackets of (2-9) refers to a statistical-mechanical average over initial rotational states J, M, the weighting factors being the Boltzmann populations of those states at temperature T. The double sum over J' and M' in (2-10) extends over the accessible final rotational states for given initial and final electronic and vibrational quantum numbers n, ν, n', ν' and a given initial wave number k_o. J'_{max} is the maximum J' for which k', as given by (2-3), remains real. Therefore, it depends on k_o, n, ν, J, n', and ν'.

Next, show how $I_{n\nu}^{n'\nu'}$ can be determined. If $G_j(u)$ is any complete orthonormal set of functions of a variable u (which may be multidimensional) and F(u) is any function of u, the following expression is valid:

$$\sum_{j'} \left| \int G_{j'}^*(u)\, F(u)\, G_j(u)\, du \right|^2 = \int |F(u)\, G_j(u)|^2\, du \ . \qquad (2\text{-}11)$$

This property is easily proven by expanding FG_j in the right side of (2-11) in terms of the $G_{j'}$. Applying (2-11) to the particular case in which G_j is $Y_J^M(\chi, \phi)$ furnishes

$$\sum_{J'=0}^{\infty} \sum_{M'=-J'}^{J'} \left| \int Y_{J'}^{M'^{*}}(\chi, \phi) Y_{J}^{M}(\chi, \phi) F(\chi, \phi) d\Omega \right|^2$$

$$= \int \left| Y_{J}^{M}(\chi, \phi) \right|^2 \left| F(\chi, \phi) \right|^2 d\Omega . \qquad (2\text{-}12)$$

Substitution of (2-4) into (2-10), replacement of $\mathcal{T}_{fi}$ by the quantity $\mathcal{T}_{n\nu}^{n'\nu'}$ defined below, and use of (2-12) with $F = \int \xi_{n'\nu'}^{*} \mathcal{T}_{n\nu}^{n'\nu'} \xi_{n\nu} R^2 \, dR$ furnishes:

$$I_{n\nu JM}^{n'\nu'}(k_o, \theta, \varphi) = \frac{3\bar{k}'}{k_o} \int_{\Omega} \left| \int_{R} \xi_{n'\nu'}^{*}(R) \, \mathcal{T}_{n\nu}^{n'\nu'}(k_o, \theta, \varphi; R, \chi, \;) \right.$$

$$\left. \xi_{n\nu}(R) \, R^2 \, dR \right|^2 \left| Y_{J}^{M}(\chi, \phi) \right|^2 d\Omega . \qquad (2\text{-}13)$$

Here, $\bar{k}'$ $(k_o, n, \nu, J, n', \nu')$ represents some mean value of $k'(k_o, n, \nu, J, n', \nu', J')$ over the accessible J'. The scattering amplitude $\mathcal{T}_{fi}$ depends on J' through k'. Because of their small mass, electrons are not effective in producing rotational excitation. Therefore, the change in the wave number of the incident electron due to rotational excitation is negligible compared to that due to electronic and vibrational excitation. As a result, k' should deviate very little from

$$k'' = \left[k_o^2 - \frac{2m}{\hbar^2} (E_{n'\nu'} - E_{n\nu}) \right]^{1/2} \qquad (2\text{-}14)$$

where the energies $E_{n\nu}$ and $E_{n'\nu'}$ do not include rotational contributions. Since $\mathcal{T}_{fi}$ is not a very rapidly varying function of k', $\mathcal{T}_{fi}(k')$ can be replaced by $\mathcal{T}_{n\nu}^{n'\nu'} \equiv \mathcal{T}_{fi}(k'')$ to a very good approximation. This quantity is not a function of J or J' and depends on ν and ν' only through k''. To get (2-13), the sum over J' in (2-10) was assumed to extend to infinity. The justification for this assumption is that, for the reasons just stated, I_1^f is expected to be negligible for J' very different from J. Therefore, the additional terms introduced in going from J'_{max} to ∞ should be negligible. On the same basis, since only relatively small values of J and J' are being considered, the radial wave functions $\xi_{n'\nu'J'}(R)$ and $\xi_{n\nu J}(R)$ were assumed to be independent of J' and J, respectively.

Substituting (2-13) into (2-9) and using the sum rule for spherical harmonics gives the result

$$I_{n\nu}^{n'\nu'}(k_o, \theta, \varphi; T) = \frac{3\langle \bar{k}' \rangle_T}{k_o} \int_{\Omega} \left| \int_R [R\xi^*_{n'\nu'}(R)]^* \, \mathcal{T}_{n\nu}^{n'\nu'}(k_o, \theta, \varphi; R, \chi, \phi) \right.$$

$$\left. [R\xi_{n\nu}(r)] \, dR \right|^2 \frac{d\Omega}{4\pi} \tag{2-15}$$

where

$$\langle \bar{k}' \rangle_T = \frac{\sum_J (2J+1) e^{-E_{n\nu J}/kT} \, \bar{k}'(k_o, n, \nu, J, n', \nu')}{\sum_J (2J+1) e^{-E_{n\nu J}/kT}} . \tag{2-16}$$

To a first very good approximation, $\langle \bar{k}' \rangle_T$ can be replaced by the quantity k'' defined by (2-14), for the reasons given above. This substitution is even more reasonable if the incident electron beam is not monoenergetic enough to resolve rotational transitions, which is the usual case in the experiments performed to date. The resulting expression for the differential, rotationally averaged, excitation cross section is

$$I_{n\nu}^{n'\nu'}(k_o, \theta, \varphi) = \frac{3k''}{k_o} \int_{\Omega} \left| \int_{R} [R\xi_{n'\nu'}(R)]^* \mathcal{I}_{n\nu}^{n'\nu'}(k_o, \theta, \varphi; R, \chi, \phi) \right.$$

$$\left. [R\xi_{n\nu}(R)] \right|^2 \frac{d\Omega}{4\pi} \, . \qquad (2\text{-}17)$$

As a result of the replacement of $\langle \bar{k}' \rangle_T$ by k'', the temperature (T) has been dropped as a variable in $I_{n\nu}^{n'\nu'}$.

In (2-17), ν', the quantum number for the vibrational level of the excited state, is implicitly assumed to be discrete. However, if some of the symbols are redefined, this equation still holds when ν' is continuous, i.e., when $E_{n'\nu'} - E_{n'o}$ is larger than the dissociation energy of electronic state n' or when that state is a repulsive one. In such cases, $I_{n\nu}^{n'\nu'} d\nu'$ represents the differential, rotationally averaged, excitation cross section from state n, ν into any state in the range n', ν' to $n', \nu' + d\nu'$. In addition, the radial wave function $R\xi_{n'\nu'}(R)$, which now represents a state in the continuum, is assumed to be normalized according to[48]

$$\lim_{\eta \to 0} \left[\frac{1}{\eta} \int_0^{\infty} \left| \int_{\nu'}^{\nu'+\eta} R\xi_{n'\nu''}(R) d\nu'' \right|^2 dR \right] = 1 \, . \qquad (2\text{-}18)$$

It should be noted that (2-17) states that the differential scattering cross section $I_{n\nu}^{n'\nu'}$ for excitation from state $(n\nu)$ to state $(n'\nu')$ can be obtained by assuming the molecular axis fixed at some orientation (χ, ϕ), averaging the electronic transition amplitude $\mathcal{T}_{n\nu}^{n'\nu'}$ over the vibrational wave functions ($\xi_{n\nu}$ and $\xi_{n'\nu'}$) and then performing an angular average on the square of this quantity over all possible orientations.

It is customary to introduce an additional approximation[49] into (2-17) by assuming that $\mathcal{T}_{n\nu}^{n'\nu'}(R)$ is a very slowly varying function of R and replacing it by its value at the equilibrium internuclear distance $R_e^{(n\nu)}$ of the $(n\nu)$ initial state. As will be seen in Section 5.2.2, this approximation is not always justified. However, it significantly simplifies (2-17) to

$$I_{n\nu}^{n'\nu'}(k_o, \theta, \varphi) = \frac{3k''}{k_o} g_{n\nu}^{n'\nu'} \langle |\mathcal{T}_{n\nu}^{n'\nu'}(R_e^{(n\nu)})|^2 \rangle \qquad (2\text{-}19)$$

where

$$\langle |\mathcal{T}_{n\nu}^{n'\nu'}(R)|^2 \rangle \equiv \int |\mathcal{T}_{n\nu}^{n'\nu'}(k_o, \theta, \varphi; R, \chi, \phi)|^2 \frac{d\Omega}{4\pi} \qquad (2\text{-}20)$$

is the average of $|\mathcal{T}_{n\nu}^{n'\nu'}|^2$ over all orientations of the internuclear axis and

$$g_{n\nu}^{n'\nu'} \equiv \left| \int_0^\infty [R\xi_{n'\nu'}(R)]^* [R\xi_{n\nu}(R)] \, dR \right|^2 \qquad (2\text{-}21)$$

is the Franck-Condon factor for the $(n\nu) \rightarrow (n'\nu')$ electronic-vibrational transition. The quantity $\langle | \mathcal{T}_{n\nu}^{n'\nu'}(R_e^{(n\nu)}) |^2 \rangle$ is a function of the transition $(n\nu) \rightarrow (n'\nu')$, the incident electron wave number k_o, and the scattering direction only.

The total cross section for the $(n\nu) \rightarrow (n'\nu')$ transition can be obtained by integrating (2-17) [or its approximate equivalent (2-19)] over all scattering angles:

$$\sigma_{n\nu}^{n'\nu'}(k_o) = \int_{\theta,\varphi} I_{n\nu}^{n'\nu'}(k_o, \theta, \varphi) \sin\theta d\theta d\varphi \, . \qquad (2\text{-}22)$$

The total electronic excitation cross section from the initial $(n\nu)$ state to <u>all</u> accessible vibrational states of the excited electronic state (n') is given by

$$\sigma_{n\nu}^{n'}(k_o) = \int \sigma_{n\nu}^{n'\nu'}(k_o) \, d\nu' \qquad (2\text{-}23)$$

where $\int$ is a Stieltjes integral used to represent a sum over the discrete values of ν' plus an integral over its continuum values which are energy-wise accessible in the sense that $k''^2 \geq 0$.

3. <u>Molecular Wave Functions</u>

The wave functions used in calculating the excitation of H_2 from its ground electronic vibrational state ($X\ ^1\Sigma_g^+$; $\nu = 0$) to its first and second triplet states ($b\ ^3\Sigma_u^+$ and $a\ ^3\Sigma_g^+$, respectively) are described in this section. For the ground state, three different approximate wave functions[50a] were used: the two-parameter wave function of Weinbaum[50b]

$$\psi_o(\vec{r}_1,\vec{r}_2) = N_o\,[(1s_A^Z(1)\,1s_B^Z(2) + 1s_A^Z(2)\,1s_B^Z(1)) + C\,(1s_A^Z(1)\,1s_A^Z(2) + 1s_B^Z(1)\,1s_B^Z(2))]\,, \qquad (3\text{-}1)$$

the valence bond wave function of Wang:[50c]

$$\psi_o(\vec{r}_1,\vec{r}_2) = N_o\,[1s_A^Z(1)\,1s_B^Z(2) + 1s_A^Z(2)\,1s_B^Z(1)]\,, \qquad (3\text{-}2)$$

and the simple molecular orbital wave function of Coulson:[50d]

$$\psi_o(\vec{r}_1,\vec{r}_2) = N_o[(1s_A^Z(1) + 1s_B^Z(1))\cdot(1s_A^Z(2) + 1s_B^Z(2))]. \qquad (3\text{-}3)$$

For the first triplet state ($b^3\Sigma_u^+$) the two-parameter wave function of Phillipson-Mulliken[51a] was used:

$$\psi_3(\vec{r}_1,\vec{r}_2) = \frac{1}{\sqrt{2}}\left\{\varphi_g(1)\,\varphi_u(2) - \varphi_g(2)\,\varphi_u(1)\right\} \qquad (3\text{-}4)$$

where

$$\varphi_g \equiv N_g(1s_A^{Z_1} + 1s_B^{Z_1}) \qquad (3\text{-}5)$$

and

$$\varphi_u \equiv N_u(1s_A^{Z_2} - 1s_B^{Z_2}); \qquad (3\text{-}6)$$

and the less accurate Hurley[51b] two-parameter wave function

$$\psi_3(r_1, r_2) = N_3 \left[1s^{Z}_{A'}(1)\, 1s^{Z}_{B'}(2) - 1s^{Z}_{A'}(2)\, 1s^{Z}_{B'}(1)\right], \qquad (3\text{-}7)$$

where the centers A', B' are permitted to be displaced from the nuclei A, B, the displacement being the second variational parameter which, however, turns out to be practically zero for this state. Finally, a two parameter Hartree-Fock function was calculated for the second triplet state ($a\,^3\Sigma_g^+$) using computer programs furnished by Prof. W. A. Goddard of the California Institute of Technology. The form of this function was:

$$\psi_3(\vec{r}_1, \vec{r}_2) = \frac{1}{\sqrt{2}} \left\{\varphi_{1g}(1)\, \varphi_{2g}(2) - \varphi_{1g}(2)\, \varphi_{2g}(1)\right\} \qquad (3\text{-}8)$$

where

$$\varphi_{1g} = N_{1g}(1s_A^{Z_1} + 1s_B^{Z_2}) \qquad (3\text{-}9)$$

and

$$\varphi_{2g} = N_{2g}(2s_A^{Z_2} + 2s_B^{Z_2}) - N'_{1g}(1s_A^{Z_1} + 1s_B^{Z_1}). \qquad (3\text{-}10)$$

In Eqs. (3-1) through (3-10), the symbol $1s^{Z}_{X}(j) \equiv e^{-zr_{jX}/a_o}$ stands for a 1s atomic orbital for electron j(= 1, 2) centered on nucleus X(= A, B) with screening parameters; and $2s^{Z(j)}_{X} \equiv e^{-zr_{jX}/a_o}$ is a similar 2s Slater atomic orbital.

To perform cross section calculations, it is necessary to know the molecular electronic wave functions of the ground and excited states as well as the vertical excitation energies from the ground to the appropriate excited state as parametric functions of the internuclear distance R. In all cases, considered in this paper these parametric functions varied quite slowly over the pertinent range of R determined by the classical turning points of the ground electronic vibrational state ($1.20\ a_o < R < 1.67\ a_o$), and it was possible to use, with a high degree of accuracy (error < 3%), polynomial representation of this R variation obtained from least squares fitting to values calculated for a few R values. The R variation of the screening parameters for the first triplet states were found in the literature,[51a, b] while for the ground states the R dependence was obtained from unpublished work.[50a] The R variation of the parameters for the second triplet state was determined in the calculation of the wave function. The values used in determining the R variation of the excitation energies were taken from theoretical calculations of the potential energy as a function of the internuclear distance for the ground and the two excited triplet states.[52] Figure 1 illustrates the potential energy curves for these and some additional singlet states. The classical range of R variation and the Franck-Condon region are indicated by the shading.

In Table I are summarized some of the important parameters for the wave functions used. The last column gives the variationally determined energy at $R_e = 1.40\ a_o$. Included in this table is a listing of the R variation of the screening parameters and normalization constants for the wave functions used.

TABLE I. Parameters of molecular wave functions.

Wave Function	Parameters				Energy (Rydbergs)
Ground State[50a] ($X\,^1\Sigma_g^+$)	$R(a_o)$	$N_o^2(a_o^{-6})$	z	C	
Weinbaum[50b]	1.20	.0802	1.2493	0.2606	
	1.40	.0668	1.2005	0.2647	-2.2956
	1.60	.0571	1.1592	0.2589	
Wang[50c]	1.20	.1099	1.2226	0.	
	1.40	.0881	1.1695	0.	-2.2780
	1.60	.0731	1.1257	0.	
Coulson[50d]	1.20	.0310	1.2412	1.0	
	1.40	.0255	1.1895	1.0	-2.2564
	1.60	.0214	1.1449	1.0	
Accurate[50e]	R_e = 1.40				-2.3490
First Triplet ($b\,^3\Sigma_u^+$)	$R(a_o)$	$N_g^2N_u^2(a_o^{-6})$	z_1	z_2	
Phillipson-Mulliken[51a]	1.20	.0908	1.3868	0.5055	
	1.40	.0720	1.3250	0.5754	-1.5638
	1.60	.0588	1.2715	0.6412	
Hurley[51b]	1.20	.1466	1.0		
	1.40	.1170	1.0		-1.0574
	1.60	.0977	1.0		
Accurate[51c]					-1.5910
Second Triplet ($a\,^3\Sigma_g^+$)	$R(a_o)$	$N_{1g}{}^2N_{2g}{}^2(a_o^{-6})$	z_1	z_2	
Hartree-Fock	1.20	.00020	1.4463	0.4733	
	1.40	.00027	1.3497	0.5120	-1.3830
	1.60	.00033	1.2399	0.5477	
Accurate[52d]	R_e = 1.864				-1.4258

4. Evaluation of Multicenter Integrals

The scattering amplitude T_{fi} ((O) or (OR)) was calculated for fixed q, R, and orientation (χ, ϕ) in the following manner. When the two-center molecular wave functions are inserted into Eqs. (2-6) or (2-7), two- and three-center one-electron integrals appear. The two-center integrals can be performed analytically while the three-center ones require numerical evaluation. The general form of these three-center one-electron integrals is

$$I = N_p N_t \int e^{i\vec{q}\cdot\vec{r}_1} r_{1A}^{p-1} e^{-zr_{1A}} r_{1B}^{t-1} e^{-z'r_{1B}} d\vec{r}_1 \qquad (4\text{-}1)$$

where $p, t = 1, 2$, N_p and N_t are the normalization constants for the corresponding atomic orbitals, $\vec{r}_1$ is the position vector of electron 1 with respect to the center (0) of the molecule, r_{1A} and r_{1B} are the distances of this electron from the nuclei (see Fig. 2), and z, z' are the screening parameters of the atomic wave functions considered. These integrals are evaluated by expanding the plane wave as

$$e^{i\vec{q}\cdot\vec{r}_1} = 4\pi \sum_{\ell=0}^{\infty} \sum_{m=-\ell}^{\ell} i^{\ell} j_{\ell}(qr_1)\, Y_{\ell}^{m*}(\hat{q})\, Y_{\ell}^{m}(\hat{r}_1) \qquad (4\text{-}2)$$

where j_ℓ is the spherical Bessel function of order ℓ, Y_ℓ^m is the spherical harmonic and $\hat{q}$ and $\hat{r}_1$ are the unit vectors in the $\vec{q}$ and $\vec{r}_1$ directions. The atomic orbitals are expanded in Legendre polynomials about the center of the molecule according to the zeta function expansion[53] which for the wave functions used in these calculations takes the form:

$$r_{1X}^{p-1} e^{-zr_{1X}} = \sum_{u=0}^{\infty} \frac{(2u+1)}{\frac{(r_1 R)^{1/2}}{\sqrt{2}}} P_u(\cos\theta_1)\, \zeta_{p,u}(z, r_1; R/2) \qquad (4\text{-}3)$$

where (r_1, θ_1) are the coordinates of the electron measured from the diatomic center as indicated in Fig. 2; r_{1j} is the distance of the electron from nucleus j = A, B; P_u is the Legendre polynomial of order u and $\zeta_{p,u}$ is the zeta function.[53] Although the integrals I of Eq. (4-3) can be reduced to two-center integrals about the nuclei, an expansion about their midpoint has the advantage that it enables the averaging over all orientations of the molecular axis to be performed easily and without any great increase in the complexity of the numerical work. When the expansions are inserted into this equation, one obtains, after choosing the laboratory-fixed z axis along $\vec{q}$ and performing the integration over φ_1, the following:

$$I = \sum_{\ell=0}^{\infty} (2\ell+1)(i)^{\ell} P_{\ell}(\cos\chi) \sum_{u=0}^{\infty} \sum_{u'=0}^{\infty} N_p N_t (-1)^{u'} (2u+1)(2u'+1) \int j_{\ell}(qr_1)$$

$$\zeta_{p,u}(z, r_1; R/2)\, \zeta_{t,u'}(z', r_1; R/2) \left(\frac{2}{r_1 R}\right) P_{\ell}(\cos\theta_1)\, P_u(\cos\theta_1)\, P_{u'}(\cos\theta_1)$$

$$2\pi r_1^2 dr_1 \sin\theta_1 d\theta_1 \equiv \sum_{\ell=0}^{\infty} (2\ell+1)(i)^{\ell} P_{\ell}(\cos\chi)\, Z_{t,z'}^{p,z}(\ell; q, R)\,. \qquad (4\text{-}4)$$

Equation (4-4) serves to define the quantity $Z_{t,z'}^{p,z}$ as used in these calculations.

The three-center scattering integral program for Eq. (4-1) was developed using the methods just described. It was generated by modification of a three-center energy integral program kindly supplied by Prof. R. M. Pitzer of the California Institute of Technology. In the actual computation the terms for each ℓ in Eq. (4-4) decreased rapidly in magnitude with increasing ℓ so the series was truncated after $\ell = 2$. The error due to this truncation is less than 5%. For fixed q, R, and χ, each $Z_{t,z'}^{p,z}$ function can be evaluated with 5 or 6 decimal place accuracy in about 7 seconds on an IBM 7094. This includes an integration over θ_1 using the recursion relations of the P_u functions and a numerical integration over r_1 by a Gauss-Legendre integration.[53] Some of the details of these numerical methods, including a listing of this modified three-center program, is given in Appendix F.

5. Method of Calculating Cross Sections

Total cross sections for the exchange excitation of the hydrogen molecule from the ground state ($X^1\Sigma_g^+$) to the first ($b^3\Sigma_u^+$) and second ($a^3\Sigma_g^+$) triplet states have been calculated. The (OR) and (O) approximations to the scattering amplitude T_{fi} [Eqs. (2-7) and (2-6), respectively] have been used, the necessary integrals, including the three-center ones, having been evaluated as indicated in the previous section. Even though the (OR) approximation is superior to the (O) one (see Section I-5 and Appendix E), calculations with the latter were also performed for comparison with the (OR) results since this (O) approximation appears frequently in the literature. The difference in computational efforts between the (OR) and (O) approximations is very small, since they differ only in the energy dependent factors which appear outside of the integral in the expressions for the corresponding scattering amplitudes.

In addition, the calculations were repeated using the (OR) and (O) approximations with the separated atom (SA) approximation to the scattering amplitude. This latter approximation, introduced by Khare and Moiseiwitsch,[54] consists in neglecting the two- and three-center integrals in the expression for $T_{n\nu}^{n'\nu'}$ as if the two atoms were infinitely separated. Except for this, the molecule is treated as if the nuclei were at a finite distance, R. Although this (SA) approximation greatly simplifies the calculations by eliminating the need to evaluate the difficult three-center integrals, there seems to be little physical justification for it, as shown in Section 6.2. However, since such an approximation has appeared in the literature, the cross sections were calculated using it for comparison with the complete calculations.

5.1 Electronic scattering amplitude

Using the wave functions described in Section 3, the (OR) and (O) scattering amplitudes for the transition from the ground vibrational-electronic state ($X^1\Sigma_g^+$) to the first ($b^3\Sigma_u^+$) and second ($a^3\Sigma_g^+$) states are given respectively by

$$T_{\nu'}^{(1)} \equiv 2^{1/2}\pi a_o N_o N_g N_u (1+C)\beta F(k_o, k')i[H_1 \sin(q\frac{R}{2}\cos\chi) - 6M_1\cos\chi] \tag{5-1}$$

$$T_{\nu'}^{(2)} \equiv 2^{1/2}\pi a_o N_o N_{1g} N_{2g} (1+C)\epsilon F(k_o,k')[H_2\cos(q\frac{R}{2}\cos\chi)+2K_2-10L_2P_2(\cos\chi)]. \tag{5-2}$$

In the expressions above the laboratory-fixed system of coordinates was chosen so that its z-axis is parallel to $\vec{q}$. With this choice the values of $\mathcal{T}_{\nu'}^{(1)}$ and $\mathcal{T}_{\nu'}^{(2)}$ are independent of ϕ, which is now the angle of rotation of $\vec{R}$ around $\vec{q}$. The new quantities in (5-1) are defined by (5-3) through (5-7) and those in (5-2) by (5-8) through (5-13):

$$H_1(q,R) \equiv \frac{16(z+z_2)}{[(z+z_2)^2 + (a_o q)^2]^2} + W_1 \frac{16(z+z_1)}{[(z+z_1)^2 + (a_o q)^2]^2} \tag{5-3}$$

$$W_1(R) \equiv \frac{\gamma(1-C)}{\beta(1+C)} \tag{5-4}$$

$$\gamma(R) \equiv a_o^3 \int 1s_A^z(r_{2A})\, 1s_A^{z_2}(r_{2A})\, d\vec{r}_2 - a_o^3 \int 1s_A^z(r_{2A})\, 1s_B^{z_2}(r_{2B})\, d\vec{r}_2 \tag{5-5}$$

$$\beta(R) \equiv a_o^3 \int 1s_A^z(r_{2A})\, 1s_A^{z_1}(r_{2A})\, d\vec{r}_2 + a_o^3 \int 1s_A^z(r_{2A})\, 1s_B^{z_1}(r_{2B})\, d\vec{r}_2 \tag{5-6}$$

$$M_1(q,R) \equiv \frac{\pi}{(zz_2)^{3/2}} Z_{1,z_2}^{1,z}(1;q,R) + W_1 \frac{\pi}{(zz_1)^{3/2}} Z_{1,z}^{1,z_1}(1;q,R) \tag{5-7}$$

$$H_2(q,R) \equiv \frac{16(z+z_1)}{[(z+z_1)^2 + (a_o q)^2]^2} - W_2 \frac{16[3(z+z_2)^2 - (a_o q)^2]}{[(z+z_2)^2 + (a_o q)^2]^3} \tag{5-8}$$

$$W_2(R) \equiv \frac{\alpha}{\epsilon} \tag{5-9}$$

$$\alpha(R) \equiv a_o^3 \int 1s_A^{z}(r_{2A})\, 1s_A^{z_1}(r_{2A})\, d\vec{r}_2 + a_o^3 \int 1s_A^{z}(r_{2A})\, 1s_B^{z_1}(r_{2B})\, d\vec{r}_2 \quad (5\text{-}10)$$

$$\epsilon(R) \equiv a_o^3 \int 1s_A^{z}(r_{2A})\, 2s_A^{z_2}(r_{2A})\, d\vec{r}_2 + a_o^3 \int 1s_A^{z}(r_{2A})\, 2s_B^{z_2}(r_{2B})\, d\vec{r}_2 \quad (5\text{-}11)$$

$$K_2(q,R) \equiv \frac{\pi}{(zz_1)^{3/2}} Z_{1,z}^{1,z_1}(0;q,R) - W_2\left(\frac{3\pi^2}{z^3 z_2^5}\right)^{1/2} Z_{2,z_2}^{1,z}(0;q,R) \quad (5\text{-}12)$$

$$L_2(q,R) \equiv \frac{\pi}{(zz_1)^{3/2}} Z_{1,z}^{1,z_1}(2;q,R) - W_2\left(\frac{3\pi^2}{z^3 z_2^5}\right)^{1/2} Z_{2,z_2}^{1,z}(2;q,R) \quad (5\text{-}13)$$

The quantity $F(k_o, k')$ is defined by:

$$(OR):\ F = \frac{1}{[a_o k' - (I_o/R)^{1/2} i]^2} \qquad (O):\ F = \frac{1}{a_o^2 k_o^2} \quad (5\text{-}14)$$

where $I_o = 15.279$ (eV)[52a] and the value of C depends on which ground state function is used. It is 0 for the Wang function, 1 for the Coulson function, and given in Table I as a function of R for the Weinbaum function. The quantities H_1, H_2, α, β, γ, ϵ, W_1, and W_2 depend on R due to the dependence of the molecular wave function parameters on this quantity, as indicated in Table I.

As seen in Section 2.3 [(2-19)], it is also useful to calculate the quantity $\langle |\mathcal{I}_{\nu'}^{(j)}(R)|^2 \rangle$. This can be done using the above equations and gives:

$$\langle |T_{\nu'}^{(1)}|^2 \rangle = 2\pi^2 a_o^2 N_o^2 N_g^2 N_u^2 (1+C)^2 \beta^2 |F(k_o, k')|^2 [H_1^2 \Theta_{11} - \frac{12}{\pi} H_1 M_1 \Theta_{12} + \frac{36}{\pi^2} M_1^2 \Theta_{13}] \tag{5-15}$$

$$\langle |T_{\nu'}^{(2)}|^2 \rangle = 2\pi^2 a_o^2 N_o^2 N_{1g}^2 (1+C)^2 \epsilon^2 |F(k_o, k')|^2 [H_2^2 \Theta_{21} + \frac{4}{\pi} H_2 K_2 \Theta_{22} -$$

$$\frac{20}{\pi} H_2 L_2 \Theta_{23} + \frac{4}{\pi^2} K_2^2 \Theta_{24} + \frac{100}{\pi^2} L_2^2 \Theta_{25}] \ . \tag{5-16}$$

The quantities Θ_{ij} result from the orientation averaging process and are defined by:

$$\Theta_{11} \equiv \langle \sin^2 (\frac{qR}{2} \cos \chi) \rangle = (1/2)(1 - \sin \frac{qR}{2}) \tag{5-17}$$

$$\Theta_{12} \equiv \langle \sin (\frac{qR}{2} \cos \chi) \cos \chi \rangle = (\frac{2}{qR})^2 (\sin \frac{qR}{2} - \frac{qR}{2} \cos \frac{qR}{2}) \tag{5-18}$$

$$\Theta_{13} \equiv \langle \cos^2 \chi \rangle = 1/3 \tag{5-19}$$

$$\Theta_{21} \equiv \langle \cos^2 (\frac{qR}{2} \cos \chi) \rangle = (1/2)(1 + \sin \frac{qR}{2}) \tag{5-20}$$

$$\Theta_{22} \equiv \langle \cos (\frac{qR}{2} \cos \chi) \rangle = \frac{2}{qR} \sin \frac{qR}{2} \tag{5-21}$$

$$\Theta_{23} \equiv \langle \cos\left(\frac{qR}{2}\cos\chi\right) P_2(\cos\chi)\rangle = 3\left(\frac{2}{qR}\right)^2 \cos\frac{qR}{2} + \frac{2}{qR}\left[1 - 3\left(\frac{2}{qR}\right)^2\right] \sin\frac{qR}{2} \tag{5-22}$$

$$\Theta_{24} \equiv \langle P_0^2(\cos\chi)\rangle = 1 \tag{5-23}$$

$$\Theta_{25} \equiv \langle P_2^2(\cos\chi)\rangle = 1/5 \tag{5-24}$$

The actual calculations were done using atomic units throughout (see Appendix B).

5.2 Excitation cross sections

To calculate the total cross sections for the electronic excitation processes of interest we must evaluate the quantities defined by (2-17), (2-22), and (2-23). It is convenient to consider the two triplet state excitations separately. [The details of the numerical techniques, including listings and error checks for the important programs used in this section are given in Appendices F and G.]

5.2.1 $X^1\Sigma_g^+ \rightarrow b^3\Sigma_u^+$ excitation

The first triplet state ($b^3\Sigma_u^+$) is a non-bound one. Let its continuum vibrational wave function be $\xi_\nu^{(1)}(R)$ and let $\xi_0^{(0)}(R)$ be the $\nu = 0$ vibrational wave function of the ground electronic state. According to (2-17), the following quantity must be evaluated:

$$J^{(1)}_{\nu'}(k_o, \theta, \varphi; \chi, \phi) \equiv \left| \int_0^\infty [R\xi^{(1)}_{\nu'}(R)]^* \mathcal{T}^{(1)}_{\nu'}(k_o, \theta, \varphi; R, \chi, \phi)[R\xi^{(0)}_o(R)]\, dR \right|^2. \tag{5-25}$$

Similar type quantities for H_2 have been considered in the past[55] in connection with spectral intensities in optical emissions from the $a^3\Sigma^+_g$ to the $b^3\Sigma^+_u$ state. As above, this was a discrete to continuum state transition. The integrals in question involved either the product of the radial wave functions alone[55a] or this product times the electric dipole transition momentum.[55b] In either case it was shown that these integrals could be evaluated with good accuracy by substituting the radial function of the continuum state by a delta function at the classical turning point for the transition energy being considered. We will use here the same approximation and replace $R\xi^{(1)}_{\nu'}(R)$ in (5-25) by $A\delta(R - R^{(1)})$:

$$J^{(1)}_{\nu'} = |A|^2 \left| \mathcal{T}^{(1)}_{\nu'}(k_o, \theta, \varphi; R^{(1)}, \chi, \phi)\, R^{(1)} \xi^0_o(R^{(1)}) \right|^2. \tag{5-26}$$

In this expression, A is a proportionality constant to be determined as indicated below. $R^{(1)}$ is the classical turning point, and is depicted in Fig. 1. It is a function of the excitation energy E_1, determined by the relation

$$V^{(1)}(R^{(1)}) = E_1 = E^{(1)}_{\nu'} - E^{(0)}_o \tag{5-27}$$

where $E^{(0)}_o$ is the energy of the ground vibrational-electronic state and $E^{(1)}_{\nu'}$ that of the ν' level of the first triplet state. $V^{(1)} = V^{(1)}(R)$ is the equation for the potential energy curve for the first triplet state,

measured with respect to the ground vibrational-electronic state. Therefore, the function $R^{(1)} - R^{(1)}(E_1)$ is simply the inverse of the function $V^{(1)} = V^{(1)}(R)$. Since (5-27) relates ν' and E_1, either of them can be considered as the variable which defines the continuum vibrational level under consideration. We shall use them interchangeably.

The proportionality constant A can be evaluated from the condition that replacement of $R\xi^{(1)}_{\nu'}(R)$ by $A\delta(R - R^{(1)})$ should also furnish a very good approximation[55a] to the Franck-Condon factor

$$g^{(1)}_{\nu'} \equiv \left| \int_0^\infty [R\xi^{(1)}_{\nu'}(R)]^* \, [R\xi^{(0)}_{o}(R)] \, dR \right|^2 . \qquad (5\text{-}28)$$

Expanding the normalized square integrable function $R\xi^{(0)}_{o}(R)$ in terms of the complete orthonormal set of wave functions $R\xi^{(1)}_{\nu'}(R)$ and using the orthonormality properties of such continuum functions,[48] it is easy to prove that

$$\int g^{(1)}_{\nu'} d\nu' = 1 . \qquad (5\text{-}29)$$

Introducing into (5-28) the δ-function substitution just mentioned, and requiring that the approximate $g^{(1)}_{\nu'}$ which results still be normalized according to (5-29) furnishes

$$|A|^2 = \left[\int_{D_o}^\infty |R^{(1)}(E_1) \, \xi^0_o(R^{(1)}(E_1))|^2 dE_1 \right]^{-1} \qquad (5\text{-}30)$$

where D_o is the dissociation energy of the $X^1\Sigma_g^+$ state measured from its lowest vibrational level.

Substitution of (5-26), (5-27), and into (2-17) furnishes for the rotationally averaged differential cross section per unit energy range:

$$I^{(1)}_{\nu'}(k_o, \theta, \varphi) = \frac{3k''}{k_o} P^{(1)}(E_1) \langle | \mathcal{T}^{(1)}_{\nu'}[R^{(1)}(E_1)] |^2 \rangle \qquad (5\text{-}31)$$

where

$$P^{(1)}(E_1) \equiv |A|^2 \, |R^{(1)}(E_1) \, \xi^{(0)}_o[R^{(1)}(E_1)]|^2 \qquad (5\text{-}32)$$

satisfies the normalization relation

$$\int_{D_o}^{\infty} P^{(1)}(E_1) \, dE_1 = 1 \qquad (5\text{-}33)$$

as can easily be seen from (5-30). In addition to depending on the excitation energy E_1 (and hence ν') through $R^{(1)}$, the quantity $\langle | \mathcal{T}^{(1)}_{\nu'}[R^{(1)}(E')] |^2 \rangle$ [defined for arbitrary R by Eq. (2-20)] is also a function of k_o, θ, and φ.

The product $R\xi^{(0)}_o(R)$ is well represented by a ground linear harmonic oscillator wave function,[57] which was used in these calculations:

$$R\xi^{(0)}_o(R) = \left(\frac{\mu}{\pi}\right)^{1/4} \exp\left[-\frac{\mu}{2}(R - R_e)^2\right] . \qquad (5\text{-}34)$$

Here, $\mu = 18.4\ a_o^{-2}$, and R_e, the ground state equilibrium internuclear distance is $1.40\ a_o$.[57] The range of R for which this wave function contributes non-negligibly to the total cross section $\sigma^{(1)}(k_o)$ is relatively small. Over this range, (5-27) can be represented to within 3% accuracy by

$$E_1 = a^{(1)} - b^{(1)} R^{(1)} \tag{5-35}$$

where $a^{(1)} = 21.01$ eV and $b^{(1)} = 7.40$ eV/a_o.

Substitution of (5-31) into (2-22) furnishes

$$\sigma^{(1)}_{\nu'}(k_o) = \frac{3k''}{k_o} P^{(1)}(E_1) \int \langle | T^{(1)}_{\nu'}[R^{(1)}(E_1)] |^2 \rangle \sin\theta d\theta d\varphi. \tag{5-36}$$

Although $\langle | T^{(1)}_{\nu'}[R^{(1)}(E_1)] |^2 \rangle$ depends in principle on both θ and φ it can be seen from (5-15) and (5-17) through (5-24) that this dependence occurs through the quantity q, which according to (2-8) and (2-14) depends only on θ:

$$q = [k_o^2 + k''^2 - 2k_o k'' \cos\theta]^{1/2}. \tag{5-37}$$

Therefore, the integration over φ results in a multiplicative factor 2π whereas the integration θ can be easily calculated by changing to variable q. Since, from (5-37)

$$\sin\theta d\theta = \frac{q dq}{k_o k''} \tag{5-38}$$

(5-36) becomes

$$\sigma^{(1)}_{\nu'}(k_o) = \frac{6\pi^2}{k_o^2} P^{(1)}(E_1) \int_{q_{min}(E_1)}^{q_{max}(E_1)} \langle | \mathcal{T}^{(1)}_{\nu'}[R^{(1)}(E_1)] |^2 \rangle \, q dq \qquad (5\text{-}39)$$

where

$$q_{min}(E_1) \equiv k_o - k''(E_1)$$
$$q_{max}(E_1) \equiv k_o + k''(E_1) \quad . \qquad (5\text{-}40)$$

The quantity $P^{(1)}(E)$ was calculated from (5-30), (5-32), (5-34), and (5-35) whereas $\langle | \mathcal{T}^{(1)}_{\nu'} |^2 \rangle$ was obtained from (5-15). The most convenient method of evaluating numerically the integral over q in (5-39) is to perform a Simpson integration taking advantage of the fact that as the incident energy increases, q_{min} and q_{max} monotonically decrease and increase, respectively. Therefore, it is convenient to start at the lowest desired incident energy and for each new energy value just add the contributions of the two new integration regions to the integral which has already been calculated. This is the method adopted here.

Finally, the total cross section $\sigma^{(1)}(k_o)$ for excitation from the ground vibrational-rotational state of H_2 to all vibrationally accessible levels of the first triplet state by electrons of initial energy $E_o = \hbar^2 k_o^2/2m$ can be obtained by substitution of (5-39) into (2-23), and use of E_1 rather than ν' as the vibrational state label. The resulting expression is:

$$\sigma^{(1)}(k_o) = \frac{6\pi}{k_o^2} \int_{D_o}^{E_o} P^{(1)}(E_1) \left[\int_{q_{min}(E_1)}^{q_{max}(E_1)} \langle | T_{\nu'}^{(1)}(R^{(1)}(E_1)) |^2 \rangle \, qdq \right] dE_1 . \tag{5-41}$$

It is convenient to change integration variables from E_1 to $R^{(1)}$ through (5-27) [and specifically (5-35)]. The resulting expression is:

$$\sigma^{(1)}(k_o) = \frac{6\pi}{k_o^2} \int_{R(E_o)}^{\infty} P^{(1)}[E_1(R)] \left[\int_{q_{min}(R)}^{q_{max}(R)} \langle | T_{\nu'}^{(1)}(R) |^2 \rangle \, qdq \right] \left(- \frac{dE_1}{dR}\right) dR \tag{5-42}$$

where the superscript on the new integration variable has been dropped. The integral over R in this equation was performed by a three-point Gauss-Hermite quadrature[58] to 4 significant digit accuracy.

5.2.2 $X^1\Sigma_g^+ \rightarrow a^3\Sigma_g^+$ excitation

The second triplet state is a shallow (dissociation energy of 2.91 eV) bound state which has a minimum at $R_e^{(2)} = 1.864\ a_o$. It has 16 bound vibrational states and no continuum states whose left classical turning points fall within the Franck-Condon vertical band depicted in Fig. 1. In principle, the calculation of the total cross section for the excitation of this state [according to (2-17), (2-22), and (2-23) requires inserting expressions for the $\xi^{(0)}$ and $\xi_{\nu'}^{(2)}$ vibrational wave functions, and performing the integration over R. Then the absolute value of the result obtained

must be squared and averaged over all possible orientation angles of the molecular axis. This process requires very extensive numerical work in view of the large number of vibrational states involved, but is unnecessary within the scope of this paper, since only the total electronic excitation cross section as defined by (2-23) is desired here. Instead of using (2-17), two approximate methods were used. In one of them, (2-17) was replaced by (2-19). The validity of this approximation is discussed later in this section. The total excitation cross section which results from (2-19), (2-22), and (2-23), after making the change of variables defined by (5-37), is

$$\sigma^{(2)}(k_o) = \frac{6\pi}{k_o^2} \int g_{\nu'}^{(2)} \left[\int_{q_{min}(\nu')}^{q_{max}(\nu')} \langle | T_{\nu'}^{(2)}(R_e) |^2 \rangle \, q dq \right] d\nu' \qquad (5\text{-}43)$$

where R_e is the equilibrium internuclear distance of the ground electronic-vibrational state, and q_{min} and q_{max} are defined by (5-40) with ν' replacing E_1. $\langle | T_{\nu'}^{(2)} |^2 \rangle$ was calculated using (5-16). For each incident energy $E_o = \hbar^2 k_o^2 / 2m$ the integral over q in (5-43) was calculated for all of the allowed ν' [for which k'', defined by (2-14), is real]. The corresponding Franck-Condon factors $g_{\nu'}^{(2)}$ were calculated by numerical integration[59] and the total cross section obtained by performing the sum over ν' indicated in (5-43). Because these Franck-Condon factors decrease rapidly with increasing ν', essentially all the contribution to $\sigma^{(2)}(k_o)$ comes from the first 8 vibrational levels ($\nu' = 0, \cdots, 7$). In addition, contributions to $\sigma^{(2)}(k_o)$ from continuum values of ν' were neglected since the corresponding values of $g_{\nu'}^{(2)}$ are very small.

The assumption used to derive (2-19), and hence (5-43), was that $T_{n\nu}^{n'\nu'}$ was approximately independent of R over the important range of R as determined by the ground vibrational state. To test this assumption the quantity $\langle | T_{\nu'}^{(2)}(R) | \rangle$ was calculated for different values of the momentum transfer q, by using (5-2) and (5-8) through (5-13). It was found to vary linearly over this range of R with a slope that decreased rapidly with increasing q. From these considerations, the error introduced in this approximation is expected to be largest in the threshold region where it might be as high as 15%. Above 20 eV incident energy, the error associated with this approximation is estimated to be less than 8%.

An alternate approximation to (2-17) was used which is much faster computationally while still giving essentially the same total cross section as (5-43). This approximation consists of replacing the function $R\xi_{\nu'}^{(2)}(R)$ by a δ-function at the classical turning point of the ν'-state in a manner analogous to that done for the first triplet excitation. The total cross section for excitation of the second triplet is then given by expressions analogous to (5-42), (5-32), and (5-30), with the superscript and subscript (1) replaced everywhere by (2). In particular, the exprcssion corresponding to (5-42) is:

$$\sigma^{(2)}(k_o) = \frac{6\pi}{k_o^2} \int_{R^{(2)}(E_o)}^{\infty} P^{(2)}[E_2(R^{(2)})] \left[\int_{q_{min}(R^{(2)})}^{q_{max}(R^{(2)})} \langle | T_{\nu'}^{(2)}(R^{(2)}) |^2 \rangle \, q dq \right] \left(- \frac{dE_2}{dR^{(2)}} \right) dR^{(2)} \quad . \tag{5-44}$$

Although this is a rather drastic approximation, especially for small ν', it does not assume that $T^{(2)}_{\nu'}$ is independent of R, as the previous method did.

Over the region of R of importance, the counterpart of (5-35) was obtained by a least squares fit to the potential energy curve for the second triplet state as calculated by Wakefield and Davidson,[52d] yielding (to within 1%)

$$E_2 = a^{(2)} - b^{(2)}R^{(2)} + c^{(2)}[R^{(2)}]^2 \qquad (5\text{-}45)$$

where $a^{(2)} = 20.22$ eV, $b^{(2)} = 7.48$ eV/a_o, and $c^{(2)} = 1.44$ eV/a_o^2.

A comparison of the total electronic excitation cross section obtained from (5-43) and (5-44) is given in Table II for a few energies in the threshold region. The total computing time necessary to obtain the cross section by (5-44) was 125 minutes while that using (5-43) was 350 minutes. Therefore, the δ-function method is faster than the Franck-Condon one but the results are equivalent. For this reason, all other calculations done for the second triplet state used the faster method. The good agreement of the two methods could be due in part to errors of the same size and in the same direction in the two different approximations. More likely, it is a consequence of the fact that the general behavior of the total electronic cross section is determined primarily by the parameters of the electronic states involved. In other words, the range of excitation energies due to excitation of different vibrational states is relatively small and hence the integral over q varies slowly over the range of ν'. The distributions $g^{(2)}_{\nu'}$ and $P^{(2)}(E_2)$ are both normalized:

TABLE II. Comparison of δ-function and Franck-Condon methods

	Total Cross Section $\sigma^{(2)}(\pi a_o^2)$	
Incident Energy E_o(eV)	δ-function (5-44)	Franck-Condon (5-43)
11.90	.0072	.0117
12.30	.0376	.0418
12.70	.0710	.0841
13.43	.1312	.1321
15.00	.1783	.1787
18.00	.1602	.1634
Computer Time (min)	125	350

$$\sum_{\nu'} g^{(2)}_{\nu'} \, d\nu' = 1 \tag{5-46}$$

and

$$\int P^{(2)}(E_2)dE_2 = \sum_{\nu'} P^{(2)}_{\nu'} = 1 \tag{5-47}$$

where

$$P^{(2)}_{\nu'} \equiv \int_{E_2(\nu')}^{E_2(\nu'+1)} P^{(2)}(E_2)dE_2 \ . \tag{5-48}$$

These relationships can be proved in a manner analogous to that used to verify (5-29) and (5-33). In addition to being normalized, $g^{(2)}_{\nu'}$ and $P^{(2)}_{\nu'}$ have approximately the same shape, as can be seen from Fig. 3. Therefore, the result of Stieltjes integrating over ν' (or E_2) is relatively insensitive to the details of the ν' dependence of $\sigma^{(2)}_{\nu'}(k_o)$.

As for the first triplet, the integration over R in (5-44) was performed by a Gauss-Hermite quadrature.[58]

6. Results and Discussions

6.1 The effect of different approximate wave functions

Fig. 4 shows the effect on the calculated total excitation cross sections of using different approximate wave functions for the ground state of the molecule. Only the results using the

complete (OR) approximation are illustrated since the (O) curves show the same relative differences. It can be seen from this figure that the first triplet cross section is quite sensitive to the choice of the ground state wave function while the second triplet one is not, which is at first surprising. In addition, the relative magnitude of the first triplet cross section does not change monotonically as the quality of the ground state wave function is improved. Indeed, in order of increasing quality (from an energy criterion viewpoint), the ground state wave functions are Coulson, Wang, and Weinbaum, but in order of increasing relative cross section they are Coulson, Weinbaum, and Wang. This suggests that the relative sizes of two cross sections calculated from two different ground-state wave functions depends on properties of the wave functions other than those optimized by the energy minimization. This is indeed the case and both the relative magnitudes and ordering of the calculated cross sections can be qualitatively understood as follows. From the expression for the scattering amplitude T_{fi} [(2-6) or (2-7)], it is seen that the effect of the electronic wave functions on the excitation cross section is entirely contained in the one-electron overlap charge density defined as:

$$\rho_{n'n}(\vec{r}_1; R) \equiv \int \psi^*_{n'}(\vec{r}_1, \vec{r}_2; R)\, \psi_n(\vec{r}_1, \vec{r}_2; R)\, d\vec{r}_2 . \qquad (6\text{-}1)$$

Therefore, any change in the ground state wave function also produces a change in the overlap charge density. The nature and magnitude of this effect is expected to depend on the symmetries of the ground and excited state wave functions.

Consider the excitation to the first triplet state. The ground and first triplet state wave functions are both symmetric with respect to reflection of one of the electrons (electron 2, for example) through a plane containing the internuclear axis. However, the former one is even with respect to inversion of one electron through the center of the molecule whereas the latter one is odd. Therefore, the plane passing through the origin and perpendicular to the internuclear axis is a one-electron plane of symmetry for the ground state function and a nodal plane for the first triplet state. The effect of this nodal plane is to reduce the contribution to ρ of spatial regions of the ground state wave function close to it, i.e., of regions for which $|z_2|$ is small (Oz being the direction of the internuclear axis). As a result, the relative importance of the spatial extent of the ground state wave function in the x and y directions is greatly reduced whereas the contribution to ρ from regions of large $|z_2|$ is relatively enhanced. Consequently, slight differences in the z-direction tails (outer regions) of different ground state wave functions will have their effect on ρ amplified by this nodal plane, and appreciable differences in the resulting cross sections might be expected, as is indeed found to be the case. From these arguments, the ground state wave function with largest extend in the z-direction might be expected to give the largest excitation cross section since the region in which ρ is appreciable has then the largest spatial extent. Table III contains the values of the second-order moments of the ground state charge density of the hydrogen molecule as calculated for the three ground state wave functions used and as determined experimentally. As suggested by these qualitative considerations, the relative ordering of the values of $\langle z^2 \rangle$ for the

TABLE III. Moments of the charge distribution of the ground electronic state[60a]

Ground State Wave Functions	Binding Energy (eV)	$\langle x^2 \rangle = \langle y^2 \rangle$ (a_o^2)	$\langle z^2 \rangle$ (a_o^2)	$\langle r^2 \rangle$ (a_o^2)
Weinbaum*	4.04	0.738	1.082	2.558
Wang*	3.76	0.767	1.131	2.665
Coulson*	3.47	0.742	1.073	2.557
Experiment[60b]	4.476[57]	0.7663	1.0604	2.593

*Calculated at $R_e = 1.40\ a_o$.

TABLE III. Moments of the charge distribution of the ground electronic state[60a]

Ground State Wave Functions	Binding Energy (eV)	$\langle x^2 \rangle = \langle y^2 \rangle$ (a_o^2)	$\langle z^2 \rangle$ (a_o^2)	$\langle r^2 \rangle$ (a_o^2)
Weinbaum*	4.04	0.738	1.082	2.558
Wang*	3.76	0.767	1.131	2.665
Coulson*	3.47	0.742	1.073	2.557
Experiment[60b]	4.476[57]	0.7663	1.0604	2.593

*Calculated at $R_e = 1.40\ a_o$.

three ground state wave functions used is indeed the same as the relative ordering of the magnitude of the corresponding cross sections for excitation to the first triplet state.

In the case of excitation to the second triplet, the excited state wave function has the same one-electron symmetry characteristics as the ground state wave function, that is, no one-electron nodal planes. As a result, the second triplet wave function does not strongly emphasize the importance of the ground state wave function along any one axial direction over the other two. Consequently, the relative differences in $\rho_{nn'}(\vec{r}_1)$ as calculated for different ground state wave functions is expected to be much smaller than in the first triplet case, and the resulting cross sections are expected to be much less sensitive to the choice of ground state wave function. Fig. 4 shows that this is indeed the case.

The cross section for excitation to the first triplet state was also calculated using the best (Weinbaum) ground state wave function and the Hurley[51b] wave function for the excited state. This excited state wave function is much less accurate than the Phillipson-Mulliken one (from an energy standpoint) and from the above arguments should predict a significantly different cross section. This is indeed the case as shown in Fig. 5 which illustrates the first triplet cross section as calculated using the Weinbaum ground state and the two different excited state wave function, in the complete (OR) approximation. The large discrepancy between the two curves further serves to indicate the magnitude of errors which can result from the use of excessively inaccurate wave functions.

6.2 Comparison of Ochkur, Ochkur-Rudge, and separated atom approximations

Fig. 6 shows the theoretical cross sections for excitation to the first triplet state from the ground state as calculated in the complete Ochkur-Rudge (ORC), complete Ochkur (OC), the separated atom Ochkur-Rudge (ORSA) and the separated atom-Ochkur (OSA) approximations. The wave functions used for the ground and excited states were the Weinbaum and Phillipson-Mulliken ones, respectively (see Section 3). From the curves in this figure it can be seen that the (OR) and (O) calculations give significantly different results. As will be indicated in Section 6.3, the (ORC) results agree better with experiment than the (OC) ones. Two differences between the (OR) and the (O) approximations can be noted. First, in either the complete or the (SA) approximations the cross section obtained using the (O) form for the transition amplitude [(2-6)] is about two times the corresponding (OR) cross section [(2-7)], a result that might be expected from a comparison of the energy dependent coefficients which precede the integral in (2-6) and (2-7). Second, the location of the maximum in the (O) cross sections occurs at a lower energy (by about .5 to .75 eV) than the corresponding (OR) cross sections. In addition, the (SA) approximation, applied to either the (O) or the (OR) transition amplitudes, produces cross sections that have the proper shape but whose magnitude will generally be significantly smaller (by about 30%) than those predicted by the corresponding complete calculations. This is due to the fact that in the (SA) approximation all multicenter terms that appear in the normalization constants and scattering amplitude are ignored. For purposes of illustration of the effect of multicenter terms the

following approximations were applied to (5-41). The quantity $\langle |\mathcal{T}^{(1)}_{\nu'}(R^{(1)}(E_1))|^2 \rangle$ was evaluated at $R_e = 1.40\ a_o$ only and the excitation was assumed to occur at only one energy (8.8 eV). From these approximations and the normalization property of $P(E_1)$ [see (5-33)]

$$\sigma^{(1)}(k_o) \cong \frac{6\pi}{k_o^2} \int_{q_{min}}^{q_{max}} \langle |\mathcal{T}^{(1)}(R_e)|^2 \rangle\, q dq \qquad (6\text{-}2)$$

where $\langle |\mathcal{T}^{(1)}(R_e)|^2 \rangle$ can be calculated from (5-15). Table IV gives the contribution to the total cross section of the various terms in this equation as obtained in the complete and (SA) calculations for an incident energy of 14.0 eV. The (OR) approximation was used along with the Weinbaum and Phillipson-Mulliken wave functions for the ground and excited states. Columns I, II, and III contain the energy-independent constants associated with the molecular (electronic) wave functions. Columns IV, V, and VI show respectively the values of each of the three terms in the bracket of (5-15) after they have been multiplied by q, integrated over q and finally multiplied by $|F|^2/k_o^2$. Column VII is the sum of the three preceding columns and Column VIII gives the total cross section (Column III times Column VII) in units of πa_o^2. Note that in the (SA) approximation, the second and third terms in this bracket are zero because they are three-center terms. It is evident from Table IV that application of the (SA) approximation leads to significant changes in all of the quantities involved in the scattering amplitude, some increasing and some decreasing. These changes are not justifiable on either physical or mathematical grounds, and as a

TABLE IV. Comparison between complete and separated-atom (OR) calculations of the total cross section for excitation to the first-triplet state ($R = 1.40\ a_o$, $E_o = 14.0$ eV, $E_f - E_i = 8.8$ eV)

Calculation	I N_o^2 (a_o^{-6})	II $N_g^2 N_u^2$ (a_o^{-6})	III $12\pi^2 N_o^2 N_g^2 N_u^2 (1+C)^2 \beta^2$	IV $(\lvert F\rvert^2/k_o^2)\cdot \int H_1^2 \Theta_{11} q dq$	V $(\lvert F\rvert^2/k_o^2)\cdot \int_{\pi/2}^{12} H_1 M_1 \Theta_{12} q dq$
Complete	0.0668	0.0720	0.9610	1.274	-0.734
Separated atom	0.1417	0.0056	0.1165	3.517	0.000

VI $(\lvert F\rvert^2/k_o^2)\cdot \int_{\pi/2}^{36} M_1^2 \Theta_{13} q dq$	VII Sum of columns IV, V, VI	VIII Cross Section (πa_o^2)
0.106	0.646	0.621
0.000	3.517	0.410

result, the (SA) approximation should not be relied on to give more than order of magnitude results.

Fig. 7 is a comparison of the (OC) and (ORC) calculations (using the Weinbaum and Phillipson-Mulliken wave functions) with two other recent calculations of the excitation cross section to the first triplet state. The curve labeled (E1) is the first-order exchange approximation of Khare and Moiseiwitsch[44] in which the excitation was assumed to occur for a fixed energy loss of 11.0 eV and at the fixed internuclear distance $R_e = 1.404\ a_o$. In addition, the authors found it necessary to apply the (SA) approximation in order to evaluate the cross section. The curve labeled (K) is a recent calculation by Khare[45] in which the (O) approximation was employed along with the assumption that the excitation occurred at a fixed energy loss of 10.62 eV and at a fixed internuclear distance $R_e = 1.40\ a_o$. To facilitate the evaluation of the integrals, only one-center molecular (electronic) wave functions were used in this last calculation. From Fig. 7, it is apparent that the assumption of fixed energy loss for the incident electrons and fixed internuclear distance predicts a steeper rise of the excitation cross section as a function of energy than either the (ORC) calculation, the (OC) calculation, or experiment (see Section 6.3).

Fig. 8 is a comparison of the total cross section for excitation of the second triplet as calculated in the (ORC) and (ORSA) approximations using the three different ground state wave functions. Included for comparison is the corresponding (K) cross section calculated by Khare[45] in the (O) approximation using one-center molecular (electronic) wave functions, a single energy loss (11.7 eV) and single internuclear distance $R_e = 1.40\ a_o$. As can be seen from the figure,

the cross sections calculated with the (ORSA) approximation are smaller and more sensitive to the choice of ground state wave function than those calculated in the (ORC) approximation. In this latter calculation, the cross sections obtained from the three ground state wave functions coincide within the plotting accuracy of Fig. 8. It is difficult to explain the large difference between the (K) and the (ORC) results but it is probably due to the use by Khare of the (O) approximation [which always leads to larger results than the (OR) one] and of one-center electronic wave functions which are less accurate than the two-center ones employed in the (ORC) calculations. It is interesting to note that the threshold energy in the (K) curve was normalized to the approximately correct value of 11.7 eV by using this as the single excitation energy, although the excitation energy consistent with the equilibrium internuclear distance used is 12.55 eV.[52d] This mode of normalization makes the maximum cross section occur at an energy about 1.2 eV lower than the (ORC) one.

6.3 Comparison with experiment

The only experimental results with which these calculations can be directly compared are the approximate measurements by Corrigan[42] of the total cross section for the electron impact dissociation of H_2 into two H atoms. This experiment essentially measured the sum of the total cross sections for the excitation to all the triplets in molecular hydrogen. These states then decay radiatively to the lowest repulsive triplet ($b^3\Sigma_u^+$), which dissociates into two ground state H atoms. Since experimental evidence indicates that the magnitude of the total cross sections for electronic excitation to level (n) from the ground state falls off very

rapidly with increasing n,[61] the sum of the total cross sections for excitation of the first two triplets should account for most of this experimentally measured dissociation cross section. There is also a $c^3\Pi_u$ state which lies close in energy to the $a^3\Sigma_g^+$ state. However, no minimum basis set wave function for this state could be found in the literature. Because of its Π symmetry, a calculation of this type of wave function and of the corresponding scattering amplitude would have involved an extensive amount of computer time. A decision was made not to undertake this expense because this state is not expected to contribute much to the dissociation cross section. Its total excitation cross section is expected to be smaller than that for the $a^3\Sigma_g^+$ state in view of its different symmetry.[33, 61] This behavior is indicated by the one-center calculations of Khare[45] which show the cross section for excitation to the $c^3\Pi_u$ state to be about 60% of that to the $a^3\Sigma_g^+$ state. Because of the relative smallness of the former cross section, the error in the total dissociation cross section due to the neglect of the contribution from the $c^3\Pi_u$ state should not exceed 5%.

Fig. 9 is a comparison of the experimental data (full curve) and the sum of the theoretical cross sections for the excitation to the first and second triplets (dash-dot curve) as calculated here in the complete (OR) approximation, with the methods described above, and using the best (Weinbaum) ground state wave function. The theory is seen to predict quite well the linear rise above threshold, the magnitude and the general shape of the measured dissociation cross section. Although there actually exists a sudden change in slope of the theoretical curve at the onset of the second triplet excitation ($\sim$ 11.9 eV), this change is negligible within plotting

accuracy of the figure and thus cannot be seen in the (ORC) curve. The discrepancy between the predicted and observed location (in energy) of the maximum of the cross section is perhaps due in part to the scatter in the experimental points (which are the dots shown in Fig. 9 before the effect of molecular ionization is subtracted) which is particularly bad for energies above 13 eV. In addition, neglect of the contribution of the $c^3\Pi_u$ to the cross section tends to make the theoretical maximum shift slightly towards lower energies. It is encouraging (but perhaps fortuitous) that the best agreement between the present (ORC) calculations and experiment occurs in the energy region between threshold and maximum cross section, where the experimental points have highest accuracy.

Included in Fig. 9 is the dissociation cross section curve reported by Khare,[45] in which his calculations for the cross sections for excitation of the $b^3\Sigma_u^+$, $a^3\Sigma_g^+$, and $c^3\Pi_u$ states are added together. The high threshold energy and excessively steep rise between the threshold and maximum of this curve is due to the assumption that the excitation of each state occurs only at the most probable value of the internuclear distance (the equilibrium internuclear distance of the ground electronic state).

The ionization cross-section curve used by Corrigan to subtract the effect of ionization on his experimental results was that obtained in 1932 by Tate and Smith.[62] More recent measurements[63-65] furnish somewhat larger values for that ionization cross section, which would reduce the dissociation cross section of Corrigan and decrease the discrepancy between it and the (ORC) calculations at energies above 16 eV. In Fig. 10 are illustrated two dissociation cross sections obtained by modifying the Corrigan curve using the more recent experimental ionization data of Golden and

Rapp,[64] and of Harrison.[65] The modification is a simple subtraction from the Corrigan curve of the difference between the more current data and that of Tate and Smith. The upper dash-dot curve represents the dissociation cross section obtained by modification with the Golden-Rapp[64] ionization cross section. The shaded area along this curve indicates the error in the experiment as determined by the spread in data points reported by Corrigan.[42] The lower dashed curve is the similar dissociation cross section obtained from the Corrigan and Harrison[65] data, with the experimental error in the former again denoted by the shading. It is apparent from this figure that more accurate measurements of the dissociation cross section are necessary before the quality of this exchange excitation model can be evaluated more precisely.

Finally, it should be stressed that all the calculations we made are completely ab initio and absolute, with no experimental parameters having been used and no normalization to experiment having been performed.

6.4 Conclusions - Excitation of H_2

The total cross section obtained in the (OR) model for exchange excitation appears to describe the dissociation excitation of the hydrogen molecule better than any other currently tractable model. When proper allowance for nuclear motion (vibration) is made, the results agree quite well with the experimental data in the threshold-to-maximum region. When the excitation is assumed to occur only at the equilibrium internuclear distance of the ground electronic state, an excessively high threshold energy results as well as too steep an increase in the cross section between this threshold and the energy of maximum cross section.

It is apparent from the results of these calculations that care should be exercised in the choice of the wave functions used to describe the bound system. In some cases the excitation cross sections for a molecular electronic excitation process may be quite sensitive to the "quality" of the wave functions used and in other cases not. It appears that the degree of this sensitivity on molecular (electronic) wave functions depends on the symmetries of the molecular states involved. The results of this investigation suggest that along with the energy, other properties such as moments of the one-electron charge density predicted by the approximate wave functions should be used to determine the "best" overall approximate wave function.

In addition, it is evident from the calculations here reported that the (SA) approximation to the transition amplitude should be used with caution since the cross sections predicted by it may differ by 30% from the more accurate results.

The results reported in this paper and elsewhere[33, 34] show that the (OR) approximation describes reasonably well the exchange excitation processes and indicates that more accurate experiments are now needed in order to make a complete evaluation of this model.

III. The Exchange Excitation of Helium

1. Review of Previous Calculations on He

There have been numerous calculations concerning the electronic exchange excitation of He. However, because they are superior, only the results of the more recent calculations will be discussed and compared with the present calculations.

The first detailed treatment of the exchange excitation of He was done for the 2^3S state by Massey and Moiseiwitsch.[66] They performed an elaborate exchange-distorted wave calculation which, although considered as quite complete, produced cross sections which are somewhat smaller than the experimental data. Ochkur has made[67] two calculations on the excitation of helium. The first[67a], which involved only the 2^3S and 2^3P states, demonstrated his modification of the (BO) approximation (Section I-5) and gave quite good agreement with extrapolated experimental data. In the second[67b], the excitation of the 2^3S and 2^3P states were part of a more complete calculation in which he computed all the excitation processes from the ground state for which he could obtain wave functions. He employed the Born (direct) and Ochkur (exchange) approximations. Although his theoretical cross sections show general agreement with experiment, for some processes (excitation of the 2^3P state for example) the calculated cross sections still differ, by a factor of 2 or more, from the experimental data. Bell, Eissa and Moiseiwitsch[68] have applied the first order exchange approximation to the excitation of the 2^3S and 2^3P states and obtained cross sections which are larger than the experimental data by a factor of 2 or so. Recently, Joachain and Mittleman[69] performed calculations using

8 different formulations for the transition amplitude in an effort to understand the relative importance of the different approximations used. However, they did not evaluate the possible errors in the approximate wave functions they used and were unable to arrive at a definite conclusion as to the best starting point (i. e., formulation of the T-matrix) to describe the rearrangement process. Massey and Moiseiwitsch[70] and then Lashmore-Davies[71] (who used a more accurate ground state wave function) have calculated the cross section for excitation of the 2^3P state in the distorted wave approximation. However, their results are about a factor of 5 larger than the best experimental results.

The (O) and (OR) approximations will be applied here to calculate the exchange excitation of the 2^3S and 2^3P states of helium. Some attention will be paid to possible errors introduced through the use of approximate wave functions. The total cross sections obtained using the "best" wave functions are then compared with a few of the previous calculations and the experimental data.

2. The Scattering Amplitude

The (O) and (OR) approximations to the exact scattering amplitude were discussed in Section (I-5) and are given respectively by

$$\mathcal{T}_{fi}^{O} = -\frac{2}{a_o k_o^2} \int \psi_f^*(\vec{r}_2, \vec{r}_1)\, \psi_i(\vec{r}_1, \vec{r}_2) e^{i\vec{q}\cdot\vec{r}_1}\, d\vec{r}_1 d\vec{r}_2 \; ; \qquad (2\text{-}1)$$

$$T_{fi}^{OR} = - \frac{2}{[a_o k' - (I_2/\mathcal{R})^{1/2}{}_i]^2} \int \psi_f^*(\vec{r}_2, \vec{r}_1)\psi_i(\vec{r}_1, \vec{r}_2) e^{i\vec{q}\cdot\vec{r}_1} d\vec{r}_1 d\vec{r}_2 , \tag{2-2}$$

where k' satisfies

$$k' = [k_o^2 - \frac{2m}{\hbar^2}(E_f - E_i)]^{1/2} , \tag{2-3}$$

ψ_f, ψ_i are the final, initial wave functions for the He atom, $I_i/\mathcal{R}$ is the ionization energy of the initial (ground) state of helium expressed in Rydbergs, and the rest of the notation is as introduced in Section II-2. It was pointed out in Section I-3, that the particles undergoing the exchange can be treated as distinguishable and any lack of distinguishability can be accounted for by taking certain linear combinations of the appropriate scattering amplitudes. Consequently, no specific reference to spin variables need be made and the appropriate multiplicative degeneracy factor ($\sqrt{3}$) will be introduced prior to forming the absolute square of the scattering amplitude.

3. Atomic Wave Functions

The (approximate) wave functions used to calculate the exchange excitation of He from the ground state (1^1S) to the first (2^3S) and second (2^3P) triplet states are described in this section. Rydberg-atomic units are used throughout (Appendix B).

Three different ground state wave functions were used. They all satisfy the functional form

$$\psi_o(\vec{r}_1, \vec{r}_2) = \varphi(\vec{r}_1)\,\varphi(\vec{r}_2)\,, \tag{3-1}$$

where $\varphi(\vec{r})$ is different in the three cases. The three functions are: the Clementi double minimum basis set function[72a]

$$\varphi(\vec{r}) = N_o(c_1 e^{-z_1 r} + c_2 e^{-z_2 r})\,, \tag{3-2}$$

the two-parameter function of Green, et. al.[72b]

$$\varphi(\vec{r}) = \frac{N_o}{\sqrt{\pi}}(e^{-z_1 r} + C\,e^{-z_2 r})\,,\ z_2 = 2z_1 \tag{3-3}$$

and the Hylleraas (minimum basis set Hartree-Fock) one-parameter function[72c]

$$\varphi(\vec{r}) = N_o e^{-z_1 r}\,. \tag{3-4}$$

Two different sets of wave functions were used for the two excited triplet states (2^3S and 2^3P). One set is composed of the two-parameter wave functions determined by Morse et. al.[73a]:

$$\psi_S(\vec{r}_1, \vec{r}_2) = \frac{1}{\sqrt{2}}\left\{v_1(\vec{r}_1)\,v_2(\vec{r}_2) - v_1(\vec{r}_2)\,v_2(\vec{r}_1)\right\}\,, \tag{3-5}$$

where

$$v_1(\vec{r}) = \left(\frac{\mu^3 a^3}{\pi}\right)^{1/2} e^{-\mu a r}\,, \tag{3-6}$$

$$v_2(\vec{r}) = \left(\frac{\mu^5}{3\pi M}\right)^{1/2} \left[r\, e^{-\mu r} - \frac{3A}{\mu}\, e^{-\mu b r} \right] , \tag{3-7}$$

$$A = \frac{(a+b)^3}{(1+a)^4} , \quad M = 1 - \frac{48A}{(1+b)^4} + \frac{3A^2}{b^3} ; \tag{3-8}$$

$$\psi_P(\vec{r}_1, \vec{r}_2) = \frac{1}{\sqrt{2}} \left\{ v_1(\vec{r}_1) v_m(\vec{r}_2) - v_1(\vec{r}_2) v_m(\vec{r}_1) \right\} , \tag{3-9}$$

where $v_1(\vec{r})$ is given by (3-6) and

$$v_m(\vec{r}) = \left(\frac{u^5 c^5}{\pi}\right)^{1/2} \left\{ \begin{array}{ll} \cos\theta & (m = 0) \\ \frac{1}{\sqrt{2}} \sin\theta\, e^{\pm i\varphi} & (m = \pm 1) \end{array} \right\} . \tag{3-10}$$

The other set is part of the two-parameter wave functions of Veselov et. al. [73b]:

$$\psi_S(\vec{r}_1, \vec{r}_2) = \frac{1}{\sqrt{2}} \left\{ v_1(\vec{r}_1)\, v_2(\vec{r}_2) - v_1(\vec{r}_2)\, v_2(\vec{r}_1) \right\} , \tag{3-11}$$

where

$$v_1(\vec{r}) = \frac{\alpha^3}{\pi}\, e^{-\alpha r} , \tag{3-12}$$

$$v_2(\vec{r}) = \left(\frac{3\beta^5}{\pi(\alpha^2 - \alpha\beta + \beta^2)} \right)^{1/2} \left[1 - \frac{\alpha + \beta}{3} r \right] e^{-\beta r} . \tag{3-13}$$

The ψ_P states of Veselov et. al. have exactly the same form as (3-9), (3-6), (3-10) except the variational parameters of those equations are replaced by the Veselov values

$$\mu a \rightarrow \alpha , \quad \mu c \rightarrow \gamma . \tag{3-14}$$

The values of the parameters associated with these wave functions are given in Table V.

At this point it is worthwhile making a few comments concerning the quality of the above wave functions. The ground state wave functions given in (3-2) and (3-3) are clearly better than (energy-wise) the Hylleraas ground state function (3-4) as seen from Table V. However, the latter was also used in these calculations because it has been at least tried by most of the previous investigators[74]. Using this state allows a better comparison to be made between the results reported here and previous calculations.

To see more clearly the relative superiority of the Clementi and Green et. al. ground states, the quantity

$$\langle \psi_o(\vec{r}_1, \vec{r}_2) | (r_1^2 + r_2^2) | \psi_o(\vec{r}_1, \vec{r}_2) \rangle \tag{3-15}$$

is tabulated in Table VI for the three ground state wave functions. As seen by comparison with the experimental determination, the Hylleraas wave function predicts too small a value. This means that the charge density is more concentrated near the nucleus in the "Hylleraas atom" than in the real atom. Thus, by the same reasoning used for the hydrogen molecule wave functions (see Section II-6-1), the cross sections obtained by using the Hylleraas wave function

TABLE V. Parameters of atomic wave functions (atomic units)

Wave function	Parameters					Energy (Rydbergs)
Ground State (1^1S)	N_o^2	z_1	z_2	c_1	c_2	
Clementi[72a]	1.000	1.44608	2.86222	0.83415	0.19060	-5.72334
Green et. al[72b]	1.484233	1.4558	2.9116	1.000	0.60	-5.723
Hylleraas[72c]	1.236775	1.6875	0.0	1.000	0.0	-5.695
Accurate[72d]						-5.807
First Triplet (2^3S)						
Morse et. al.[73a]	$\mu a = 2.00$	$\mu b = 1.57$	$\mu = 0.61$			-4.348
Veselov et. al.[73b]	$\alpha = 2.008$	$\beta = 0.794$				-4.344
Accurate[73c]						-4.350
Second Triplet (2^3P)						
Morse et. al.[73a]	$\mu a = 1.99$	$\mu c = 0.55$	$\mu = 0.61$			-4.261
Veselov et. al.[73b]	$\alpha = 1.991$	$\gamma = 0.544$				-4.262
Accurate[73c]						-4.266

TABLE VI

Wave function Ground state (1^1S)	$\langle r_1^2 + r_2^2 \rangle$ (in a_o^2)
Clementi[72a]	2.3694
Green et. al.[72b]	2.3593
Hylleraas[72c]	2.1070
Experiment[72d]	2.3972

should be too small. This effect does indeed appear and will be discussed in a later section.

Although the excited state wave functions are very similar (see Table V), calculations were made using both sets for the following two reasons. The first was to see if the calculated cross sections were sensitive to the small differences between the wave functions, and the second was because Ochkur used the Veselov wave functions in his original paper.[33] Thus, by using the Hylleraas ground state and the Veselov excited states, the accuracies of the present calculations could be checked against Ochkur's results.

4. Calculation of Total Cross Sections

For simplicity, the first and second triplet excitations are treated separately. Atomic units are used throughout.

4.1 Excitation of the first triplet ($1^1S \rightarrow 2^3S$)

When the wave functions (3-1) and (3-5) are inserted into the expression for the scattering amplitude, either (2-1) or (2-2), and the z-axis of the coordinate system is chosen along $\vec{q}$, the following expression results:

$$T_{fi}(1^1S \rightarrow 2^3S) = 8/6\ N^2 V_1 V_2 f(k_o, k') \left\{ \frac{D_1(z_1 + \mu a)}{[(z_1 + \mu a)^2 + q^2]^2} - \right.$$

$$\frac{D_2[3(z_1+\mu)^2 - q^2]}{[(z_1 + \mu)^2 + q^2]^3} + \left(\frac{3A}{\mu}\right) \frac{D_2(z_1 + \mu b)}{[(z_1 + \mu b)^2 + q^2]^2} + CD_1 \frac{(z_2 + \mu a)}{[(z_2+\mu a)^2+q^2]^2} -$$

$$\frac{CD_2[3(z_2+\mu)^2 - q^2]}{[(z_2+\mu)^2+q^2]^3} + \left(\frac{3AC}{\mu}\right)\frac{D_2(z_2+\mu b)}{[(z_2+\mu b)^2+q^2]^2}\Big\}, \qquad (4\text{-}1)$$

where the parameters for the wave functions are given by Table V, equation (3-8) and

$$N^2 = z_1^3 \Big/ \left\{1 + (c_2/c_1)^2 + 16(c_2/c_1)\left[\frac{z_1 z_2}{(z_1+z_2)^2}\right]^{3/2}\right\}; \qquad (4\text{-}2)$$

$$c_2/c_1 = C\left(\frac{z_1}{z_2}\right)^{3/2}; \quad V_1^2 = \frac{(\mu a)^3}{\pi}; \quad V_2^2 = \frac{\mu^5}{3\pi M}; \qquad (4\text{-}3)$$

$$D_1 = (24\pi)\left\{\frac{1}{(z_1+\mu)^4} - \frac{A/\mu}{(z_1+\mu b)^3} + \frac{C}{(z_2+\mu)^4} - \frac{AC/\mu}{(z_2+\mu b)^3}\right\}; \qquad (4\text{-}4)$$

$$D_2 = 8\pi\left\{\frac{1}{(z+\mu a)^3} + \frac{C}{(z_2+\mu a)^3}\right\}; \qquad (4\text{-}5)$$

$$\text{(OR):}\ f(k_o,k') = \frac{1}{[k' - I_o^{1/2}i]^2}; \quad \text{(O):}\ f(k_o,k') = \frac{1}{k_o^2} \qquad (4\text{-}6)$$

where I_o is the ionization energy of the 1^1S state expressed in Rydbergs. The Morse et. al.[73a] excited state wave function is used above.

Equations (4-1), (4-2), and (4-3) have been written in a form such that any of the three ground state wave functions given above can be used. For instance, setting C(or c_2/c_1) equal to zero and choosing the appropriate z_1, one obtains the scattering

amplitude for the Hylleraas ground state wave function. Similar manipulation of (c_2/c_1), with the appropriate z_1 and z_2, gives the scattering amplitude corresponding to the ground state wave functions (3-2) and (3-3). The cross section corresponding to the Veselov excited state is obtained from (4-1) by using the appropriate screening constants and redefining V_1 and V_2 consistent with (3-12), (3-13).

The differential cross section for the excitation is obtained by using (4-1) and forming

$$\frac{d\sigma}{d\Omega}(k_o, \theta) = \frac{k'}{k_o} |T_{fi}|^2 . \qquad (4-7)$$

The total cross section is found by integrating (4-7) over all scattered angles, or more conveniently by integrating over momentum transfer:

$$\sigma(k_o) = \int\int \frac{d\sigma}{d\Omega}(k_o, \theta) d\Omega = \frac{2\pi}{k_o k'} \int_{q_{min}}^{q_{max}} \frac{d\sigma}{d\Omega}(q) q dq. \qquad (4-8)$$

4.2 Excitation of the second triplet $(1^1S \rightarrow 2^3P)$

The scattering amplitude for the excitation of the second triplet state is obtained from the appropriate wave functions exactly as done in section 4.1 above. Note that the choice of the z-axis along the momentum transfer vector $\vec{q}$ simplifies the calculations by insuring that the only 2^3P wave function which contributes to the cross section is the one with (m = 0) (the z-axis is also the axis of L-quantization). The contribution from the

($m = \pm 1$) components of the 2^3P state vanish because of the resulting azimuthal symmetry. Thus, the scattering amplitude for this transition is given by (using excited state (3-10)):

$$T_{fi} = -8\sqrt{6}\, i\, N^2 V_1 V_2 G_2 f(k,k') \frac{1}{q} \left\{ \frac{(z_1 + \mu c)}{[(z_1 + \mu c)^2 + q^2]^2} + \frac{C(z_2 + \mu c)}{[(z_2 + \mu c)^2 + q^2]^2} - \right.$$

$$\left. \frac{(z_1 + \mu c)[(z_1 + \mu c)^2 - 3q^2]}{[(z_1 + \mu c)^2 - q^2]^3} - \frac{C(z_2 + \mu c)[(z_2 + \mu c)^2 - 3q^2]}{[(z_2 + \mu c)^2 + q^2]^3} \right\} \qquad (4\text{-}9)$$

where the wave function parameters are given in Table V; N^2 is given by (4-2); and

$$V_1^2 = \frac{\mu a^3}{\pi} \; ; \quad V_2^2 = \frac{\mu c^5}{\pi} \qquad (4\text{-}10)$$

$$G_2 = 8\pi \left\{ 1/(z_1 + \mu a)^3 + C/(z_2 + \mu a)^3 \right\} . \qquad (4\text{-}11)$$

As in the case of the first triplet excitation, the appropriate choice of (c_2/c_1 or C) and z_1, z_2 determines the particular ground state wave function being used.

The differential and total cross sections are again given by (4-7) and (4-8) respectively.

5. Results and Discussion

5.1 The effect of approximate wave functions

Figures 11 and 12 show the effect on the total excitation cross section of using different approximate ground and excited state wave functions for the (2^3S) and (2^3P) states respectively. Only the results from using the (OR) approximation are illustrated since the (O) curves show the same relative differences. In Fig. 11, the curves are labeled according to the pair of ground-excited state wave functions employed: C - Clementi[72a]; G-Green, et. al.[72b]; H-Hylleraas[72c]; MYH-Morse, et. al.[73a]; VES-Veselov, et. al.[73b]. Figure 12 could not be labeled this way because the curves are too close together but it contains the same information (see figure captions for the labeling of Fig. 12).

As seen from Fig. 11, the 2^3S cross section is quite sensitive to the particular choice of ground and excited state wave functions employed. As is perhaps expected from the data in Tables V and VI, the Clementi and Green et. al. ground states give essentially the same total cross section for a given excited state. They agree within the plotting accuracy of the figure. One also sees that the cross section obtained from the Hylleraas wave function is significantly smaller than from the other ground states. As suggested in Section (III-3), this is due to the over-concentration of the electron charge density near the nucleus for the Hylleraas wave function (see Table VI). Consequently, the one-electron overlap charge density (defined in (6-1) of Section II-6-1) will be smaller which will lead to a smaller total cross section. It is worth noting that, although the cross sections obtained from the

Green et. al. and Clementi ground states are nearly the same, their relative magnitude is as expected from the values in Table VI. That is, relative to the Green et. al. ground state function, the Clementi wave function gives a slightly larger expectation value for $(r_1^2 + r_2^2)$ and hence yields a cross section that is slightly larger. The differences in the 2^3S excited states is more difficult to assess since there is no experimental parameter (other than the energy) to which the excited states can be referenced. However, by correlating the energy eigenvalues for the (MYH) and (VES) 2^3S excited states with the relative magnitudes of the 2^3S total cross section (for a given ground state) one notices that the state with the better energy eigenvalue (MYH) gives the lower cross section. This same property for excited state wave functions is observed in the 2^3P case although the relative difference is much smaller because the 2^3P excited states (MYH and VES) are so similar in this case (their energy eigenvalues are almost the same).

From Fig. 12 one notices that the cross section for excitation of the 2^3P state is much less sensitive to the various approximate wave functions. As just mentioned, the magnitude of the total cross section is only slightly sensitive to which excited (2^3P) wave function is used because the two excited states (MYH or VES) are so similar. The reason the 2^3P cross section is only slightly sensitive to the ground state wave function is probably due to the fact that the excited state has "p_z-symmetry" [see (3-10), (m = 0)]. As a result, the difference in $(r_1^2 + r_2^2)$ for the ground state wave functions is "sampled" in only the z-direction. This is in contrast to the case when the excited state is spherically symmetric (e. g. the 2^3S state), and the difference in $(r_1^2 + r_2^2)$ is accumulated along all three axial directions.

5.2 Comparison of Ochkur and Ochkur-Rudge approximations

Figure 13 shows the theoretical total cross section for excitation of the 2^3S state as calculated using the (O) and (OR) approximations. Figure 14 is a similar comparison for the 2^3P state. The curves in both figures were calculated using the G and MYH wave functions for the ground and excited states. The (O) approximation is seen to always give a larger cross section than the (OR) approximation. This is indeed expected by inspection of $|f(k_o, k')|$ as given by (4-6) since

$$\frac{1}{k_o^2} > \frac{1}{k'^2 + I_o} . \tag{5-1}$$

As stated earlier (Section I-5), the (OR) approximation is superior to the (O) approximation on theoretical grounds and as will be shown in the next section, indeed gives better agreement with existing experimental data.

5.3 Comparison with experiment

No consistent set of absolute measurements of the total cross sections for excitation of the 2^3S and 2^3P levels exist at present. The basic reason for this state of affairs is because so far it has not been possible to overcome all the technical difficulties in the experiments. The cross sections that can be determined more conveniently are the ones for states with higher ($n = 3, 4, \cdots$) principal quantum numbers, whose excitations can be measured by the light they emit when they radiatively decay.[75]

As discussed in references (33) and (61) the excitation cross sections decrease with the cube of the principal quantum number n. Thus, the cross sections for excitation of the 2^3S and 2^3P states can be reasonably well estimated by extrapolating to lower n the results for the higher level excitations. This was done by Ochkur in his original paper[33] using the Gabriel and Heddle data[61] and Yakhontova data.[75b] These results, along with the isolated absolute measurements that exist, will be compared with the theoretical calculations. The cross section for excitation of the two triplet states will be considered separately.

5.3.1 Excitation ($1^1S \rightarrow 2^3S$)

In Figure 15, the total cross section for excitation of the 2^3S state, as calculated using the (OR) approximation and the (C) and (MYH) wave functions, is compared with the extrapolated Gabriel and Heddle data.[33] The error bars denote estimates of the error due to the extrapolation method. The cross section obtained by extrapolating the Yakhontova data[75b] has a maximum value represented by the symbol (▲) in Fig. 15 and agrees quite well with the extrapolated Gabriel and Heddle data over the whole energy range. At an energy value 0.3 eV above the excitation threshold of the 2^3S state (19.81 eV), Schulz and Fox[76a] found a maximum value equal to $4.5 \times 10^{-2}\ \pi a_o^2$ which is denoted by (O) in the figure. This value agrees somewhat with the measurement $4.2 \times 10^{-2}\ \pi a_o^2$ determined by Maier-Leibnitz[75b], which is denoted by the symbol (□) in Fig. 15. Included in Fig. 15 is the cross section calculated by Massey and Moiseiwitsch[66] using a very elaborate distorted wave method. As seen from the figure, the

Massey and Moiseiwitsch cross section possesses a very sharp first maximum very close to the excitation threshold. The location of this sharp peak agrees well with the measurements of Fox and Schulz and Maier-Leibnitz. This sharp peak is attributed to a near-resonance in the distortion of the electron-wave in the final channel.[66] This is interesting as the existence of such a resonance has been verified experimentally.[77] It is clear that the present calculations cannot be expected to produce such a "fine-structure" because they are based on a model which does not contain the necessary flexibility. However, the (OR) calculations are seen to agree remarkably well with the extrapolated experimental data. It is worth noting that the (O) approximation, using the same wave functions, would be $\sim 40\%$ larger than the (OR) curve in Fig. 15 (ref. Fig. 13). Also, the (BO) approximation for this excitation gives a cross section whose maximum value is $1.3\pi a_o^2$.[66] It is interesting to note that Massey and Moiseiwitsch used the (MYH) wave function for the 2^3S state but the Hylleraas wave function for the ground state. By the discussion of Section 5.1 and Fig. 11, the Hylleraas wave function is clearly a poor representation of the ground state. As a result, their reported cross section could be as much as 40% too low. This would account for some of the disagreement between their calculations and the extrapolated data.

5.3.2 Excitation ($1^1S \rightarrow 2^3P$)

In Figure 16, the cross section for excitation of the 2^3P state, as calculated using the (OR) approximation and the (C) and (VES) wave functions, is compared with the available experimental data. As evident from the figure, there is a wide range in the experimental data. The extrapolated Gabriel and Heddle data[69b],

denoted by (x), possess error bars due to error in the original data and error intrinsic in the extrapolation. The Frost and Phelps data[78a] (⊙) as well as the Holt and Krotkov data[78b] (Δ) are taken from the analysis of Joachain and Mittleman[69b]. Frost and Phelps collected all the available data for incident electrons with less than 45 eV which had been published through 1956 and analyzed it with the hope of arriving at a good consistent set of excitation cross sections. The values reported by Frost and Phelps are the lowest of all the experimental data. The Holt and Krotkov data, which extended only a few eV above threshold, were obtained by assuming a value of $3.5 \times 10^{-2} \pi a_o^2$ for the 2^3S cross section. The reported error associated with that determination is indicated by the vertical bar. There is one other set of data for which one point is included. This is the data of St. John et. al.[79] who used optical methods to make measurements of the cross section for excitation of the $n = 3, 4, \cdots$ levels of helium. The St. John value, denoted by (▼), was obtained by extrapolation and is larger than the other experimental values.

All present theoretical cross sections[68], [69b], [70], [71], except for the (O) curve, predict values which are much too large to be plotted in Fig. 16. The failures of the other theories also includes a distorted-wave calculation[70] similar to the 2^3S calculation discussed above. There is no simple explanation as to why the distorted wave should fail so for the 2^3P state but it seems clear from Fig. 16 that the (OR) approximation has the best chance of agreeing with the experimental data.

IV. Angular Distribution of Electrons After the Exchange Excitation of Molecular Hydrogen and Helium

1. General Comments

In this section, the terms differential cross section (DCS), angular distribution, or simply cross section will be used interchangeably and are supposed to mean the same thing.

The angular distributions of the electrons scattered after undergoing a rearrangement collision with H_2 or He are discussed separately from the total cross sections for two reasons. The first is because this separation is probably less confusing to the reader and the second is because the analysis of the results requires special treatment since there is so little experimental date available.

To date, there are no published differential cross sections for the electron-exchange scattering processes in molecular hydrogen. For the electron-exchange processes in helium there are three sets of data which will be discussed in Section (IV-3). However, there are no published theoretical angular distributions for any of the excitation processes of interest with which the present calculations can be compared. The differential cross sections for the electron excitation of the two lowest-lying triplet states of molecular hydrogen and atomic helium are presented here as calculated in the (OR) approximation and using the "best" wave functions for the respective states. The results obtained from using the (O) approximation and the other wave functions discussed in earlier sections are not presented here since they contain no new information. The comments of Sections II and III concerning the (O) approximation and the effect of the less accurate wave functions apply here also.

The last section will be devoted to an analysis of why the maximum in the (DCS) appears where it does.

2. Molecular Hydrogen

The (DCS) for excitation of the $b^3\Sigma_u^+$ and $a^3\Sigma_g^+$ states of molecular hydrogen were calculated by slightly modifying the equations and techniques discussed in Section II. For completeness, the equations applicable for the two excitations will be reproduced here.

2.1 $X^1\Sigma_g^+ \rightarrow b^3\Sigma_u^+$ Excitation

From equations (5-31) through (5-35) of Section (II-5.2.1), the differential, rotationally averaged, excitation cross section per unit energy range is given by:

$$I^{(1)}_{\nu'}(k_o, \theta, \varphi) = \frac{3k''}{k_o} P^{(1)}(E_1) \langle |\mathcal{T}^{(1)}_{\nu'}[R^{(1)}(E_1)]|^2 \rangle \quad , \tag{2-1}$$

where $P^{(1)}$, E_1 and k'' are defined in the equations referred to above, and $\mathcal{T}^{(1)}_{\nu'}$ is defined by (5-15) of Section (II-5.1). Since the (DCS) is the quantity of interest, (2-1) was not integrated over the scattered angles. The (DCS) for excitation from the ground vibrational-rotational state to all final vibrational states that are energetically accessible is given by

$$I^{(1)}(k_o, \theta, \varphi) = \frac{3k''}{k_o} \int_{D_o}^{E_o} P^{(1)}(E_1) \langle |\mathcal{T}^{(1)}_{\nu'}[R^{(1)}(E_1)]|^2 \rangle dE_1, \tag{2-2}$$

where

$$E_o = \frac{\hbar^2 k_o^2}{2m} ,$$

and D_o is the dissociation energy of the ground electronic-vibrational state. It should be noted that due to the azimuthal symmetry of the H_2 molecule and the form of the (OR) matrix element (see equation (5-8) of Section (I-5.2)), (2-2) depends only on the scattered angle θ but not on φ. The numerical techniques used to evaluate (2-2) are the same as those discussed in Sections (II-4, 5).

Three "views" of the (DCS) for the excitation process ($X\,^1\Sigma_g^+ \rightarrow b\,^3\Sigma_u^+$) are illustrated[80] in Figures 17, 18, and 19. The definition of a "view" is the following. Since the (DCS) is a function of two variables, the incident energy and the scattered angle, it can be represented by a surface in a system of coordinates whose axis are E(incident energy), θ(scattering angle) and (DCS). Figs. 17, 18, and 19 represent different perspective views of this surface. The range of the scattered angle (θ) is from 0^o to 180^o in steps of 5^o starting at the origin. The values of the incident energy range from 10 eV to 85 eV in steps of 5 eV also starting from the origin. The spherical-polar angles from which direction the surface is viewed are given at the lower left in each figure. The curves on the figures are intersections of the surface with planes of constant E and of constant θ. Fig. 17 is a special case of perspective plotting, namely an x-y plot. The vertical lines are lines of constant angle and the smoothly varying horizontal contours are lines of constant energy. Figs. 18 and 19 are the same (DCS) array but "viewed" from different angular orientations.

Since there is no experimental data available for these excitation processes, it is difficult to evaluate the quality of the (OR) approximation in predicting the (DCS). However, the (DCS) does possess the properties expected on physical grounds. That is, at 10 eV (. 2 eV above threshold) the (DCS) is nearly isotropic. This is consistent with the physical picture of the scattered electron having almost equal probability of going in any direction since it, so to speak, "barely escapes". As the incident energy increases, the maximum in the (DCS) moves more and more toward the forward direction. This is also expected since for high enough energy the electron will be only slightly deflected.

2.2 $X\,^1\Sigma_g^1 \rightarrow a\,^3\Sigma_g^+$ excitation

The equations and the methods used in the calculation of the (DCS) for this process are very similar to those described above in Section (2.1). The differences are associated with the details of the $a\,^3\Sigma_g^+$ state. Thus, the differential cross section, rotationally averaged and summed over all energetically allowable final vibrational states is given by

$$I^{(2)}(k, \theta, \varphi) = \frac{3k''}{k_o} \int_{D_o}^{E_o} P^{(2)}(E_2) \langle |T^{(2)}_{\nu'}[R^{(2)}(E_2)]|^2 \rangle dE_2, \qquad (2\text{-}3)$$

where the symbols are the same as defined in Section (II-5.2.2). Again, because of the azimuthal symmetry, (2-5) depends only on the scattered angle θ.

The (DCS) for the excitation of the $a\,^3\Sigma_g^+$ state is displayed in Figs. 20, 21 and 22. These "views" have exactly the

same meaning as those for the first triplet excitation described in Part 2.1 above except for one slight difference. Since the excitation threshold is ~ 11.9 eV, the lowest incident energy value in these figures is 12 eV. Thereafter, the energy values are 15, 20, 25 etc. up to 85 eV in steps of 5 eV. The angular range is the same as in Figs. 17, 18 and 19.

As mentioned above, there is no experimental data with which to check these calculations. A possible explanation as to the shape of these cross sections is presented in Part 4.

3. Helium

The differential cross section for the excitation from the ground state to the first (2^3S) and second (2^3P) triplet states were calculated using the (OR) approximation and the "best" wave functions. The (DCS) for each excitation process will be treated separately.

3.1 $1^1S \rightarrow 2^3S$ excitation

The (DCS) for this process is given by equations (4-7) and (4-1) of Section (III-4.1). Again note that because of the symmetry involved, the (DCS) depends only on the scattered angle θ. The Green et. al.[72b] and MYH[73a] wave functions were used for the ground and excited states respectively. Using the Clementi[72a] ground state wave function produced a negligible change in the (DCS).

Three perspective "views" of the (DCS) for this process are illustrated in Figs. 23, 24 and 25. As expected, the (DCS) possesses the same qualitative features as the angular distributions for the excitation processes in H_2 which were discussed

above. There are three "pieces" of experimental information concerning the (DCS) for this process. Schulz and Philbrick[81] measured the change with incident energy of the (DCS) at the fixed scattering angle of 72^{o}. Unfortunately, they were able to measure this dependence to only a few eV above threshold (19.81 eV), and their measured cross section exhibits a good deal of complex structure. The very limited energy range and resonance type effects in their results does not permit a direct comparison with the calculations reported here.

The other two "bits" of information involve experiments in which the angular distribution was measured for fixed incident energy. Ehrhardt and Willmann just recently measured[82] the angular distribution of electrons scattered after exciting the $2^{3}S$ state for energies from threshold to 24 eV. They observed three resonances at energies of $19.90 \pm .05$, $20.45 \pm .05$ and $21.00 \pm .05$ eV. The calculations here are not refined enough to see such resonances but can be compared with two "off-resonance" angular distributions at 20 and 24 eV which they measured. To facilitate the comparison, the calculated cross sections corresponding to the experimental incident energies are plotted with the Ehrhardt and Willmann data in Fig. 26. The experimental data were reported as relative and is consequently normalized to the calculated cross section at a scattered angle of 70^{o}. This particular angle is an arbitrary choice representing a value half-way in the experimental range. For an incident energy of 20 eV (the upper plot in Fig. 26), the theory and normalized experimental data are seen to agree very well. Both theory and experiment describe a preferential back-scattering of the incident electrons. It should be noticed that for this 20 eV case, the particular angle chosen for normalization

doesn't affect the agreement because both theory and experiment are approximately straight lines of the same slope.

The bottom half of Fig. 26 contains the comparison between theory and experiment for the 24 eV case. To be consistent with the 20 eV comparison, the data were again normalized to theory at a scattered angle of 70^{o}. The agreement here is not as good as for the 20 eV case although the theory and experiment possess very similar characteristics. The theory has a maximum in the angular distribution at $\sim 120^{o}$ while the experimental maximum falls at $\sim 90^{o}$. Both theory and experiment predict the same relative difference between the maximum and minimum of the angular distribution. It is worth noting that a different choice of angle for the normalization of the data could improve the agreement between theory and experiment over sections of the angular range. However, it seems evident that no choice of normalization will allow the curves to coincide over the entire angular range.

Simpson et. al. [83] have measured the angular distribution of 56.5 eV electrons scattered after exciting the $2^{3}S$ state. Their reported cross section is in disagreement with the present calculations. They determined that for this incident energy the angular distribution peaks at $\sim 0^{o}$ while the calculated one peaks at $\sim 55^{o}$. There seems to be no simple explanation for this disagreement. It is the opinion of this writer that the measurements of Simpson et. al. are not consistent with those of Ehrhardt and Willmann. This is because to this writer the two measurements imply angular distributions at the same energy which possess completely different shapes. This discrepancy will probably persist until more experimental measurements are made for this excitation process.

3.2 $1^1S \rightarrow 2^3P$ excitation

The angular distributions for this excitation process are displayed in Figs. 27, 28 and 29. They were calculated in the (OR) approximation using the Green et. al.[72b] and MYH[73a] wave functions for the ground and excited states respectively. Use of the Clementi[72a] and/or Veselov et. al.[73b] wave functions introduced no significant changes in the cross sections. There are no published calculations or experimental measurements for this excitation process so the quality of this calculation can't be readily evaluated. About all that can be said is that the angular distributions possess shapes that are physically reasonable for the same reasons outlined in Section 2.1 above.

4. The Shape of the Angular Distributions

In this section, a few general comments will be made concerning the shape of the angular distributions for the triplet excitation processes as governed by the (OR) approximation.

By inspection of the matrix element in the (OR) approximation (suppressing all but electronic coordinates)

$$\mathcal{F}_{(q)} = \langle \psi_f | e^{i\vec{q}\cdot\vec{r}_1} | \psi_i \rangle \ , \qquad (4\text{-}1)$$

one sees that the angular distribution is related to the Fourier transform of a one-electron overlap charge density. Thus, if this one-electron overlap charge density is appreciable only in a region of radius (a), then the Fourier transform takes appreciable values only in a region of linear dimensions (1/a) about the origin.[84]

Consequently, (4-1) will possess its maximum somewhere in the region $q \lesssim 1/a$. The precise "a-priori" location of the maxima of (4-1) requires a knowledge of the range of the one-electron charge density and the details of the interaction process. Although not enough information seems to be available at present a semi-quantitative analysis can be carried out as will be shown below.

The intrinsic complexity of this type of scattering process can be made more evident by considering the classical analog of the scattering of electromagnetic radiation by a partially absorbing body. One thinks of the body absorbing the incident electromagnetic radiation and then re-emitting the radiation at a different energy. If the wave length of the incident radiation is large compared to the size of the object, one can treat the re-emitted radiation as coming only from an induced dipole. However, if the wave length of the incident radiation is of the order of the size of the object, the case of interest here, many multipoles are important and the details become quite complicated. This is called by the general name of Mie Scattering.[85] Some insight into the quantum case can be gained from this classical analog when one notes that the quantity which determines the angular distribution in Mie Scattering is[85c]

$$\rho = \frac{2\pi a}{\lambda} \equiv q_\lambda a \,, \qquad (4\text{-}2)$$

where (a) is the radius of the particle and (λ) is the wave length of the incident radiation. This is very similar to the quantum requirement $qa \lesssim 1$ obtained in conjunction with (4-1).

For the analysis of the electron scattering angular distributions, these qualitative arguments need to be made more quantitative. To do so, it is assumed that the maximum in the angular distributions are characterized by the equation (atomic units)

$$aq(k_o^2, \theta) = 1 , \tag{4-3}$$

where (a) is the radius of the one-electron charge distribution and q is the momentum transfer wave number which depends on the incident energy and scattered angle according to

$$q^2 = k_o^2 + k'^2 - 2k_o k' \cos\theta , \tag{4-4}$$

$$k'^2 = k_o^2 - \Delta E . \tag{4-5}$$

The quantity ΔE is the excitation energy of the particular process being considered. The choice of the value 1 for the right hand side of (4-3) is somewhat arbitrary (although the value is close to unity) and was chosen so for convenience. Although the actual value may be different from 1 and may also be a function of the particular scattering process, this choice is quite consistent with the discussion above and does not affect the principle of the analysis that follows.

By using (4-3), the location of the maxima in the angular distributions can be explained as follows. Since (a) is fixed for a given excitation process, q is always determined for the same process by solving (4-3). It follows from (4-4) that in order for q to maintain its same value as the energy changes, the

scattered angle must change. To demonstrate that this type of analysis does indeed characterize the maxima of the angular distributions, the excitation of the first triplet ($b^3\Sigma_u^+$) state of H_2 is analyzed using (4-3). In Fig. 30, the vector relation between $\vec{q}$, $\vec{k}_o$ and $\vec{k}'$ is displayed in the upper left corner. The lower portion represents this vector relation plotted out explicitly for a number of incident energies. The horizontal axis represents k_o in atomic units. The large semi-circles whose centers are located at different points along the k_o-axis represent the magnitude and possible orientations of the $\vec{k}'$-vector with respect to the tip of the $\vec{k}_o$ vector. For purposes of this discussion, just one possible energy-loss has been used in obtaining k' from (4-5); namely 10.62 eV. If (4-3) is valid, the vectors q (for all possible energies) must lie on a circle whose origin is at the tail of the vector $\vec{k}_o$. In Fig. 30, the magnitude of q was taken to be 1, which corresponds to a value of 1 for the radius of the one-electron overlap charge distribution. Then for each incident energy, the intersection of the q-semicircle with the k'-semicircle uniquely defines the scattered angle θ. The vector diagram is explicitly for the case of 10 eV incident electrons. By measuring the scattered angle (with a protractor) and comparing it with the one corresponding to the maximum in the angular distributions of Fig. 17, one sees that the agreement is quite good. For instance, at energies of 10, 20 and 30 eV both the maxima predicted by Fig. 30 and that displayed in Fig. 17 are respectively 110^o, 54^o and 42^o.

In Fig. 31 are displayed the maximum in the angular distribution (θ_{max}) as function of the incident energy (E) as found from Fig. 30 and calculated in the (OR) approximation (Fig. 17). The solid line is the (OR) result, the crosses are the results from

Fig. 30. It is worth mentioning that for an incident energy of 200 eV, the maximum in the angular distribution will occur at 15^{o} according to the (OR) model for the excitation. This is an interesting result because it has been speculated that at this energy the maximum in the angular distribution will be at 0^{o}. Experimental measurements will be necessary to determine if this is indeed the case. Note that the choice of $a = 1a_{o}$ is consistent with knowledge of the charge distribution for the hydrogen molecule. This value corresponds to a (rotationally averaged!) diameter of $2a_{o}$. A similar analysis can of course be carried out for the second triplet excitation of H_2 and the He excitation processes. The only changes that are necessary are in the excitation energy and perhaps the value of a. In this model, these two quantities are the ones that determine the shape of the angular distribution! This is a physically appealing result.

The discussion carried out in this section shows that the calculated angular distributions are indeed consistent with both the classical picture of the scattering process and the mathematical model employed. As more experimental data for electron-atom rearrangement processes becomes available one will be able to perform a better evaluation of the validity of the (OR) approximation for differential cross sections.

References

(1) a) M. L. Goldberger and K. M. Watson, Collision Theory (John Wiley and Sons, Inc., New York (1964)).

b) T. Y. Wu and T. Ohmura, Quantum Theory of Scattering (Prentice Hall Inc., New Jersey (1962)).

c) A. Messiah, Quantum Mechanics Vols. I and II, (John Wiley and Sons Inc., New York (1961)).

d) N. F. Mott and H. S. W. Massey, The Theory of Atomic Collisions (Oxford University Press, London (1965)).

(2) The treatment in Sections (I-1) and (I-2) is basically a summary of that found in refs. 1b) and 1c).

(3) Ref. 1c, Vol. II, p. 831, 834; Vol. I, p. 421.

(4) Ref. 1d, p. 75.

(5) The derivation of this quantity can be found in any number of texts. See for instance ref. 1d, p. 20.

(6) Ref. 1c, p. 803.

(7) Ref. 1d, p. 80.

(8) Ref. 1c, Vol. II, p. 810.

(9) Ref. 1d, p. 77, 86.

(10) Ref. 1c, Vol. II, p. 819.

(11) Ref. 1a, p. 81.

(12) E. Gerjuoy, Ann. Phys. 5, 58 (1958). Collisions involving more (or less) than two particles/channel are discussed in this reference.

(13) This separation is treated in numerous texts on many body motion. See for instance: ref. 1c, Vol. I, pp. 384 and 409; Vol. II, p. 833.

(14) See for instance a) L. I. Schiff, Quantum Mechanics (McGraw Hill, New York (1949)) pp. 97-99; or b) ref. 1c, Vol. I, p. 409.

(15) Ref. 1c, Vol. II, p. 836.

(16) For instance, in the case of rearrangement collisions, the vectors are not orthogonal: see ref. 1c, Vol. II, pp. 847-8; For a discussion of uniqueness see: ref. (12) and B. A. Lippmann, Phys. Rev. 102, 264 (1956).

(17) a) The requirements on the boundary conditions to insure uniqueness for the general case is discussed in: E. Gerjuoy, Phys. Rev. 109, 1806 (1958).

b) The reason for non-uniqueness in some approximate solutions is discussed in: L. L. Foldy and W. Tobocman, Phys. Rev. 105, 1099 (1957).

c) The problem is also discussed in: S. Epstein, Phys. Rev. 106, 598 (1957).

(18) The details of this derivation are given in ref. 1c, Vol. II, pp. 837, 8.

(19) The results presented here for a massive core can be modified to the case of a finite core as discussed in: T. B. Day, L. S. Rodberg, G. A. Snow and J. Sucher, Phys. Rev. 123, 1051 (1961). (See footnote (6) in this paper.); The approach used here to obtain (3-35) and (3-38) is different than that used by Day et al..

(20) See ref. (19), p. 1052.

(21) a) The "prior", "post" discrepancy is discussed at length in: D. R. Bates, A. Fundaminsky, J. W. Leech, and H. S. W. Massey, Trans. Roy. Soc. A243, 93 (1950);

b) The "first order exchange approximation" was developed to correct for lack of orthogonality: K. L. Bell and B. L. Moiseiwitsch, Proc. Phys. Soc. A276, 346 (1963).

(22) In ref. 1b, p. 334 and pp. 246-7, this paradox is discussed and some additional references are given.

(23) J. D. Jackson, Proc. Phys. Soc. A70, 26 (1957).

(24) See ref. 14a, p. 230, p. 238 or ref. 17a.

(25) See ref. 1d in which most of the commonly used approximations are discussed and results obtained from their use are evaluated.

(26) The Born approximation becomes the Born-Oppenheimer approximation when the rearrangement involves identical particles. See the original treatment in: J. R. Oppenheimer, Phys. Rev. 32, 361 (1928).

(27) Many references to the results of Born calculations are given in ref. 1d.

(28) L. D. Landau and E. M. Lifshitz, Quantum Mechanics (Addison-Wesley Inc., Massachusetts (1958)), p. 153.

(29) See ref. 1b section M3 for the details of the "close-coupling" approximation.

(30) Two new books have appeared which discuss the close-coupling approximation as applied to electron-atom collision. They are:
a) Atomic Collisions, edited by V. Ya. Veldre (The MIT Press, Cambridge, Mass. (1966)).
b) The Theory of Electron Atom Collisions by G. F. Drukarev (Academic Press, New York (1965)).

(31) This comparison is made in ref. 21a, p. 100, 102.

(32) The failure of the BOA is explicitly discussed in ref. 21a.

(33) V. I. Ochkur, Soviet Physics -- JETP 18, 503 (1964).

(34) a) M. R. H. Rudge, Proc. Phys. Soc. 85, 607 (1965).
b) M. R. H. Rudge, Proc. Phys. Soc. 86, 763 (1965).

(35) The treatment used by Rudge is contained in: Y. N. Demkov, Variational Principles in the Theory of Collisions (Pergamon Press, London (1963)), Chap. 1.

(36) See ref. (35), pp. 97-102 and ref. 34b, p. 765.

(37) See for instance ref. 1c, Vol. II, p. 806.

(38) These arguments on the lack of detailed balance in general when using the Rudge expression for exchange were presented simultaneously by:
a) D. S. F. Crothers, Proc. Phys. Soc. 87, 1003 (1966);
b) O. Bely, Proc. Phys. Soc. 87, 1010 (1966).

(39) An excellent review of electron collision processes up to November 1966 is contained in: L. J. Kieffer, "Bibliography of Low Energy Electron Collision Cross Section Data", National Bureau of Standards Miscellaneous Publication 289, March 10, 1967. (50 cents).

(40) H. S. W. Massey and C. B. O. Mohr; Proc. Roy. Soc. A135, 258 (1932).

(41) See ref. 21a, p. 134, for a brief discussion on this violation.

(42) S. J. B. Corrigan, J. Chem. Phys. 43, 4381 (1965).

(43) L. A. Edelstein, Nature 182, 932 (1958).

(44) S. P. Khare and B. L. Moiseiwitsch, Proc. Phys. Soc. 88, 685 (1966).

(45) S. P. Khare, Phys. Rev. (to be published).

(46) M. Born and J. R. Oppenheimer, Ann. der Physik 84, 457 (1927).

(47) J. D. Craggs and H. S. W. Massey, Handbuch der Physik, edited by S. Flügge (Springer-Verlag, Berlin, 1959) 37, p. 333.

(48) E. C. Kemble, The Fundamental Principles of Quantum Mechanics (Dover Publications, Inc., New York, 1958), pp. 162-170.

(49) E. N. Lassettere and M. E. Krasnow, J. Chem. Phys. 40, 1248 (1964).

(50) a) The optimized values of the screening constants for the various internuclear distances of the ground states were made available by Dr. G. O. Hultgren, now at Battelle Institute, Columbus, Ohio;

b) C. Weinbaum, J. Chem. Phys. 1, 593 (1933);

c) S. C. Wang, Phys. Rev. 31, 579 (1929);

d) C. A. Coulson, Trans. Faraday Soc. 33, 1479 (1937);

e) W. Kolos and C. C. J. Roothaan, Rev. Mod. Phys. 32, 219 (1960).

(51) a) P. E. Phillipson and R. S. Mulliken, J. Chem. Phys. 28, 1248 (1958);

b) A. C. Hurley, Proc. Roy. Soc. A226, 187 (1954);

c) A. S. Coolidge and H. M. James, J. Chem. Phys. 6, 730 (1938).

(52) a) For the ionization energy: V. A. Johnson, Phys. Rev. 60, 373 (1941);

b) for the states $X^1\Sigma_g^+$, $b^3\Sigma_u$, and $c^1\Pi_u$: W. Kolos and L. Wolniewicz, J. Chem. Phys. 43, 2429 (1965);

c) for the $B^1\Sigma_u^+$ state: W. Kolos and L. Wolniewicz, LMSS Technical Report (1965), University of Chicago, p. 85;

d) for the $a^3\Sigma_g^+$ state: C. B. Wakefield and E. R. Davidson, J. Chem. Phys. 43, 834 (1965);

e) for the $c^3\Pi_u$ state: J. C. Browne, J. Chem. Phys. 40, 43 (1964).

(53) M. P. Barnett, Methods in Computational Physics, Vol. 2 (edited by B. Alder, S. Fernbach, and M. Rotenberg, Academic Press, New York 1963), pp. 95-120.

(54) S. P. Khare and B. L. Moiseiwitsch, Proc. Phys. Soc. 85, 821 (1965).

(55) a) A. S. Coolidge, H. M. James, and R. D. Present, J. Chem. Phys. 4, 193 (1936);

b) H. M. James and A. S. Coolidge, Phys. Rev. 55, 184 (1939).

(56) In Ref. (55), the replacement was $A'E^{1/4}\delta(R-R_c)$ where E was the energy of the continuum state above its value at infinite internuclear separation. However, the continuum wave function was normalized so as to have unit amplitude

at large R. It is simple to show from the information in Ref. (48) that if the normalization of (2-18) is used, the $E^{1/4}$ factor should be omitted.

(57) G. Herzberg, Spectra of Diatomic Molecules (Second Edition, Van Nostrand, 1953), pp. 76-78, 532.

(58) A. Kopal, Numerical Analysis (Second Edition, Wiley, New York, 1961), p. 569.

(59) R. N. Zare, J. Chem. Phys. 40, 1934 (1964); R. N. Zare, University of California Radiation Laboratory, Report 10925 (1963). Dr. Zare kindly provided the programs necessary for this calculation.

(60) a) T. P. Das and R. Bersohn, Phys. Rev. 115, 897 (1959);
b) N. F. Ramsey, Molecular Beams (Oxford University Press, Oxford, 1956).

(61) A. H. Gabriel and D. W. O. Heddle, Proc. Phys. Soc. A258, 124 (1960).

(62) J. T. Tate and P. T. Smith, Phys. Rev. 39, 270 (1932).

(63) L. J. Kieffer and G. H. Dunn, Rev. Mod. Phys. 38, 1 (1966).

(64) P. Englander-Golden and D. Rapp, Lockheed Missiles and Space Co. Report No. 6-74-64-12.

(65) H. Harrison, The Experimental Determination of Ionization Cross Sections of Gases under Electron Impact (Catholic University of America Press, Washington, D. C., 1956), Table 4.

(66) H. S. W. Massey and B. L. Moiseiwitsch, Proc. Roy. Soc. A227, 38 (1950).

(67) a) See ref. (33) for the first calculation.

b) V. I. Ochkur and V. F. Brattsev, Optics and Spectroscopy 19, 274 (1966).

(68) K. L. Bell, H. Eissa and B. L. Moiseiwitsch, Proc. Phys. Soc. 88, 57 (1966).

(69) a) For the 2^3S state: C. J. Joachain and M. H. Mittleman, Phys. Rev. 140, A432 (1965);

b) For the 2^3P state: C. J. Joachain and M. H. Mittleman, Phys. Rev. 151, 7 (1966).

(70) H. S. W. Massey and B. L. Moiseiwitsch, Proc. Roy. Soc. A258, 147 (1960).

(71) C. N. Lashmore-Davies, Proc. Phys. Soc. 86, 783 (1965).

(72) a) E. Clementi, J. Chem. Phys. 40, 1944 (1964); IBM Corp. Research Paper RJ-256 (1963).

b) L. G. Green, M. M. Mulder, M. N. Lewis, and J. W. Woll, Phys. Rev. 93, 757 (1954).

c) H. Bethe and E. Salpeter, Quantum Mechanics of One and Two Electron Atoms (Academic Press Inc., New York, 1957), pp. 128, 147.

d) Reference (71).

(73) a) P. M. Morse, L. A. Young, and E. S. Haurwitz, Phys. Rev. 48, 948 (1935).

b) M. G. Veselov, I. M. Antonova, V. F. Brattsev and I. V. Kirillova, Optics and Spectroscopy 10, No. 6, 367 (1961).

c) C. E. Moore, "Atomic Energy Levels as Derived from the Analysis of Optical Spectra", U. S. Nat. Bur. Standards Circ. 467, Atomic Energy Levels 1, 309 (1949).

(74) For the states of interest here, the Hylleraas ground state was used in references (33), (66), (69).

(75) a) See ref. (61),
b) and the results of V. E. Yakhontova, Thesis, Leningrad State University, quoted in refs. (33) and (68).

(76) a) G. J. Schulz and R. E. Fox, Phys. Rev. 106, 1179 (1957).
b) H. Maier-Leibnitz, z. Physik 95, 499 (1935).

(77) G. J. Schulz and J. W. Philbrick, Phys. Rev. Letters 13, 477 (1964). (This was the first verification of the resonance.)

(78) a) L. S. Frost and A. V. Phelps, Westinghouse Lab. Res. Report No. 6-94439-6-R3, 1957.
b) H. K. Holt and R. Krotkov, Phys. Rev. 144, 82 (1966).

(79) R. M. St. John, F. L. Miller and C. C. Lin, Phys. Rev. 134, A888 (1964).

(80) The computer program which generates these perspective plots is a slight modification of a program written by David L. Nelson, Technical Report 553, Univ. of Maryland, Dept. of Physics, March 1966.

(81) G. J. Schulz and J. W. Philbrick, Phys. Rev. Letters 13, 477 (1964).

(82) H. Ehrhardt and K. Willmann (1967), to be published.

(83) J. A. Simpson, M. G. Menendez and S. R. Mielczarek, Phys. Rev. 150, 76 (1966).

(84) This result is a general property of the Fourier transform. For a realistic example see ref. 1c, Vol. II, p. 816.

(85) a) A discussion of Mie scattering is contained in: K. Bullrich, Electromagnetic Scattering, edited by M. Kerker (1962), p. 162;

b) P. Beckman and A. Spizzichino, The Scattering of Electromagnetic Waves (1963), p. 404;

c) K. Ya. Kondrat'yev, Aetinometry, a translation of Aktinometriya, Gidrometeorologicheskoye Izdatel'stvo, Leningrad (1965), p. 163-168. (Available from NASA TT F-9712);

d) J. D. Jackson, Classical Electrodynamics, (John Wiley and Sons, New York (1963)), p. 294.

(86) R. J. Fleming and G. S. Higginson, Proc. Phys. Soc., 84, 531 (1964).

FIGURE 1

Potential energy as a function of internuclear distance for low-lying states of H_2.[52] Quantities $R^{(1)}$ and E_1 are defined in Section 5.2.1. The shaded area represents the Franck-Condon region for excitation from the ground vibrational state. The horizontal full line to the right of the $b^3\Sigma_u^+$ curve represents a continuum vibrational energy level, ν'.

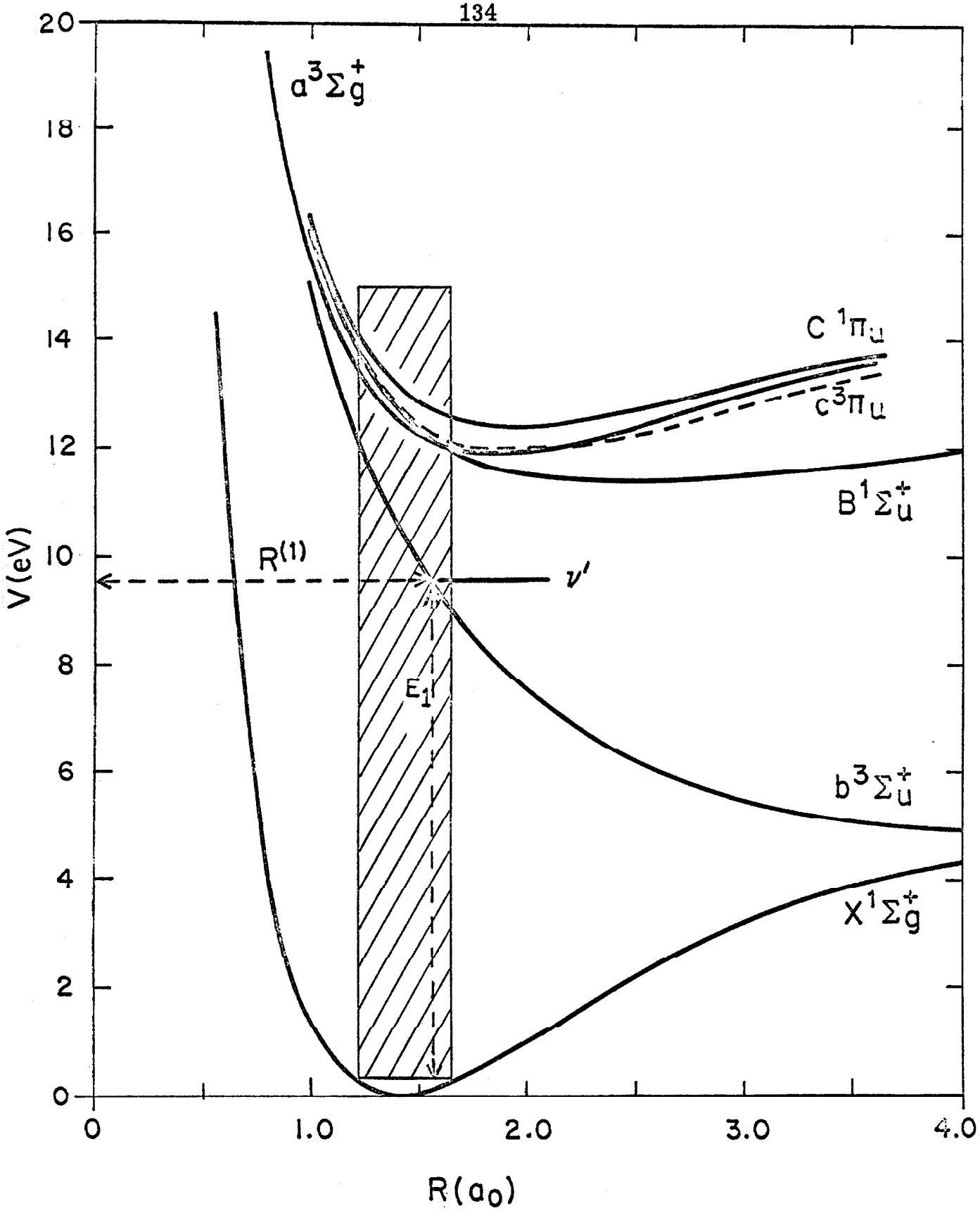
20
18
16
14
12
10
8
6
4
2
0
V(eV)
0
1.0
2.0
3.0
4.0
R(a0)
a 3Σg+
C 1Πu
c 3Πu
B 1Σu+
b 3Σu+
X 1Σg+
R(1)
v'
E1

FIGURE 1

FIGURE 2

Diagram indicating distances and angles for the evaluation of multicenter integrals.

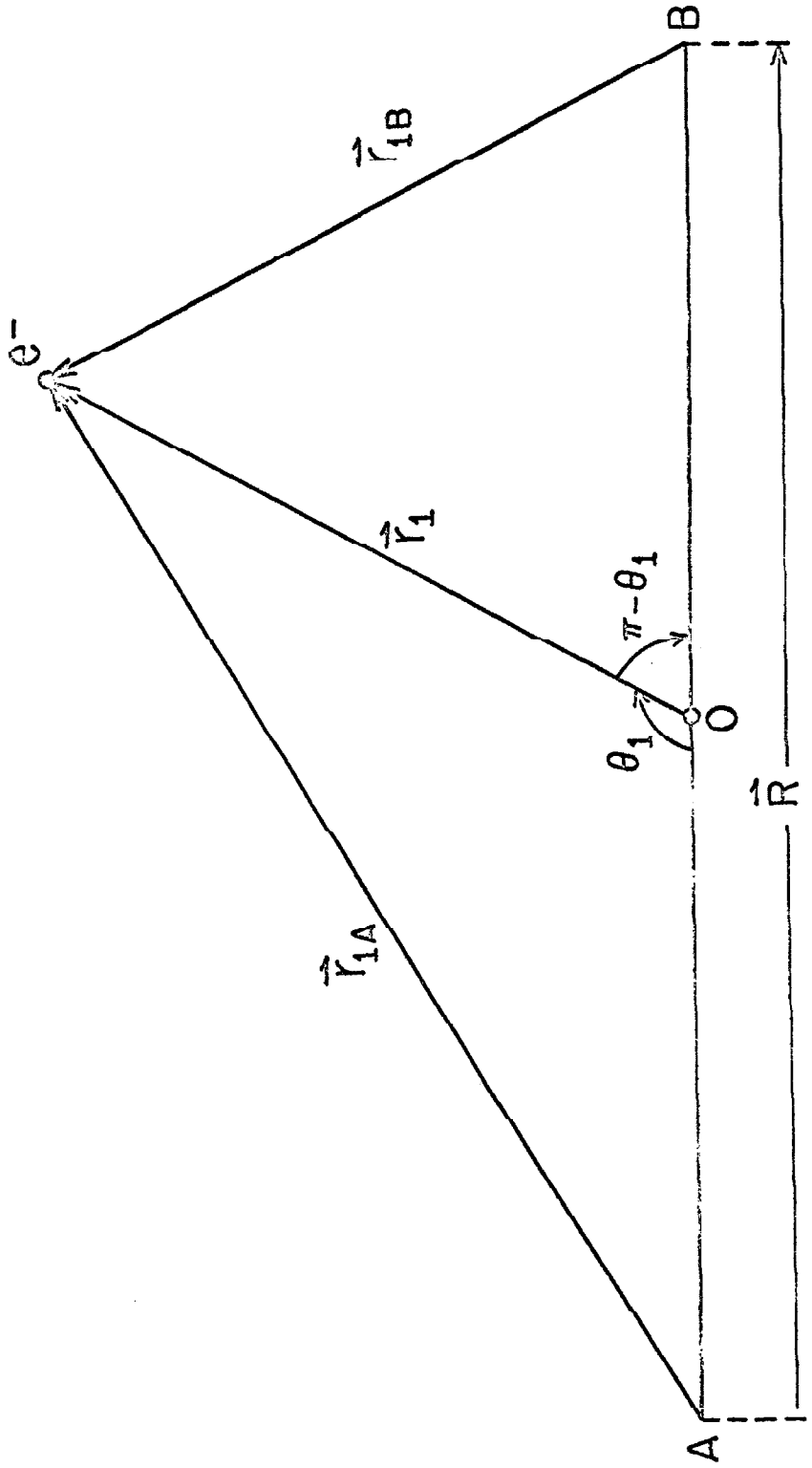

FIGURE 2

FIGURE 3

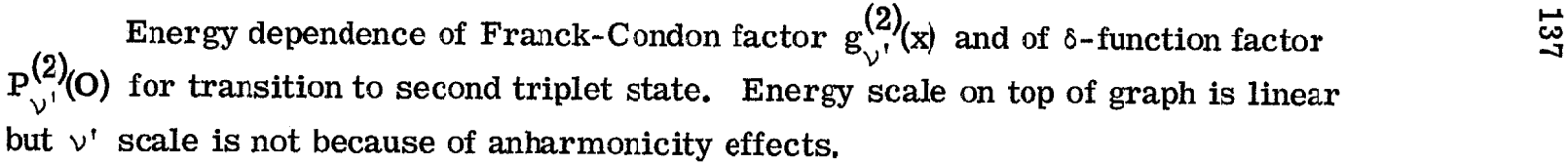

Energy dependence of Franck-Condon factor $g^{(2)}_{\nu'}(x)$ and of δ-function factor $P^{(2)}_{\nu'}(O)$ for transition to second triplet state. Energy scale on top of graph is linear but ν' scale is not because of anharmonicity effects.

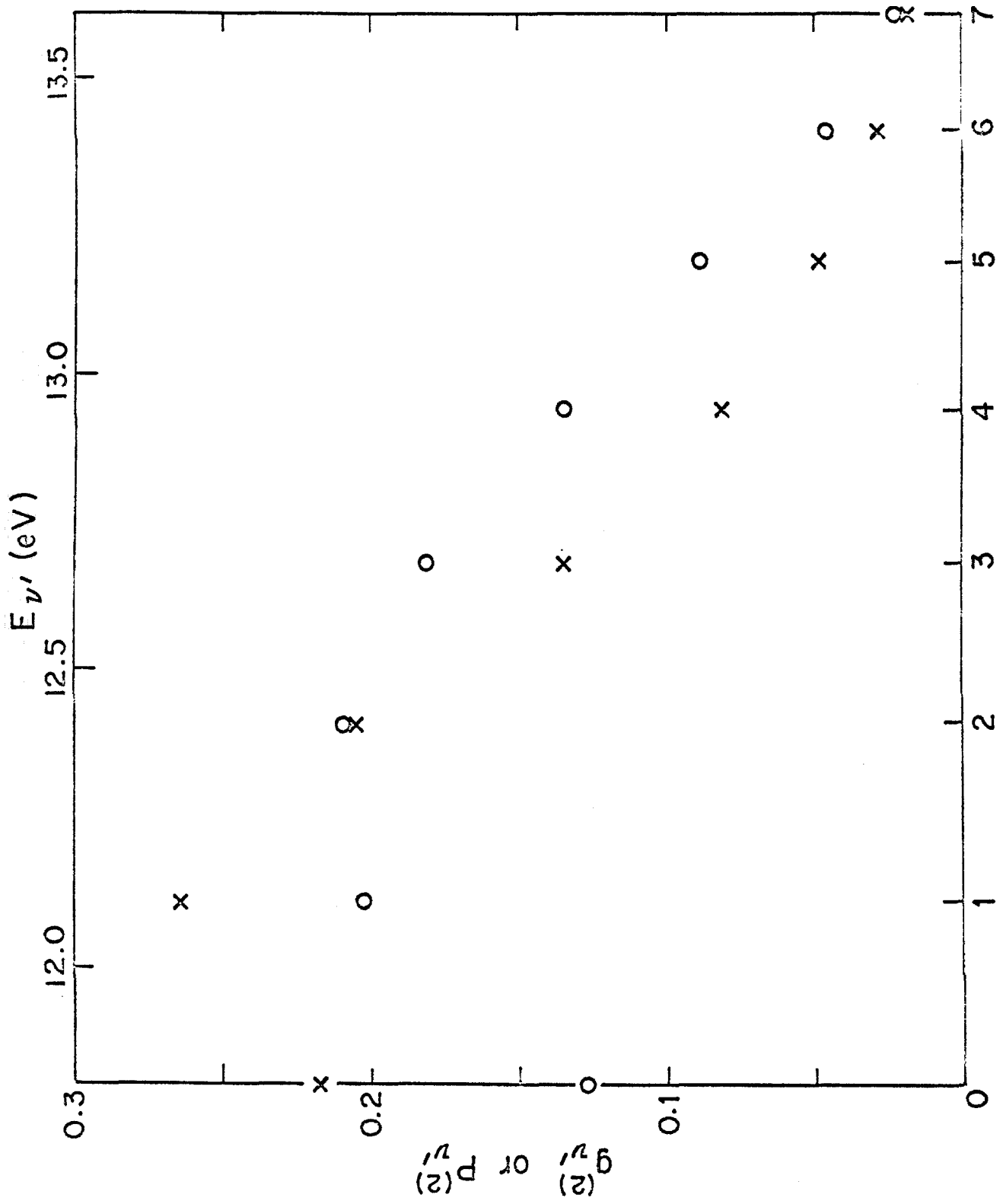

FIGURE 3

FIGURE 4

Effect of ground state wave function on cross section for excitation to first and second triplets: (1) Wg--first triplet, Wang; (1) Wb--first triplet, Weinbaum; (1) C--first triplet, Coulson; (2)--second triplet (curves corresponding to the three different ground state wave functions coincide within plotting accuracy).

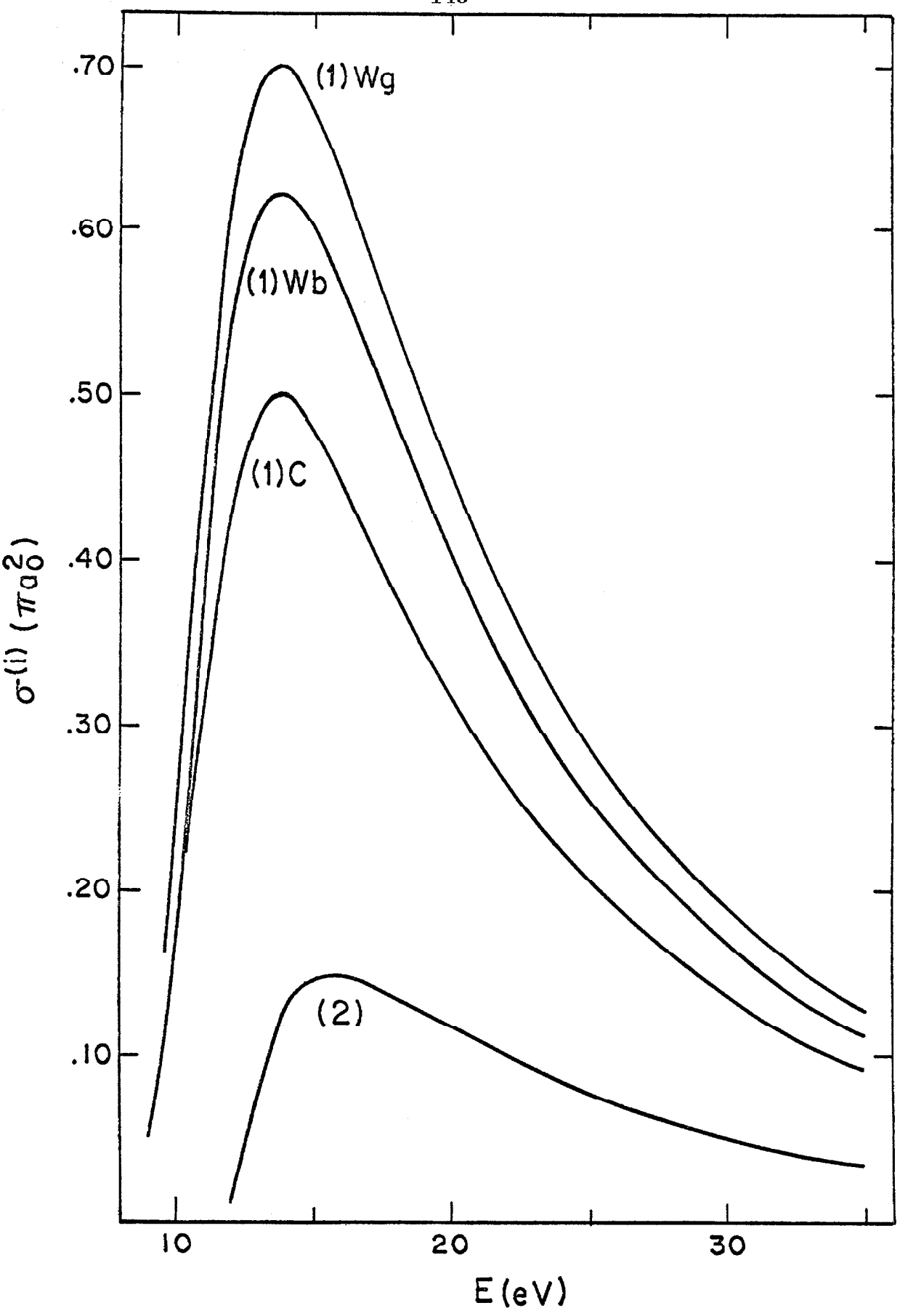

FIGURE 4

FIGURE 5

Effect of different excited state wave functions on the cross section for excitation to the first triplet. Ground state is Weinbaum for both (PM)--Phillipson-Mulliken, (H) Hurley.

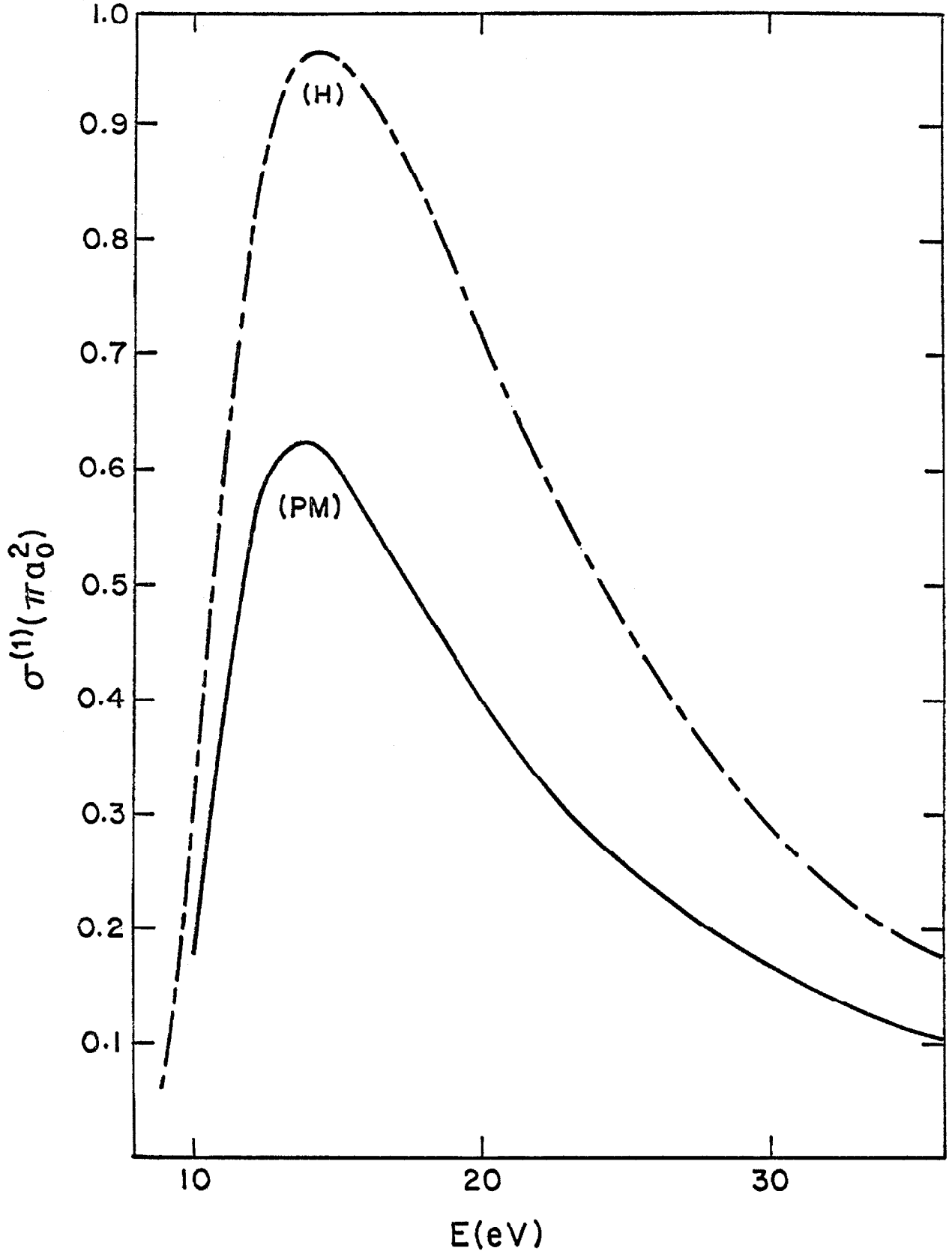

FIGURE 5

FIGURE 6

Energy dependence of excitation cross section to first triplet: (OC)--Ochkur, complete; (OSA)--Ochkur, separated atom; (ORC)--Ochkur Rudge, complete; (ORSA)--Ochkur Rudge, separated atom.

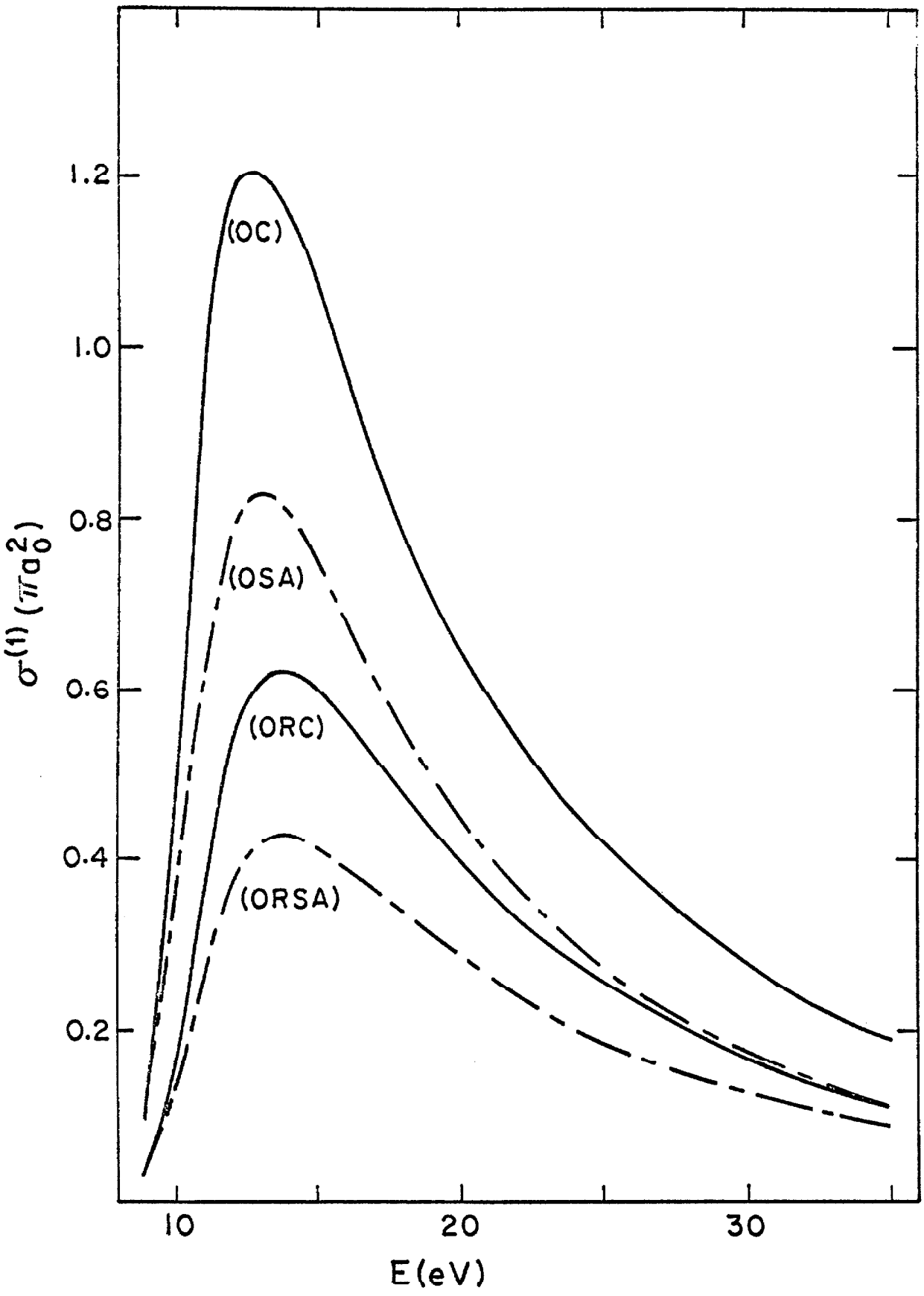

FIGURE 6

FIGURE 7

Energy dependence of excitation cross section to first triplet: (ORC)--Ochkur Rudge, complete; (OC)--Ochkur complete; (E1)--first order exchange; (K)--Khare-one center, Ochkur.

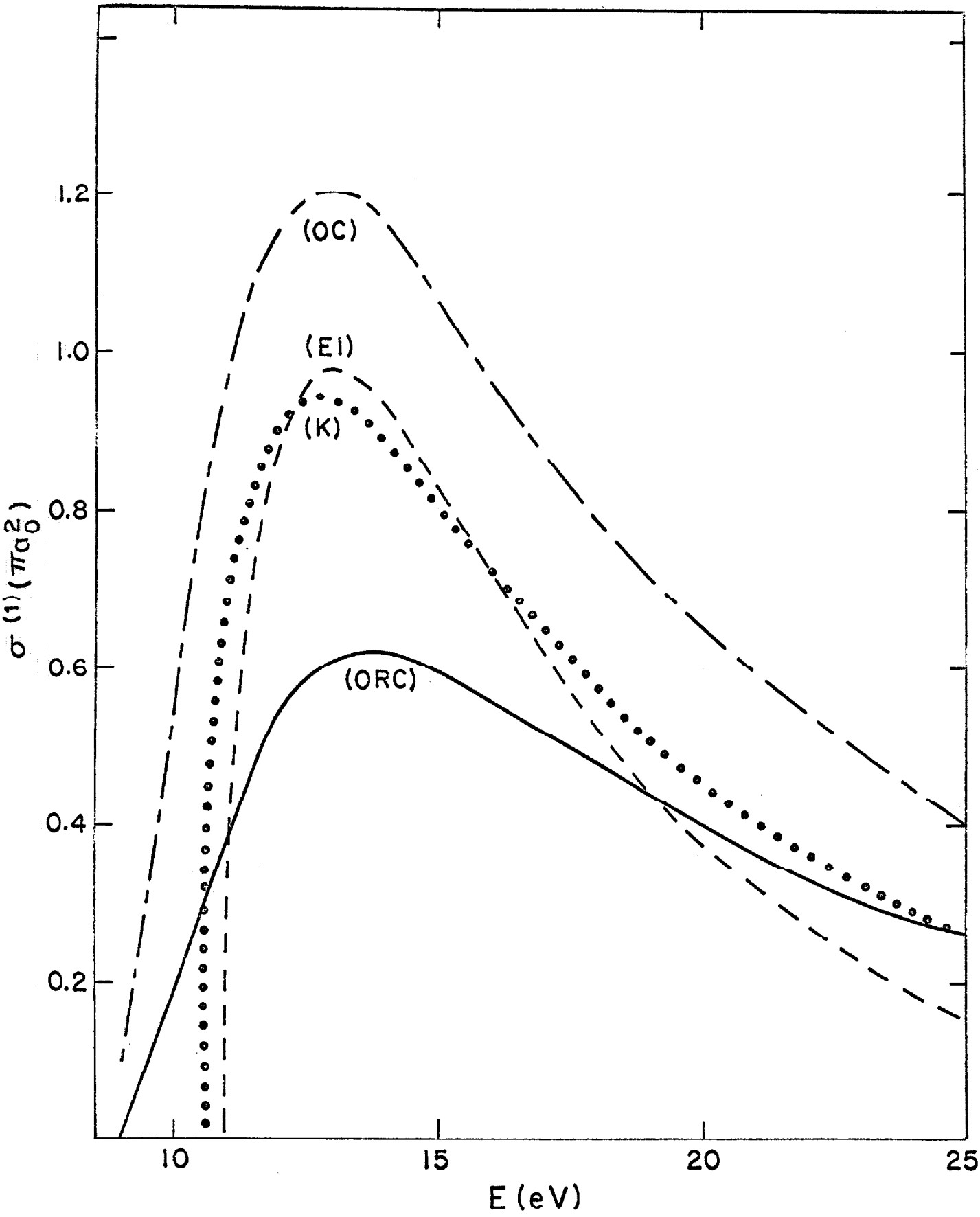

FIGURE 7

FIGURE 8

Effect of ground state wave function on cross section for excitation to second triplet state, for (OR), complete and separated atom approximations:— — — —separated atom (SA): (C)--Coulson; (WB)--Weinbaum; (Wg)--Wang; ————————complete (curves corresponding to the three different ground state wave functions coincide within plotting accuracy); — — — — (K), Khare one-center Ochkur.

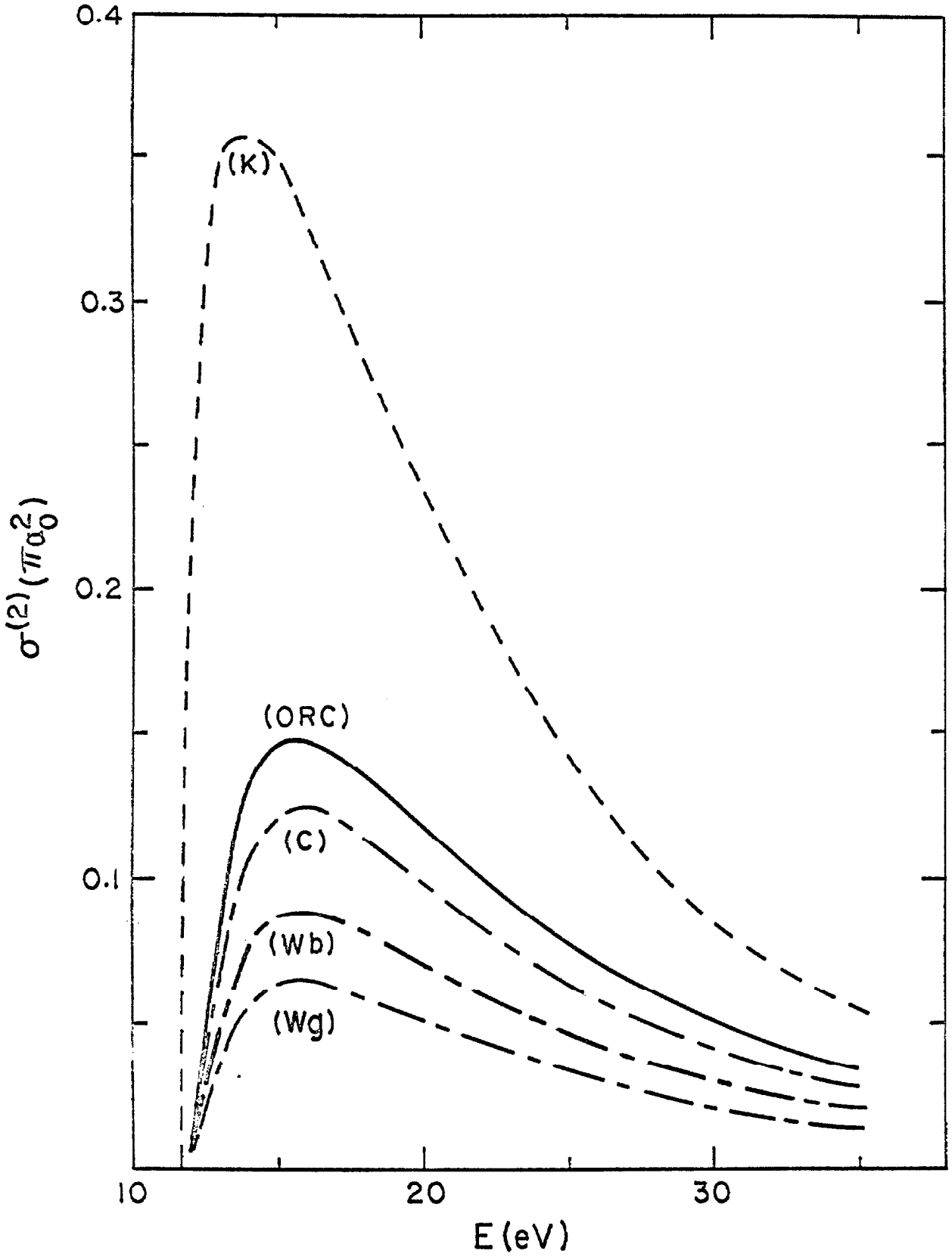

FIGURE 8

FIGURE 9

Dissociation cross section of H_2 into 2H by electron impact. The points are experimental but include the effect of ionization.[42] ——— (Exp), experimental curve[42] after subtraction of molecular ionization cross section; — – — – (ORC), present calculations of the sum of excitation cross sections to first two triplet states (using Weinbaum ground state), including effect of variation of excitation energy; — — — — (K) Khare's one-center Ochkur dissociation cross section.[45]

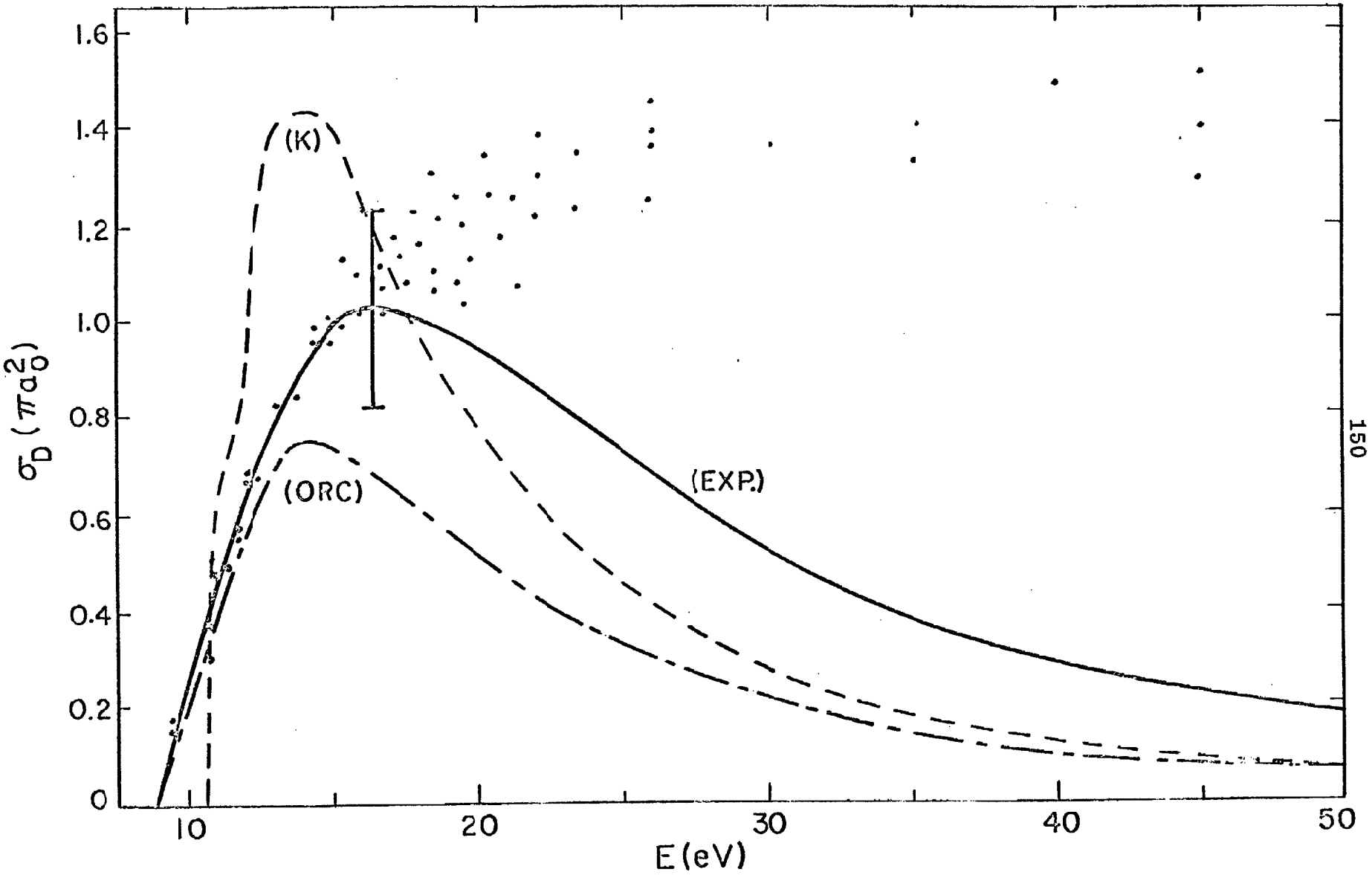
1.6
1.4
1.2
1.0
0.8
0.6
0.4
0.2
0
σ_D (πa_0^2)
(K)
(ORC)
(EXP.)
10
20
30
40
50
E(eV)
150

FIGURE 9

FIGURE 10

Dissociation cross section of H_2 into 2H by electron impact. ——(ORC), present calculations (same as in Fig. 9); — – — – — Corrigan data as modified by using ionization cross section of Golden and Rapp;[64] ----- Corrigan data as modified using ionization data of Harrison.[65] The shading along the two experimental curves indicates the spread in experimental data as reported by Corrigan.[42]

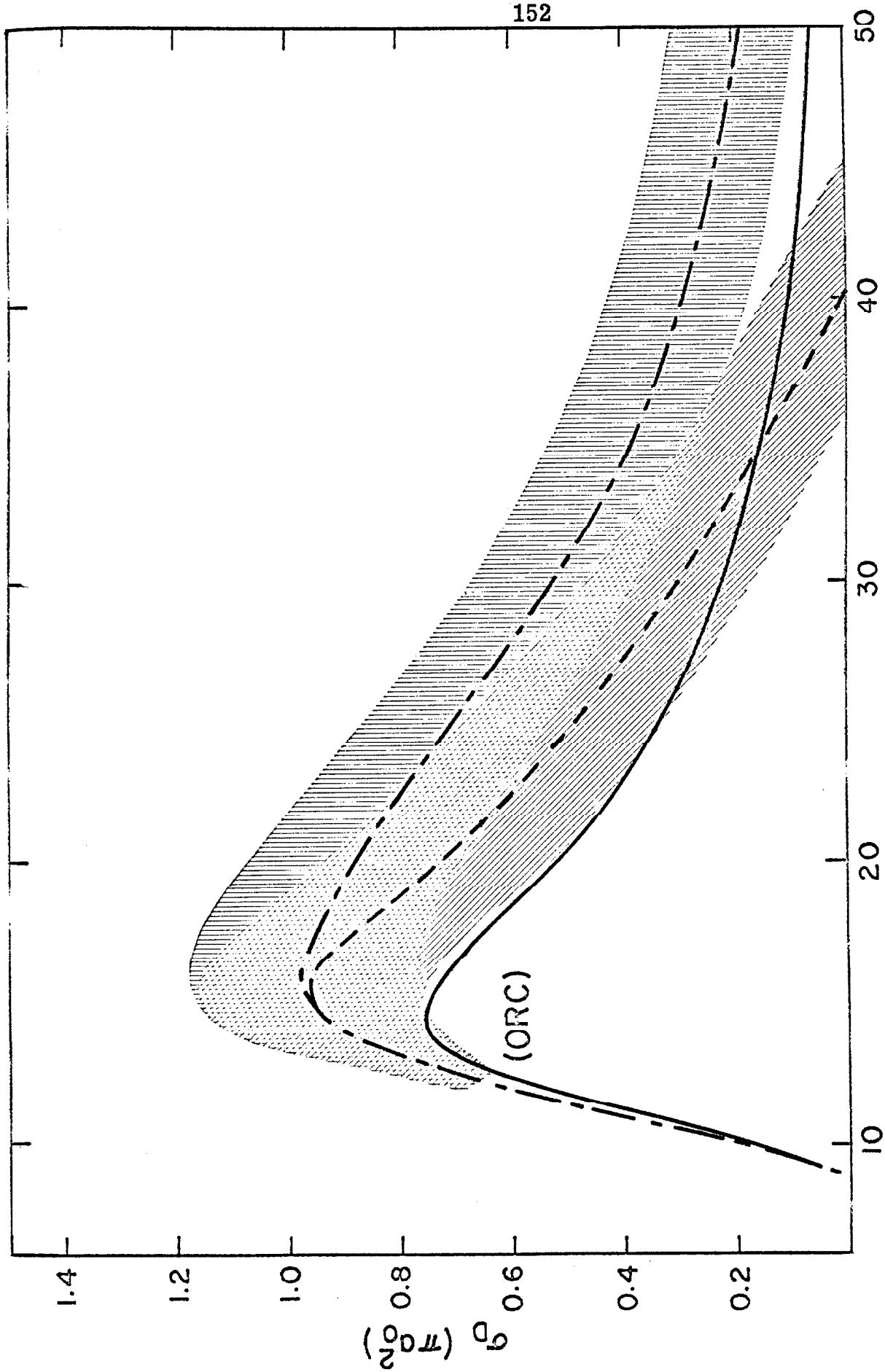

FIGURE 10

FIGURE 11

The effect of different wave functions on the total cross section for excitation of the 2^3S state of helium in the (OR) approximation. The ground state wave functions are: C-Clementi, G-Green et. al., H-Hylleraas; the excited state wave functions are: MYH-Morse, et. al., VES-Veselov et. al..

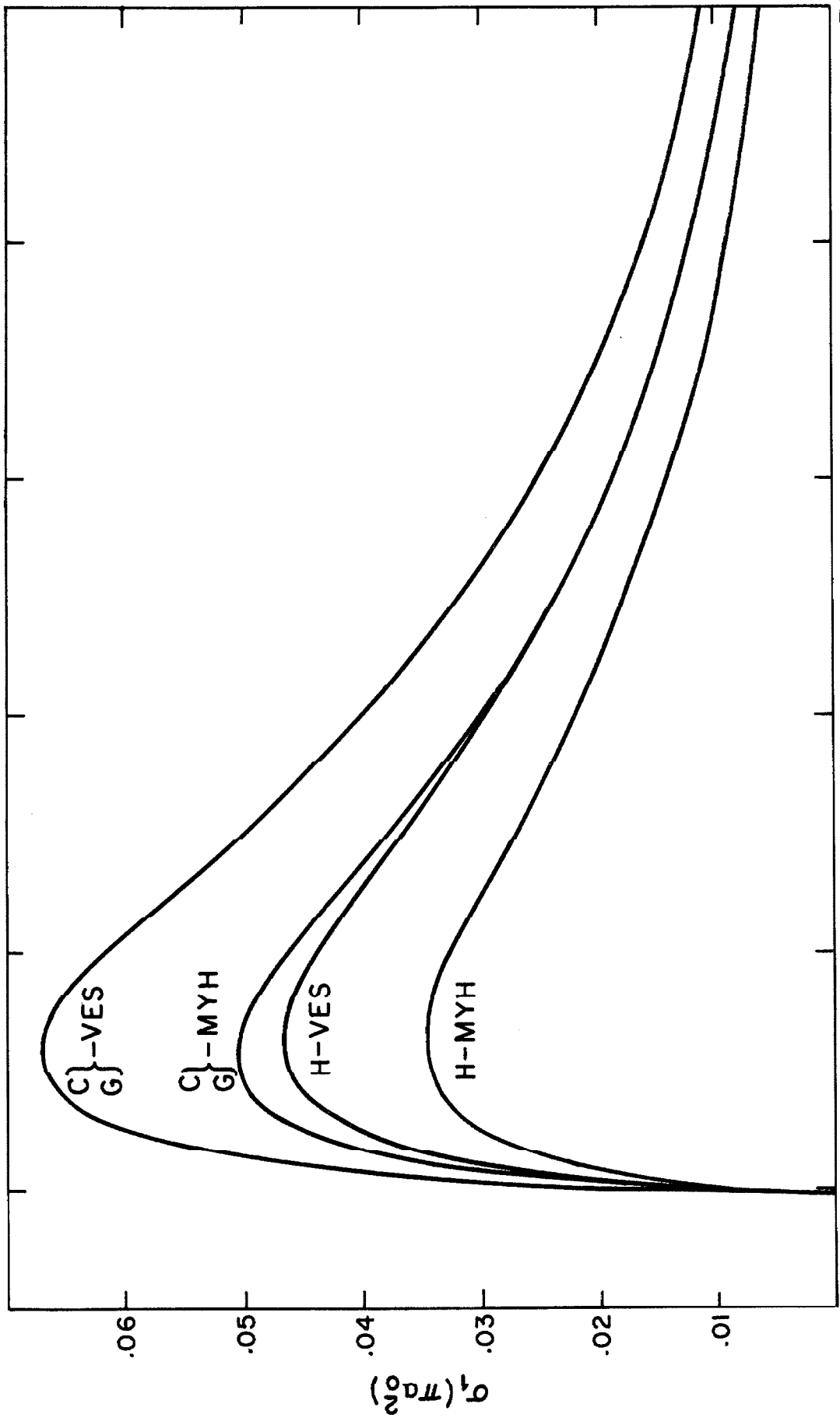
.06
.05
.04
.03
.02
.01
$\sigma_1(\pi a_o^2)$
20
30
40
50
60
70
E (eV)
Cl
G
-VES
Cl
G
-MYH
H-VES
H-MYH

FIGURE 11

FIGURE 12

The effect of different wave functions on the total cross section for excitation of the 2^3P state of helium in the (OR) approximation. (———), C or G and MYH; (·····), C or G and VES; (– ——–), H and MYH; (-----), H and VES. The abbreviations are the same as for Fig. 11.

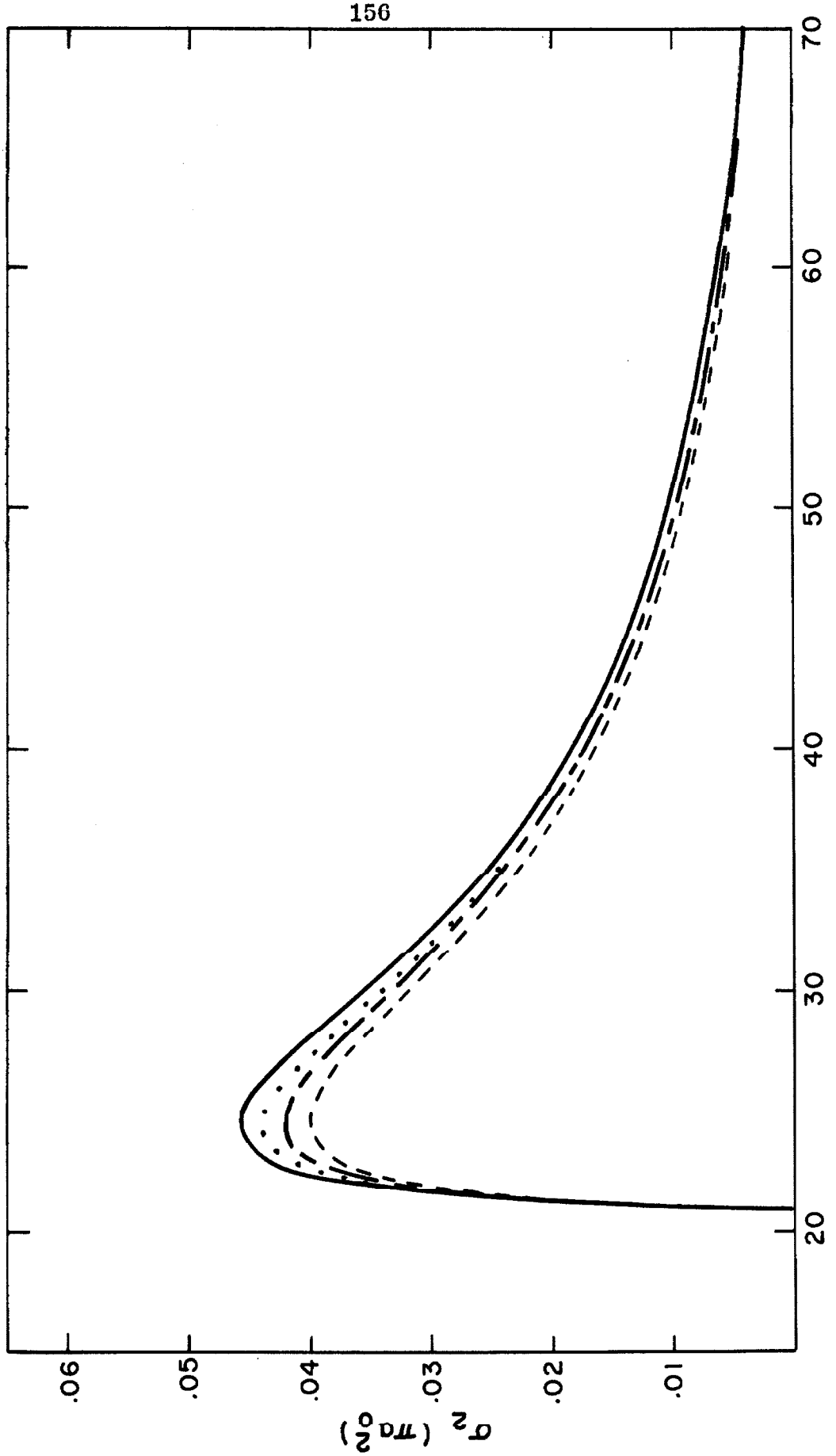

FIGURE 12

FIGURE 13

Comparison of the total cross sections for the excitation of the 2^3S state of helium as calculated in the (O) and (OR) approximations. The wave functions used in both cases were the Green et. al. and MYH for the ground and excited states.

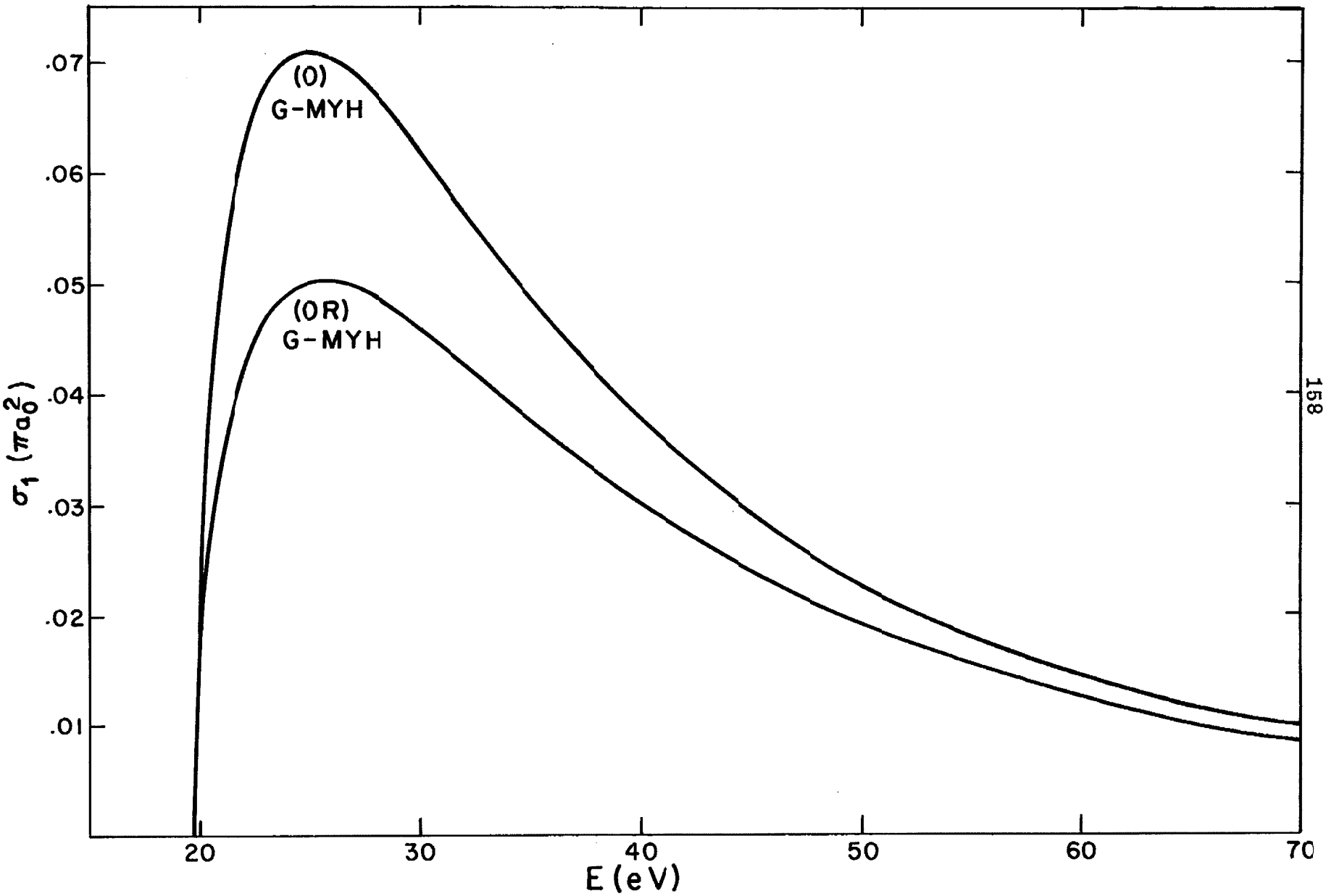
(0)
G-MYH
(0R)
G-MYH
.07
.06
.05
.04
.03
.02
.01
σ_1 (πa_0^2)
20
30
40
50
60
70
E (eV)

FIGURE 13

FIGURE 14

Comparison of the total cross sections for the excitation of the 2^3P state of helium as calculated in the (O) and (OR) approximation. The wave functions used in both cases were the Green et. al. and MYH for the ground and excited states.

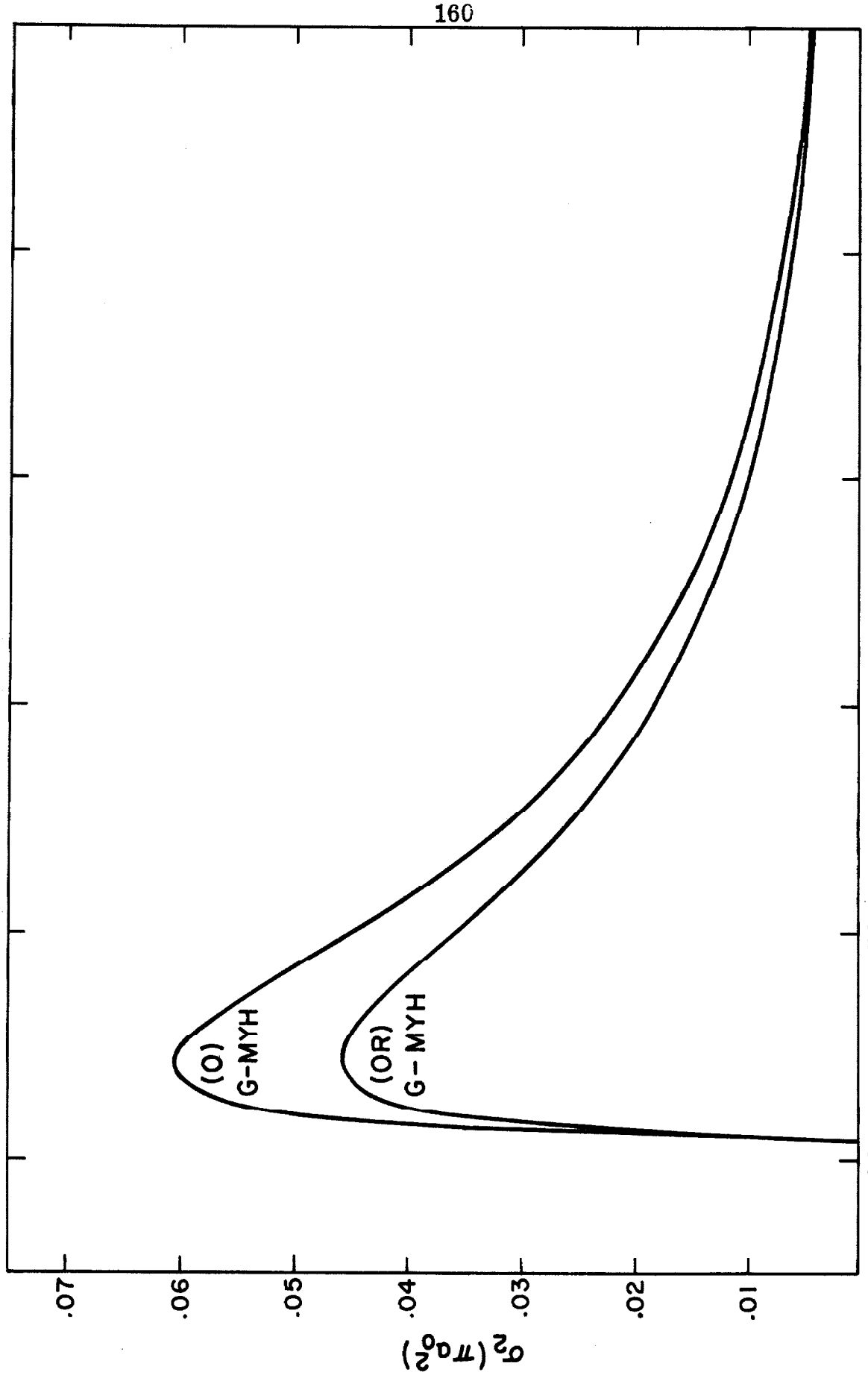
.07
.06
.05
.04
.03
.02
.01
$\sigma_2(\pi a_0^2)$
20
30
40
50
60
70
E (eV)
(O)
G-MYH
(OR)
G-MYH

FIGURE 14

FIGURE 15

Total cross section for the excitation of the 2^3S state of helium. (———), present (OR) calculations using Clementi and Morse et. al. wave functions; (— — — —), distorted wave calculations of Massey and Moiseiwitsch[66]; (x), extrapolated data of Gabriel and Heddle[61]; (▲), extrapolated maximum of Yakhontova[75b] data; (O), Schulz and Fox[76] maximum value; (□), Maier-Liebnitz[76] maximum value; (▽), maximum value of Fleming and Higginson[86].

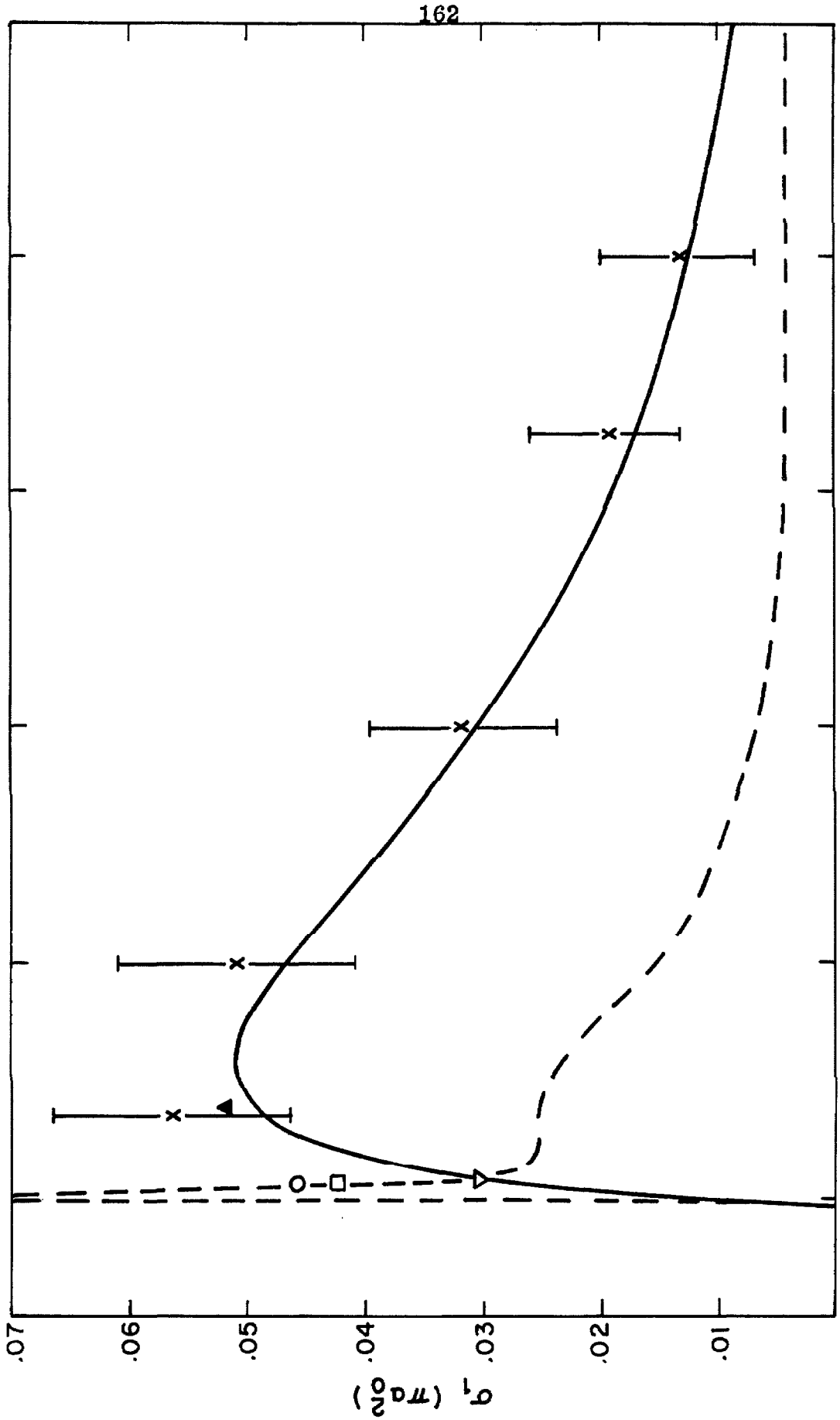

FIGURE 15

FIGURE 16

The total cross section for the excitation of the 2^3P state of helium. (———), present (OR) calculations using Clementi and Veselov et. al. wave functions; (x), extrapolated data of Gabriel and Heddle[61]; (o), data of Frost and Phelps[78a]; (Δ), data point of Holt and Krotkov[78b]; (▼), data point of St. John et. al.[79].

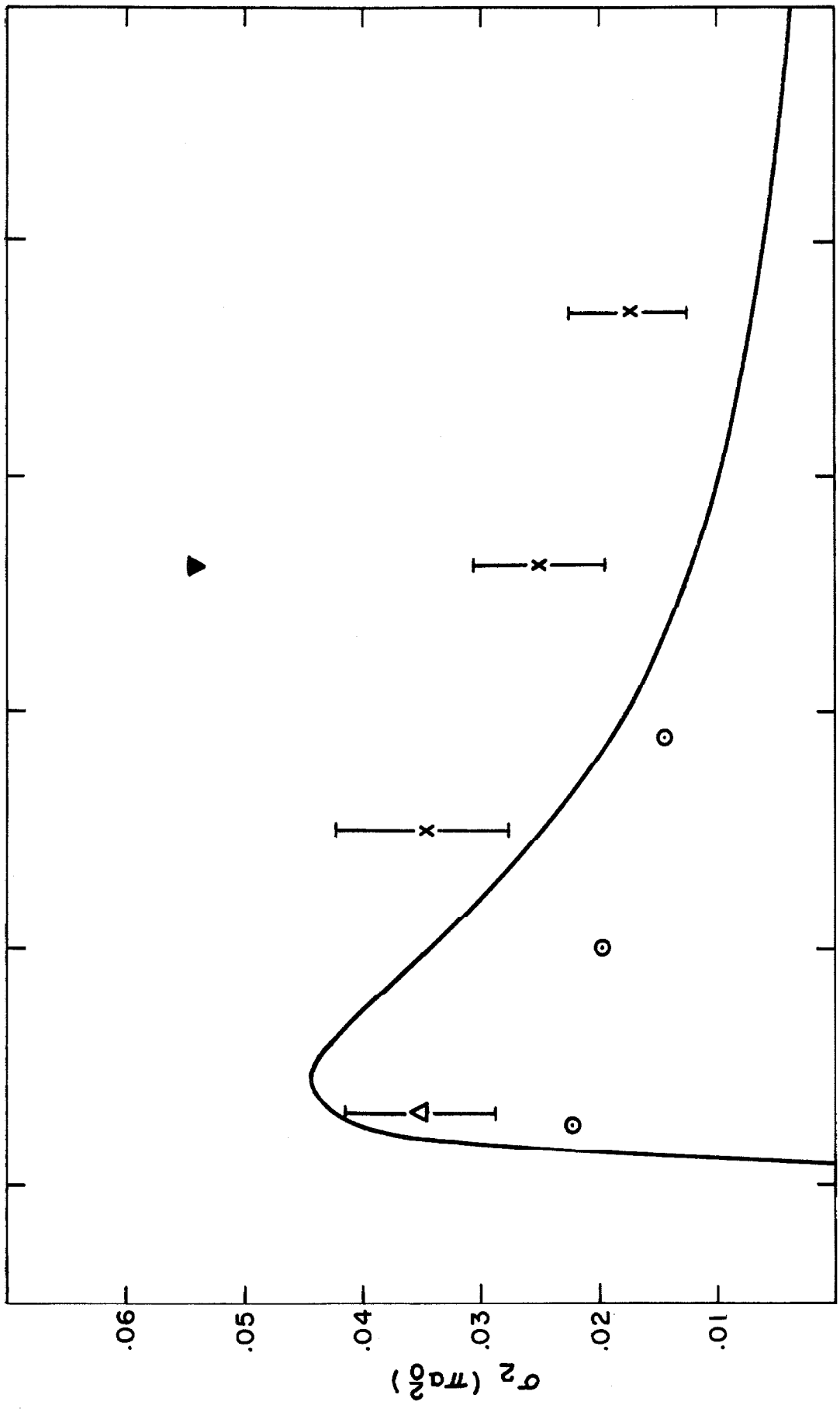

FIGURE 16

FIGURE 17

Perspective view of the differential cross section for excitation of the $b^3\Sigma_u^+$ state of molecular hydrogen. Calculated using the (OR) approximation with Weinbaum[50b] and Phillipson-Mulliken[51a] wave functions. The axis is as labeled and the spherical polar angles from which direction the array is viewed are indicated on the lower portion of the figure.

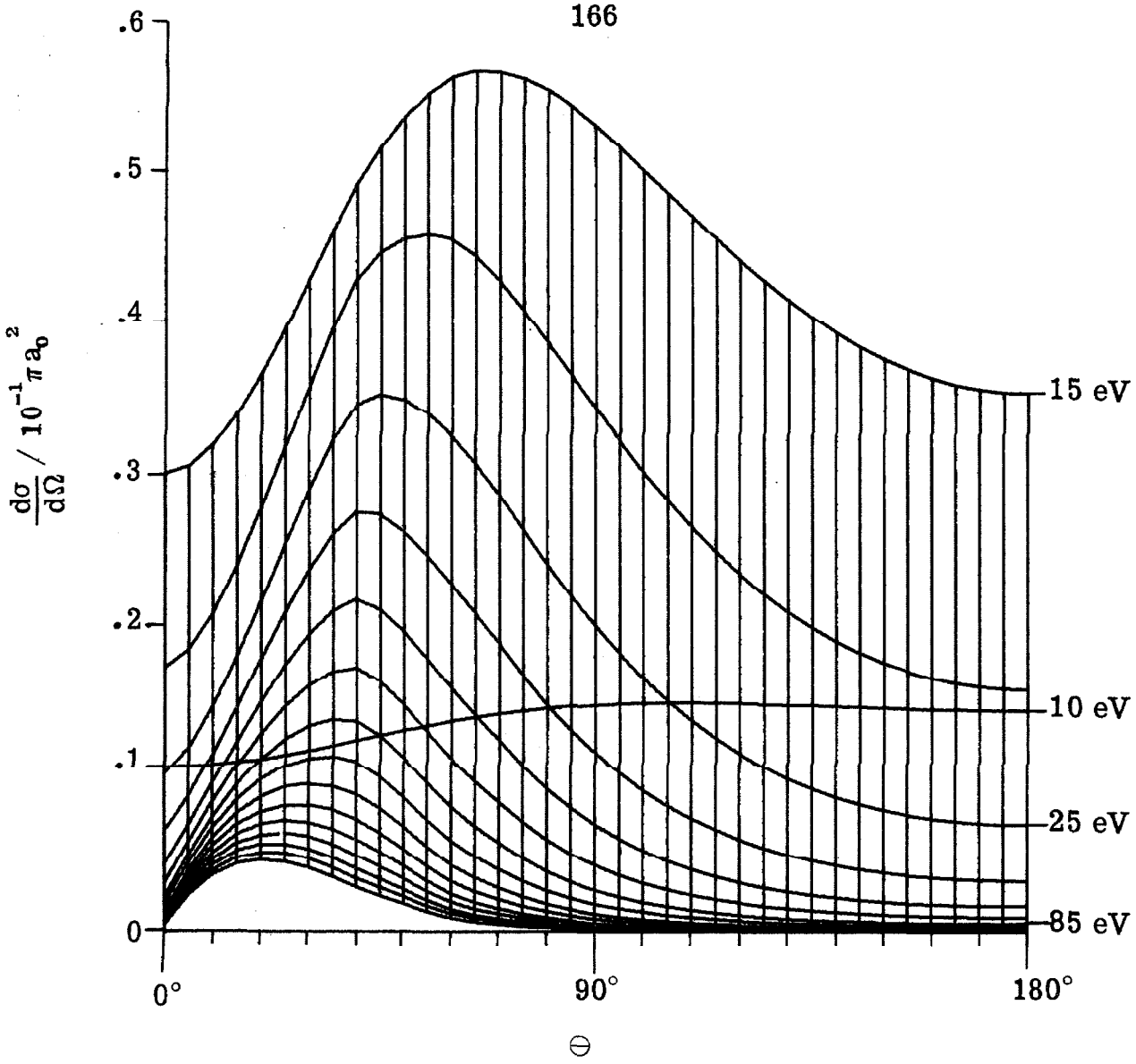

Molecular Hydrogen $X^1\Sigma_g^+ \rightarrow b^3\Sigma_u^+$

AMAX= .057

VIEWING ANGLE
THETA = 90.00
PHI = 0.00

EXECUTION TIME .14 MIN
MODE = 1
RUDGE H2 1ST-TR WEIN-PM

ARRAY SIZE

	NATURAL DIMENSION	REGION PLOTTED
X	16	1 THRU 16
Y	37	1 THRU 37

FIGURE 17

FIGURE 18

Perspective view of the differential cross section for excitation of the $b^3\Sigma_u^+$ state of molecular hydrogen. Calculated using the (OR) approximation with Weinbaum[50b] and Phillipson-Mulliken[51a] wave functions. The axis is as labeled and the spherical polar angles from which direction the array is viewed are indicated on the lower portion of the figure.

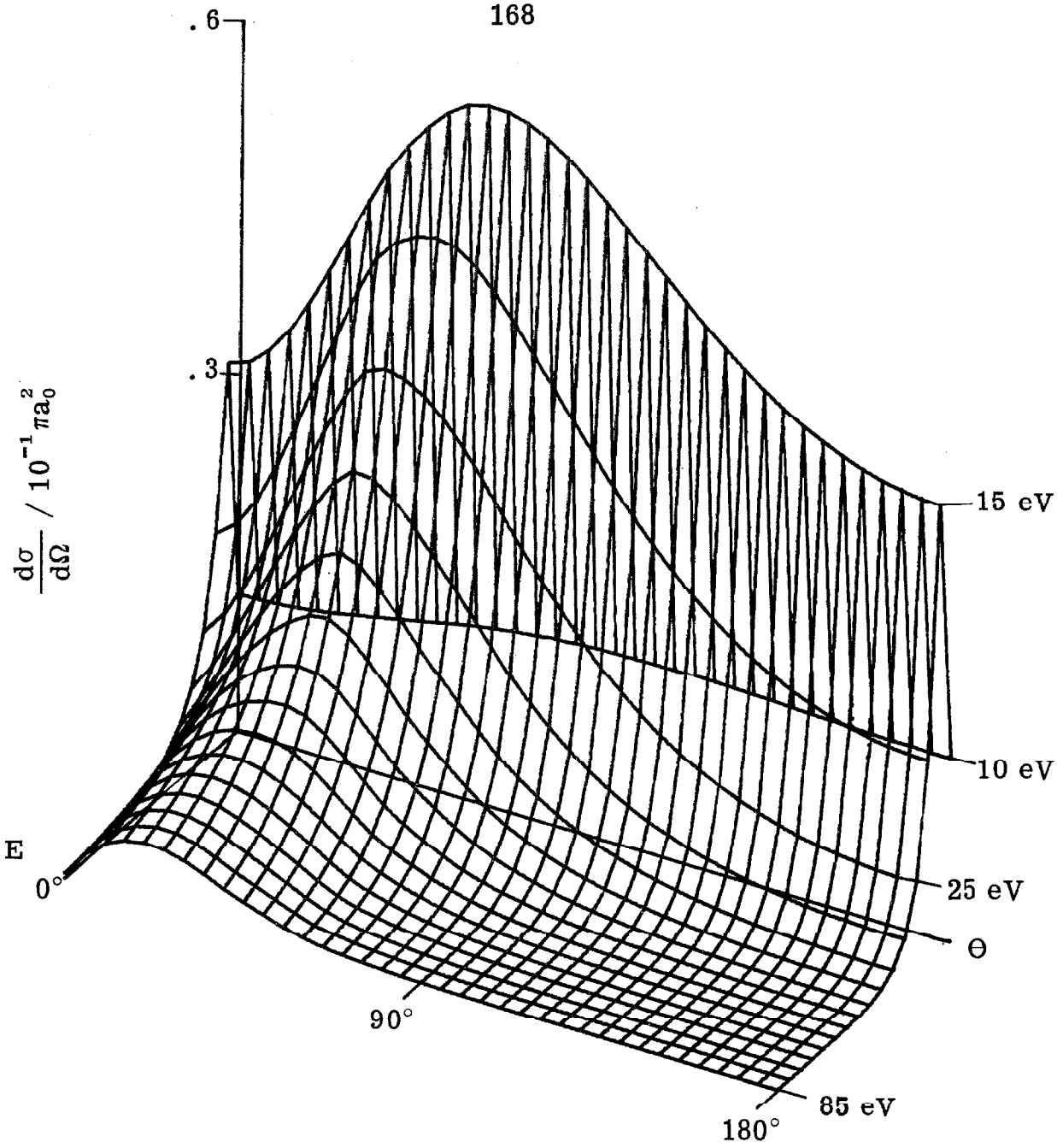

Molecular Hydrogen $X^1\Sigma_g^+ \longrightarrow b^3\Sigma_u^+$

AMAX= .057

VIEWING ANGLE
THETA = 60.00
PHI = 30.00

EXECUTION TIME .09 MIN
MODE = 1
RUDGE H2 1ST-TR WEIN-PM

ARRAY SIZE

	NATURAL DIMENSION	REGION PLOTTED
X	16	1 THRU 16
Y	37	1 THRU 37

FIGURE 18

FIGURE 19

Perspective view of the differential cross section for excitation of the $b^3\Sigma_u^+$ state of molecular hydrogen. Calculated using the (OR) approximation with Weinbaum[50b] and Phillipson-Mulliken[51a] wave functions. The axis is as labeled and the spherical polar angles from which direction the array is viewed are indicated on the lower portion of the figure.

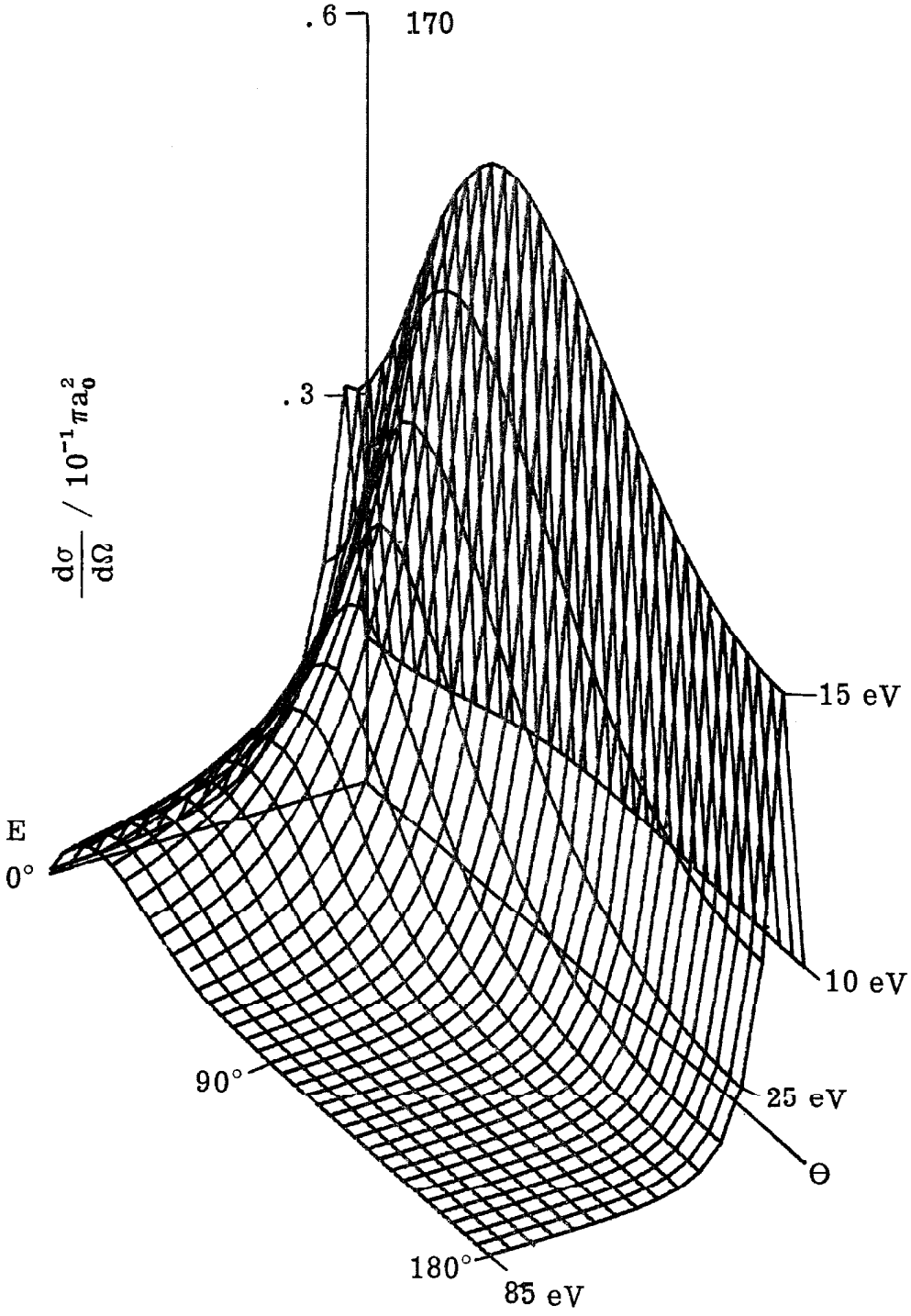

Molecular Hydrogen $X\,^1\Sigma_g^+ \longrightarrow b\,^3\Sigma_u^+$

AMAX= .057

VIEWING ANGLE
THETA = 60.00
PHI = 60.00

EXECUTION TIME .09 MIN
MODE = 1
RUDGE H2 1ST-TR WEIN-PM

ARRAY SIZE

	NATURAL DIMENSION	REGION PLOTTED
X	16	1 THRU 16
Y	37	1 THRU 37

FIGURE 19

FIGURE 20

Perspective view of the differential cross section for excitation of the $a^3\Sigma_g^+$ state of molecular hydrogen. Calculated using the (OR) approximation with Weinbaum[50b] and Hartree-Fock wave functions. The axis is as labeled and the spherical polar angles from which direction the array is viewed are indicated on the lower portion of the figure.

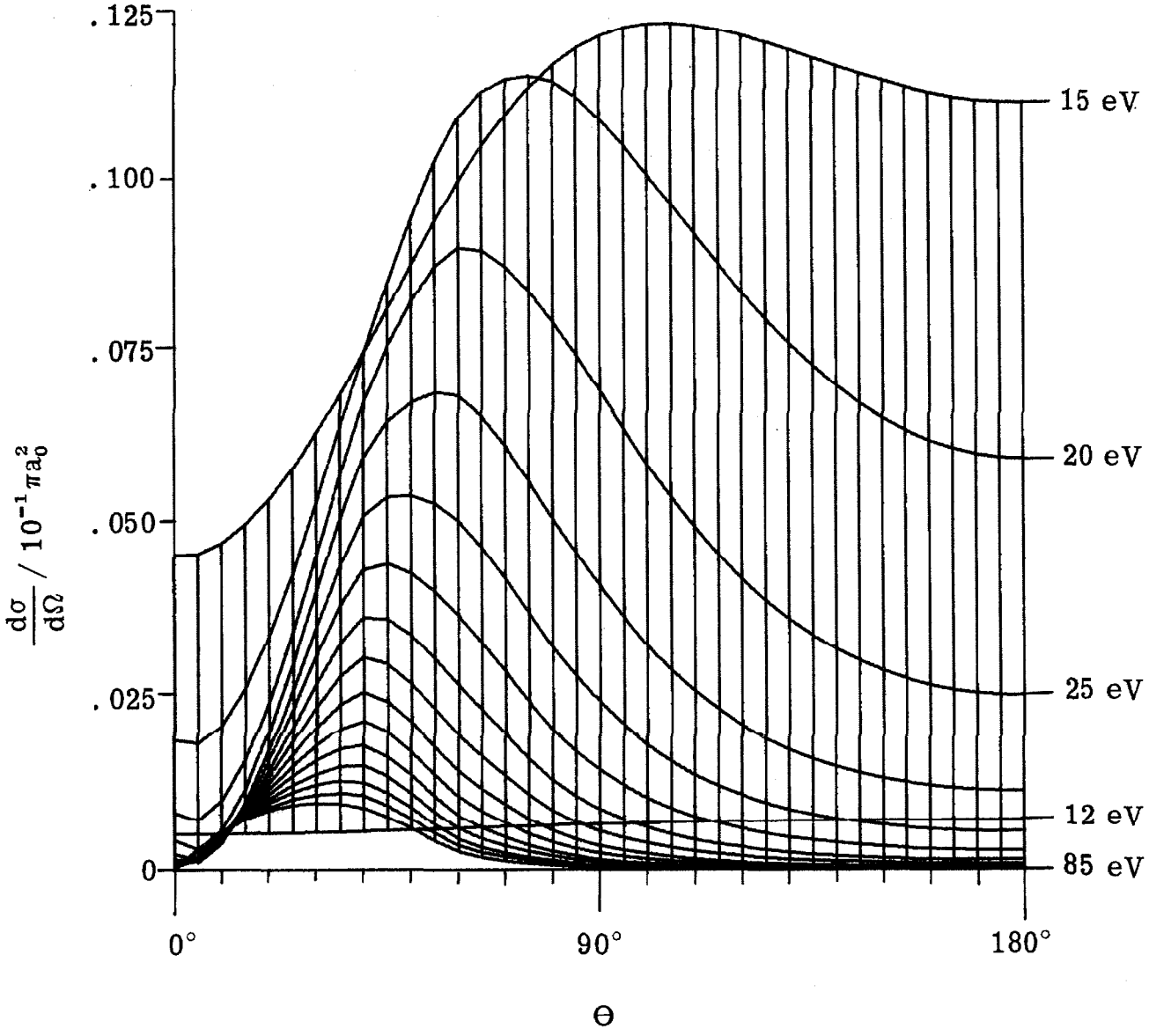

Molecular Hydrogen $X^1\Sigma_g^+ \rightarrow a^3\Sigma_g^+$

AMAX= .012
VIEWING ANGLE
THETA = 90.00
PHI = 0.00
EXECUTION TIME .11 MIN
MODE = 1
RUDGE H2 2ND-TR WEIN-G1

ARRAY SIZE

	NATURAL DIMENSION	REGION PLOTTED
X	16	1 THRU 16
Y	37	1 THRU 37

FIGURE 20

FIGURE 21

Perspective view of the differential cross section for excitation of the $a^3\Sigma_g^+$ state of molecular hydrogen. Calculated using the (OR) approximation with Weinbaum[50b] and Hartree-Foch wave functions. The axis is as labeled and the spherical polar angles from which direction the array is viewed are indicated on the lower portion of the figure.

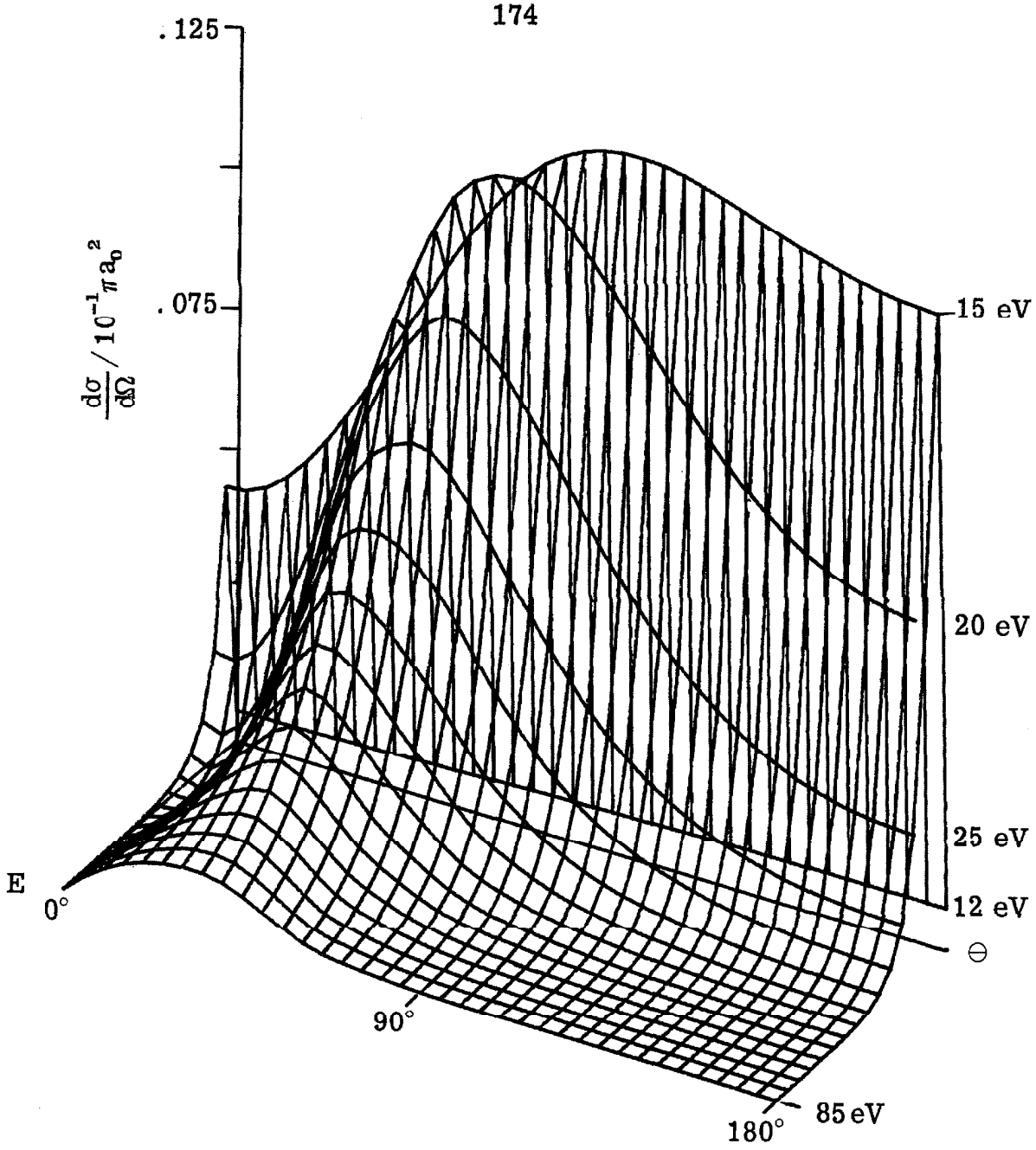

Molecular Hydrogen $X^1\Sigma_g^+ \rightarrow a^3\Sigma_g^+$

AMAX= .012

VIEWING ANGLE
THETA = 60.00
PHI = 30.00

EXECUTION TIME .10 MIN
MODE = 1
RUDGE H2 2ND-TR WEIN-G1

ARRAY SIZE

	NATURAL DIMENSION	REGION PLOTTED
X	16	1 THRU 16
Y	37	1 THRU 37

FIGURE 21

FIGURE 22

Perspective view of the differential cross section for excitation of the $a^3\Sigma_g^+$ state of molecular hydrogen. Calculated using the (OR) approximation with Weinbaum[50b] and Hartree-Foch wave functions. The axis is as labeled and the spherical polar angles from which direction the array is viewed are indicated on the lower portion of the figure.

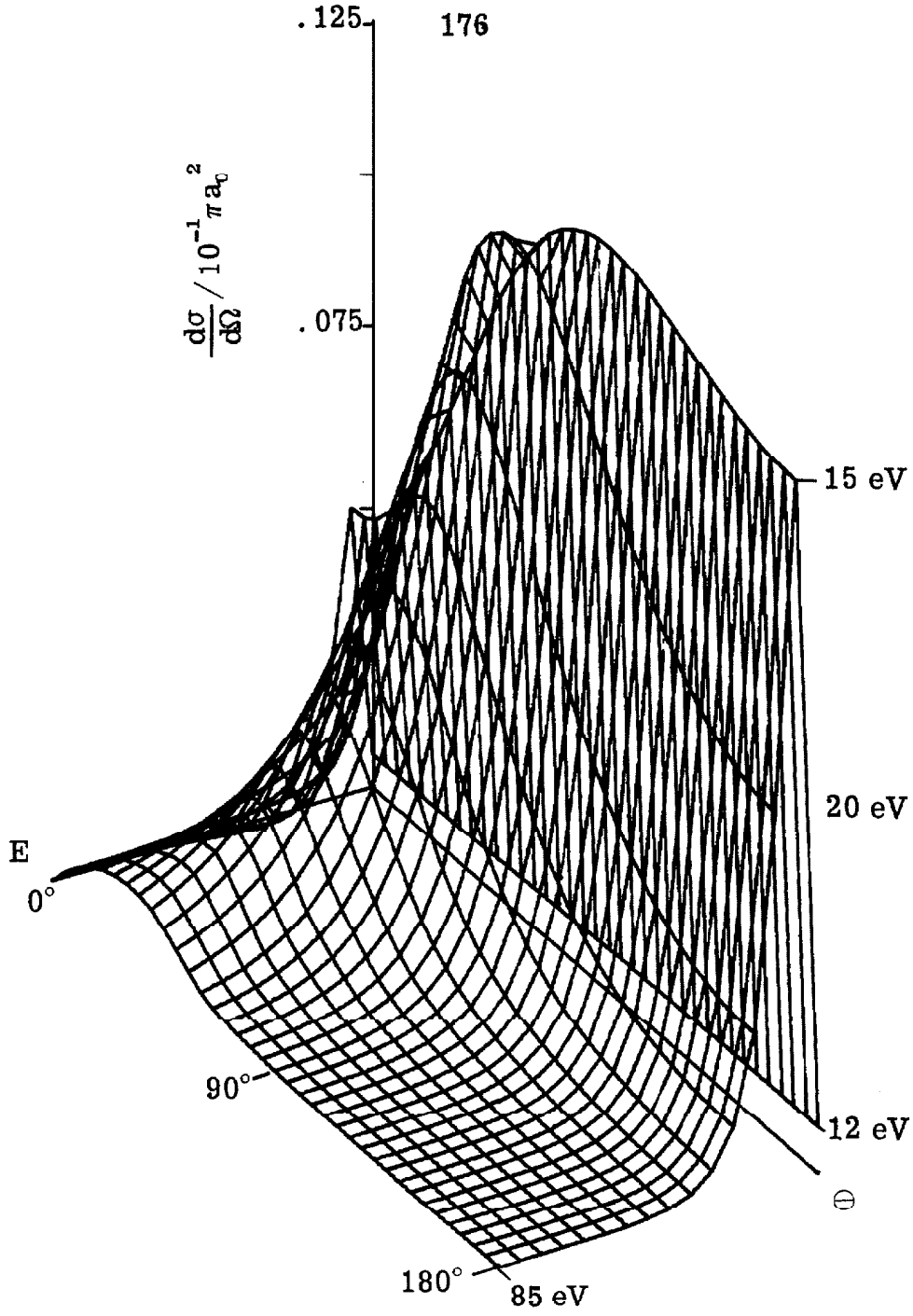

Molecular Hydrogen $X^1\Sigma_g^+ \rightarrow a^3\Sigma_g^+$

AMAX= .012

VIEWING ANGLE
THETA = 60.00
PHI = 60.00

EXECUTION TIME .10 MIN
MODE = 1
RUDGE H2 2ND-TR WEIN-G1

ARRAY SIZE

	NATURAL DIMENSION	REGION PLOTTED
X	16	1 THRU 16
Y	37	1 THRU 37

FIGURE 22

FIGURE 23

Perspective view of the differential cross section for excitation of the 2^3S state of helium. Calculated using the (OR) approximation with Green et. al. [72b] and MYH[73a] wave functions. The axis is as labeled and the spherical polar angles from which direction the array is viewed are indicated on the lower portion of the figure.

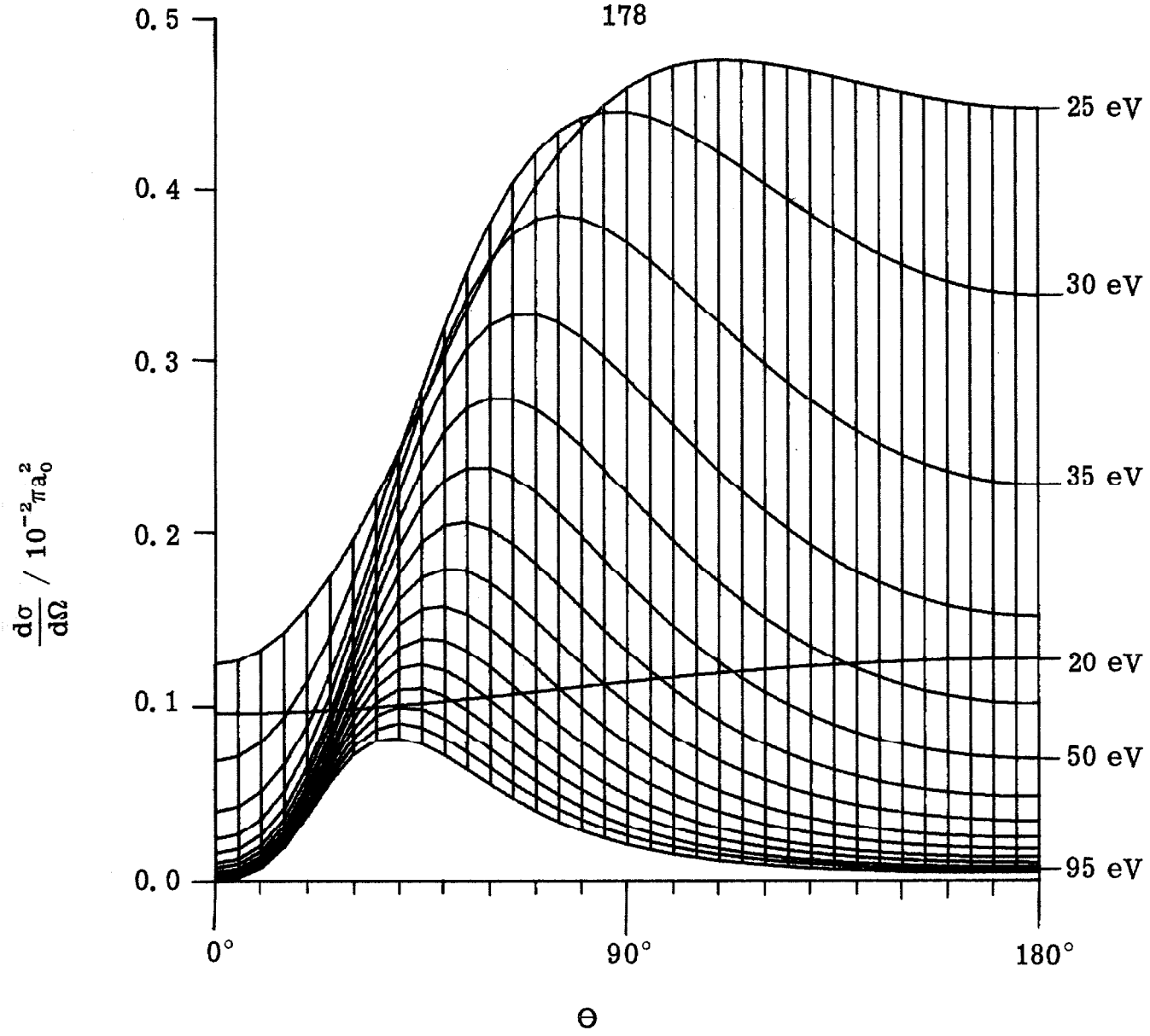

Helium $1^1S \longrightarrow 2^3S$

AMAX= .0047
VIEWING ANGLE
THETA = 90.00
PHI = 0.00
EXECUTION TIME .15 MIN
MODE = 1
RUDGE 1S-2ST GREEN-MYH

ARRAY SIZE

	NATURAL DIMENSION	REGION PLOTTED
X	16	1 THRU 16
Y	37	1 THRU 37

FIGURE 23

FIGURE 24

Perspective view of the differential cross section for excitation of the 2^3S state of helium. Calculated using the (OR) approximation with Green et. al.[72b] and MYH[73a] wave functions. The axis is as labeled and the spherical polar angles from which direction the array is viewed are indicated on the lower portion of the figure.

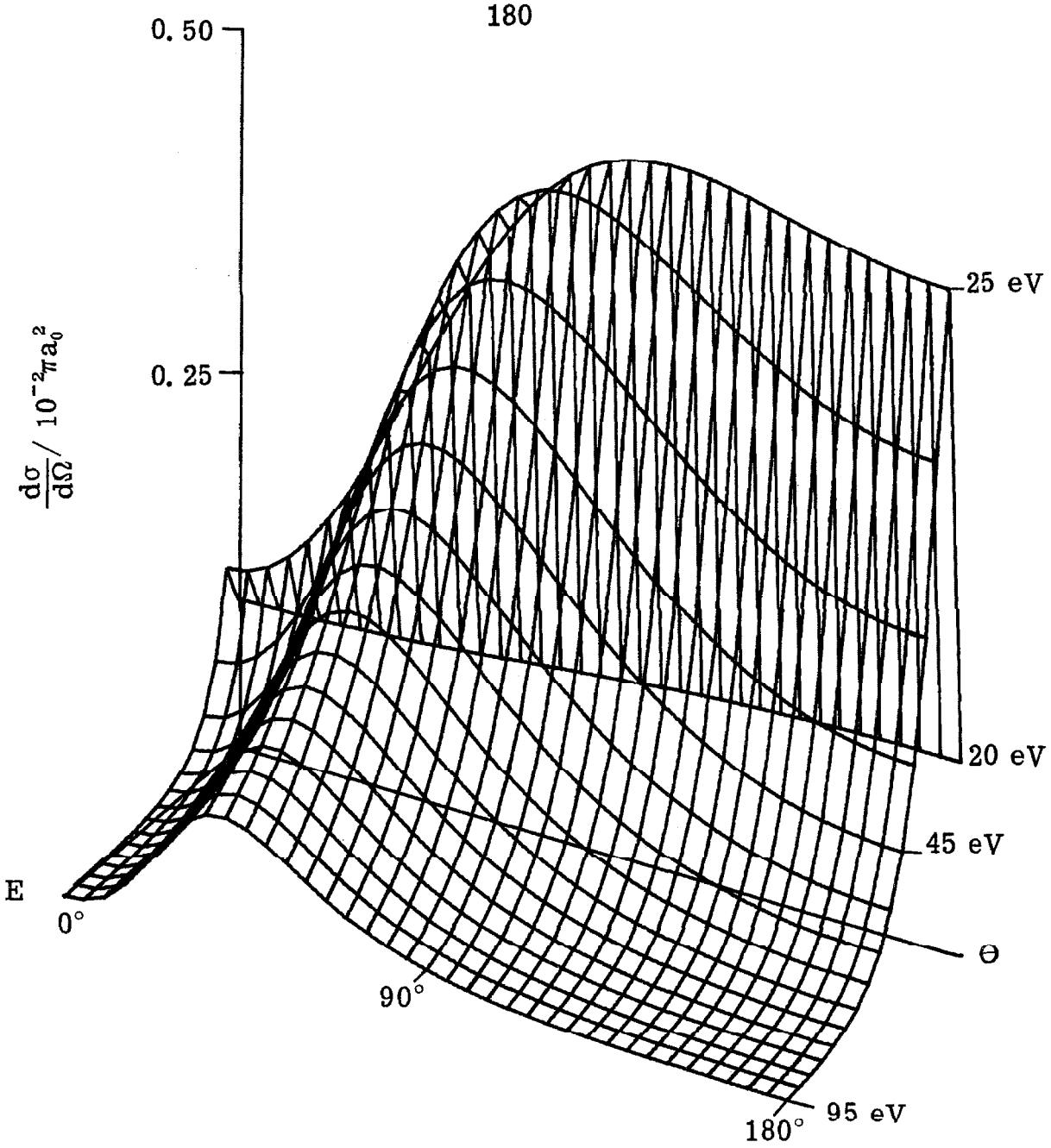

Helium $1^1S \longrightarrow 2^3S$

AMAX= .0047

VIEWING ANGLE
THETA = 60.00
PHI = 30.00

EXECUTION TIME .10 MIN
MODE = 1
RUDGE 1S-2ST GREEN-MYH

ARRAY SIZE

	NATURAL DIMENSION	REGION PLOTTED
X	16	1 THRU 16
Y	37	1 THRU 37

FIGURE 24

FIGURE 25

Perspective view of the differential cross section for excitation of the 2^3S state of helium. Calculated using the (OR) approximation with Green et. al.[72b] and MYH[73a] wave functions. The axis is as labeled and the spherical polar angles from which direction the array is viewed are indicated on the lower portion of the figure.

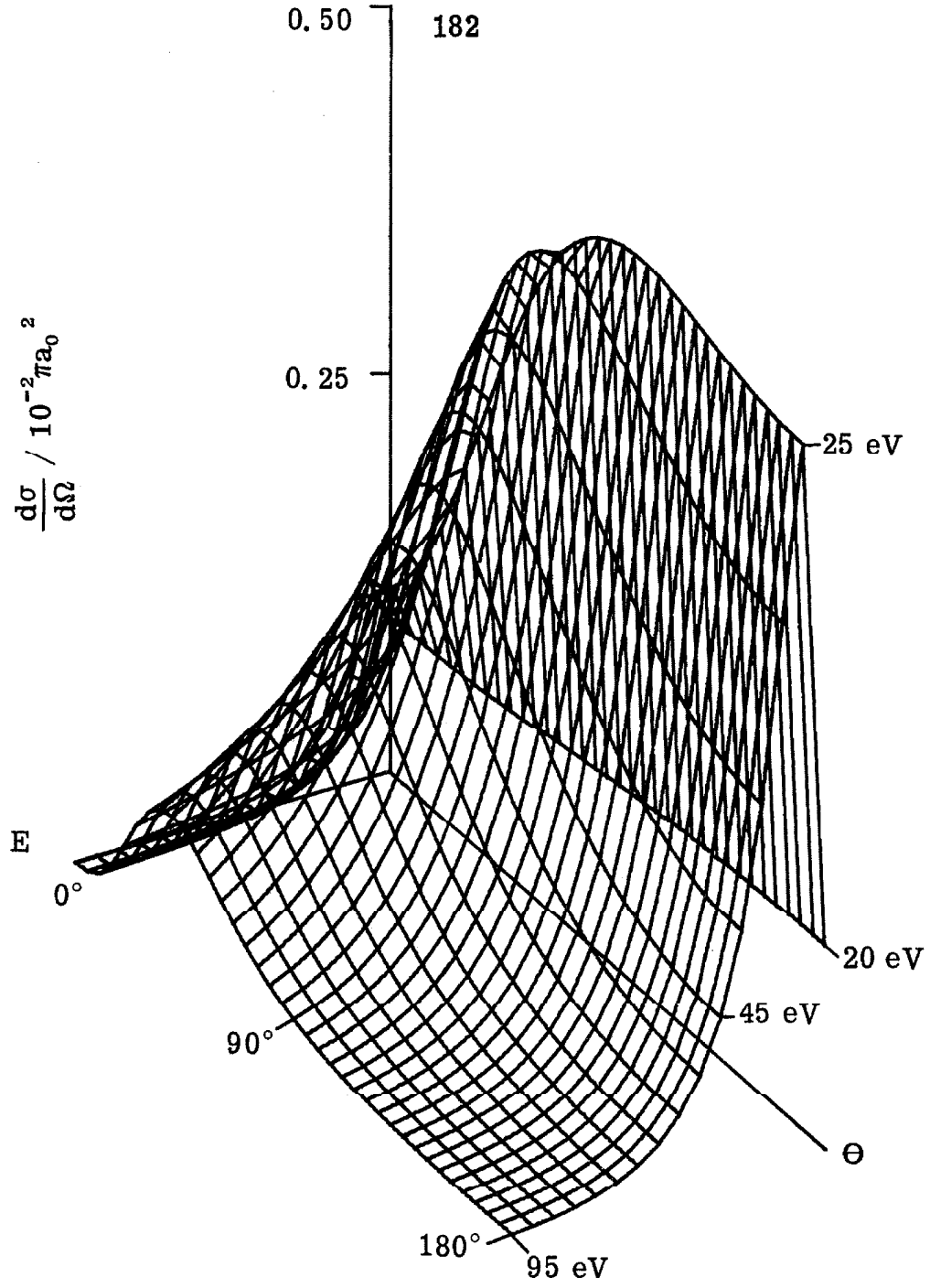

Helium $1^1S \longrightarrow 2^3S$

AMAX= .0047

VIEWING ANGLE
THETA = 60.00
PHI = 60.00

EXECUTION TIME .10 MIN
MODE = 1
RUDGE 1S-2ST GREEN-MYH

ARRAY SIZE

	NATURAL DIMENSION	REGION PLOTTED
X	16	1 THRU 16
Y	37	1 THRU 37

FIGURE 25

FIGURE 26

Comparison of theoretical and experimental angular distributions for excitation of the 2^3S state of helium. Upper plot is for electrons of 20 eV incident energy; lower plot is for electrons of 24 eV incident energy. Vertical bars are experimental points of Ehrhardt and Willmann[82]; solid lines are theoretical results in the (OR) approximation using Green et. al.[72b] and MYH[73a] wave functions.

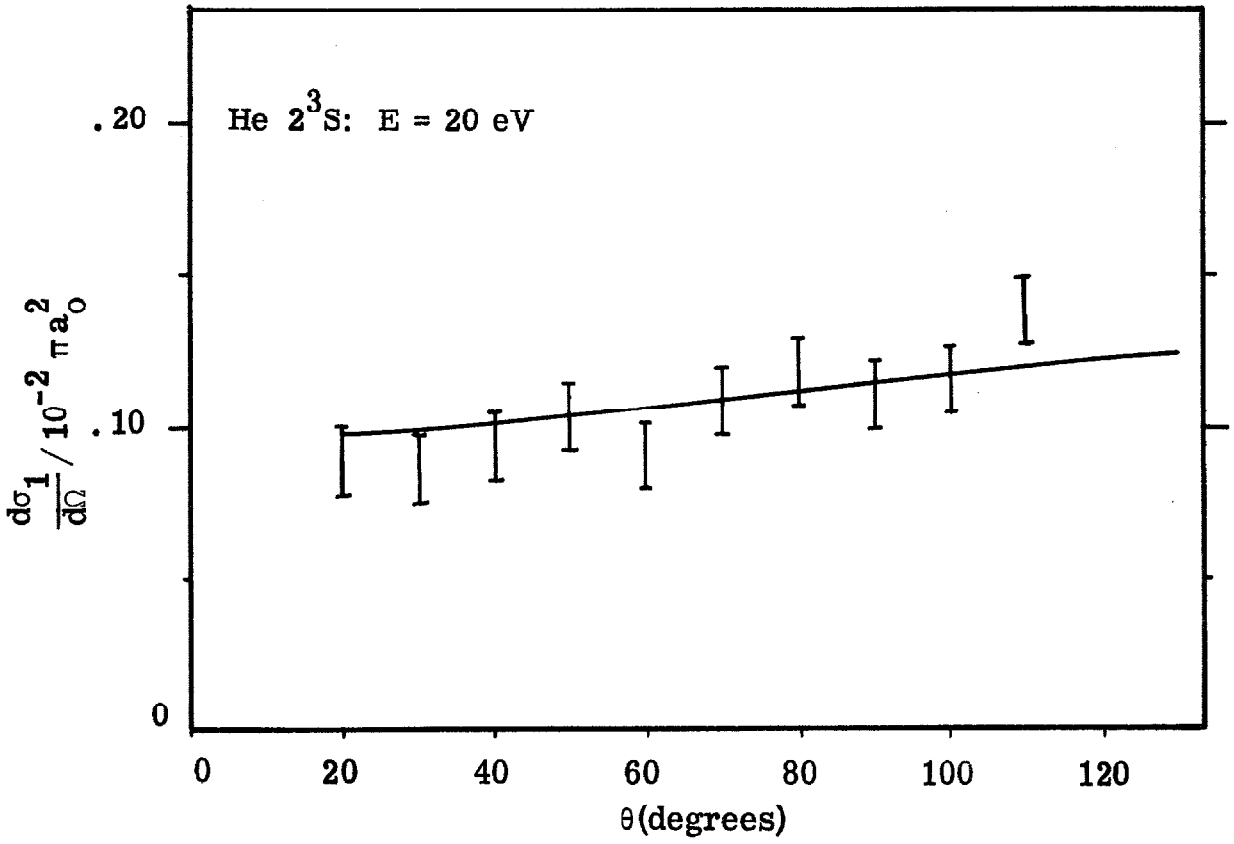
He 2^3S: E = 20 eV
.20
.10
0
$\frac{d\sigma_1}{d\Omega} / 10^{-2} \pi a_o^2$
0
20
40
60
80
100
120
θ(degrees)

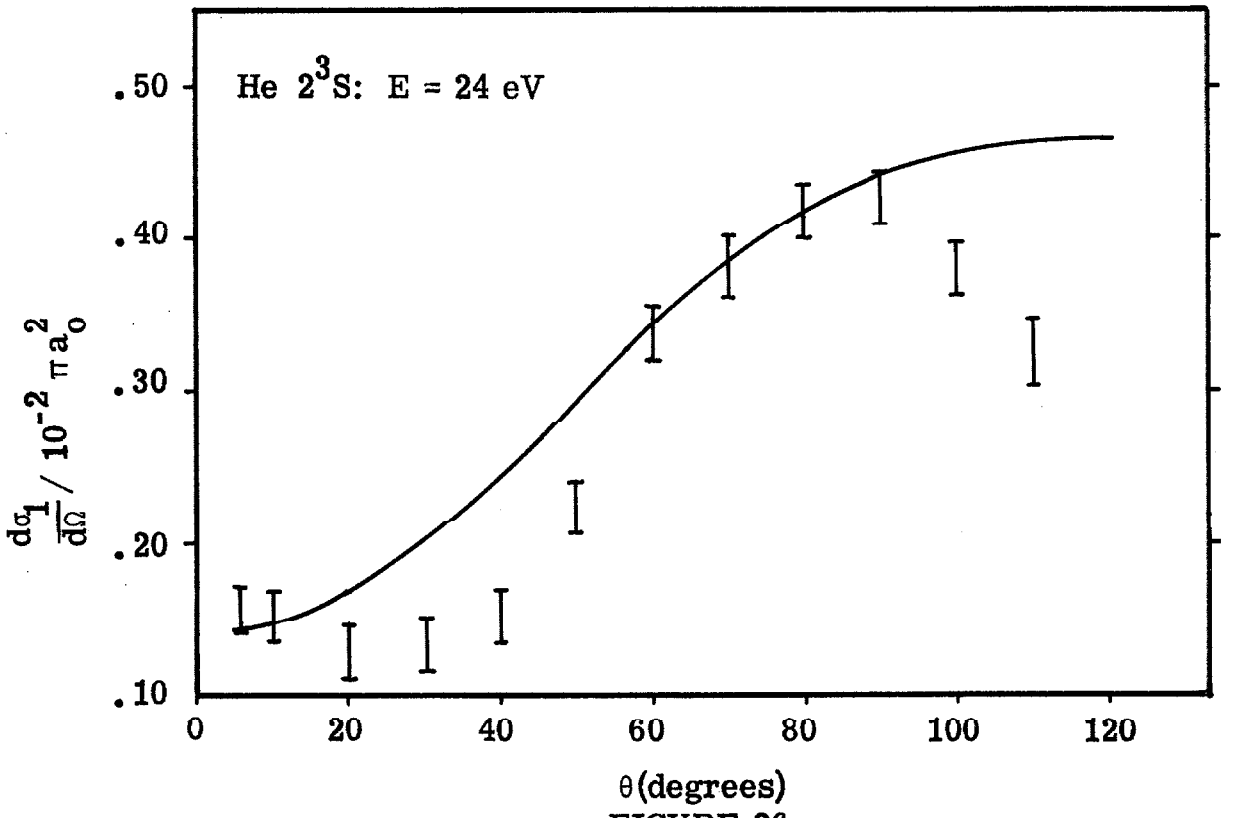
He 2^3S: E = 24 eV
.50
.40
.30
.20
.10
$\frac{d\sigma_1}{d\Omega} / 10^{-2} \pi a_o^2$
0
20
40
60
80
100
120
θ(degrees)

FIGURE 26

FIGURE 27

Perspective view of the differential cross section of the 2^3P state of helium. Calculated using the (OR) approximation with Green et. al. [72b] and MYH[73a] wave functions. The axis is as labeled and the spherical polar angles from which direction the array is viewed are indicated on the lower portion of the figure.

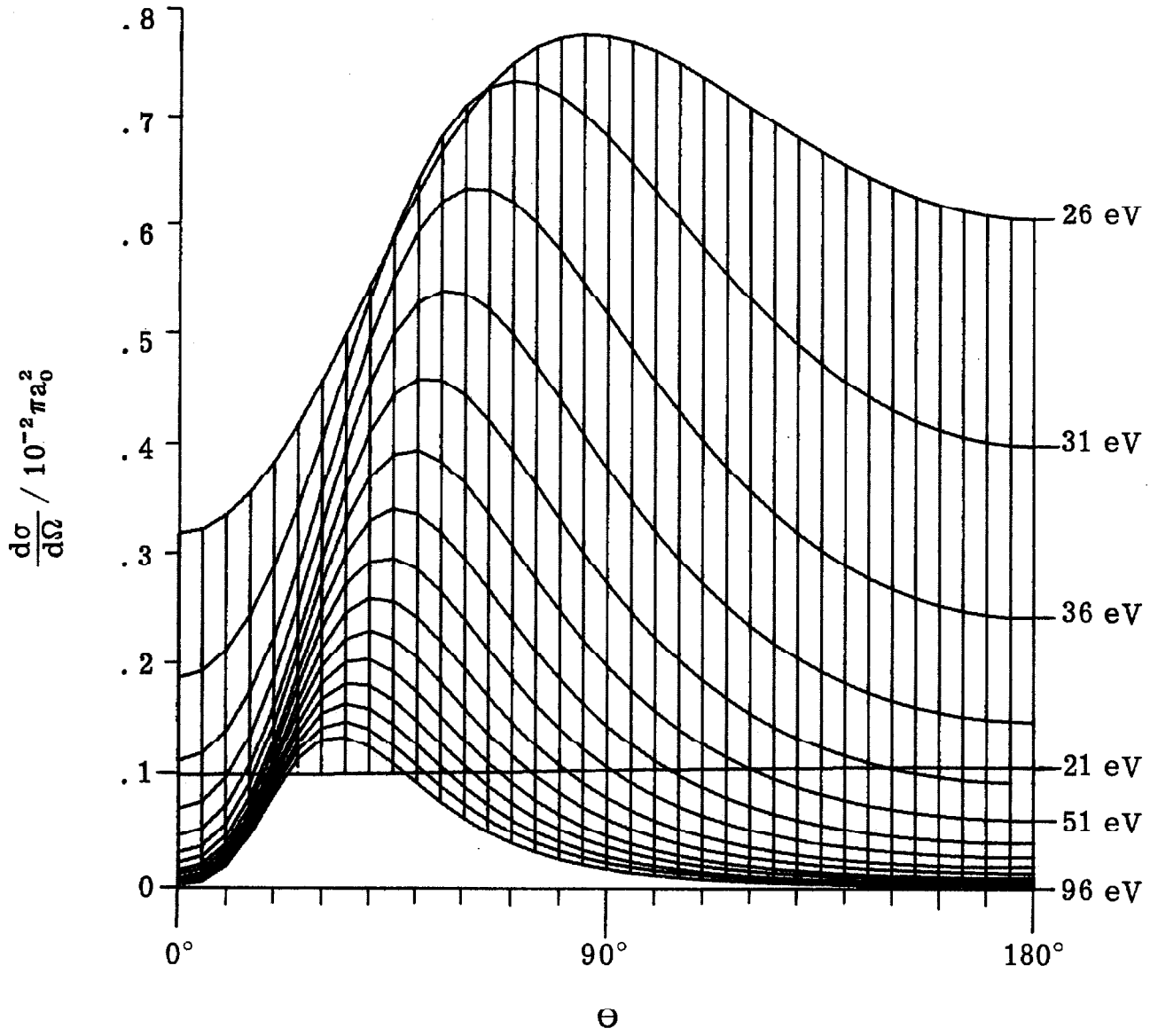

Helium $1^1S \rightarrow 2^3P$

AMAX= .0077

VIEWING ANGLE
THETA = 90.00
PHI = 0.00

EXECUTION TIME .19 MIN
MODE = 1
RUDGE HE TR-2P GREEN-MYH

ARRAY SIZE

	NATURAL DIMENSION	REGION PLOTTED
X	16	1 THRU 16
Y	37	1 THRU 37

FIGURE 27

FIGURE 28

Perspective view of the differential cross section of the 2^3P state of helium. Calculated using the (OR) approximation with Green et. al. [72b] and MYH[73a] wave functions. The axis is as labeled and the spherical polar angles from which direction the array is viewed are indicated on the lower portion of the figure.

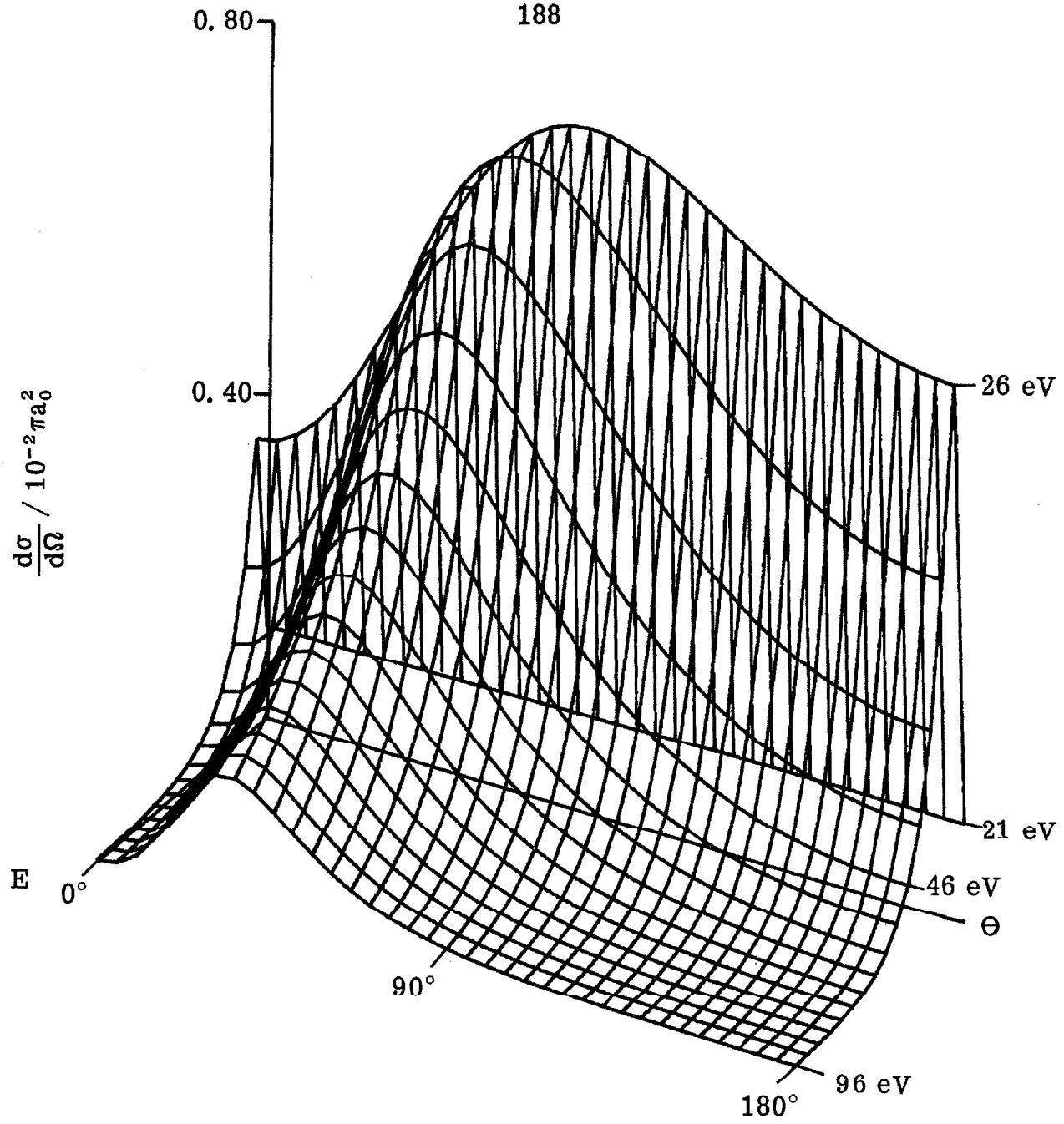

Helium $1^1S \longrightarrow 2^3P$

AMAX= .0077

VIEWING ANGLE
THETA = 60.00
PHI = 30.00

EXECUTION TIME .11 MIN
MODE = 1
RUDGE HE TR-2P GREEN-MYH

ARRAY SIZE

	NATURAL DIMENSION	REGION PLOTTED
X	16	1 THRU 16
Y	37	1 THRU 37

FIGURE 28

FIGURE 29

Perspective view of the differential cross section of the 2^3P state of helium. Calculated using the (OR) approximation with Green et. al.[72b] and MYH[73a] wave functions. The axis is as labeled and the spherical polar angles from which direction the array is viewed are indicated on the lower portion of the figure.

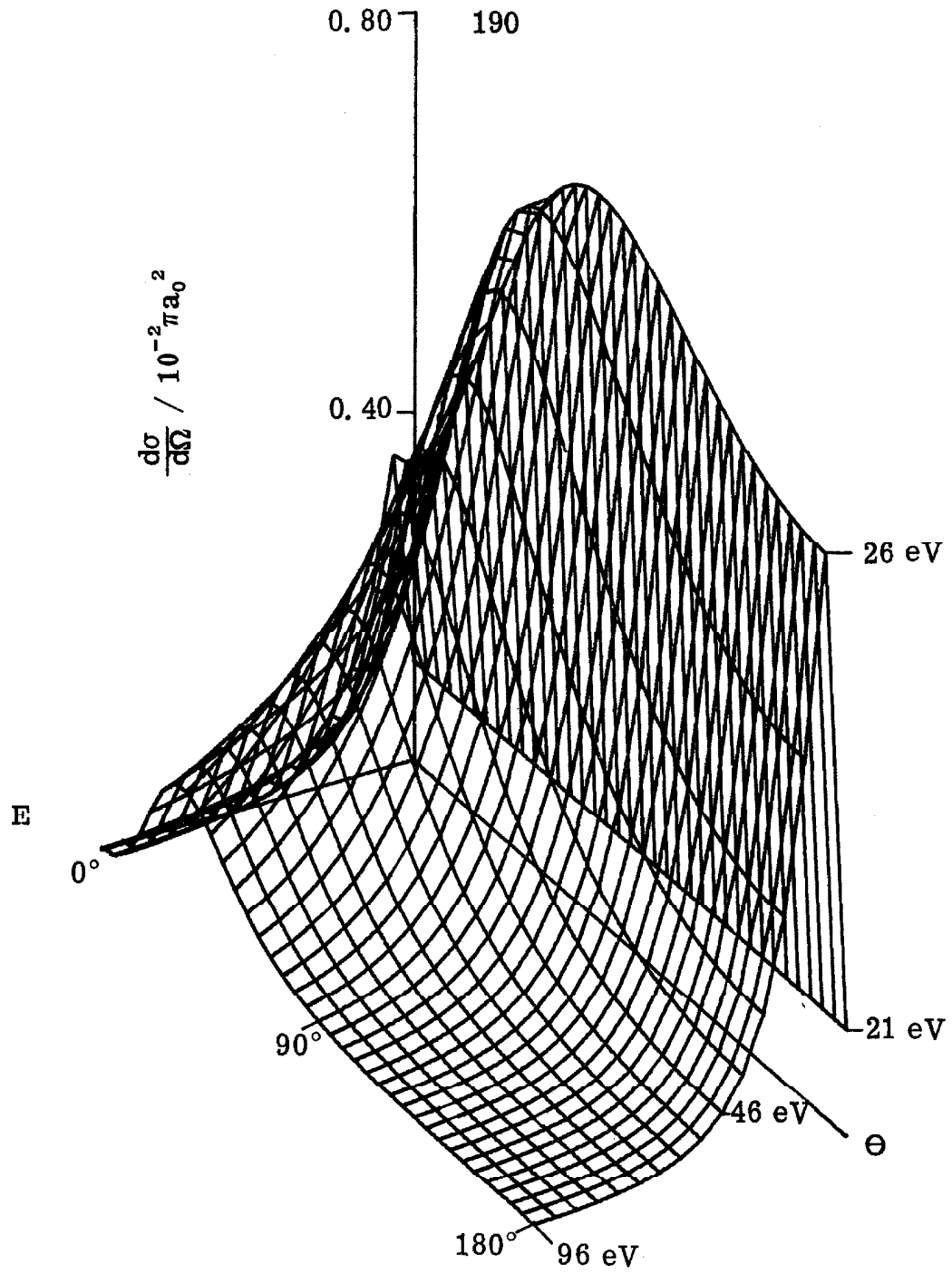

Helium $1^1S \longrightarrow 2^3P$

AMAX= .0077

VIEWING ANGLE
THETA = 60.00
PHI = 60.00

EXECUTION TIME .11 MIN
MODE = 1
RUDGE HE TR-2P GREEN-MYH

ARRAY SIZE

	NATURAL DIMENSION	REGION PLOTTED
X	16	1 THRU 16
Y	37	1 THRU 37

FIGURE 29

FIGURE 30

The vector relation $\vec{q} = \vec{k}_o - \vec{k}'$ plotted as a function of incident energy assuming that $q = 1$. The solid semi-circles indicate the possible length and direction of $\vec{k}'$ for a given incident energy. The intersection of the $q = 1$ semi-circle and k' semi-circle gives the location in angle of the maximum in the angular distribution for the given energy.

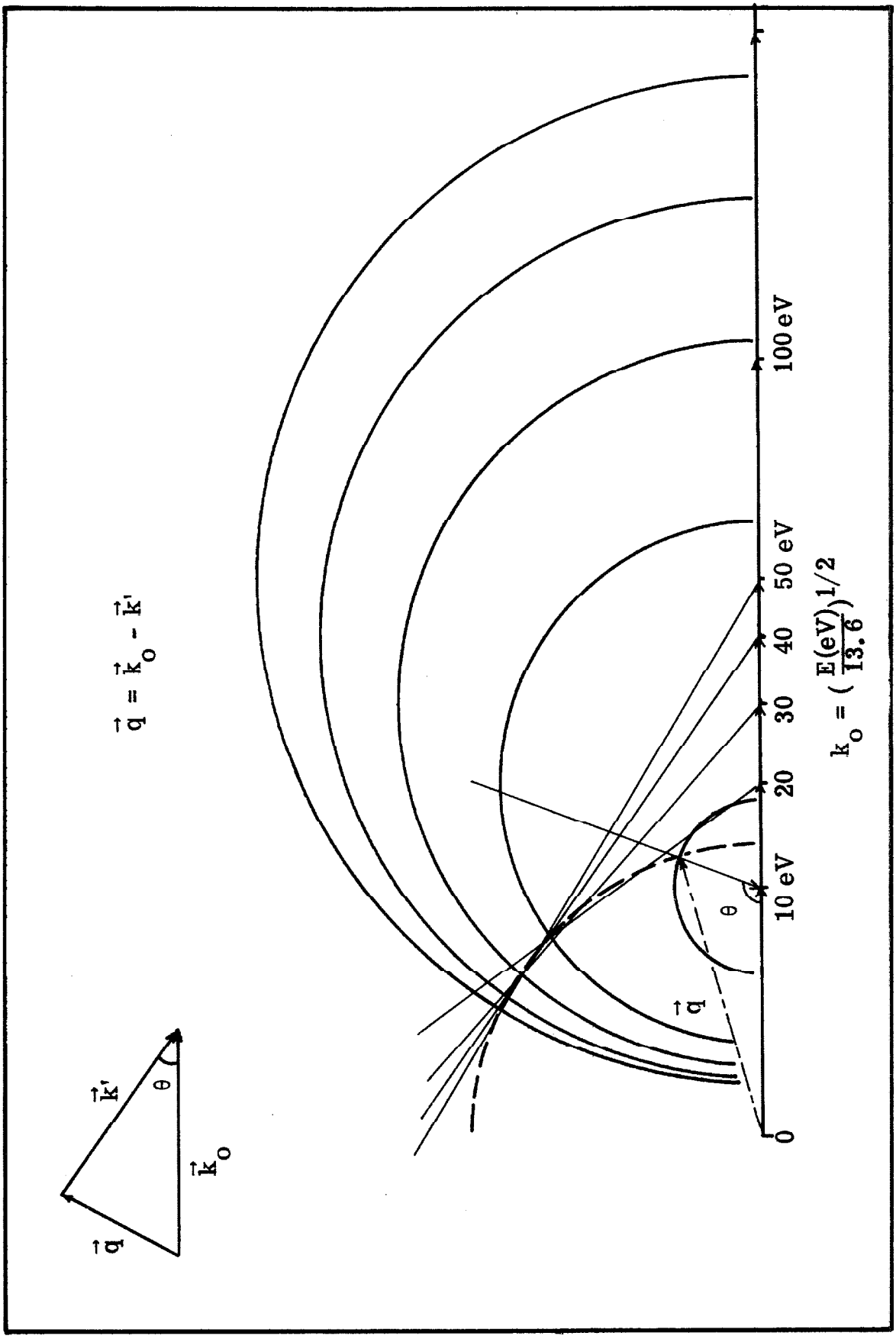
$\vec{q} = \vec{k}_o - \vec{k}'$
$\vec{k}'$
θ
$\vec{k}_o$
$\vec{q}$
$k_o = \left(\frac{E(eV)}{13.6}\right)^{1/2}$
0
10 eV
20
30
40
50 eV
100 eV
θ
$\vec{q}$

FIGURE 30

FIGURE 31

Plot of maximum in the angular distribution (θ_{max}) as a function of incident energy (E) for the excitation of the $b^3\Sigma_u^+$ state of molecular hydrogen. (———), as calculated in the (OR) approximation (Fig. 17); (x), as determined assuming q and a equal to unity.

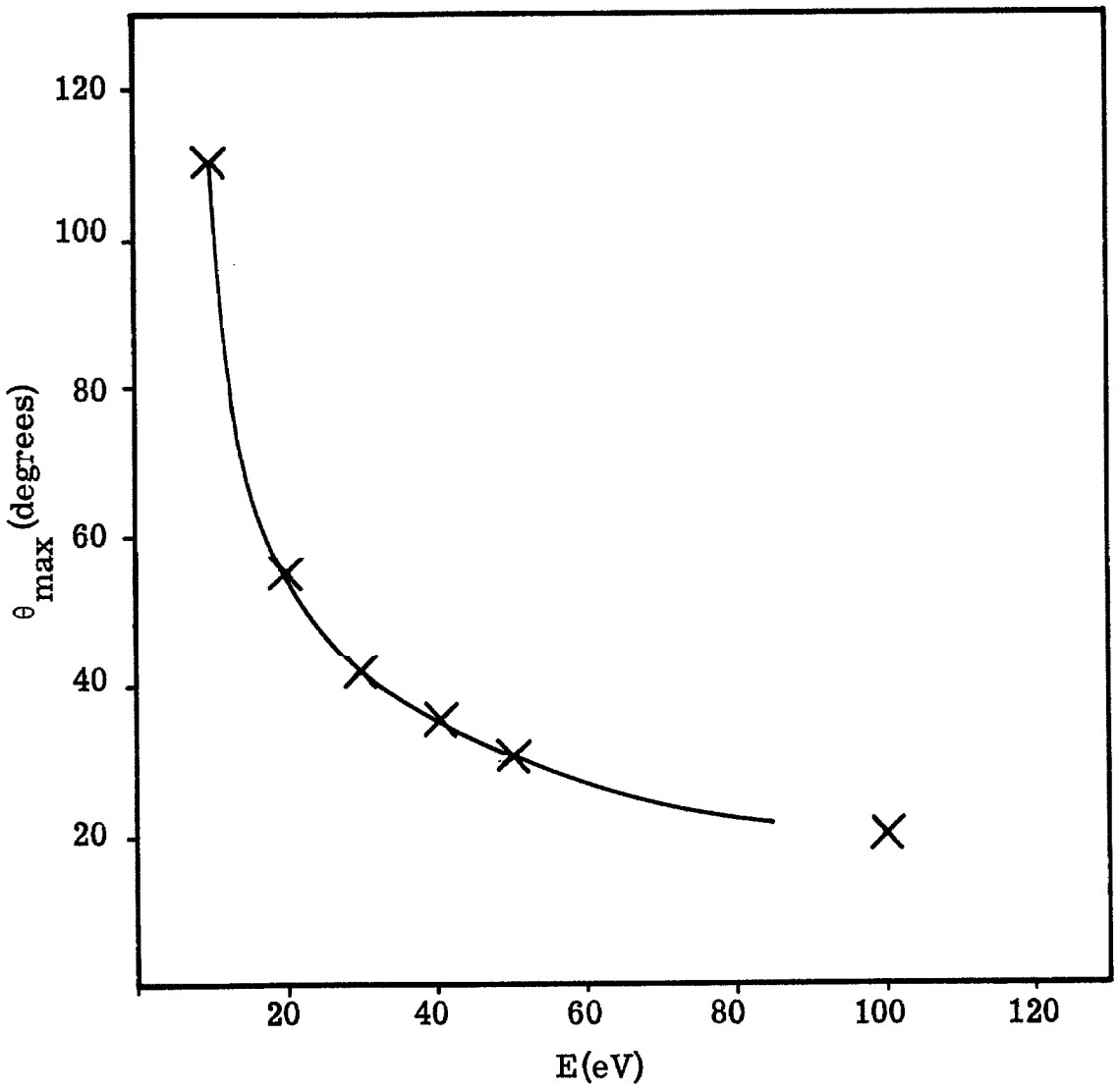

FIGURE 31

Appendix A

In this appendix, the proofs of some of the useful identities used in Section I are given. The proof of (I-1-45) and (I-1-46) will not be given since they are demonstrated on pp. 826-7 of Ref. 1c. In the following discussion, the limiting process will not be written but just assumed.

The proof of (I-1-47) proceeds as follows: Take $G^{\pm}$ and write it as

$$\frac{1}{E - H \pm i\epsilon} = \frac{1}{E - H_o \pm i\epsilon}(E - H_o \pm i\epsilon)\frac{1}{E - H \pm i\epsilon}. \tag{A-1}$$

In the above, the "right" identity

$$G_o^{\pm}(E - H_o \pm i\epsilon) = 1 \tag{A-2}$$

has been used. Add and subtract V to the quantity $(E - H_o \pm i\epsilon)$ in (A-1) to give

$$\frac{1}{E - H \pm i\epsilon} = \frac{1}{E - H_o \pm i\epsilon}[(E - H_o - V \pm i\epsilon) + V]\frac{1}{E - H \pm i\epsilon} \tag{A-3}$$

$$= \frac{1}{E - H_o \pm i\epsilon}(E - H \pm i\epsilon)\frac{1}{E - H \pm i\epsilon} + \frac{1}{E - H_o \pm i\epsilon} V \frac{1}{E - H \pm i\epsilon}. \tag{A-4}$$

Using the "left" identity for $G^{\pm}$;

$$(E - H \pm i\epsilon)G^{\pm} = 1 \tag{A-5}$$

equation (A-4) becomes

$$\frac{1}{E - H \pm i\epsilon} = \frac{1}{E - H_o \pm i\epsilon} + \frac{1}{E - H_o \pm i\epsilon} V \frac{1}{E - H \pm i\epsilon} . \qquad (A-6)$$

Rearranging produces the identity (I-1-47):

$$\frac{1}{E - H \pm i\epsilon} - \frac{1}{E - H_o \pm i\epsilon} = \frac{1}{E - H_o \pm i\epsilon} V \frac{1}{E - H \pm i\epsilon} . \qquad (A-7)$$

Identity (I-1-48) is obtained in a very similar manner using the "pre"-identities for $G_o^{\pm}$ and $G^{\pm}$:

$$\frac{1}{E - H \pm i\epsilon} = \frac{1}{E - H \pm i\epsilon} (E - H_o \pm i\epsilon) \frac{1}{E - H_o \pm i\epsilon}$$

$$= \frac{1}{E - H \pm i\epsilon} [(E - H \pm i\epsilon) + V] \frac{1}{E - H_o \pm i\epsilon}$$

$$= \frac{1}{E - H_o \pm i\epsilon} + \frac{1}{E - H \pm i\epsilon} V \frac{1}{E - H_o \pm i\epsilon} . \qquad (A-8)$$

Rearranging gives (I-1-48)

$$\frac{1}{E - H \pm i\epsilon} - \frac{1}{E - H_o \pm i\epsilon} = \frac{1}{E - H \pm i\epsilon} V \frac{1}{E - H_o \pm i\epsilon} . \qquad (A-9)$$

The very useful identities (I-1-49) and (I-1-50)

$$(1 + G^{\pm}V)(1 - G_0^{\pm}V) = 1 \qquad \text{(A-10)}$$

$$(1 - G_0^{\pm}V)(1 + G^{\pm}V) = 1 \qquad \text{(A-11)}$$

follow at once from the application of (A-6) and (A-8). To illustrate, (A-10) is obtained as follows: Write (A-9) as

$$G^{\pm} - G_0^{\pm} = G^{\pm} V G_0^{\pm} \ , \qquad \text{(A-12)}$$

right-multiply by V and rearrange to

$$G^{\pm}V - G_0^{\pm}V - G^{\pm}V G_0^{\pm}V = 0. \qquad \text{(A-13)}$$

Now add the identity to both sides of (A-13) to give

$$1 + G^{\pm}V - G_0^{\pm}V - G^{\pm}V G_0^{\pm}V = 1 \ . \qquad \text{(A-14)}$$

The left hand side of (A-14) can be factored at once to give (I-1-49)

$$(1 + G^{\pm}V)(1 - G_0^{\pm}V) = 1 \ . \qquad \text{(A-15)}$$

The identity (I-1-49) is obtained in a similar manner by using (A-7).

Note that care must be exercised so that these operators act only on vectors of finite norm.

Appendix B

There are two commonly used sets of atomic units. The principle difference is in the unit of energy; in one case it is the Rydberg and the other it is the Hartree. In table B below the value of the constants are given for these two sets of atomic units.

Table B

Constant	Rydberg A. U.	Hartree A. U.
$\hbar$	$=\sqrt{2}$	$= 1$
m_e	$= 1$	$= 1$
$\lvert e \rvert$	$=\sqrt{2}$	$= 1$
$a_o \equiv \frac{\hbar^2}{m_e^2}$	$= 1$	$= 1$
$c = \frac{e^2}{\hbar}\ \frac{1}{\alpha} = \frac{e^2}{\hbar}\ 137$	$=\sqrt{2}\ (137)$	$= 137$

Consider the effect of these units on the Schrödinger equation for, say, an electron in the field of the hydrogen atom:

$$(-\frac{\hbar^2}{2m}\nabla^2 - \frac{e^2}{r_1} + \frac{e^2}{r_{12}} - E)\psi(\vec{r}_1, \vec{r}_2) = 0. \qquad \text{(B-1)}$$

First scale the length quantities with a_o; that is, let $r = a_o\rho$ in (B-1), so that it becomes (rewrite all the constants in terms of a_o)

$$(\nabla_\rho^2 + \frac{2}{\rho_1} - \frac{2}{\rho_{12}} + \frac{E}{e^2/2a_o})\psi = 0 \ . \qquad \text{(B-2)}$$

If Rydberg A. U. 's are used, $e^2/2a_o = 1$ and the energy unit is measured in terms of 13.595 eV = $e^2/2a_o$. If Hartree A. U. 's are used, $e^2/2a_o = 1/2$. Equation (B-2) is multiplied by 1/2 so that it becomes

$$(\frac{1}{2}\nabla_\rho^2 + \frac{1}{\rho_1} - \frac{1}{\rho_{12}} + \frac{E}{e^2/a_o})\psi = 0 \ , \qquad \text{(B-3)}$$

and energy is measured in terms of $2 \times e^2/2a_o = 27.19$ eV. Thus, the advantage with either set of units is that the Schrödinger equation is rendered dimensionless; the choice of either set is therefore arbitrary.

It is worthwhile to mention the effect of atomic units on the quantities of interest in scattering problems. If the interaction potential for the rearrangement collision is electrostatic, the amplitude is the same in <u>either</u> set of atomic units:

$$T_{fi} \equiv -\frac{m_e^2}{2\pi\hbar^2} \langle \psi_b^{(-)} | g(i,j) | \chi_A^{(+)} \eta_B \rangle = -\frac{1}{2\pi} \langle \psi_b^{(-)} | g(i,j) | \chi_A^{(+)} \eta_B \rangle \ . \qquad \text{(B-4)}$$

(for electron scattering, $g(i,j) \equiv W_{AB}$ = inter electron repulsion.) This is of course a result of the fact that T_{fi} has dimensions of a length which is scaled the same in both sets of units.

The energy ($E = \hbar^2 k^2/2m_e$, in eV) is related to the wave number k in the same way in both sets of units, as seen from

$$\text{(Rydberg A. U. 's)} \quad \frac{E}{\mathcal{E}_o} = \frac{\hbar^2 k_R^2}{2m_e} = k_R^2 \qquad E(eV) = \mathcal{E}_o k_R^2$$

$$\text{(Hartree A. U. 's)} \quad \frac{E}{2\mathcal{E}_o} = \frac{\hbar^2 k_H^2}{2m_e} = \frac{k_H^2}{2} \qquad E(eV) = \mathcal{E}_o k_H^2 .$$

($\mathcal{E}_o$ = 1 Rydberg)

Note also that

$$k'^2 \equiv k^2 - \frac{2m_e}{\hbar^2}(E_i - E_f) \tag{B-5}$$

is also the same in both sets of units, since

$$\text{(Rydbergs)} \quad k'^2_R = k^2_R - \frac{2(1)}{2}\left(\frac{E_i}{\mathcal{E}_o} - \frac{E_f}{\mathcal{E}_o}\right)$$

$$\text{(Hartrees)} \quad k'^2_H = k^2_H - \frac{2(1)}{1}\left(\frac{E_i}{2\mathcal{E}_o} - \frac{E_f}{2\mathcal{E}_o}\right) .$$

Finally, since k^2, k'^2 are the same in both units,

$$q^2 \equiv k^2 + k'^2 - 2k'k\cos\theta$$

is also the same. Thus, as far performing calculations using the transition amplitudes as defined in Section I, either set of atomic units can be used.

Appendix C

There are two possible approaches to the determination of the proper spin symmetries involved; the first involves a brute force anti-symmetrization of the total wave function for the three-electron system which of course works but somewhat disguises the principles when more than two electrons are involved. The second relies on the understanding of which of the possible collision processes are really indistinguishable. Of course, this latter approach is not general but it is felt to be superior since it stresses the physical aspects and hence is the one which will be used here. For the general treatment of indistinguishable particles, the interested reader can refer to the literature [Ca]

The basic necessity here is that the total wave function for any one of the three-electron states of the system be anti-symmetric with respect to interchange of indistinguishable electrons. It is worth pointing out now that the free electron is considered as distinguishable from the two bound electrons. This is because the free electron can be separated from the bound electrons (which, of course, is the way the experiment is performed). For the two-electron bound states of the scatterer, the space and spin parts can be written in product form, each of which have their own symmetry appropriate to that state. Let $u_1(\vec{r}_1, \vec{r}_2)$ and $u_3(\vec{r}_1, \vec{r}_2)$ denote the singlet and triplet spatial bound state wave functions of the scatterer, and $\varphi(\vec{r}_3)$ the free particle wave functions. If $v(12;3)$ and $\chi(12;3)$ denote the respective initial and final state spin functions for the three electrons, then the initial singlet state can be written as

$$\psi_1(12;3) = \varphi(\vec{r}_3)\, u_1(\vec{r}_1, \vec{r}_2)\, v(12;3) \qquad (C-1)$$

and the final triplet state as

$$\psi_3(32;1) = \varphi(\vec{r}_1)\, u_3(\vec{r}_3, \vec{r}_2)\, \chi(32;1) \qquad \text{(C-2)}$$

where in (C-2) the exchange as been assumed to involve electrons 3 and 1, an arbitrary but not restrictive choice as will be demonstrated later. Note that the last electron (free) has been separated from the first two (bound) in the writing of the spin functions since this free electron is considered distinguishable.

The eigenfunctions (u_1 and u_3) are solutions of the bound state Hamiltonian and must possess the symmetry associated with their respective states. For instance, the singlet wave function u_1 must be symmetric with respect to interchange of the bound electrons; and the triplet wave function u_3 must be anti-symmetric with such interchange. Since the Hamiltonian governing the scattering process is assumed independent of spin (a good approximation), the total wave functions for each state must be eigenfunctions of $(S_1 + S_2 + S_3)^2$ and say $(S_{z1} + S_{z2} + S_{z3})$.

Thus, for the scattering off a bound state initially in a singlet state, the spin function v(12;3) must take the form

$$v(12;3) = \frac{1}{\sqrt{2}}(\alpha_1\beta_2\alpha_3 - \beta_1\alpha_2\alpha_3) \qquad \text{(C-3)}$$

which represents a doublet (total spin 1/2) state. Since the total spin is a constant of the motion, the final state spin function must also be a doublet with the same z-projection. It is taken as

$$\chi(12;3) = \frac{1}{\sqrt{6}}(\alpha_1\beta_2\alpha_3 + \beta_1\alpha_2\alpha_3 - 2\alpha_1\alpha_2\beta_3). \qquad \text{(C-4)}$$

Note that both the initial and final spin functions have symmetry only with respect to interchange of electrons 1 and 2 as written in (C-3) and (C-4). As mentioned before, no special symmetry need be attached to the free electron. Note also that in equations (C-3) and (C-4) only one polarization of incident electrons has been assumed. This again is no restriction and can be accounted for as will be shown later.

It is important at this point to observe that in producing the exchange excitation, the incident electron can exchange with only one of the two electrons bound in the scatterer. However, the two bound electrons are really indistinguishable and hence the final state can be reached by two experimentally indistinguishable paths. These two paths are denoted symbolically as

$$\underset{3}{\uparrow} + \underset{2\ 1}{\uparrow\downarrow} \longrightarrow \underset{3\ 2}{\uparrow\uparrow} + \underset{1}{\downarrow} \qquad \text{(C-5)}$$

and

$$\underset{3}{\uparrow} + \underset{1\ 2}{\uparrow\downarrow} \longrightarrow \underset{3\ 1}{\uparrow\uparrow} + \underset{2}{\downarrow} \ . \qquad \text{(C-6)}$$

Then, in forming the scattering amplitude using (C-1) and (C-2) there will be two contributions which will have equivalent spatial portions but the spin factors will be:

$$\begin{aligned} &\text{(C-5):} \quad \sum \chi^*(32;1)\, v(12;3) = \frac{\sqrt{3}}{2} \\ &\text{(C-6):} \quad \sum \chi^*(31;2)\, v(21;3) = \frac{\sqrt{3}}{2} \end{aligned} \qquad \text{(C-7)}$$

where these were evaluated by using (C-3) and (C-4) along with the usual rules for matrix multiplication. Since these processes leading to the same final state are indistinguishable, their corresponding amplitudes must be added. This produces one spatial matrix element (for example (I-5-3)) and the multiplicative factor $\sqrt{3}$. (+ superscript means spin projection up)

$$g_{03}^{+} \equiv \sqrt{3}\ T_{fi}^{\text{spatial}} \ . \qquad \text{(C-8)}$$

The above discussion represents the solution for the incident electrons with a fixed projection of $+\hbar/2$ in some preferred direction. Most experiments of interest here are carried out with an unpolarized incident beam of electrons. This means that the incident electrons have equal probability (1/2) of being polarized with + and - spin projection. An analysis for the negative polarization analogous to that carried out for the plus polarization ((C-5) and (C-6)) will produce exactly the same spin factor and spatial matrix element as found in (C-8), a result which is expected on physical grounds.

To obtain the total probability that the excitation occurs when the incident beam is unpolarized, one "averages over initial states". Each initial state is the probability of the excitation taking place for a given polarization of the incident beam multiplied by the probability of that polarization occurring in the incident beam. The various (two in this case) initial states are then added to give the total transition amplitude. In this case, since each incident polarization is weighted with the factor 1/2 one finds from (C-8) that

$$\frac{1}{2}|g_{03}^{+}|^2 + \frac{1}{2}|g_{03}^{-}|^2 = |g_{03}|^2 , \qquad \text{(C-9)}$$

since $g_{03}^{+} = g_{03}^{-}$. Because of the equal probability of positive and negative polarization in the incident electron beam authors usually forget about formally averaging over initial states since it introduces no changes, and just derive the spin factor for one fixed incident polarization.

It is interesting to point out that people are still making errors concerning this spin manipulation. In the first[(Cb-1)] of a series of two papers on the triplet excitation of helium[(Cb)], the authors used spin functions for the excited state which were not eigenfunctions of $(S_1 + S_2 + S_3)^2$ and proceeded to obtain the correct spin factor $((\sqrt{3})^2)$ by summing <u>probabilities</u> over two final states. This approach implies that the excitation proceeds by two experimentally distinguishable intermediate states which is certainly not the case. In the second of their series[(Cb-2)], the authors use the correct excited state spin functions and just introduce the final correct result $((\sqrt{3})^2)$ without elaboration on the details of forming the transition probability.

References for Appendix C

Ca. 1) For the 2-electron case see, for instance, ref. 14a, p. 235.

2) For the N-electron case see ref. 30b, Chapters 7 and 8.

Cb. 1) C. J. Joachain and M. H. Mittleman, Phys. Rev. 140, A432 (1965).

2) C. J. Joachain and M. H. Mittleman, Phys. Rev. 151, 151 (1966).

Appendix D

The Ochkur modification proceeds by considering separately the three terms in (II-5-5-6). (Ochkur kept the core terms.)

$$\mathcal{T}_{fi}^{BO} = - G_{31} - G_{32} + G_{3A} \tag{D-1}$$

where the subscripts on the G functions refer to the subscripts on the electron interaction terms. Working just with G_{31} and using the vector relation $\vec{r}_{31} = \vec{r}_3 - \vec{r}_1$ one can write:

$$G_{31} \equiv \frac{1}{2\pi} \int \frac{1}{r_{31}} e^{i(\vec{k}_\circ \cdot \vec{r}_3 - \vec{k}' \cdot \vec{r}_1)} \psi_f^*(\vec{r}_3, \vec{r}_2)\, \psi_i(\vec{r}_1, \vec{r}_2) d\vec{r}_1 d\vec{r}_2 d\vec{r}_3$$

$$= \frac{1}{2\pi} \int \psi_i(\vec{r}_1, \vec{r}_2)\, I_f(\vec{r}_1, \vec{r}_2) e^{i(\vec{k}_\circ - \vec{k}') \cdot \vec{r}_1} d\vec{r}_1\, dr_2 \tag{D-2}$$

where

$$I_f \equiv \int \frac{1}{r_{31}} \psi_f^*(\vec{r}_3, \vec{r}_2) e^{i\vec{k}_\circ \cdot \vec{r}_{31}} d\vec{r}_3 \,. \tag{D-3}$$

In (D-3), change integration variables from $\vec{r}_3$ to $\vec{r}_{31}$, which just amounts to relocation of the coordinate system origin. Choose the z-axis along $\vec{k}_\circ$ and employ the spherical coordinates (r_{31}, θ, χ). Then (D-3) becomes

$$I_f \equiv \int \psi_f^*(\vec{r}_{31} + \vec{r}_1, \vec{r}_2) e^{ikr_{31}\cos\theta} r_{31} dr_{31} \sin\theta d\theta d\chi \qquad \text{(D-4)}$$

$$= \int_{-1}^{1} \int_{0}^{\infty} \Psi_f(\vec{r}_1, r_{31}, x, \vec{r}_2) e^{ikr_{31}x} r_{31} dr_{31} dx \qquad \text{(D-5)}$$

where

$$x = \cos\theta \text{ and } \Psi_f(\vec{r}_1, r_{31}, x, \vec{r}_2) \equiv \int_0^{2\pi} \psi_f^*(\vec{r}_1 + \vec{r}_{31}, \vec{r}_2) d\chi. \qquad \text{(D-6)}$$

Now integrate (D-5) by parts with respect to x by letting

$$u = \Psi_f r_{31} \qquad \partial u = \frac{\partial \Psi_f}{\partial x} r_{31} dx$$

$$dv = e^{ikr_{31}x} dx \qquad v = \frac{e^{ikr_{31}x}}{ikr_{31}}$$

and (D-5) becomes

$$I_f = \int_0^{\infty} \left[\Psi_f r_{31} \frac{1}{ikr_{31}} e^{ikr_{31}x} \right]_{-1}^{1} dr_{31} - \frac{1}{ik} \int_{-1}^{1} \int_{0}^{\infty} \frac{\partial \Psi_f}{\partial x} e^{ikr_{31}x} dx dr_{31}. \qquad \text{(D-7)}$$

The second term in (D-7) is neglected as being a higher order smallness than the first term (seen by integrating this term again by parts). Then evaluating the limits in the first term gives

$$I_f \cong \frac{1}{ik_o}\int_0^\infty \left[\Psi_f(\vec{r}_1, r_{31}, 1, \vec{r}_2)e^{ikr_{31}} - \Psi_f(\vec{r}_1, r_{31}, -1, \vec{r}_2)e^{-ikr_{31}}\right] dr_{31}. \tag{D-8}$$

Integrate (D-8) again by parts, this time with respect to r_{31}, by letting

$$u = \Psi_f \frac{1}{ik_o} \qquad du = \frac{1}{ik_o}\frac{\partial \Psi_f}{\partial r_{31}} dr_{31}$$

$$dv = e^{ikr_{31}} dr_{31} \qquad v = \frac{1}{ik_o} e^{ikr_{31}}$$

and (D-8) becomes

$$I_f \cong -\frac{1}{k_o^2}\left\{\Psi_f(\vec{r}_1, r_{31}, 1, \vec{r}_2)e^{ikr_{31}} + \Psi_f(\vec{r}_1, r_{31}, -1, \vec{r}_2)e^{-ikr_{31}}\right\}\Bigg|_0^\infty$$

$$+ \text{(terms of higher order smallness).} \tag{D-9}$$

Using the fact that

$$\Psi_f(\vec{r}_1, r_{31}, \pm 1, \vec{r}_2) \to 0 \quad \text{for} \quad r_{31} \to \infty$$

means that (D-9) becomes

$$I_f \cong \frac{1}{k_o^2}\left\{\Psi_f(\vec{r}_1, 0, 1, \vec{r}_2) + \Psi_f(\vec{r}_1, 0, 1, \vec{r}_2)\right\}. \tag{D-10}$$

By using the definition of Ψ_f (D-6), we can see that

$$\Psi_f(\vec{r}_1, 0, \pm 1, \vec{r}_2) = \int_0^{2\pi} \psi_f^*(\vec{r}_1 + \vec{0}, \vec{r}_2) d\chi = 2\pi \psi_f^*(\vec{r}_1, \vec{r}_2) \ . \tag{D-11}$$

The last step was possible since the integrand is independent of φ. The two terms in (D-10) then add to give

$$I_f \cong \frac{4\pi}{k_o^2} \psi_f^*(\vec{r}_1, \vec{r}_2) \ . \tag{D-12}$$

Using (D-12), the expression for G_{31}, (D-2), becomes

$$G_{31} \cong \frac{2}{k_o^2} \int \psi_i(\vec{r}_1, \vec{r}_2) \, \psi_f^*(\vec{r}_1, \vec{r}_2) e^{i\vec{q} \cdot \vec{r}_1} \, d\vec{r}_1 \, d\vec{r}_2 \tag{D-13}$$

where $\vec{q} \equiv \vec{k}_o - \vec{k}'$ is the momentum transferred by the incident electron to the bound system.

The treatment of G_{32} proceeds in the same manner and yields $G_{32} = O(k_o^{-6})$ for ψ_α, ψ_β of the same symmetry and $G_{32} = O(k_o^{-7})$ for ψ_α, ψ_β of different symmetry. G_{3A} is also $O(k_o^{-6})$.

Appendix E

In this appendix a derivation of the Rudge[34] approximation will be outlined. Although Rudge approached the problem from variational considerations a more direct method will be used here. It will be similar to a discussion presented by Crothers.[Ea] For simplicity the electron-hydrogen atom will be used although the end result is general.

In Hartree atomic units, the Schrödinger equation for the electron-hydrogen atom system in the j^{th} channel is

$$(\frac{1}{2}\nabla_1^2 + \frac{1}{2}\nabla_2^2 + \frac{1}{r_1} + \frac{1}{r_2} - \frac{1}{r_{12}} + E)\Psi_j^{\pm}(\vec{r}_1, \vec{r}_2) = 0 \,. \qquad \text{(E-1)}$$

If ψ_n is used to denote the n^{th} bound state of the atom

$$(\frac{1}{2}\nabla^2 + \frac{1}{r} + E_n)\,\psi_n = 0 \,, \qquad \text{(E-2)}$$

then

$$\Psi_j^{\pm}(\vec{r}_1, \vec{r}_2) \underset{r_2 \to \infty}{\sim} \psi_j(\vec{r}_1)e^{i\vec{k}_j \cdot \vec{r}_2} + \sum_m \psi_m(\vec{r}_1) f_{jm}^{\pm}(\vec{r}_2, \vec{k}_j)\frac{e^{\pm ik_m r_2}}{r_2} \qquad \text{(E-3)}$$

represents the asymptotic boundary condition that total wave function satisfies.

If, without loss of generality, the total wave function is assumed to have the form

$$\Psi_j^{\pm}(\vec{r}_1, \vec{r}_2) = \psi_j(\vec{r}_1)\, g_j^{\pm}(\vec{r}_1, \vec{r}_2), \tag{E-4}$$

and use is made of the identity

$$\nabla_1^2(\psi_j g_j) = \psi_j \nabla_1^2 g_j + g_j \nabla_1^2 \psi_j + 2(\nabla_1 \psi_j) \cdot (\nabla_1 g_j), \tag{E-5}$$

(E-1) can be rearranged as follows:

$$\left[\frac{1}{2} \psi_j \nabla_1^2 g_j + (\nabla_1 \psi_j) \cdot (\nabla_1 g) + \frac{1}{2} \psi_j \nabla_2^2 g_j + \frac{1}{r_2} \psi_j g_j - \frac{1}{r_{12}} \psi_j g_j + \frac{k_j^2}{2} \psi_j g_j \right] +$$

$$g_j \left[\frac{1}{2} \nabla_1^2 + \frac{1}{r_1} + E_j \right] \psi_j = 0 \ . \tag{E-6}$$

Using (E-2), and multiplying (E-1) through by $2/\psi_j$ gives

$$\left(\nabla_1^2 g_j + \frac{2(\nabla_1 \psi_j)}{\psi_j} \cdot (\nabla_1 g_j) + \nabla_2^2 g_j + \frac{2}{r_2} g_j - \frac{2}{r_{12}} g_j + k_j^2 g_j \right) = 0. \tag{E-7}$$

Since

$$\nabla_1 g_j \equiv (\nabla_1 \ln g_j) g_j \tag{E-8}$$

(E-7) can be written as

$$\left[\frac{1}{k_j^2} \left\{ \nabla_1^2 + \nabla_2^2 + 2 (\nabla_1 \ln \psi_j) \cdot (\nabla_1 \ln g_j^{\pm}) \right\} + 1 \right] g_j^{\pm} = \frac{2}{k_j^2} \left(\frac{1}{r_{12}} - \frac{1}{r_2} \right) g_j^{\pm}. \tag{E-9}$$

The solution to (E-9) for high energy, which is consistent with (E-3), is

$$g_j^{(\pm)}(\vec{r}_1, \vec{r}_2) \underset{k_j^2 \to \infty}{\sim} e^{i\vec{k}_j \cdot \vec{r}_2} \tag{E-10}$$

which is just the Born solution, as expected.

The transition amplitude for the rearrangement excitation in the Born-Oppenheimer approximation is thus

$$T^{BO}(p, q) = \langle \psi_q(\vec{r}_2) e^{i\vec{k}_q \cdot \vec{r}_1} | \frac{1}{r_{12}} | \psi_p(\vec{r}_1) e^{i\vec{k}_p \cdot \vec{r}_2} \rangle \tag{E-11}$$

where p, q are the initial, final quantum numbers of the bound system. Note that energy conservation relates the energy of the free electron and the atom as

$$k_q^2 = k_p^2 - \Delta W = k_p^2 - \left(\frac{1}{p^2} - \frac{1}{q^2}\right) . \tag{E-12}$$

To proceed in the analysis, the Fourier transforms of the bound functions are introduced as

$$\Phi_j(\vec{s}) = \frac{1}{(2\pi)^{3/2}} \int \psi_j(\vec{r}) e^{i\vec{s} \cdot \vec{r}} \, d\vec{r}$$

$$\psi_j(\vec{r}) = \frac{1}{(2\pi)^{3/2}} \int \Phi_j(\vec{s}) e^{-i\vec{s} \cdot \vec{r}} \, d\vec{s} , \tag{E-13}$$

then

$$(2\pi)^{3/2}\psi_j^*(\vec{r})e^{i\vec{k}_{p+q-j}\cdot\vec{r}} \equiv \int \Phi_j^*(\vec{s})e^{i(\vec{s}+\vec{k}_{p+q-j})\cdot\vec{r}}d\vec{s}. \qquad \text{(E-14)}$$

Using (E-14), and grouping the terms with the same coordinates, (E-11) becomes (letting $p \to j$, $q \to p+q-j$)

$$T^{BO}(p,q) = (2\pi)^{-3}\int \frac{1}{r_{12}}\Phi^*_{p+q-j}(\vec{s})e^{i(\vec{s}+\vec{k}_j)\cdot\vec{r}_2}\Phi_j(\vec{t}\,')e^{-i(\vec{t}\,'+\vec{k}_{p+q-j})\cdot\vec{r}_1}d\vec{r}_1 d\vec{r}_2 d\vec{s} d\vec{t}\,'. \qquad \text{(E-15)}$$

Make the substitution in (E-15)

$$\vec{t}\,' = \vec{t} + \vec{s} + \vec{k}_j - \vec{k}_{p+q-j} \qquad \text{(E-16)}$$

which corresponds to a translation of the origin of the $\vec{t}\,'$ integration. Then (E-15) becomes

$$T^{BO}(p,q) = \int \frac{1}{r_{12}}\Phi^*_{p+q-j}(\vec{s})e^{i(\vec{s}+\vec{k}_j)\cdot\vec{r}_2}\Phi_j(\vec{t}+\vec{s}+\vec{k}_j-\vec{k}_{p+q-j})$$
$$e^{-i(\vec{t}+\vec{s}+\vec{k}_j)\cdot\vec{r}_1}d\vec{r}_1 d\vec{r}_2 d\vec{s} d\vec{t}(2\pi)^{-3} \qquad \text{(E-17)}$$

The exponents in (E-17) can be regrouped to give

$$T^{BO}(p,q) = (2\pi)^{-3}\int\int\int\int \Phi^*_{p+q-j}(\vec{s})\Phi_j(\vec{t}+\vec{s}+\vec{k}_j-\vec{k}_{p+q-j})e^{i(\vec{s}+\vec{k}_j)\cdot(\vec{r}_2-\vec{r}_1)-i\vec{t}\cdot\vec{r}_1}\frac{1}{r_{12}}$$
$$d\vec{r}_1 d\vec{r}_2 d\vec{s} d\vec{t}. \qquad \text{(E-18)}$$

The above expression can be simplified by utilizing the identity[Eb]

$$\frac{1}{r_{12}} = \frac{1}{2\pi^2} \int \frac{e^{i\vec{u}\cdot(\vec{r}_1 - \vec{r}_2)}}{u^2} d\vec{u} \qquad \text{(E-19)}$$

in the following fashion:

$$T^{BO} = \frac{(2\pi)^{-3}}{2\pi^2} \iiint\iiint \Phi^*_{p+q-j}(\vec{s})\, \Phi_j(\vec{t} + \vec{s} + \vec{k}_j - \vec{k}_{p+q-j})$$

$$e^{i(\vec{s}+\vec{k}_j)\cdot(\vec{r}_2-\vec{r}_1) - i\vec{t}\cdot\vec{r}_1 + i\vec{u}\cdot(\vec{r}_1-\vec{r}_2)} \frac{1}{u^2}\, d\vec{u} d\vec{r}_1 d\vec{r}_2 d\vec{s}\, dt$$

$$= \frac{1}{2^4\pi^5} \int \Phi^*_{p+q-j}(\vec{s}) \Phi_j(\vec{t}+\vec{s}+\vec{k}_j-\vec{k}_{p+q-j}) \frac{1}{u^2} \int e^{i(\vec{s}+\vec{k}_j-\vec{u})\cdot\vec{r}_2}\, d\vec{r}_2$$

$$\int e^{i(\vec{u}-\vec{s}-\vec{k}_j-\vec{t})\cdot\vec{r}_1}\, d\vec{r}_1\, d\vec{u}\, d\vec{s}\, d\vec{t}$$

$$= (4\pi) \int \Phi^*_{p+q-j}(\vec{s})\, \Phi_j(\vec{t}+\vec{s}+\vec{k}_j-\vec{k}_{p+q-j}) \int \frac{1}{u^2}\, \delta(\vec{s}+\vec{k}_j-\vec{u})\, \delta(\vec{u}-\vec{s}-\vec{k}_j-\vec{t}) d\vec{u}\, d\vec{s} d\vec{t}$$

$$= (4\pi) \int \Phi^*_{p+q-j}(\vec{s})\, \Phi_j(\vec{t}+\vec{s}+\vec{k}_j-\vec{k}_{p+q-j}) \frac{\delta(\vec{t})}{(\vec{s}+\vec{k}_j)^2}\, d\vec{s}\, d\vec{t}$$

$$T^{BO} = (4\pi) \int \Phi^{*}_{p+q-j}(\vec{s})\, \Phi_j(\vec{s} + \vec{k}_j - \vec{k}_{p+q-j}) \frac{1}{(\vec{s} + \vec{k}_j)^2}\, d\vec{s}\,. \qquad \text{(E-20)}$$

If in (E-20) the limit $k_j^2 \to \infty$ is taken, then (E-20) becomes

$$T^{BO} \underset{k_j^2 \to \infty}{\sim} \frac{4\pi}{k_j^2} \int \Phi^{*}_{p+q-j}(\vec{s})\, \Phi_j(\vec{s} + \vec{k}_j - \vec{k}_{p+q-j})\, d\vec{s}$$

which can be written in terms of the ψ_j functions as

$$T^{BO} \underset{k_j^2 \to \infty}{\sim} \frac{4\pi}{k_j^2} \frac{1}{(2\pi)^3} \iint \psi^{*}_{p+q-j}(\vec{r}_1)\psi_j(\vec{r}'_1) \int e^{-i\vec{s}\cdot\vec{r}_1} e^{i(\vec{s}+\vec{k}_j-\vec{k}_{p+q-j})\cdot\vec{r}'_1}\, d\vec{s}\, d\vec{r}_1\, d\vec{r}'_1$$

$$= \frac{4\pi}{k_j^2} \iint \psi^{*}_{p+q-j}(\vec{r}_1)\, \psi_j(\vec{r}'_1) e^{i(\vec{k}_j - \vec{k}_{p+q-j})\cdot\vec{r}'_1}\, \delta(-\vec{r}_1 + \vec{r}'_1) d\vec{r}_1 d\vec{r}'_1$$

$$= \frac{4\pi}{k_j^2} \int \psi^{*}_{p+q-j}(\vec{r}_1)\, \psi_j(\vec{r}_1) e^{i(\vec{k}_j - \vec{k}_{p+q-j})\cdot\vec{r}_1}\, d\vec{r}_1 \qquad \text{(E-21)}$$

which is just the Ochkur result.

Given (E-21), the above process is now reversed to determine the specific form of $g_j^{\pm}(\vec{r}_1, \vec{r}_2)$ in (E-4) which, when inserted into

$$T(p, q) = T_{\alpha}(p, q) = \langle \psi^{-}_{q}(\vec{r}_2, \vec{r}_1) | W_{AB} | \psi_p(\vec{r}_1) e^{i\vec{k}_p\cdot\vec{r}_2} \rangle \qquad \text{(E-22)}$$

$$= T_\beta(p, q) = \langle \psi_q(\vec{r}_2) e^{i\vec{k}_q \cdot \vec{r}_1} | W_{AB} | \Psi_p^+(\vec{r}_1, \vec{r}_2) \rangle \qquad \text{(E-23)}$$

will reduce to (E-21). The above two equations (E-22), (E-23) are the familiar "prior", "post" forms for the scattering amplitude respectively.

The reversal proceeds as follows: From (E-21)

$$T^O = \frac{4\pi}{k_j^2} \int \psi^*_{p+q-j}(\vec{r}_1)\, \psi_j(\vec{r}'_1) e^{i(\vec{k}_j - \vec{k}_{p+q-j}) \cdot \vec{r}'_1}\, \delta(\vec{r}_1 - \vec{r}'_1) d\vec{r}_1 d\vec{r}'_1. \qquad \text{(E-24)}$$

Motivated by the technique used in the "forward" derivation, insert into (E-24)

$$\delta(\vec{r} - \vec{r}') = \frac{1}{(2\pi)^3} \int e^{i(\vec{r}_1 - \vec{r}'_1) \cdot \vec{t}}\, d\vec{t} \qquad \text{(E-25)}$$

to give

$$T^O = \frac{4\pi}{(2\pi)^3 k_j^2} \int \psi^*_{p+q-j}(\vec{r}'_1) \psi_j(\vec{r}_1) e^{i(\vec{t} + \vec{k}_j - \vec{k}_{p+q-j}) \cdot \vec{r}_1}\, e^{-i\vec{t} \cdot \vec{r}'_1}\, d\vec{r}_1 d\vec{r}'_1 d\vec{t}\,. \qquad \text{(E-26)}$$

Using the definitions (E-13), (E-26) becomes

$$T^O = \frac{4\pi}{k_j^2} \int \Phi^*_{p+q-j}(\vec{t})\, \Phi_j(\vec{t} + \vec{k}_j - \vec{k}_{p+q-j})\, d\vec{t} \qquad \text{(E-27)}$$

Insert u^{-2} by writing

$$T^O = \frac{4\pi}{k_j^2} \int \Phi_j(\vec{u} - \vec{k}_{p+q-j})\, \Phi^*_{p+q-j}(\vec{t})\, [\vec{t}+\vec{k}_j]^2\, \frac{\delta}{u^2}\, (\vec{t}+\vec{k}_j-\vec{u}) d\vec{t}\, d\vec{u} \quad \text{(E-28)}$$

$$= \frac{(2\pi)^6}{(2\pi)^3 2\pi^2} \frac{1}{k_j^2} \int \Phi_j(\vec{s}+\vec{t}+\vec{k}_j-\vec{k}_{p+q-j})\, \Phi^*_{p+q-j}(\vec{t})[\vec{t}+\vec{k}_j]^2\, \frac{\delta}{u^2}\, (\vec{t}+\vec{k}_j-\vec{u})$$

$$\delta\, (\vec{u}-\vec{s}-\vec{t}-\vec{k}_j) d\vec{s}\, d\vec{t}\, d\vec{u}\,. \quad \text{(E-29)}$$

Restore the integrations over $d\vec{r}_1 d\vec{r}_2$ in (E-29):

$$T^O = \frac{1}{(2\pi)^3 2\pi^2} \frac{1}{k_j^2} \int \Phi_j(\vec{s}+\vec{t}+\vec{k}_j-\vec{k}_{p+q-j}) \Phi^*_{p+q-j}(\vec{t})[\vec{t}+\vec{k}_j] \frac{1}{u^2}$$

$$e^{i(\vec{t}+\vec{k}_j-\vec{u})\cdot\vec{r}_2}\, e^{i(\vec{u}-\vec{s}-\vec{t}-\vec{k}_j)\cdot\vec{r}_1}\, d\vec{r}_1 d\vec{r}_2 d\vec{s}\, d\vec{t}\, d\vec{u}\,. \quad \text{(E-30)}$$

Collect the exponents involving $\vec{u}$ and use the identity (E-19) to write:

$$T^O = \frac{1}{(2\pi)^3} \frac{1}{k_j^2} \int \Phi_j(\vec{s}+\vec{t}+\vec{k}_j-\vec{k}_{p+q-j}) \Phi^*_{p+q-j}(\vec{t})\, [\vec{t}+\vec{k}_j]^2 \frac{1}{r_{12}}$$

$$e^{i(\vec{t}+\vec{k}_j)\cdot\vec{r}_2}\, e^{-i(\vec{s}+\vec{t}+\vec{k}_j)\cdot\vec{r}_1}\, d\vec{r}_1 d\vec{r}_2 d\vec{s}\, d\vec{t}\,. \quad \text{(E-31)}$$

Let $\vec{s} = \vec{s}' - \vec{t} - \vec{k}_j + \vec{k}_{p+q-j}$ in (E-31)

$$T^{O} = \frac{1}{(2\pi)^3}\frac{1}{k_j^2}\int \Phi_j(\vec{s}')\,\Phi^{*}_{p+q-j}(\vec{t})\,[\vec{t}+\vec{k}_j]^2\,\frac{1}{r_{12}}\,e^{i(\vec{t}+\vec{k}_j)\cdot\vec{r}_2}$$

$$e^{-i(\vec{s}'+\vec{k}_{p+q-j})\cdot\vec{r}_1}\,d\vec{r}_1 d\vec{r}_2 d\vec{s}'\,d\vec{t}.$$

Instead of (E-24), proceed from

$$0 = \frac{1}{(2\pi)^3}\frac{1}{k_j^2}(-\nabla_2^2)\int \Phi_j(\vec{s}')\,\Phi^{*}_{p+q-j}(\vec{t})\,\frac{1}{r_{12}}\,e^{i(\vec{t}+\vec{k}_j)\cdot\vec{r}_2}\,e^{-i(\vec{s}'+\vec{k}_{p+q-j})\cdot\vec{r}_1}$$

$$d\vec{r}_1 d\vec{r}_2 d\vec{s}'\,d\vec{t} \qquad \text{(E-32)}$$

or,

$$0 = \frac{1}{k_j^2}(-\nabla_2^2)\int \frac{1}{(2\pi)^{3/2}}\int \Phi_j(\vec{s}')e^{-i\vec{s}'\cdot\vec{r}_1}\,d\vec{s}'\;e^{-i\vec{k}_{p+q-j}\cdot\vec{r}_1}\,\frac{1}{r_{12}}$$

$$\frac{1}{(2\pi)^{3/2}}\int \Phi^{*}_{p+q-j}(\vec{t})e^{i\vec{t}\cdot\vec{r}_2}d\vec{t}\;e^{i\vec{k}_j\cdot\vec{r}_2}d\vec{r}_1 d\vec{r}_2. \qquad \text{(E-33)}$$

Use equations (E-13), (E-21) to give

$$T^{O} = \int \psi_j(\vec{r}_1)e^{-i\vec{k}_{p+q-j}\cdot\vec{r}_1}\,\frac{1}{r_{12}}\left[-\frac{1}{k_j^2}\nabla_2^2\left\{\psi^{*}_{p+q-j}(\vec{r}_2)e^{i\vec{k}_j\cdot\vec{r}_2}\right\}\right]d\vec{r}_1 d\vec{r}_2$$

$$= \int \psi^{*}_{p+q-j}(\vec{r}_2)e^{-i\vec{k}_{p+q-j}\cdot\vec{r}_1}\,\frac{1}{r_{12}}\,\psi_j(\vec{r}_1)\left[-\frac{1}{k_j^2}\,\frac{\nabla_2^2\left\{\psi^{*}_{p+q-j}(\vec{r}_2)e^{i\vec{k}_j\cdot\vec{r}_2}\right\}}{\psi^{*}_{p+q-j}(\vec{r}_2)}\right]$$

$$d\vec{r}_1 d\vec{r}_2\,. \qquad \text{(E-34)}$$

The "prior" and "post" forms for the transition amplitude are thus

$$\text{("prior")}\ T^{O} = \langle \psi_q(\vec{r}_2)\, {}^{o}g_q^{-}(\vec{r}_1, \vec{r}_2) \left| \frac{1}{r_{12}} \right| \psi_p(\vec{r}_1) e^{i\vec{k}_p \cdot \vec{r}_2} \rangle \qquad \text{(E-35)}$$

$$\text{("post")}\ T^{O} = \langle \psi_q(\vec{r}_2) e^{i\vec{k}_q \cdot \vec{r}_1} \left| \frac{1}{r_{12}} \right| \psi_p(\vec{r}_1)\, {}^{o}g_p^{+}(\vec{r}_1, \vec{r}_2) \rangle \qquad \text{(E-36)}$$

$$\text{where}\ {}^{o}g_j^{\pm} = -\frac{1}{k_j^2} \frac{\nabla^2 \left\{ \psi^*_{p+q-j}(\vec{r}) e^{i\vec{k}_j \cdot \vec{r}} \right\}}{\psi^*_{p+q-j}(\vec{r})} \,. \qquad \text{(E-37)}$$

The r-subscript in (E-37) depends on whether the "prior" or "post" form is being considered.

However, (E-37) is not quite correct as it stands since it does not satisfy (E-3) and (E-4). This can be seen by expanding (E-37) and investigating its asymptotic behavior. Choosing the "post" form (E-36) one has

$${}^{o}g_p^{+} = -\frac{1}{k_p^2} \frac{e^{i\vec{k}_p \cdot \vec{r}_2}}{\psi^*_q(r_2)} \left\{ \nabla_2^2 \psi^*_q + 2i\vec{k}_p \cdot \nabla_2 \psi^*_q - k_p^2 \psi^*_q \right\}, \qquad \text{(E-38)}$$

and by using

$$\left\{ \nabla_2^2 + \frac{2}{r_2} - \frac{1}{q^2} \right\} \psi^*_q(\vec{r}_2) = 0$$

$$\frac{1}{\psi_q^*}\nabla_2\psi_q^* \underset{r_2\to\infty}{\sim} -\frac{\hat{r}}{q} \tag{E-39}$$

$$e^{i\vec{k}_p\cdot\vec{r}_2} \underset{r_2\to\infty}{\sim} \frac{2\pi}{ik_p r_2}\left\{\delta(\hat{r}-\hat{k}_p)e^{ik_p r_2} - \delta(\hat{r}+\hat{k}_p)e^{-ik_p r_2}\right\}, \tag{E-40}$$

(E-38) asymptotically becomes

$${}^{o}g_p^{+} \underset{r_2\to\infty}{\sim} \frac{e^{i\vec{k}_p\cdot\vec{r}_2}}{k_p^2}\left\{k_p^2 + 2i\vec{k}_p\cdot\hat{r} - \frac{1}{q^2}\right\} + \frac{e^{i\vec{k}_p\cdot\vec{r}_2}}{k_p^2}\left(\frac{2}{r_2}\right). \tag{E-41}$$

The last term in (E-41) must be neglected to be consistent with (E-39). The boundary condition (E-3) says ${}^{o}g_p^{+}$ should have outgoing spherical waves and by (E-40) this means $\hat{r} = \hat{q}$. Using this in (E-41) gives

$${}^{o}g_p^{+} \underset{r_2\to\infty}{\sim} \frac{\left(k_p + i\frac{1}{q}\right)^2}{k_p^2} e^{i\vec{k}_1\cdot\vec{r}_2}. \tag{E-42}$$

Hence, although the Ochkur result is not properly normalized, the following quantity is:

$${}^{OR}g_p^{+} \equiv \frac{k_p^2}{\left(k_p + i\frac{1}{p}\right)^2}\,{}^{o}g_p^{+}. \tag{E-43}$$

In general, the proper expression should be

$$OR_{g_j^{\pm}} = \frac{k_j^2}{\left\{k_j \pm i/(p+q-j)\right\}^2} \, {}^{o}g_j^{\pm} \, . \tag{E-44}$$

Thus, the Ochkur expression for the transition amplitude (E-21) should be corrected to

$$T^{OR} = \frac{4\pi}{\left\{k_j \pm i/(p+q-j)\right\}^2} \int \psi^*_{p+q-j}(\vec{r}_1)\, \psi_j(\vec{r}_1) e^{i(\vec{k}_j - \vec{k}_{p+q-j})\cdot \vec{r}_1} \, d\vec{r}_1 . \tag{E-45}$$

Equation (E-45) represents the Rudge modification of the Ochkur result.

Notice that when the given collision process also can proceed by direct excitation, the total transition amplitude will be such that the cross sections will not satisfy detailed balance. This is because although the Born direct transition amplitude satisfies this principle,[Ec] (E-45) does not since

$$\frac{1}{(k_p + i\frac{1}{q})^2} \neq \frac{1}{(k_q - i\frac{1}{p})^2} \, .$$

However, if no direct excitation can occur, then (E-45) does satisfy detailed balance because

$$\left| \frac{1}{(k_p + i\frac{1}{q})^2} \right|^2 = \left| \frac{1}{(k_q - i\frac{1}{q})^2} \right|^2 \tag{E-46}$$

is just the statement of conservation of energy. Since the processes considered here proceed only by exchange excitation, the cross sections reported here satisfy detail balance.

References for Appendix E

(Ea) The initial modification of the Ochkur result was published by:

(1) M. R. H. Rudge, Proc. Phys. Soc. 85, 607 (1965)
M. R. H. Rudge, Proc. Phys. Soc. 86, 763 (1965)

and subsequently the Rudge result was shown to fail at detailed balance by

(2) D. S. F. Crothers, Proc. Phys. Soc. 87, 1003 (1966)

(3) O. Bely, Proc. Phys. Soc. 87, 1010 (1966).

(Eb) L. D. Landau and M. M. Lifshitz, Quantum Mechanics (Addison-Wesley, Second edition (1965)) p. 485.

(Ec) See for example ref. Ea-3.

Appendix F

This appendix contains a brief description of the numerical methods used to evaluate the three-center integrals described in Section II-4. The essential features of the technique are contained in the three-center Coulomb integral program (aa/bc)[F1] written in FORTRAN II and FAP. The important changes that were made to adapt (aa/bc) to the scattering integrals are as follows.

The MAIN of (aa/bc) was replaced by the subroutine FNOV which still performed the initializations that MAIN did. However, FNOV, along with FKBSJ, "faked" two Slater orbitals of screening constants 1/2 q (momentum transfer). FKBSJ unnormalized these Slater orbitals and called BESSEL[F2] to evaluate the spherical BESSEL functions needed in the expansion of $e^{i\vec{q}\cdot\vec{r}_1}$. These changes, along with a few other minor changes are given in the listings of these subroutines on the following pages. A listing of the subroutines BESSEL and GAMMA (called by BESSEL), along with the unaltered subroutines of (aa/bc) are not included but can be obtained via the references.

In the case of the second triplet, it was found convenient to construct four subroutines to initialize prior to FNOV. They were OSOS, OSTS, TSOS, TSTS which call FNOV and then proceed as outlined above. They are also included in these listings.

It was important to test these programs and this was accomplished as follows. If the angle THETA was set equal to 0, the three center integral reduced to a series of two center integrals which could be integrated analytically. This test calculation was done for a few representative values of q and the screening constants. The computer results agreed with hand calculations to 5 decimal places. The final listing in this appendix is the program used to run this test.

References for Appendix F

(F1) This program can be obtained from The Quantum Chemistry Program Exchange, Chemistry Department Room 204, Indiana University, Bloomington, Indiana 47401. The designation of the program is: QCPE 22-25.

(F2) This program was taken from SHARE 1315. It is capable of calculating BESSEL functions of complex order and complex argument. It was written in FT II also.

```
CFNOV
*       LIST
        SUBROUTINE FNOV(VALINT,Q,SC3,SC4)
        COMMON IZXX,IUPVXX,ALF,D1,IMX,THETA,RHOB,RHOC,SK1,SK2,SK3,SK4,SKA,
       1   X,Y,P,M,N,IABSMX,ABSCIS,WEIGHT,IABS2F,ZETA,ZETAPM,TJ,NTERM,NE,
       2      IL,IU,IV,IW,IUS,IVS,IH,IPS,IHS,IUPV,JSUBN,BLSTM1,BLAST
        COMMON   NA,NB,NC,ND,IMX,NU
        COMMON NA1,NA2,NA3,NA4,NB1,NB2,NB3,NB4,NC1,NC2,NC3,NC4,ND1,ND2,
       2   ND3,ND4,IMX,NU,S1,S2,V,SS1,SS2,SS3,SS4,SQ7,SQA,SQB,DELQ,DELQP
        DIMENSION IZXX(5),IUPVXX(5),ALF(5,5,5),D1(30,86),P(30,5),
       1   ABSCIS(48),WEIGHT(48),ZETA(2,34,48),ZETAPM(2,30,48),TJ(8,48),
       2      NE(4),IL(4),IU(4),IV(4),IW(4),IH(4),BLSTM1(2),BLAST(2)
       $   ,TITLE(24)
        THETAP=500.0
        IZXX(1)=1
        IZXX(2)=2
        IZXX(3)=6
        IZXX(4)=18
        IZXX(5)=42
        IUPVXX(1)=0
        IUPVXX(2)=1
        IUPVXX(3)=2
        IUPVXX(4)=4
        IUPVXX(5)=6
        CALL PRPD1
        SK3=SC3
        SK4=SC4
        RHOC=RHOB
        SK1=0.5*Q
        SK2=SK1
        IMX=XMINOF(IMX,29)
        SKA=SK1+SK2
        IZVINT=0
        IF(NC-2) 42,41,42
   41   M=2
        GO TO 43
   42   M=1
   43   IF(ND-2) 45,44,45
   44   N=2
        GO TO 47
   45   N=1
   47   IF(IMX-IMXP) 49,49,48
   48   THETAP=THETA
        CALL PRPLEG
        GO TO 80
   49   IF(THETA-THETAP) 50,58,50
   50   THETAP=THETA
        CALL PRPLEG
   58   IF(NU-NUP) 80,60,80
   60   IF(ABSF(RHOB-RHOBP)+ABSF(RHOC-RHOCP)) 80,61,80
   61   IF(SK3-SK3P) 63,62,63
   62   IF(M-MMX) 64,64,63
   63   CALL PRPZTB
        MMX=M
        IZVINT=1
   64   IF(SK4-SK4P) 66,65,66
   65   IF(N-NMX) 70,70,66
   66   CALL PRPZTC
        NMX=N
        IZVINT=1
   70   IF(SKA-SKAP) 71,130,71
```

```
   71 CALL LITLJ
      IZVINT=1
      GO TO 130
   80 CALL QUAD1(RHOB,RHOC,IABSMX,ABSCIS,WEIGHT,NU)
      IZVINT=1
      CALL PRPZTB
      MMX=M
      CALL PRPZTC
      NMX=N
      CALL LITLJ
      NUP=NU
      RHOBP=RHOB
      RHOCP=RHOC
  130 NTERM=0
      IMXP=IMX
      SK3P=SK3
      SK4P=SK4
      SKAP=SKA
      VALINT=AABC(NA,NB,NC,ND,IZVINT)
      RETURN
      END
```

```
CFKBSJ
*       LIST
*       SYMBOL TABLE
        SUBROUTINE LITLJ
        COMMON IZXX,IUPVXX,ALF,D1,IMX,THETA,RHOB,RHOC,SK1,SK2,SK3,SK4,SKA,
       1   X,Y,P,M,N,IABSMX,ABSCIS,WEIGHT,IABS2F,ZETA,ZETAPM,TJ,NTERM,NE,
       2      IL,IU,IV,IW,IUS,IVS,IH,IPS,IHS,IUPV,JSUBN,BLSTM1,BLAST
        COMMON   NA,NB,NC,ND,IMX,NU
        COMMON NA1,NA2,NA3,NA4,NB1,NB2,NB3,NB4,NC1,NC2,NC3,NC4,ND1,ND2,
       2   ND3,ND4,IMX,NU,S1,S2,V,SS1,SS2,SS3,SS4,SQZ,SQA,SQB,DELO,DELOP
        DIMENSION IZXX(5),IUPVXX(5),ALF(5,5,5),D1(30,86),P(30,5),
       1   ABSCIS(48),WEIGHT(48),ZETA(2,34,48),ZETAPM(2,30,48),TJ(8,48),
       2      NE(4),IL(4),IU(4),IV(4),IW(4),IH(4),BLSTM1(2),BLAST(2)
        DO 100 I=1,IABSMX
        QR=SKA*ABSCIS(I)
        CALL BESSEL(0.5,0.0,QR,0.0,BES0,BI,BRD,BID,15)
        TJ(1,I)=2.0*BES0/SKA
        CALL BESSEL(1.5,0.0,QR,0.0,BES1,BI,BRD,BID,15)
        TJ(4,I)=4.0*ABSCIS(I)*BES1
        CALL BESSEL(2.5,0.0,QR,0.0,BES2,BI,BRD,BID,15)
        TJ(8,I)=-2.0*QR*ABSCIS(I)*BES2
100     TJ(7,I)=-6.0*TJ(8,I)
        RETURN
        END
```

```
COSOS
*       LIST
*       SYMBOL TABLE
        SUBROUTINE OSOS(JA,JB,JC,JD,Q,SS1,SS2,ANS)
        COMMON IZXX,IUPVXX,ALF,D1,IMX,THETA,RHOB,RHOC,SK1,SK2,SK3,SK4,SKA,
       1    X,Y,P,M,N,IABSMX,ABSCIS,WEIGHT,IABS2F,ZETA,ZETAPM,TJ,NTERM,NE,
       2       IL,IU,IV,IW,IUS,IVS,IH,IPS,IHS,IUPV,JSUBN,BLSTM1,BLAST
        COMMON    NA,NB,NC,ND,IMX,NU
        COMMON NA1,NA2,NA3,NA4,NB1,NB2,NB3,NB4,NC1,NC2,NC3,NC4,ND1,ND2,
       2    ND3,ND4,IMX,NU,S1,S2,V,SS1,SS2,SS3,SS4,SQZ,SQA,SQB,DELO,DELOP
        DIMENSION IZXX(5),IUPVXX(5),ALF(5,5,5),D1(30,86),P(30,5),
       1    ABSCIS(48),WEIGHT(48),ZETA(2,34,48),ZETAPM(2,30,48),TJ(8,48),
       2       NE(4),IL(4),IU(4),IV(4),IW(4),IH(4),BLSTM1(2),BLAST(2)
        NA=JA
        NB=JB
        NC=JC
        ND=JD
        CALL FNOV(ANSA,Q,SS1,SS2)
        ANS=ANSA
        RETURN
        END
COSTS
*       LIST
*       SYMBOL TABLE
        SUBROUTINE OSTS(JA,JB,JC,JD,Q,SS3,SS4,ANS)
        COMMON IZXX,IUPVXX,ALF,D1,IMX,THETA,RHOB,RHOC,SK1,SK2,SK3,SK4,SKA,
       1    X,Y,P,M,N,IABSMX,ABSCIS,WEIGHT,IABS2F,ZETA,ZETAPM,TJ,NTERM,NE,
       2       IL,IU,IV,IW,IUS,IVS,IH,IPS,IHS,IUPV,JSUBN,BLSTM1,BLAST
        COMMON    NA,NB,NC,ND,IMX,NU
        COMMON NA1,NA2,NA3,NA4,NB1,NB2,NB3,NB4,NC1,NC2,NC3,NC4,ND1,ND2,
       2    ND3,ND4,IMX,NU,S1,S2,V,SS1,SS2,SS3,SS4,SQZ,SQA,SQB,DELO,DELOP
        DIMENSION IZXX(5),IUPVXX(5),ALF(5,5,5),D1(30,86),P(30,5),
       1    ABSCIS(48),WEIGHT(48),ZETA(2,34,48),ZETAPM(2,30,48),TJ(8,48),
       2       NE(4),IL(4),IU(4),IV(4),IW(4),IH(4),BLSTM1(2),BLAST(2)
        NA=JA
        NB=JB
        NC=JC
        ND=JD
        CALL FNOV(ANSB,Q,SS3,SS4)
        ANS=ANSB
        RETURN
        END
CTSOS
*       LIST
*       SYMBOL TABLE
        SUBROUTINE TSOS(JA,JB,JC,JD,Q,SS1,SS2,ANS)
        COMMON IZXX,IUPVXX,ALF,D1,IMX,THETA,RHOB,RHOC,SK1,SK2,SK3,SK4,SKA,
       1    X,Y,P,M,N,IABSMX,ABSCIS,WEIGHT,IABS2F,ZETA,ZETAPM,TJ,NTERM,NE,
       2       IL,IU,IV,IW,IUS,IVS,IH,IPS,IHS,IUPV,JSUBN,BLSTM1,BLAST
        COMMON    NA,NB,NC,ND,IMX,NU
        COMMON NA1,NA2,NA3,NA4,NB1,NB2,NB3,NB4,NC1,NC2,NC3,NC4,ND1,ND2,
       2    ND3,ND4,IMX,NU,S1,S2,V,SS1,SS2,SS3,SS4,SQZ,SQA,SQB,DELO,DELOP
        DIMENSION IZXX(5),IUPVXX(5),ALF(5,5,5),D1(30,86),P(30,5),
       1    ABSCIS(48),WEIGHT(48),ZETA(2,34,48),ZETAPM(2,30,48),TJ(8,48),
       2       NE(4),IL(4),IU(4),IV(4),IW(4),IH(4),BLSTM1(2),BLAST(2)
        NA=JA
        NB=JB
        NC=JC
        ND=JD
        CALL FNOV(ANSC,Q,SS1,SS2)
        ANS=ANSC
```

```
      RETURN
      END
CTSTS
*     LIST
*     SYMBOL TABLE
      SUBROUTINE TSTS(JA,JB,JC,JD,Q,SS3,SS4,ANS)
      COMMON IZXX,IUPVXX,ALF,D1,IMX,THETA,RHOB,RHOC,SK1,SK2,SK3,SK4,SKA,
     1   X,Y,P,M,N,IABSMX,ABSCIS,WEIGHT,IABS2F,ZETA,ZETAPM,TJ,NTERM,NE,
     2      IL,IU,IV,IW,IUS,IVS,IH,IPS,IHS,IUPV,JSUBN,BLSTM1,BLAST
      COMMON   NA,NB,NC,ND,IMX,NU
      COMMON NA1,NA2,NA3,NA4,NB1,NB2,NB3,NB4,NC1,NC2,NC3,NC4,ND1,ND2,
     2   ND3,ND4,IMX,NU,S1,S2,V,SS1,SS2,SS3,SS4,SQZ,SQA,SQB,DELO,DELOP
      DIMENSION IZXX(5),IUPVXX(5),ALF(5,5,5),D1(30,86),P(30,5),
     1   ABSCIS(48),WEIGHT(48),ZETA(2,34,48),ZETAPM(2,30,48),TJ(8,48),
     2      NE(4),IL(4),IU(4),IV(4),IW(4),IH(4),BLSTM1(2),BLAST(2)
      NA=JA
      NB=JB
      NC=JC
      ND=JD
      CALL FNOV(ANSD,Q,SS3,SS4)
      ANS=ANSD
      RETURN
      END
```

```
      DIMENSION IZXX(5),IUPVXX(5),ALF(5,5,5),D1(30,86),P(30,5),
     1   ABSCIS(48),WEIGHT(48),ZETA(2,34,48),ZETAPM(2,30,48),TJ(8,48),
     2      NE(4),IL(4),IU(4),IV(4),IW(4),IH(4),BLSTM1(2),BLAST(2)
     3   ,TITLE(24)
      DIMENSION DUMMY(3)
C*****************************************************************************
C THE FOLLOWING STATEMENT(S) HAVE BEEN MANUFACTURED BY THE TRANSLATOR TO
C   COMPENSATE FOR THE FACT THAT EQUIVALENCE DOES NOT REORDER COMMON---
C*****************************************************************************
      0COMMON/LOCA/IZXX,IUPVXX,ALF,D1,IMX,THETA,RHOB,RHOC,SK1,SK2,SK3,SK4
     1,SKA,X,Y,M,N,IABSMX,IABS2F,P,ABSCIS,WEIGHT,ZETA,ZETAPM,BLAST,BLSTM
     21,TJ,NTERM,NE,IL,IU,IV,IW,IUS,IVS,IH,IPS,IHS,IUPV,JSUBN,NTEST,LAST
      COMMON/MOCA/NA,NB,NC,ND,NU
C*****************************************************************************
C      COMMON IZXX,IUPVXX,ALF,D1,IMX,THETA,RHOB,RHOC,SK1,SK2,SK3,SK4,SKA,
C     1   X,Y,P,M,N,IABSMX,ABSCIS,WEIGHT,IABS2F,ZETA,ZETAPM,TJ,NTERM,NE,
C     2      IL,IU,IV,IW,IUS,IVS,IH,IPS,IHS,IUPV,JSUBN,BLSTM1,BLAST,
C     3   NA,NB,NC,ND,IMX,NU
C      DIMENSION IZXX(5),IUPVXX(5),ALF(5,5,5),D1(30,86),P(30,5),
C     1   ABSCIS(48),WEIGHT(48),ZETA(2,34,48),ZETAPM(2,30,48),TJ(8,48),
C     2      NE(4),IL(4),IU(4),IV(4),IW(4),IH(4),BLSTM1(2),BLAST(2)
C     3   ,TITLE(24)
C*****************************************************************************
10    READ(5,20) NA,NB,NC,ND,IMX,NU,NON
20    FORMAT(7I3)
      READ(5,37) RHOB,SS1,SS2,SS3,SS4
37    FORMAT(5F10.7)
      THETA=0.00
C*****************************************************************************
C    NOTE THAT THIS IS A TWO CENTER INTEGRAL NOW.  WHEN DOING THE
C      THREE CENTER INTEGRALS MUST ALSO CHANGE THE VALUE OF THETA IN
C      THE SUBROUTINE FNOV.
C*****************************************************************************
      WRITE(6,20) NA,NB,NC,ND,IMX,NU,NON
      WRITE(6,88) RHOB,SS1,SS2,SS3,SS4
88    FORMAT(5F10.7)
      DO 17 I=1,3
      XNUM=DUMMY(I)
      RF=I-1
      Q=1.000+RF*1.0
      CALL FNOV(VALNT1,Q,SS1,SS2)
      CALL FNOV(VALNT2,Q,SS3,SS4)
17    WRITE(6,2) Q,VALNT1,VALNT2
2     FORMAT(F10.3,2E25.5///)
      IF(NON) 10,31,10
31    STOP
      END
```

Appendix G

This appendix sketches the methods used to calculate numerically the cross sections of interest. As seen from (II-2-23), the calculation of the total cross section requires a three-fold numerical integration: the outermost over R (or E'), the middle over q, and the innermost for the evaluation of the matrix element (the three-center integrals). The matrix element integration is described in Appendix F so only the outer two integrations will be treated here. Because of the quantity of words that would be necessary to describe these programs, only flow charts and listings will be given.

The first flow chart is for the calculation of the total cross section. The second flow chart is for the Simpson's rule integration over q, which utilizes the monotonic nature of q_{min} and q_{max}. A flow chart for the angular distribution calculation can be obtained by a simple modification of the total cross section flow chart.

The first four listings are subroutines used to calculate the molecular constants as functions of the internuclear distance R. They are SCREEN and CONSTS for the first triplet, and STSCR and STCONS for the second triplet. The next two listings are typical programs used to calculate a total cross section; the example being used is excitation of the first triplet state. The first of these two is the main program and the second is the Simpson's rule integration scheme. The seventh listing is a typical angular distribution program, the excitation of the second triplet being used as an example. The final listing is the program used to calculate the weight and abscissa values[(Ga)] for the outer Gauss-Hermite integration (over R or E').

The accuracy of the Simpson's rule integration was checked by integrating a decaying exponential times a polynomial in q. This

choice was made because it could be done analytically and yet possessed the proper fall-off with increasing q. This method was used to determine the optimum step sizes (DELO and DELOP) such that 4 decimal place accuracy could be expected.

References for Appendix G

(Ga) The techniques used in the determination of the weights and abscissa values are those outlined in ref. (58) p. 350. Note that a n-point quadrature will integrate a 2n - 1 degree polynomial exactly. The accuracy of this program was checked by letting the integral approach the usual Gauss-Hermite integral:

$$\int_{z}^{\infty} e^{ix^2} f(x)dx \xrightarrow[z \to -\infty]{} \int_{-\infty}^{\infty} e^{-x^2} f(x)dx .$$

The weights and abscissa values calculated by this program agreed with the tabulated values to 6 decimal places.

Total Cross Section

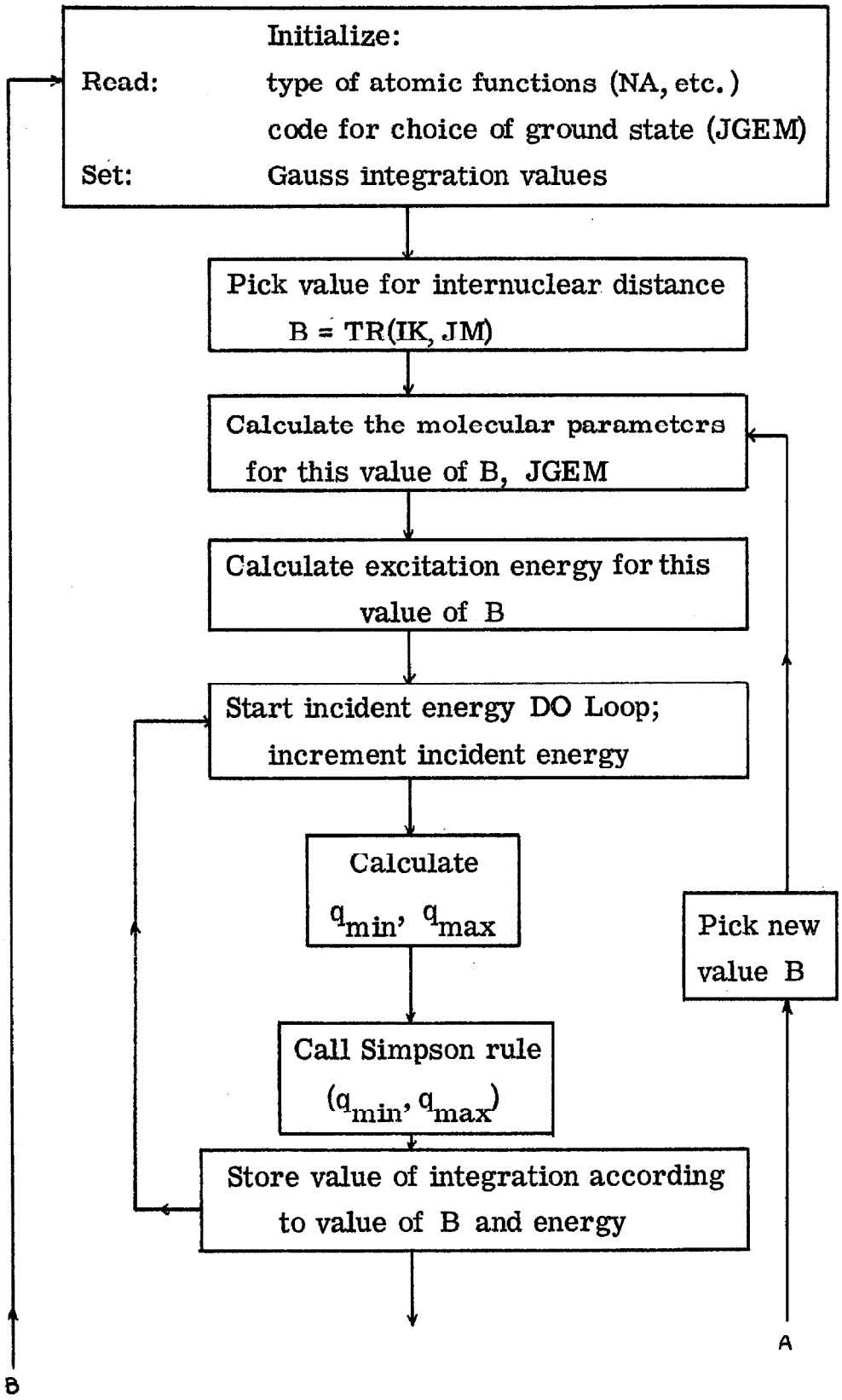

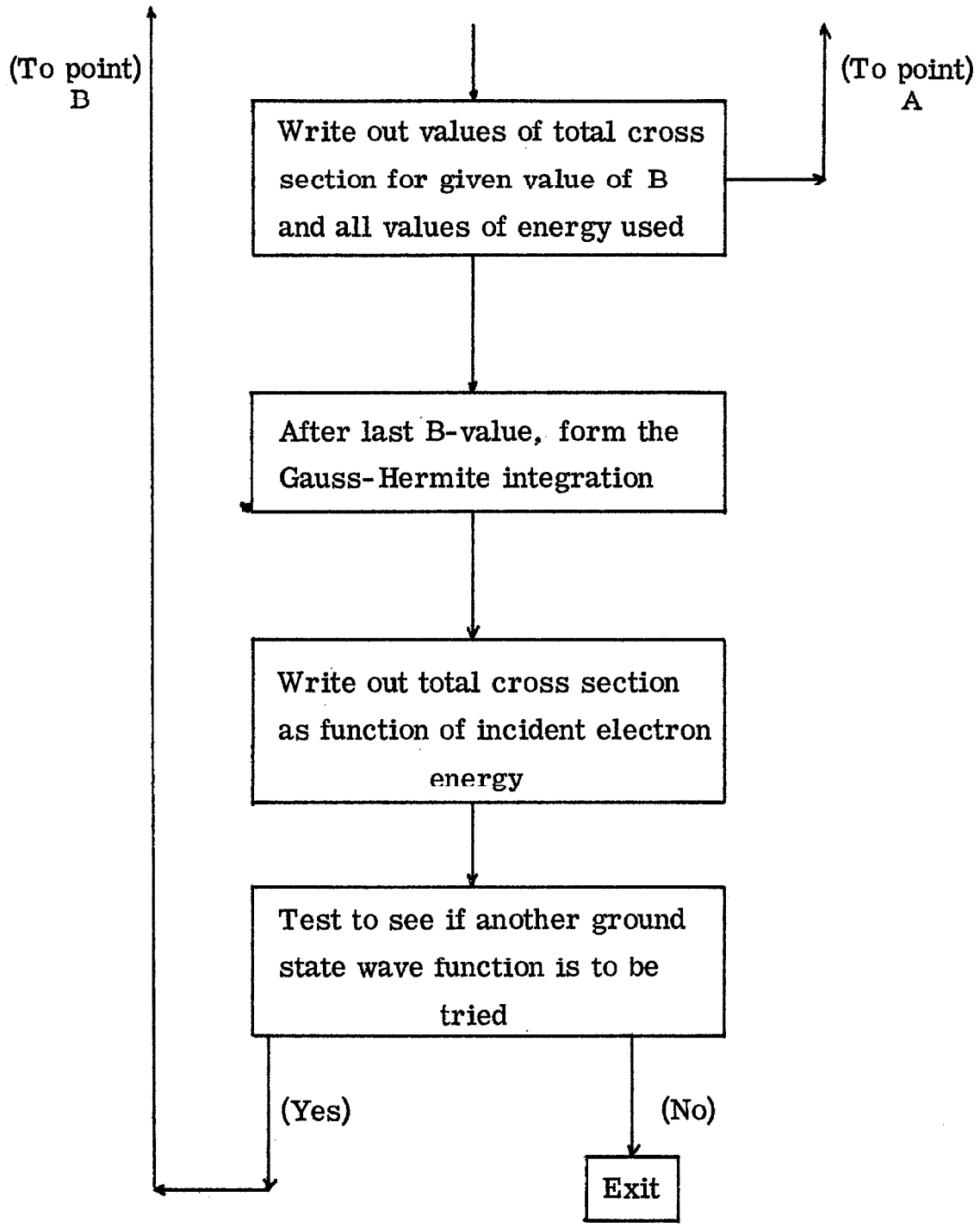
(To point) B
(To point) A
Write out values of total cross section for given value of B and all values of energy used
After last B-value, form the Gauss-Hermite integration
Write out total cross section as function of incident electron energy
Test to see if another ground state wave function is to be tried
(Yes)
(No)
Exit

Simpson Integration Scheme

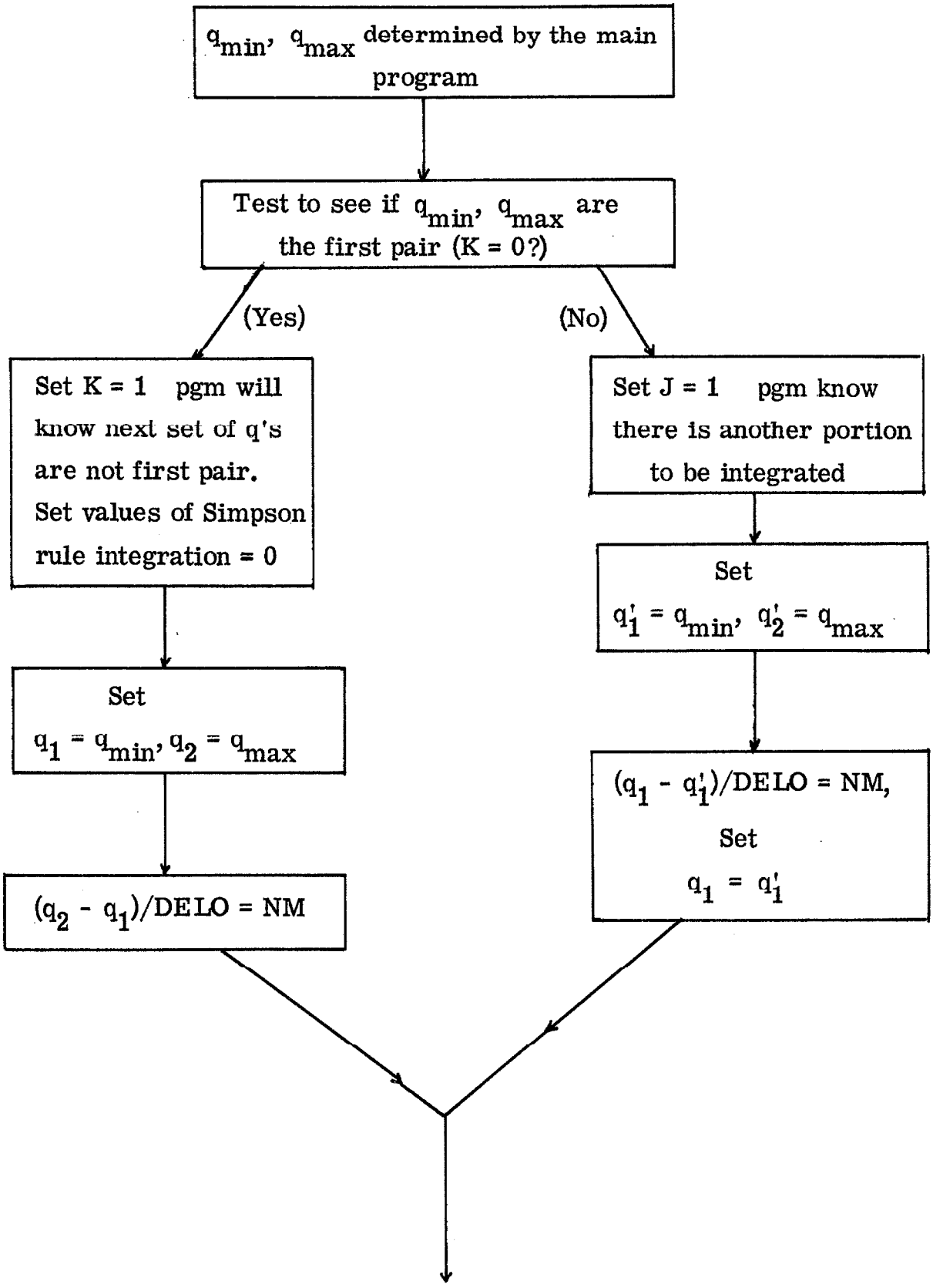

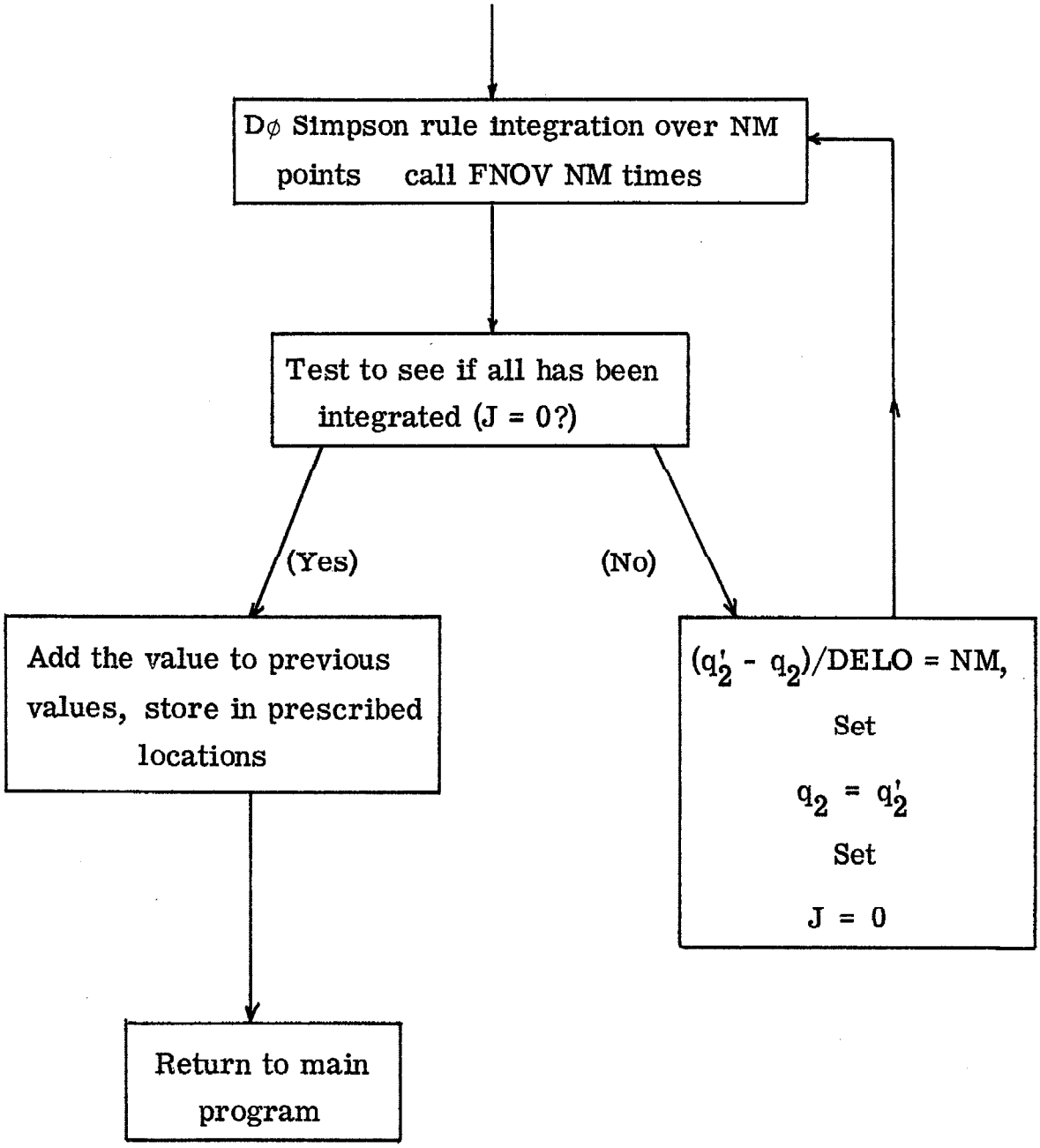
Dφ Simpson rule integration over NM points call FNOV NM times
Test to see if all has been integrated (J = 0?)
(Yes)
(No)
Add the value to previous values, store in prescribed locations
$(q_2' - q_2)/DELO = NM$,
Set
$q_2 = q_2'$
Set
J = 0
Return to main program

```
$IBFTC SCREEN  DECK     GIVES 7,Z1,Z2 FOR GROUNDS AND FIRST EXCITED TRIP
      SUBROUTINE SCREEN (AR,JI,AZ,AZ1,AZ2)
C     JI=1,2,3 MEANS WEINBAUM,WANG,COULSON GROUND STATES  RESPECTIVELY.
      R=AR
      IF(JI.EQ.1) GO TO 600
      IF(JI.EQ.2) GO TO 610
      IF(JI.EQ.3) GO TO 620
600   AZ=1.75812-0.61451*R+0.18466*R*R-0.02158*(R**3)
      GO TO 630
610   AZ=1.80975-0.724746*R+0.22766*R*R-0.02618*(R**3)
      GO TO 630
620   AZ=1.76254-0.62635*R+0.18896*R*R-0.02423*(R**3)
630   AZ1=1.99346-0.71167*R+0.19879*R*R-0.02250*(R**3)
      AZ2=-0.19289+0.79983*R-0.20391*R*R+0.01864*(R**3)
      RETURN
      END
```

```
CCONSTS
      SUBROUTINE CONSTS(TZ,T1,T2,TD,TS1,TS2,TV,TCONS,TFF1,TFF2,JG)
C     THIS SUBROUTINE CALCULATES THE NORMALIZATION CONSTANTS FOR THE
C     GROUND STATES AND EXCITED STATE WAVEFUNCTIONS.  IT ALSO CALCS V.
      PI=3.14159266
      IF(JG-2) 43,44,42
42    C=1.0
      GO TO 33
44    C=0.0
      GO TO 33
43    C=0.047059+0.31286*TD-0.11245*TD*TD
33    CP=1.+C
      CF=1.+C*C
      CM=1.-C
      Z=TZ
      TS1=Z+T1
      TS2=Z+T2
      SZ1=SQRTF(T1*Z)
      SZ2=SQRTF(T2*Z)
      TFF1=PI/(T1*Z*SZ1)
      TFF2=PI/(Z*T2*SZ2)
      SOZ=EXPF(-Z*TD)*(1.+Z*TD+Z*Z*TD*TD/3.)
      SO1=EXPF(-T1*TD)*(1.+T1*TD+T1*T1*TD*TD/3.)
      SO2=EXPF(-T2*TD)*(1.+T2*TD+T2*T2*TD*TD/3.)
      BLIP=1.-SO2+SO1-SO2*SO1
      ORMES=((T2**3.)*(T1**3.)/(PI*PI))*(1./(8.*BLIP))
      AEG=2.*PI*PI*CF*(1.+SOZ*SOZ+4.*C/CF*SOZ)
      ORMGS=(Z**6.)/AEG
      A1=8.*PI/(TS1**3)
      RHH=TD/2.*TS1
      GAM=TD/2.*(T1-Z)
      SONH=0.5*(EXPF(GAM)-EXPF(-GAM))
      CISH=SONH+EXPF(-GAM)
      TMID=SONH/GAM*(1./RHH+1./(RHH*RHH)-1./(GAM*GAM))+CISH/(GAM*GAM)
      B1=PI*TD*TD*TD*EXPF(-RHH)/RHH*TMID
      BET=A1+B1
      A2=8.*PI/(TS2**3)
      RHI=TD/2.*TS2
      GAI=TD/2.*(Z-T2)
      SONI=0.5*(EXPF(GAI)-EXPF(-GAI))
      CISI=SONI+EXPF(-GAI)
      TMII=SONI/GAI*(1./RHI+1./(RHI*RHI)-1./(GAI*GAI))+CISI/(GAI*GAI)
      B2=PI*TD*TD*TD*EXPF(-RHI)/RHI*TMII
      GAFF=A2-B2
      TV=(CM*GAFF)/(CP*BET)
      TCONS=12.*PI*ORMGS*ORMES*CP*CP*BET*BET
      RETURN
      END
```

```
*       LIST
        SUBROUTINE STSCR(AR,JI,BZ,BZ1,BZ2)
C     JI=1,2,3 MEANS WEINBAUM,WANG,COULSON GROUND STATES  RESPECTIVELY.
        R=AR
        IF(JI-1) 599,600,601
599     PRINT 650
650     FORMAT(11HJI IN ERROR)
        GO TO 660
601     IF(JI-2) 599,610,620
600     BZ=1.75812-0.61451*R+0.18466*R*R-0.02158*(R**3)
        GO TO 630
610     BZ=1.80975-0.724746*R+0.22766*R*R-0.02618*(R**3)
        GO TO 630
620     BZ=1.76254-0.62635*R+0.18896*R*R-0.02423*(R**3)
630     BZ1=1.54616+0.38585*R-0.48119*(R**2)+0.075253*(R**3)
        BZ2=0.24065+0.15509*R+0.06026*(R**2)-0.02328*(R**3)
660     RETURN
        END
```

```
CSTCONS
      SUBROUTINE STCONS(TZ,T1,T2,DD,TS1,TS2,TV,TCONS,TQZ,TQA,TQB,JG)
      COMMON NA,NB,NC,ND,IMX,NU,C
      PI=3.14159266
      IF(JG-2) 43,44,42
42    C=1.0
      GO TO 33
44    C=0.0
      GO TO 33
43    C=0.047059+0.31286*DD-0.11245*DD*DD
33    CP=1.+C
      CW=1.+C*C
      Z=TZ
      Z1=T1
      Z2=T2
      S1=Z+Z1
      S2=Z+Z2
      TS1=S1
      TS2=S2
      TQZ=SQRTF(PI/(Z**3))
      TQA=SQRTF(PI/(Z1**3))
      TQB=SQRTF(3.*PI/(Z2**5))
      SOZ=EXPF(-Z*DD)*(1.+Z*DD+Z*Z*DD*DD/3.)
      BIF=1.+SOZ*SOZ+4.*C*SOZ/CW
      ORMGS=(Z**6)/(PI*PI)*(1./(2.*CW*BIF))
C     TERM=(0.3643*0.5436-0.0186*0.2085)/(TQA*TQB)  WAS THE OLD CARD
      TRRR=(0.427213-0.267873*DD+0.127455*(DD*DD))
      TERM=TRRR/(TQA*TQB)
      ORMES=TERM*TERM
      A1=8.*PI/(S1**3)
      RA=S1*DD/2.
      GA=(Z1-Z)*DD/2.
      RB=S2*DD/2.
      GB=(Z-Z2)*DD/2.
      SOAA=0.5*(EXPF(GA)-EXPF(-GA))
      CISA=SOAA+EXPF(-GA)
      BOA=SOAA/GA*(1./RA+1./(RA*RA)-1./(GA*GA))
      BOB=CISA/(GA*GA)
      B1=PI*DD*DD*DD*EXPF(-RA)/RA*(BOA+BOB)
      ALPHA=A1+B1
      A2=24.*PI/(S2**4)
      BTA=1./RB+3./(RB**2)+3./(RB**3)+1./GB-1./(RB*GB)-1./(GB*RB*RB)
     2+3./(GB**3)-1./(GB**2)-1./(RB*GB*GB)
      BTB=1./RB+1./(RB**2)+1./GB+1./(GB*RB)-3./(GB**2)
      SOAB=0.5*(EXPF(GB)-EXPF(-GB))
      CISB=SOAB+EXPF(-GB)
      B2=PI*(DD**4)/2.*EXPF(-RB)/RB*(SOAB/GB*BTA+CISB/GB*BTB)
      DELT=A2+B2
      TV=ALPHA/DELT
      TCONS=6.*PI*ORMGS*ORMES*CP*CP*DELT*DELT
      RETURN
      END
```

```
C*************************************************************************
C     THIS PROGRAM CALCULATES THE TOTAL CROSS SECTION FOR EXCITATION
C     OF TRIPLET LEVELS IN H2 BY ELECTRON IMPACT ALA THE GENERAL
C     METHOD OF OCHKUR OR RUDGE.  THE APPLICATION INCLUDES AN INTEGRA-
C     OVER THE INTERNUCLEAR DISTANCE.  THE OUTER INTEGRATION IS GAUSS-
C     IAN AND THE INNER IS SIMPSON.  THE OUTER GAUSSIAN INVOLVES A
C     SPECIFIC SET OF ABCISSA AND WEIGHTS FOR THE DELTA-ENERGY OF THE
C     TRANSITITON.  THESE WEIGHTS ARE OBTAINED BY PROGRAM HJAJ.
C     THE GROUND STATES CAN BE WEINBAUM,WANG,COULSON AND THE EXCITED
C     STATE IS PHILLIPSON-MULLIKAN.
C*************************************************************************
*     LIST
*     SYMBOL TABLE
      COMMON IZXX,IUPVXX,ALF,D1,IMX,THETA,RHOB,RHOC,SK1,SK2,SK3,SK4,SKA,
     1   X,Y,P,M,N,IABSMX,ABSCIS,WEIGHT,IABS2F,ZETA,ZETAPM,TJ,NTERM,NE,
     2      IL,IU,IV,IW,IUS,IVS,IH,IPS,IHS,IUPV,JSUBN,BLSTM1,BLAST,
     4   NA,NB,NC,ND,IMX,NU,S1,S2,V,SS1,SS2,SS3,SS4,FF2,FF1,DELO,DELOP
      DIMENSION IZXX(5),IUPVXX(5),ALF(5,5,5),D1(30,86),P(30,5),
     1   ABSCIS(48),WEIGHT(48),ZETA(2,34,48),ZETAPM(2,30,48),TJ(8,48),
     2      NE(4),IL(4),IU(4),IV(4),IW(4),IH(4),BLSTM1(2),BLAST(2)
      DIMENSION TSIGT(12),TR(3,5),HHF(3,5),ENER(12),RO(3,12)
      READ 20,NA,NB,NC,ND,IMX,NU
20    FORMAT(6I3)
      PRINT 45,NA,NB,NC,ND,IMX,NU
45    FORMAT(3HNA=,I3,3X,3HNB=,I3,3X,3HNC=,I3,3X,3HND=,I3,3X,
     54HIMX=,I4,3X,3HNU=,I3)
47    READ 101, JGEM
101   FORMAT(I10)
      THETA=3.14159266
      PI=3.14159266
      DELO=0.02
      DELOP=0.005
      ALFAP=18.4
      SPI=SQRTF(PI)
      FRONT=1./SPI
      SALF=SQRTF(ALFAP)
      XVAL=1.2247449/SALF
      DELTF=1.0
      TR(1,1)=1.649955
      TR(2,1)=1.758458
      TR(3,1)=1.939779
      HHF(1,1)=0.094009
      HHF(2,1)=0.058437
      HHF(3,1)=0.004506
      TR(1,2)=1.523542
      TR(2,2)=1.656939
      TR(3,2)=1.862597
      HHF(1,2)=0.289925
      HHF(2,2)=0.217733
      HHF(3,2)=0.020587
      TR(1,3)=1.402524
      TR(2,3)=1.568075
      TR(3,3)=1.798589
      HHF(1,3)=0.515389
      HHF(2,3)=0.511151
      HHF(3,3)=0.061628
      TR(1,4)=1.291864
      TR(2,4)=1.496149
      TR(3,4)=1.749283
      HHF(1,4)=0.574782
      HHF(2,4)=0.831250
```

```
      HHF(3,4)=0.129512
      TR(1,5)=1.400-XVAL
      TR(2,5)=1.400
      TR(3,5)=1.400+XVAL
      HHF(1,5)=0.2954909
      HHF(2,5)=1.1816359
      HHF(3,5)=HHF(1,5)
      PRINT 134,    ((TR(JI,KI),KI=1,5),JI=1,3),((HHF(NI,MI),MI=1,5
     2),NI=1,3)
  134 FORMAT(1H0,9HTR MATRIX//    (3(5F10.4//)),2X,10HHHF MATRIX//
     3(3(5F10.4//)))
      PRINT 102, JGEM
  102 FORMAT(1H1,5HJGEM=,I3//)
      DO 991 IK=1,3
      JM=5
      OUTTA=0.000
      OUTTB=0.000
      OUTTC=0.000
      B=TR(IK,JM)
      CALL SCREEN (B,JGEM,Z,Z1,Z2)
      CALL CONSTS(Z,Z1,Z2,B,S1,S2,V,CONST,FF1,FF2,JGEM)
      SS1=Z
      SS2=Z2
      SS3=Z1
      SS4=Z
      PRINT 832,B,SS1,SS2,SS3,SS4,V,FF1,FF2,CONST,C
  832 FORMAT(1H1,10F13.5//)
      FNDIF=-7.401*B+21.0081
      FM=FNDIF/13.6
      DO 310 JJ=5,9
      KK=JJ-5
      RR=JJ-5
      ENERGY=13.0+RR*DELTE
  745 EN=ENERGY/13.6
      ENER(JJ)=ENERGY
      TPP=SQRTF(EN)
      TEMPS=ABSF(EN-FM)
      S=SQRTF(TEMPS)
      QMIN=TPP-S
      QMAX=TPP+S
      CALL SIMP(QMIN,QMAX,B,KK,VALUE1,VALUE2,VALUE3)
      WI=FN*(S*S+1.)*(S*S+1.)
      W=1./WI
      OUTTA=2.*PI*VALUE1*CONST*W
      OUTTB=2.*PI*VALUE2*CONST*W
      OUTTC=2.*PI*VALUE3*CONST*W
      TERM=OUTTA-OUTTB+OUTTC
  310 RO(IK,JJ)=TERM
  991 PRINT 21, B,(ENER(K),RO(IK,K),K=5,12)
   21 FORMAT(1H0,25HINTER NUCLEAR DISTANCE IS,4X,F6.4//(40X,F10.3,30X,
     2F15.5//))
      DO 750 JJ=5,12
  750 TSIGT(JJ)=FRONT*(HHF(1,5)*RO(1,JJ)+HHF(2,5)*RO(2,JJ)+HHF(3,5)*
     3RO(3,JJ))
      PRINT 753
  753 FORMAT(1H1,50X,26HTHE TOTAL CROSS SECTION IS//)
      PRINT 751, (ENER(MI),TSIGT(MI),MI=5,12)
  751 FORMAT(1H0,40X,7HENERGY=,F7.3,20X,6HTSIGT=,E15.5//)
      IF(NON-3) 47,13,47
   13 STOP
      END
```

```
CSIMP
      SUBROUTINE SIMP(QL,QU,DD,K,VAL,VALB,VALC)
      COMMON IZXX,IUPVXX,ALF,D1,IMX,THETA,RHOB,RHOC,SK1,SK2,SK3,SK4,SKA,
     1   X,Y,P,M,N,IABSMX,ABSCIS,WEIGHT,IABS2F,ZETA,ZETAPM,TJ,NTERM,NE,
     2      IL,IU,IV,IW,IUS,IVS,IH,IPS,IHS,IUPV,JSUBN,BLSTM1,BLAST,
     4   NA,NB,NC,ND,IMX,NU,S1,S2,V,SS1,SS2,SS3,SS4,FF2,FF1,DELO,DELOP
      DIMENSION IZXX(5),IUPVXX(5),ALF(5,5,5),D1(30,86),P(30,5),
     1   ABSCIS(48),WEIGHT(48),ZETA(2,34,48),ZETAPM(2,30,48),TJ(8,48),
     2      NE(4),IL(4),IU(4),IV(4),IW(4),IH(4),BLSTM1(2),BLAST(2)
      PI=3.14159266
      RHOB=DD/2.
      IF(K) 22,1,22
22    J=1
      D=QASTQL-QL
      QASTQL=QL
      QQ=QL
4     NM=D/DELO
      IF(NM) 11,11,10
10    FN=NM
      DEL=D/FN
      HH=DEL/3.
      F=QQ
      FA=16.*S2/((S2*S2+E*E)*(S2*S2+E*E))
      GA=16.*S1/((S1*S1+E*E)*(S1*S1+E*E))
      HA=FA+V*GA
      PHASA=0.5*(1.-SINF(E*DD)/(E*DD))
      CALL FNOV(VALNTA,E,SS1,SS2)
      CALL FNOV(VALNTB,E,SS3,SS4)
      VALSA=FF2*VALNTA+V*FF1*VALNTB
      YTA=E*DD/2.
      THETB=1./(YTA*YTA)*(SINF(YTA)-YTA*COSF(YTA))
      SIGA=HA*HA*E*PHASA
      SIGB=E*(12./PI)*HA*VALSA*THETB
      SIGC=E*(12./PI)*VALSA*VALSA/PI
      DO 3 I=1,NM
      R=I
      Q=QQ+R*DEL
      F=16.*S2/((S2*S2+Q*Q)*(S2*S2+Q*Q))
      G=16.*S1/((S1*S1+Q*Q)*(S1*S1+Q*Q))
      H=F+V*G
      YY=Q*DD
      PHASE=0.5*(1.-SINF(YY)/YY)
      CALL FNOV(VALNT1,Q,SS1,SS2)
      CALL FNOV(VALNT2,Q,SS3,SS4)
      VALSS=FF2*VALNT1+V*FF1*VALNT2
      YT=YY/2.
      THETT=(1./(YT*YT))*(SINF(YT)-YT*COSF(YT))
      SIG1=Q*H*H*PHASE
      SIG2=Q*(12./PI)*H*VALSS*THETT
      SIG3=Q*(12./PI)*VALSS*VALSS/PI
      SR=2.0
      IF(I-NM) 60,9,60
60    II=I/2
      II=II*2
      IF(I-II) 61,62,61
61    SR=4.0
62    SIGA=SIGA+SR*SIG1
      SIGB=SIGB+SR*SIG2
      SIGC=SIGC+SR*SIG3
      GO TO 3
9     SIGA=SIGA+SIG1
```

```
      SIGB=SIGP+SIG2
      SIGC=SIGC+SIG3
3     CONTINUE
      VAL=SIGA*HH+VAL
      VALB=SIGP*HH+VALB
      VALC=SIGC*HH+VALC
      IF(J) 97,99,97
11    PRINT 12
12    FORMAT(37H Q INTEGRATION INDEX ZERO, DELOP USED,1X,I4)
      NM=D/DELOP
      IF(NM) 14,17,10
17    PRINT 18
18    FORMAT(25HDELOP IS TOO LARGE VAL=0.)
      GO TO 99
97    J=0
      QQ=QASTQU
      D=QU-QASTQU
      QASTQU=QU
      GO TO 4
1     J=0
      K=1
C     THIS DONE SO THAT EACH SUCCEEDING CALL MISSES THE INITIALIZATION.
      VAL=0.0
      VALB=0.0
      VALC=0.0
      QQ=QL
      D=QU-QL
      QASTQL=QL
      QASTQU=QU
      GO TO 4
14    PRINT 15
15    FORMAT(18HSTEP SIZE NEGATIVE)
      GO TO 16
99    VALUE1=VAL
      VALUE2=VALB
      VALUE3=VALC
16    RETURN
      END
```

```
*       LIST
*       SYMBOL TABLE
        COMMON IZXX,IUPVXX,ALF,D1,IMX,THETA,RHOB,RHOC,SK1,SK2,SK3,SK4,SKA,
       1   X,Y,P,M,N,IABSMX,ABSCIS,WEIGHT,IABS2F,ZETA,ZETAPM,TJ,NTERM,NE,
       2      IL,IU,IV,IW,IUS,IVS,IH,IPS,IHS,IUPV,JSUBN,BLSTM1,BLAST
        COMMON NA,NB,NC,ND,IMX,NU,C
C      THE ABOVE COMMON CARD HAS BEEN ALTERED FROM THE USUAL BY THE
C       ADDITION OF  C   TO TEST THE SUBROUTINE ACCURACY.   4/20/67
        COMMON NA1,NA2,NA3,NA4,NB1,NB2,NB3,NB4,NC1,NC2,NC3,NC4,ND1,ND2,
       2   ND3,ND4,IMX,NU,S1,S2,V,SS1,SS2,SS3,SS4,SQ7,SQA,SQB,DELO,DELOP
        DIMENSION IZXX(5),IUPVXX(5),ALF(5,5,5),D1(30,86),P(30,5),
       1   ABSCIS(48),WEIGHT(48),ZETA(2,34,48),ZETAPM(2,30,48),TJ(8,48),
       2      NE(4),IL(4),IU(4),IV(4),IW(4),IH(4),BLSTM1(2),BLAST(2)
C
C       THIS PGM CALCULATES THE ANGULAR DISTRIBUTION FOR ELECTRONS
C         SCATTERED AFTER EXCITING THE SECOND TRIPLET OF H2.  USING THE
C         ZETA FUNCTION EXPANSION METHOD TO CALC THE THREE CENTER INTS.
C
C
        DIMENSION ANGLE(10),DSIGT(10),QANG(16,10),TERM(3),TR(3,5),HHF(3,5)
        READ 20,NA1,NB1,NC1,ND1,NA2,NB2,NC2,ND2,NA3,NB3,NC3,ND3,
       2NA4,NB4,NC4,ND4,IMX,NU
20      FORMAT(18I3)
47      READ 101, JGEM
101     FORMAT(I10)
        PRINT 25,NA1,NB1,NC1,ND1,NA2,NB2,NC2,ND2,NA3,NB3,NC3,ND3,
       3NA4,NB4,NC4,ND4,IMX,NU
25      FORMAT(18I3)
        THETA=3.14159266
        PI=3.14159266
        AB=15.422/13.60
        REQM=7.483-2.870*1.40
        ALFAP=18.4
        SPI=SQRTF(PI)
        FRONT=1./SPI
        SALF=SQRTF(ALFAP)
        XVAL=1.2247449/SALF
        TR(1,1)=1.603286
        TR(2,1)=1.720145
        TR(3,1)=1.910188
        HHF(1,1)=0.151864
        HHF(2,1)=0.100207
        HHF(3,1)=0.008276
        TR(1,2)=1.459127
        TR(2,2)=1.608451
        TR(3,2)=1.827239
        HHF(1,2)=0.418230
        HHF(2,2)=0.359015
        HHF(3,2)=0.038425
        TR(1,3)=1.340115
        TR(2,3)=1.526299
        TR(3,3)=1.769692
        HHF(1,3)=0.575142
        HHF(2,3)=0.693365
        HHF(3,3)=0.096276
        TR(1,4)=1.245479
        TR(2,4)=1.469012
        TR(3,4)=1.731193
        HHF(1,4)=0.535819
        HHF(2,4)=0.951534
        HHF(3,4)=0.166281
```

```
      TR(1,5)=1.400-XVAL
      TR(2,5)=1.400
      TR(3,5)=1.400+XVAL
      HHF(1,5)=0.2954909
      HHF(2,5)=1.1816359
      HHF(3,5)=HHF(1,5)
      PRINT 134,   ((TR(JI,KI),KI=1,5),JI=1,3),((HHF(NI,MI),MI=1,5
     2),NI=1,3)
  134 FORMAT(1H0,9HTR MATRIX//   (3(5F10.4//)),2X,10HHHF MATRIX//
     3(3(5F10.4//)))
      PRINT 102, JGEM
  102 FORMAT(1H1,5HJGEM=,I3//)
      DO 2 J=14,16
C     THE FOLLOWING PRINT STATEMENT HAS BEEN ADDED FOR THIS RUN ONLY.
      PRINT 301, DD,Z1,V,SQA,SQB,C, CONST
  301 FORMAT(1H0,3HDD=,F7.4,5X,3HZ1=,F7.4,5X,2HV=,F7.4,5X,4HSQA=,F7.4,
     2   5X,4HSQB=,F7.4,5X,2HC=,F7.4,5X,6HCONST=,F8.4)
      XX=J-2
      IF(J-1) 200,200,201
  200 JM=1
      EN=0.8823529
      GO TO 202
  201 JM=5
      EN=1.1029412+0.367647*XX
  202 ENERGY=EN*13.6
      PP=SQRTF(EN)
      DO 3 K=1,10
      R=K-1
      RAD=0.3490658*R
      ANGLE(K)=RAD*180./PI
      DO 15 IK=1,3
      DD=TR(IK,JM)
      FACTOR=(7.483-2.870*DD)/REQM
      RHOR=DD/2.
      ENDIF=20.2203-7.483*DD+1.435*DD*DD
      FM=ENDIF/13.6
      TEMPS=ABSF(EN-FM)
      S=SQRTF(TEMPS)
      Q=SQRTF(EN+S*S-2.*PP*S*COSF(RAD))
      W=S/(PP*(S*S+AB)*(S*S+AB))
      CALL STSCR(DD,JGEM,7,Z1,Z2)
      CALL STCONS(Z,Z1,Z2,DD,S1,S2,V,CONST,SQZ,SQA,SQB,JGEM)
      SS1=Z1
      SS2=Z
      SS3=Z
      SS4=ZZ
      YY=Q*DD
      YT=YY/2.
      PHASE=0.5*(1.+SINF(YY)/YY)
      PHASB=1./YT*SINF(YT)
      PHASC=3./(YT*YT)*COSF(YT)+1.5*(1.-2./(YT*YT))*PHASB-0.5*PHASB
      F=16.*S1/((S1*S1+Q*Q)*(S1*S1+Q*Q))
      G=16.*(3.*S2*S2-Q*Q)/((S2*S2+Q*Q)**3)
      H=F-V*G
      CALL OSOS(NA1,NB1,NC1,ND1,Q,SS1,SS2,VALA)
      CALL OSTS(NA2,NB2,NC2,ND2,Q,SS3,SS4,VALB)
      CALL TSOS(NA3,NB3,NC3,ND3,Q,SS1,SS2,VALC)
      CALL TSTS(NA4,NB4,NC4,ND4,Q,SS3,SS4,VALD)
      SBESA=SQZ*SQA*VALA-V*SQZ*SQB*VALB
      SBFSB=SQZ*SQA*VALC-V*SQZ*SQB*VALD
      DSIG1=CONST*W*H*H*PHASE*FACTOR
```

```
      DSIG2=CONST*W*4./PI*H*SBESA*PHASB*FACTOR
      DSIG3=CONST*W*20./PI*H*SBESB*PHASC*FACTOR
      DSIG4=CONST*W*4./PI*SBESA*SBESA/PI*FACTOR
      DSIG5=CONST*W*20./PI*SBESB*SBESB/PI*FACTOR
15    TERM(IK)=DSIG1+DSIG2-DSIG3+DSIG4+DSIG5
      DSIGT(K)=FRONT*(HHF(1,JM)*TERM(1)+HHF(2,JM)*TERM(2)+HHF(3,JM)*
     2TERM(3))
3     QANG(J,K)=DSIGT(K)
2     PRINT 8,ENERGY,(ANGLE(K),DSIGT(K),K=1,10)
8     FORMAT(1H1,F10.3//(F10.3, F25.4//))
      WRITE OUTPUT TAPE 3, 83, ((QANG(I,J),J=1,10),I=1,16)
83    FORMAT(5E12.4)
      CALL EXIT
      END
```

```
$IBFTC HJAJ    NODECK
      DIMENSION A(50,3),B(50,1),COE(4),ROOTR(3),ROOTI(3),AJ(3)
      COMMON/THREE/ALFC(6)
      ALFAP=18.4
      PI=3.14159265
      SPI=SQRT(PI)
      SALF=SQRT(ALFAP)
C     FOR THE FIRST TRIPLET THE FOLLOWING CARD IS  DO 900 JK=1,4
      DO 900 JK=1,4
      RJK=JK-1
C     FIRST TRIP HAS THE NEXT CARD AS   ENERGY=9.0+1.0*RJK
      ENERGY=12.0+0.5*RJK
C     FIRST TRIP HAS THE NEXT CARD AS       R=(21.0081-ENERGY)/7.401
      R=7.483/2.870-SQRT(7.483*7.483-4.*1.435*(20.2203-ENERGY))/2.870
      ZO=SALF*(R-1.40)
      WRITE(6,901) R,ZO
901   FORMAT(1H1,20X,21HA NEW VALUE OF R, R=,F7.4,20X,3HZO=,F7.4)
C
C     NOW CALCULATE THE K-ALFA MOMENTS OF THE WEIGHTING FUNCTION W(X).
C
      CALL MOMENT(ZO)
      WRITE(6,202) ALFC
202   FORMAT(1H0,50X,4HALFC//(50X,F10.6/))
C
C     FORM THE A,B,C MATRICES
C
      DO 300 J=1,3
      A(J,1)=ALFC(J)
      A(J,2)=ALFC(J+1)
300   A(J,3)=ALFC(J+2)
      WRITE(6,301) ((A(N,M),N=1,3),M=1,3)
301   FORMAT(1H0,50X,29HTHE A MATRIX COMPOSED OF ALFC///(40X,3F15.6//))
      B(1,1)=-ALFC(4)
      B(2,1)=-ALFC(5)
      B(3,1)=-ALFC(6)
      WRITE(6,401) (B(N,1),N=1,3)
401   FORMAT(1H0,65X,8HB MATRIX///(55X,F15.6//))
      CALL MATINV(A,3,B,1,DETERM)
      WRITE(6,501) IT,DETERM,(B(N,1),N=1,3)
501   FORMAT(1H0,25X,3HIT=,I3,10X,7HDETERM=,F7.5//8HC MATRIX///
     33(40X,F15.6//))
C
C     FIND THE ROOTS OF THE POLY--THE AJ VALUES.
C
      COF(1)=1.0
      COF(2)=B(3,1)
      COF(3)=B(2,1)
      COF(4)=B(1,1)
      WRITE(6,502) COF
502   FORMAT(1H0,50X,16HCOEFFICIENTS COF//(55X,F16.5//))
      CALL MULLER(COF,3,ROOTR,ROOTI)
      WRITE(6,503) ROOTR,ROOTI
503   FORMAT(1H0,25X,5HROOTR,75X,5HROOTI///3(10X,F15.6//),3(80X,F15.6/))
      AJ(1)=ROOTR(1)/SALF+1.40
      AJ(2)=ROOTR(2)/SALF+1.40
      AJ(3)=ROOTR(3)/SALF+1.40
      WRITE(6,940) AJ
940   FORMAT(1H0,22HTHE ABCISSA VALUES ARE/(30X,F15.6//))
C
C     DETERMINE THE WEIGHTS HJ
C
```

```
      B(1,1)=ALFC(2)
      B(2,1)=ALFC(3)
      B(3,1)=ALFC(4)
      DO 601 N=1,3
      A(1,N)=ROOTR(N)
      A(2,N)=ROOTR(N)**2
  601 A(3,N)=ROOTR(N)**3
      WRITE(6,602) (((A(K,L),K=1,3),L=1,3),(B(N,1),N=1,3))
  602 FORMAT(1H0,30X,15HSECOND A MATRIX25X,15HSECOND B MATRIX//
     23(20X,3F15.6///),3(85X,F15.6//))
      CALL MATINV(A,3,B,1,DETERM)
      WRITE(6,603) IT,DETERM,(B(N,1),N=1,3)
  603 FORMAT(1H0,3HIT=,I3,30X,7HDETERM=,F7.5//50X,21HWEIGHT COEFFICIENTS
     4 H//3(30X,F15.6//))
      CALCUL=B(1,1)+B(2,1)+B(3,1)
      TRUE=ALFC(1)
      WRITE(6,700) CALCUL,TRUE
  700 FORMAT(1H0,20X,7HCALCUL=,F12.7,20X,5HTRUE=,F12.7)
  900 CONTINUE
      STOP
      END
$IBFTC MOMENT  DECK
      SUBROUTINE MOMENT(B)
      COMMON/THREE/ALFC(6)
      SPI=SQRT(3.14159265)
      EPP=EXP(-B*B)
      ALFC(1)=SPI/2.*(1.-ERF(B))
      ALFC(3)=0.5*(ALFC(1)+B*EPP)
      ALFC(5)=1.5*ALFC(3)+0.5*(B**3)*EPP
      ALFC(2)=0.5*EPP
      ALFC(4)=ALFC(2)+B*B*EPP/2.
      ALFC(6)=2.*ALFC(4)+(B**4)*EPP/2.
      RETURN
      END
```

```
CFNOV
*       LIST
        SUBROUTINE FNOV(VALINT,Q,SC3,SC4)
        COMMON IZXX,IUPVXX,ALF,D1,IMX,THETA,RHOB,RHOC,SK1,SK2,SK3,SK4,SKA,
       1   X,Y,P,M,N,IABSMX,ABSCIS,WEIGHT,IABS2F,ZETA,ZETAPM,TJ,NTERM,NE,
       2      IL,IU,IV,IW,IUS,IVS,IH,IPS,IHS,IUPV,JSUBN,BLSTM1,BLAST
        COMMON   NA,NB,NC,ND,IMX,NU
        COMMON NA1,NA2,NA3,NA4,NB1,NB2,NB3,NB4,NC1,NC2,NC3,NC4,ND1,ND2,
       2   ND3,ND4,IMX,NU,S1,S2,V,SS1,SS2,SS3,SS4,SQ7,SQA,SQB,DELO,DELOP
        DIMENSION IZXX(5),IUPVXX(5),ALF(5,5,5),D1(30,86),P(30,5),
       1   ABSCIS(48),WEIGHT(48),ZETA(2,34,48),ZETAPM(2,30,48),TJ(8,48),
       2      NE(4),IL(4),IU(4),IV(4),IW(4),IH(4),BLSTM1(2),BLAST(2)
       $   ,TITLE(24)
        THETAP=500.0
        IZXX(1)=1
        IZXX(2)=2
        IZXX(3)=6
        IZXX(4)=18
        IZXX(5)=42
        IUPVXX(1)=0
        IUPVXX(2)=1
        IUPVXX(3)=2
        IUPVXX(4)=4
        IUPVXX(5)=6
        CALL PRPD1
        SK3=SC3
        SK4=SC4
        RHOC=RHOB
        SK1=0.5*Q
        SK2=SK1
        IMX=XMINOF(IMX,29)
        SKA=SK1+SK2
        IZVINT=0
        IF(NC-2) 42,41,42
   41   M=2
        GO TO 43
   42   M=1
   43   IF(ND-2) 45,44,45
   44   N=2
        GO TO 47
   45   N=1
   47   IF(IMX-IMXP) 49,49,48
   48   THETAP=THETA
        CALL PRPLEG
        GO TO 80
   49   IF(THETA-THETAP) 50,58,50
   50   THETAP=THETA
        CALL PRPLEG
   58   IF(NU-NUP) 80,60,80
   60   IF(ABSF(RHOB-RHOBP)+ABSF(RHOC-RHOCP)) 80,61,80
   61   IF(SK3-SK3P) 63,62,63
   62   IF(M-MMX) 64,64,63
   63   CALL PRPZTB
        MMX=M
        IZVINT=1
   64   IF(SK4-SK4P) 66,65,66
   65   IF(N-NMX) 70,70,66
   66   CALL PRPZTC
        NMX=N
        IZVINT=1
   70   IF(SKA-SKAP) 71,130,71
```

```
   71 CALL LITLJ
      IZVINT=1
      GO TO 130
   80 CALL QUAD1(RHOB,RHOC,IABSMX,ABSCIS,WEIGHT,NU)
      IZVINT=1
      CALL PRPZTB
      MMX=M
      CALL PRPZTC
      NMX=N
      CALL LITLJ
      NUP=NU
      RHOBP=RHOB
      RHOCP=RHOC
  130 NTERM=0
      IMXP=IMX
      SK3P=SK3
      SK4P=SK4
      SKAP=SKA
      VALINT=AABC(NA,NB,NC,ND,IZVINT)
      RETURN
      END
```

```
CFKBSJ
*       LIST
*       SYMBOL TABLE
        SUBROUTINE LITLJ
        COMMON IZXX,IUPVXX,ALF,D1,IMX,THETA,RHOB,RHOC,SK1,SK2,SK3,SK4,SKA
       1   X,Y,P,M,N,IABSMX,ABSCIS,WEIGHT,IABS2F,ZETA,ZETAPM,TJ,NTERM,NE,
       2      IL,IU,IV,IW,IUS,IVS,IH,IPS,IHS,IUPV,JSUBN,BLSTM1,BLAST
        COMMON   NA,NB,NC,ND,IMX,NU
        COMMON NA1,NA2,NA3,NA4,NB1,NB2,NB3,NB4,NC1,NC2,NC3,NC4,ND1,ND2,
       2   ND3,ND4,IMX,NU,S1,S2,V,SS1,SS2,SS3,SS4,SQZ,SQA,SQB,DELO,DELOP
        DIMENSION IZXX(5),IUPVXX(5),ALF(5,5,5),D1(30,86),P(30,5),
       1   ABSCIS(48),WEIGHT(48),ZETA(2,34,48),ZETAPM(2,30,48),TJ(8,48),
       2      NE(4),IL(4),IU(4),IV(4),IW(4),IH(4),BLSTM1(2),BLAST(2)
        DO 100 I=1,IABSMX
        QR=SKA*ABSCIS(I)
        CALL BESSEL(0.5,0.0,QR,0.0,BES0,BI,BRD,BID,15)
        TJ(1,I)=2.0*BES0/SKA
        CALL BESSEL(1.5,0.0,QR,0.0,BES1,BI,BRD,BID,15)
        TJ(4,I)=4.0*ABSCIS(I)*BES1
        CALL BESSEL(2.5,0.0,QR,0.0,BES2,BI,BRD,BID,15)
        TJ(8,I)=-2.0*QR*ABSCIS(I)*BES2
100     TJ(7,I)=-6.0*TJ(8,I)
        RETURN
        END
```

```
COSOS
*       LIST
*       SYMBOL TABLE
        SUBROUTINE OSOS(JA,JB,JC,JD,Q,SS1,SS2,ANS)
        COMMON IZXX,IUPVXX,ALF,D1,IMX,THETA,RHOB,RHOC,SK1,SK2,SK3,SK4,SKA,
       1   X,Y,P,M,N,IABSMX,ABSCIS,WEIGHT,IABS2F,ZETA,ZETAPM,TJ,NTERM,NE,
       2      IL,IU,IV,IW,IUS,IVS,IH,IPS,IHS,IUPV,JSUBN,BLSTM1,BLAST
        COMMON   NA,NB,NC,ND,IMX,NU
        COMMON NA1,NA2,NA3,NA4,NB1,NB2,NB3,NB4,NC1,NC2,NC3,NC4,ND1,ND2,
       2   ND3,ND4,IMX,NU,S1,S2,V,SS1,SS2,SS3,SS4,SQZ,SQA,SQB,DELO,DELOP
        DIMENSION IZXX(5),IUPVXX(5),ALF(5,5,5),D1(30,86),P(30,5),
       1   ABSCIS(48),WEIGHT(48),ZETA(2,34,48),ZETAPM(2,30,48),TJ(8,48),
       2      NE(4),IL(4),IU(4),IV(4),IW(4),IH(4),BLSTM1(2),BLAST(2)
        NA=JA
        NB=JB
        NC=JC
        ND=JD
        CALL FNOV(ANSA,Q,SS1,SS2)
        ANS=ANSA
        RETURN
        END
COSTS
*       LIST
*       SYMBOL TABLE
        SUBROUTINE OSTS(JA,JB,JC,JD,Q,SS3,SS4,ANS)
        COMMON IZXX,IUPVXX,ALF,D1,IMX,THETA,RHOB,RHOC,SK1,SK2,SK3,SK4,SKA,
       1   X,Y,P,M,N,IABSMX,ABSCIS,WEIGHT,IABS2F,ZETA,ZETAPM,TJ,NTERM,NE,
       2      IL,IU,IV,IW,IUS,IVS,IH,IPS,IHS,IUPV,JSUBN,BLSTM1,BLAST
        COMMON   NA,NB,NC,ND,IMX,NU
        COMMON NA1,NA2,NA3,NA4,NB1,NB2,NB3,NB4,NC1,NC2,NC3,NC4,ND1,ND2,
       2   ND3,ND4,IMX,NU,S1,S2,V,SS1,SS2,SS3,SS4,SQZ,SQA,SQB,DELO,DELOP
        DIMENSION IZXX(5),IUPVXX(5),ALF(5,5,5),D1(30,86),P(30,5),
       1   ABSCIS(48),WEIGHT(48),ZETA(2,34,48),ZETAPM(2,30,48),TJ(8,48),
       2      NE(4),IL(4),IU(4),IV(4),IW(4),IH(4),BLSTM1(2),BLAST(2)
        NA=JA
        NB=JB
        NC=JC
        ND=JD
        CALL FNOV(ANSB,Q,SS3,SS4)
        ANS=ANSB
        RETURN
        END
CTSOS
*       LIST
*       SYMBOL TABLE
        SUBROUTINE TSOS(JA,JB,JC,JD,Q,SS1,SS2,ANS)
        COMMON IZXX,IUPVXX,ALF,D1,IMX,THETA,RHOB,RHOC,SK1,SK2,SK3,SK4,SKA,
       1   X,Y,P,M,N,IABSMX,ABSCIS,WEIGHT,IABS2F,ZETA,ZETAPM,TJ,NTERM,NE,
       2      IL,IU,IV,IW,IUS,IVS,IH,IPS,IHS,IUPV,JSUBN,BLSTM1,BLAST
        COMMON   NA,NB,NC,ND,IMX,NU
        COMMON NA1,NA2,NA3,NA4,NB1,NB2,NB3,NB4,NC1,NC2,NC3,NC4,ND1,ND2,
       2   ND3,ND4,IMX,NU,S1,S2,V,SS1,SS2,SS3,SS4,SQZ,SQA,SQB,DELO,DELOP
        DIMENSION IZXX(5),IUPVXX(5),ALF(5,5,5),D1(30,86),P(30,5),
       1   ABSCIS(48),WEIGHT(48),ZETA(2,34,48),ZETAPM(2,30,48),TJ(8,48),
       2      NE(4),IL(4),IU(4),IV(4),IW(4),IH(4),BLSTM1(2),BLAST(2)
        NA=JA
        NB=JB
        NC=JC
        ND=JD
        CALL FNOV(ANSC,Q,SS1,SS2)
        ANS=ANSC
```

```
      RETURN
      END
CTSTS
*     LIST
*     SYMBOL TABLE
      SUBROUTINE TSTS(JA,JB,JC,JD,Q,SS3,SS4,ANS)
      COMMON IZXX,IUPVXX,ALF,D1,IMX,THETA,RHOB,RHOC,SK1,SK2,SK3,SK4,SKA,
     1   X,Y,P,M,N,IABSMX,ABSCIS,WEIGHT,IABS2F,ZETA,ZETAPM,TJ,NTERM,NE,
     2      IL,IU,IV,IW,IUS,IVS,IH,IPS,IHS,IUPV,JSUBN,BLSTM1,BLAST
      COMMON   NA,NB,NC,ND,IMX,NU
      COMMON NA1,NA2,NA3,NA4,NB1,NB2,NB3,NB4,NC1,NC2,NC3,NC4,ND1,ND2,
     2   ND3,ND4,IMX,NU,S1,S2,V,SS1,SS2,SS3,SS4,SQZ,SQA,SQB,DELO,DELOP
      DIMENSION IZXX(5),IUPVXX(5),ALF(5,5,5),D1(30,86),P(30,5),
     1   ABSCIS(48),WEIGHT(48),ZETA(2,34,48),ZETAPM(2,30,48),TJ(8,48),
     2      NE(4),IL(4),IU(4),IV(4),IW(4),IH(4),BLSTM1(2),BLAST(2)
      NA=JA
      NB=JB
      NC=JC
      ND=JD
      CALL FNOV(ANSD,Q,SS3,SS4)
      ANS=ANSD
      RETURN
      END
```

```
      DIMENSION IZXX(5),IUPVXX(5),ALF(5,5,5),D1(30,86),P(30,5),
     1   ABSCIS(48),WEIGHT(48),ZETA(2,34,48),ZETAPM(2,30,48),TJ(8,48),
     2      NF(4),IL(4),IU(4),IV(4),IW(4),IH(4),BLSTM1(2),BLAST(2)
     3   ,TITLE(24)
      DIMENSION DUMMY(3)
C*****************************************************************
C THE FOLLOWING STATEMENT(S) HAVE BEEN MANUFACTURED BY THE TRANSLATOR TO
C   COMPENSATE FOR THE FACT THAT EQUIVALENCE DOES NOT REORDER COMMON---
C*****************************************************************
      0COMMON/LOCA/IZXX,IUPVXX,ALF,D1,IMX,THETA,RHOB,RHOC,SK1,SK2,SK3,SK4
     1,SKA,X,Y,M,N,IABSMX,IABS2F,P,ABSCIS,WEIGHT,ZETA,ZETAPM,BLAST,BLSTM
     21,TJ,NTERM,NE,IL,IU,IV,IW,IUS,IVS,IH,IPS,IHS,IUPV,JSUBN,NTEST,LAST
      COMMON/MOCA/NA,NB,NC,ND,NU
C*****************************************************************
C      COMMON IZXX,IUPVXX,ALF,D1,IMX,THETA,RHOB,RHOC,SK1,SK2,SK3,SK4,SKA,
C     1   X,Y,P,M,N,IABSMX,ABSCIS,WEIGHT,IABS2F,ZETA,ZETAPM,TJ,NTERM,NE,
C     2      IL,IU,IV,IW,IUS,IVS,IH,IPS,IHS,IUPV,JSUBN,BLSTM1,BLAST,
C     3   NA,NB,NC,ND,IMX,NU
C      DIMENSION IZXX(5),IUPVXX(5),ALF(5,5,5),D1(30,86),P(30,5),
C     1   ABSCIS(48),WEIGHT(48),ZETA(2,34,48),ZETAPM(2,30,48),TJ(8,48),
C     2      NF(4),IL(4),IU(4),IV(4),IW(4),IH(4),BLSTM1(2),BLAST(2)
C     3   ,TITLE(24)
C*****************************************************************
10    READ(5,20) NA,NB,NC,ND,IMX,NU,NON
20    FORMAT(7I3)
      READ(5,37) RHOB,SS1,SS2,SS3,SS4
37    FORMAT(5F10.7)
      THETA=0.00
C*****************************************************************
C     NOTE THAT THIS IS A TWO CENTER INTEGRAL NOW.  WHEN DOING THE
C       THREE CENTER INTEGRALS MUST ALSO CHANGE THE VALUE OF THETA IN
C       THE SUBROUTINE FNOV.
C*****************************************************************
      WRITE(6,20) NA,NB,NC,ND,IMX,NU,NON
      WRITE(6,88) RHOB,SS1,SS2,SS3,SS4
88    FORMAT(5F10.7)
      DO 17 I=1,3
      XNUM=DUMMY(I)
      RF=I-1
      Q=1.000+RF*1.0
      CALL FNOV(VALNT1,Q,SS1,SS2)
      CALL FNOV(VALNT2,Q,SS3,SS4)
17    WRITE(6,2) Q,VALNT1,VALNT2
2     FORMAT(F10.3,2E25.5///)
      IF(NON) 10,31,10
31    STOP
      END
```

```
$IBFTC SCREEN  DECK     GIVES Z,Z1,Z2 FOR GROUNDS AND FIRST EXCITED TRIP
      SUBROUTINE SCREEN (AR,JI,AZ,AZ1,AZ2)
C     JI=1,2,3 MEANS WEINBAUM,WANG,COULSON GROUND STATES  RESPECTIVELY.
      R=AR
      IF(JI.EQ.1) GO TO 600
      IF(JI.EQ.2) GO TO 610
      IF(JI.EQ.3) GO TO 620
600   AZ=1.75812-0.61451*R+0.18466*R*R-0.02158*(R**3)
      GO TO 630
610   AZ=1.80975-0.724746*R+0.22766*R*R-0.02618*(R**3)
      GO TO 630
620   AZ=1.76254-0.62635*R+0.18896*R*R-0.02423*(R**3)
630   AZ1=1.99346-0.71167*R+0.19879*R*R-0.02250*(R**3)
      AZ2=-0.19289+0.79983*R-0.20391*R*R+0.01864*(R**3)
      RETURN
      END
```

```
CCONSTS
      SUBROUTINE CONSTS(TZ,T1,T2,TD,TS1,TS2,TV,TCONS,TFF1,TFF2,JG)
C     THIS SUBROUTINE CALCULATES THE NORMALIZATION CONSTANTS FOR THE
C     GROUND STATES AND EXCITED STATE WAVEFUNCTIONS.  IT ALSO CALCS V.
      PI=3.14159266
      IF(JG-2) 43,44,42
42    C=1.0
      GO TO 33
44    C=0.0
      GO TO 33
43    C=0.047059+0.31286*TD-0.11245*TD*TD
33    CP=1.+C
      CF=1.+C*C
      CM=1.-C
      Z=TZ
      TS1=Z+T1
      TS2=Z+T2
      SZ1=SQRTF(T1*Z)
      SZ2=SQRTF(T2*Z)
      TFF1=PI/(T1*Z*SZ1)
      TFF2=PI/(Z*T2*SZ2)
      SOZ=EXPF(-Z*TD)*(1.+Z*TD+Z*Z*TD*TD/3.)
      SO1=EXPF(-T1*TD)*(1.+T1*TD+T1*T1*TD*TD/3.)
      SO2=EXPF(-T2*TD)*(1.+T2*TD+T2*T2*TD*TD/3.)
      BLIP=1.-SO2+SO1-SO2*SO1
      ORMES=((T2**3.)*(T1**3.)/(PI*PI))*(1./(8.*BLIP))
      AFG=2.*PI*PI*CF*(1.+SOZ*SOZ+4.*C/CF*SOZ)
      ORMGS=(Z**6.)/AFG
      A1=8.*PI/(TS1**3)
      RHH=TD/2.*TS1
      GAM=TD/2.*(T1-Z)
      SONH=0.5*(EXPF(GAM)-EXPF(-GAM))
      CISH=SONH+EXPF(-GAM)
      TMID=SONH/GAM*(1./RHH+1./(RHH*RHH)-1./(GAM*GAM))+CISH/(GAM*GAM)
      B1=PI*TD*TD*TD*EXPF(-RHH)/RHH*TMID
      BET=A1+B1
      A2=8.*PI/(TS2**3)
      RHI=TD/2.*TS2
      GAI=TD/2.*(Z-T2)
      SONI=0.5*(EXPF(GAI)-EXPF(-GAI))
      CISI=SONI+EXPF(-GAI)
      TMII=SONI/GAI*(1./RHI+1./(RHI*RHI)-1./(GAI*GAI))+CISI/(GAI*GAI)
      B2=PI*TD*TD*TD*EXPF(-RHI)/RHI*TMII
      GAFF=A2-B2
      TV=(CM*GAFF)/(CP*BET)
      TCONS=12.*PI*ORMGS*ORMES*CP*CP*BET*BET
      RETURN
      END
```

```
CSTSCR
*       LIST
        SUBROUTINE STSCR(AR,JI,BZ,BZ1,BZ2)
C     JI=1,2,3 MEANS WEINBAUM,WANG,COULSON GROUND STATES  RESPECTIVELY.
        R=AR
        IF(JI-1) 599,600,601
599     PRINT 650
650     FORMAT(11HJI IN ERROR)
        GO TO 660
601     IF(JI-2) 599,610,620
600     BZ=1.75812-0.61451*R+0.18466*R*R-0.02158*(R**3)
        GO TO 630
610     BZ=1.80975-0.724746*R+0.22766*R*R-0.02618*(R**3)
        GO TO 630
620     BZ=1.76254-0.62635*R+0.18896*R*R-0.02423*(R**3)
630     BZ1=1.54616+0.38585*R-0.48119*(R**2)+0.075253*(R**3)
        BZ2=0.24065+0.15509*R+0.06026*(R**2)-0.02328*(R**3)
660     RETURN
        END
```

```
CSTCONS
      SUBROUTINE STCONS(TZ,T1,T2,DD,TS1,TS2,TV,TCONS,TQZ,TQA,TQB,JG)
      COMMON NA,NB,NC,ND,IMX,NU,C
      PI=3.14159266
      IF(JG-2) 43,44,42
42    C=1.0
      GO TO 33
44    C=0.0
      GO TO 33
43    C=0.047059+0.31286*DD-0.11245*DD*DD
33    CP=1.+C
      CW=1.+C*C
      Z=TZ
      Z1=T1
      Z2=T2
      S1=Z+Z1
      S2=Z+Z2
      TS1=S1
      TS2=S2
      TQZ=SQRTF(PI/(Z**3))
      TQA=SQRTF(PI/(Z1**3))
      TQB=SQRTF(3.*PI/(Z2**5))
      SOZ=EXPF(-Z*DD)*(1.+Z*DD+Z*Z*DD*DD/3.)
      BIF=1.+SOZ*SOZ+4.*C*SOZ/CW
      ORMGS=(Z**6)/(PI*PI)*(1./(2.*CW*BIF))
C     TERM=(0.5643*0.5436-0.0186*0.2085)/(TQA*TQB)  WAS THE OLD CARD
      TRRR=(0.427213-0.267873*DD+0.127455*(DD*DD))
      TERM=TRRR/(TQA*TQB)
      ORMES=TERM*TERM
      A1=8.*PI/(S1**3)
      RA=S1*DD/2.
      GA=(Z1-Z)*DD/2.
      RB=S2*DD/2.
      GB=(Z-Z2)*DD/2.
      SOAA=0.5*(EXPF(GA)-EXPF(-GA))
      CISA=SOAA+EXPF(-GA)
      BOA=SOAA/GA*(1./RA+1./(RA*RA)-1./(GA*GA))
      BOB=CISA/(GA*GA)
      B1=PI*DD*DD*DD*EXPF(-RA)/RA*(BOA+BOB)
      ALPHA=A1+B1
      A2=24.*PI/(S2**4)
      BTA=1./RB+3./(RB**2)+3./(RB**3)+1./GB-1./(RB*GB)-1./(GB*RB*RB)
     2+3./(GB**3)-1./(GB**2)-1./(RB*GB*GB)
      BTB=1./RB+1./(RB**2)+1./GB+1./(GB*RB)-3./(GB**2)
      SOAB=0.5*(EXPF(GB)-EXPF(-GB))
      CISB=SOAB+EXPF(-GB)
      B2=PI*(DD**4)/2.*EXPF(-RB)/RB*(SOAB/GB*BTA+CISB/GB*BTB)
      DELT=A2+B2
      TV=ALPHA/DELT
      TCONS=6.*PI*ORMGS*ORMES*CP*CP*DELT*DELT
      RETURN
      END
```

```
*       LIST
*       SYMBOL TABLE
        COMMON IZXX,IUPVXX,ALF,D1,IMX,THETA,RHOR,RHOC,SK1,SK2,SK3,SK4,SKA,
       1   X,Y,P,M,N,IABSMX,ABSCIS,WEIGHT,IABS2F,ZETA,ZETAPM,TJ,NTERM,NE,
       2      IL,IU,IV,IW,IUS,IVS,IH,IPS,IHS,IUPV,JSUBN,BLSTM1,BLAST
        COMMON NA,NB,NC,ND,IMX,NU,C
C      THE ABOVE COMMON CARD HAS BEEN ALTERED FROM THE USUAL BY THE
C       ADDITION OF  C   TO TEST THE SUBROUTINE ACCURACY.   4/20/67
        COMMON NA1,NA2,NA3,NA4,NB1,NB2,NB3,NB4,NC1,NC2,NC3,NC4,ND1,ND2,
       2   ND3,ND4,IMX,NU,S1,S2,V,SS1,SS2,SS3,SS4,SQ7,SQA,SQB,DELO,DELOP
        DIMENSION IZXX(5),IUPVXX(5),ALF(5,5,5),D1(30,86),P(30,5),
       1   ABSCIS(48),WEIGHT(48),ZETA(2,34,48),ZETAPM(2,30,48),TJ(8,48),
       2      NE(4),IL(4),IU(4),IV(4),IW(4),IH(4),BLSTM1(2),BLAST(2)
C
C       THIS PGM CALCULATES THE ANGULAR DISTRIBUTION FOR ELECTRONS
C         SCATTERED AFTER EXCITING THE SECOND TRIPLET OF H2.  USING THE
C         ZETA FUNCTION EXPANSION METHOD TO CALC THE THREE CENTER INTS.
C
C
        DIMENSION ANGLE(10),DSIGT(10),QANG(16,10),TERM(3),TR(3,5),HHF(3,5)
        READ 20,NA1,NB1,NC1,ND1,NA2,NB2,NC2,ND2,NA3,NB3,NC3,ND3,
       2NA4,NB4,NC4,ND4,IMX,NU
20      FORMAT(18I3)
47      READ 101, JGEM
101     FORMAT(I10)
        PRINT 25,NA1,NB1,NC1,ND1,NA2,NB2,NC2,ND2,NA3,NB3,NC3,ND3,
       3NA4,NB4,NC4,ND4,IMX,NU
25      FORMAT(18I3)
        THETA=3.14159266
        PI=3.14159266
        AB=15.422/13.60
        REQM=7.483-2.870*1.40
        ALFAP=18.4
        SPI=SQRTF(PI)
        FRONT=1./SPI
        SALF=SQRTF(ALFAP)
        XVAL=1.2247449/SALF
        TR(1,1)=1.603286
        TR(2,1)=1.720145
        TR(3,1)=1.910188
        HHF(1,1)=0.151864
        HHF(2,1)=0.100207
        HHF(3,1)=0.008276
        TR(1,2)=1.459127
        TR(2,2)=1.608451
        TR(3,2)=1.827239
        HHF(1,2)=0.418230
        HHF(2,2)=0.359015
        HHF(3,2)=0.038425
        TR(1,3)=1.340115
        TR(2,3)=1.526299
        TR(3,3)=1.769692
        HHF(1,3)=0.575142
        HHF(2,3)=0.693365
        HHF(3,3)=0.096276
        TR(1,4)=1.245479
        TR(2,4)=1.469012
        TR(3,4)=1.731193
        HHF(1,4)=0.535819
        HHF(2,4)=0.951534
        HHF(3,4)=0.166281
```

```
      TR(1,5)=1.400-XVAL
      TR(2,5)=1.400
      TR(3,5)=1.400+XVAL
      HHF(1,5)=0.2954909
      HHF(2,5)=1.1816359
      HHF(3,5)=HHF(1,5)
      PRINT 134,    ((TR(JI,KI),KI=1,5),JI=1,3),((HHF(NI,MI),MI=1,5
     2),NI=1,3)
134   FORMAT(1H0,9HTR MATRIX//    (3(5F10.4//)),2X,10HHHF MATRIX//
     3(3(5F10.4//)))
      PRINT 102, JGEM
102   FORMAT(1H1,5HJGEM=,I3//)
      DO 2 J=14,16
C     THE FOLLOWING PRINT STATEMENT HAS BEEN ADDED FOR THIS RUN ONLY.
      PRINT 301, DD,Z1,V,SQA,SQB,C, CONST
301   FORMAT(1H0,3HDD=,F7.4,5X,3HZ1=,F7.4,5X,2HV=,F7.4,5X,4HSQA=,F7.4,
     2    5X,4HSQB=,F7.4,5X,2HC=,F7.4,5X,6HCONST=,F8.4)
      XX=J-2
      IF(J-1) 200,200,201
200   JM=1
      EN=0.8823529
      GO TO 202
201   JM=5
      EN=1.1029412+0.367647*XX
202   ENERGY=EN*13.6
      PP=SQRTF(EN)
      DO 3 K=1,10
      R=K-1
      RAD=0.3490658*R
      ANGLE(K)=RAD*180./PI
      DO 15 IK=1,3
      DD=TR(IK,JM)
      FACTOR=(7.483-2.870*DD)/REQM
      RHOB=DD/2.
      ENDIF=20.2203-7.483*DD+1.435*DD*DD
      EM=ENDIF/13.6
      TEMPS=ABSF(EN-EM)
      S=SQRTF(TEMPS)
      Q=SQRTF(EN+S*S-2.*PP*S*COSF(RAD))
      W=S/(PP*(S*S+AB)*(S*S+AB))
      CALL STSCR(DD,JGEM,Z,Z1,Z2)
      CALL STCONS(Z,Z1,Z2,DD,S1,S2,V,CONST,SQZ,SQA,SQB,JGEM)
      SS1=Z1
      SS2=Z
      SS3=Z
      SS4=Z2
      YY=Q*DD
      YT=YY/2.
      PHASE=0.5*(1.+SINF(YY)/YY)
      PHASB=1./YT*SINF(YT)
      PHASC=3./(YT*YT)*COSF(YT)+1.5*(1.-2./(YT*YT))*PHASB-0.5*PHASB
      F=16.*S1/((S1*S1+Q*Q)*(S1*S1+Q*Q))
      G=16.*(3.*S2*S2-Q*Q)/((S2*S2+Q*Q)**3)
      H=F-V*G
      CALL OSOS(NA1,NB1,NC1,ND1,Q,SS1,SS2,VALA)
      CALL OSTS(NA2,NB2,NC2,ND2,Q,SS3,SS4,VALB)
      CALL TSOS(NA3,NB3,NC3,ND3,Q,SS1,SS2,VALC)
      CALL TSTS(NA4,NB4,NC4,ND4,Q,SS3,SS4,VALD)
      SBESA=SQZ*SQA*VALA-V*SQZ*SQB*VALB
      SBESB=SQZ*SQA*VALC-V*SQZ*SQB*VALD
      DSIG1=CONST*W*H*H*PHASE*FACTOR
```

```
CSIMP
      SUBROUTINE SIMP(QL,QU,DD,K,VAL,VALB,VALC)
      COMMON IZXX,IUPVXX,ALF,D1,IMX,THETA,RHOB,RHOC,SK1,SK2,SK3,SK4,SKA,
     1   X,Y,P,M,N,IABSMX,ABSCIS,WEIGHT,IABS2F,ZETA,ZETAPM,TJ,NTERM,NE,
     2      IL,IU,IV,IW,IUS,IVS,IH,IPS,IHS,IUPV,JSUBN,BLSTM1,BLAST,
     4   NA,NB,NC,ND,IMX,NU,S1,S2,V,SS1,SS2,SS3,SS4,FF2,FF1,DELO,DELOP
      DIMENSION IZXX(5),IUPVXX(5),ALF(5,5,5),D1(30,86),P(30,5),
     1   ABSCIS(48),WEIGHT(48),ZETA(2,34,48),ZETAPM(2,30,48),TJ(8,48),
     2      NE(4),IL(4),IU(4),IV(4),IW(4),IH(4),BLSTM1(2),BLAST(2)
      PI=3.14159266
      RHOB=DD/2.
      IF(K) 22,1,22
22    J=1
      D=QASTQL-QL
      QASTQL=QL
      QQ=QL
4     NM=D/DELO
      IF(NM) 11,11,10
10    FN=NM
      DEL=D/FN
      HH=DEL/3.
      F=QQ
      FA=16.*S2/((S2*S2+E*E)*(S2*S2+E*E))
      GA=16.*S1/((S1*S1+E*E)*(S1*S1+E*E))
      HA=FA+V*GA
      PHASA=0.5*(1.-SINF(E*DD)/(F*DD))
      CALL FNOV(VALNTA,F,SS1,SS2)
      CALL FNOV(VALNTB,E,SS3,SS4)
      VALSA=FF2*VALNTA+V*FF1*VALNTB
      YTA=E*DD/2.
      THETB=1./(YTA*YTA)*(SINF(YTA)-YTA*COSF(YTA))
      SIGA=HA*HA*E*PHASA
      SIGB=E*(12./PI)*HA*VALSA*THETB
      SIGC=E*(12./PI)*VALSA*VALSA/PI
      DO 3 I=1,NM
      R=I
      Q=QQ+R*DEL
      F=16.*S2/((S2*S2+Q*Q)*(S2*S2+Q*Q))
      G=16.*S1/((S1*S1+Q*Q)*(S1*S1+Q*Q))
      H=F+V*G
      YY=Q*DD
      PHASF=0.5*(1.-SINF(YY)/YY)
      CALL FNOV(VALNT1,Q,SS1,SS2)
      CALL FNOV(VALNT2,Q,SS3,SS4)
      VALSS=FF2*VALNT1+V*FF1*VALNT2
      YT=YY/2.
      THETT=(1./(YT*YT))*(SINF(YT)-YT*COSF(YT))
      SIG1=Q*H*H*PHASE
      SIG2=Q*(12./PI)*H*VALSS*THETT
      SIG3=Q*(12./PI)*VALSS*VALSS/PI
      SR=2.0
      IF(I-NM) 60,9,60
60    II=I/2
      II=II*2
      IF(I-II) 61,62,61
61    SR=4.0
62    SIGA=SIGA+SR*SIG1
      SIGB=SIGB+SR*SIG2
      SIGC=SIGC+SR*SIG3
      GO TO 3
9     SIGA=SIGA+SIG1
```

```
      SIGB=SIGB+SIG2
      SIGC=SIGC+SIG3
3     CONTINUE
      VAL=SIGA*HH+VAL
      VALB=SIGB*HH+VALB
      VALC=SIGC*HH+VALC
      IF(J) 97,99,97
11    PRINT 12
12    FORMAT(37H Q INTEGRATION INDEX ZERO, DELOP USED,1X,I4)
      NM=D/DELOP
      IF(NM) 14,17,10
17    PRINT 18
18    FORMAT(25HDELOP IS TOO LARGE VAL=0.)
      GO TO 99
97    J=0
      QQ=QASTQU
      D=QU-QASTQU
      QASTQU=QU
      GO TO 4
1     J=0
      K=1
C     THIS DONE SO THAT EACH SUCCEEDING CALL MISSES THE INITIALIZATION.
      VAL=0.0
      VALB=0.0
      VALC=0.0
      QQ=QL
      D=QU-QL
      QASTQL=QL
      QASTQU=QU
      GO TO 4
14    PRINT 15
15    FORMAT(18HSTEP SIZE NEGATIVE)
      GO TO 16
99    VALUE1=VAL
      VALUE2=VALB
      VALUE3=VALC
16    RETURN
      END
```

```
C*************************************************************************
C     THIS PROGRAM CALCULATES THE TOTAL CROSS SECTION FOR EXCITATION
C     OF TRIPLET LEVELS IN H2 BY ELECTRON IMPACT ALA THE GENERAL
C      METHOD OF OCHKUR OR RUDGE.  THE APPLICATION INCLUDES AN INTEGRA-
C      OVER THE INTERNUCLEAR DISTANCE.  THE OUTER INTEGRATION IS GAUSS-
C      IAN AND THE INNER IS SIMPSON.  THE OUTER GAUSSIAN INVOLVES A
C      SPECIFIC SET OF ABCISSA AND WEIGHTS FOR THE DELTA-ENERGY OF THE
C      TRANSITITON.  THESE WEIGHTS ARE OBTAINED BY PROGRAM HJAJ.
C      THE GROUND STATES CAN BE WEINBAUM,WANG,COULSON AND THE EXCITED
C      STATE IS PHILLIPSON-MULLIKAN.
C*************************************************************************
*      LIST
*      SYMBOL TABLE
       COMMON IZXX,IUPVXX,ALF,D1,IMX,THETA,RHOB,RHOC,SK1,SK2,SK3,SK4,SKA,
      1   X,Y,P,M,N,IABSMX,ABSCIS,WEIGHT,IABS2F,ZETA,ZETAPM,TJ,NTERM,NE,
      2      IL,IU,IV,IW,IUS,IVS,IH,IPS,IHS,IUPV,JSUBN,BLSTM1,BLAST,
      4   NA,NB,NC,ND,IMX,NU,S1,S2,V,SS1,SS2,SS3,SS4,FF2,FF1,DELO,DELOP
       DIMENSION IZXX(5),IUPVXX(5),ALF(5,5,5),D1(30,86),P(30,5),
      1   ABSCIS(48),WEIGHT(48),ZETA(2,34,48),ZETAPM(2,30,48),TJ(8,48),
      2      NE(4),IL(4),IU(4),IV(4),IW(4),IH(4),BLSTM1(2),BLAST(2)
       DIMENSION TSIGT(12),TR(3,5),HHF(3,5),ENEP(12),RO(3,12)
       READ 20,NA,NB,NC,ND,IMX,NU
20     FORMAT(6I3)
       PRINT 45,NA,NB,NC,ND,IMX,NU
45     FORMAT(3HNA=,I3,3X,3HNB=,I3,3X,3HNC=,I3,3X,3HND=,I3,3X,
      54HIMX=,I4,3X,3HNU=,I3)
47     READ 101, JGEM
101    FORMAT(I10)
       THETA=3.14159266
       PI=3.14159266
       DELO=0.02
       DELOP=0.005
       ALFAP=18.4
       SPI=SQRTF(PI)
       FRONT=1./SPI
       SALF=SQRTF(ALFAP)
       XVAL=1.2247449/SALF
       DELTE=1.0
       TR(1,1)=1.649955
       TR(2,1)=1.758458
       TR(3,1)=1.939779
       HHF(1,1)=0.094009
       HHF(2,1)=0.058437
       HHF(3,1)=0.004506
       TR(1,2)=1.523542
       TR(2,2)=1.656939
       TR(3,2)=1.862597
       HHF(1,2)=0.289925
       HHF(2,2)=0.217733
       HHF(3,2)=0.020587
       TR(1,3)=1.402524
       TR(2,3)=1.568075
       TR(3,3)=1.798589
       HHF(1,3)=0.515389
       HHF(2,3)=0.511151
       HHF(3,3)=0.061628
       TR(1,4)=1.291864
       TR(2,4)=1.496149
       TR(3,4)=1.749283
       HHF(1,4)=0.574782
       HHF(2,4)=0.831250
```

```
      HHF(3,4)=0.129512
      TR(1,5)=1.400-XVAL
      TR(2,5)=1.400
      TR(3,5)=1.400+XVAL
      HHF(1,5)=0.2954909
      HHF(2,5)=1.1816359
      HHF(3,5)=HHF(1,5)
      PRINT 134,    ((TR(JI,KI),KI=1,5),JI=1,3),((HHF(NI,MI),MI=1,5
     2),NI=1,3)
134   FORMAT(1H0,9HTR MATRIX//   (3(5F10.4//)),2X,10HHHF MATRIX//
     3(3(5F10.4//)))
      PRINT 102, JGEM
102   FORMAT(1H1,5HJGEM=,I3//)
      DO 991 IK=1,3
      JM=5
      OUTTA=0.000
      OUTTB=0.000
      OUTTC=0.000
      B=TR(IK,JM)
      CALL SCREEN (B,JGEM,Z,Z1,Z2)
      CALL CONSTS(Z,Z1,Z2,B,S1,S2,V,CONST,FF1,FF2,JGEM)
      SS1=Z
      SS2=Z2
      SS3=Z1
      SS4=Z
      PRINT 832,B,SS1,SS2,SS3,SS4,V,FF1,FF2,CONST,C
832   FORMAT(1H1,10F13.5//)
      FNDIF=-7.401*B+21.0081
      FM=FNDIF/13.6
      DO 310 JJ=5,9
      KK=JJ-5
      RR=JJ-5
      ENERGY=13.0+RR*DELTE
745   EN=ENERGY/13.6
      ENER(JJ)=ENERGY
      TPP=SQRTF(EN)
      TEMPS=ABSF(EN-FM)
      S=SQRTF(TEMPS)
      QMIN=TPP-S
      QMAX=TPP+S
      CALL SIMP(QMIN,QMAX,B,KK,VALUE1,VALUE2,VALUE3)
      WI=FN*(S*S+1.)*(S*S+1.)
      W=1./WI
      OUTTA=2.*PI*VALUE1*CONST*W
      OUTTB=2.*PI*VALUE2*CONST*W
      OUTTC=2.*PI*VALUE3*CONST*W
      TERM=OUTTA-OUTTB+OUTTC
310   RO(IK,JJ)=TERM
991   PRINT 21, B,(ENER(K),RO(IK,K),K=5,12)
21    FORMAT(1H0,25HINTER NUCLEAR DISTANCE IS,4X,F6.4//(40X,F10.3,30X,
     2F15.5//))
      DO 750 JJ=5,12
750   TSIGT(JJ)=FRONT*(HHF(1,5)*RO(1,JJ)+HHF(2,5)*RO(2,JJ)+HHF(3,5)*
     3RO(3,JJ))
      PRINT 753
753   FORMAT(1H1,50X,26HTHE TOTAL CROSS SECTION IS//)
      PRINT 751, (ENER(MI),TSIGT(MI),MI=5,12)
751   FORMAT(1H0,40X,7HENERGY=,F7.3,20X,6HTSIGT=,E15.5//)
      IF(NON-3) 47,13,47
13    STOP
      END
```

```
      DSIG2=CONST*W*4./PI*H*SBESA*PHASB*FACTOR
      DSIG3=CONST*W*20./PI*H*SBESB*PHASC*FACTOR
      DSIG4=CONST*W*4./PI*SBESA*SBESA/PI*FACTOR
      DSIG5=CONST*W*20./PI*SBESB*SBESB/PI*FACTOR
15    TERM(IK)=DSIG1+DSIG2-DSIG3+DSIG4+DSIG5
      DSIGT(K)=FRONT*(HHF(1,JM)*TERM(1)+HHF(2,JM)*TERM(2)+HHF(3,JM)*
     2TERM(3))
3     QANG(J,K)=DSIGT(K)
2     PRINT 8,ENERGY,(ANGLE(K),DSIGT(K),K=1,10)
8     FORMAT(1H1,F10.3//(F10.3, F25.4//))
      WRITE OUTPUT TAPE 3, 83, ((QANG(I,J),J=1,10),I=1,16)
83    FORMAT(5E12.4)
      CALL EXIT
      END
```

```
$IBFTC HJAJ    NODECK
      DIMENSION A(50,3),B(50,1),COE(4),ROOTR(3),ROOTI(3),AJ(3)
      COMMON/THREE/ALFC(6)
      ALFAP=18.4
      PI=3.14159265
      SPI=SQRT(PI)
      SALF=SQRT(ALFAP)
C     FOR THE FIRST TRIPLET THE FOLLOWING CARD IS  DO 900 JK=1,4
      DO 900 JK=1,4
      RJK=JK-1
C     FIRST TRIP HAS THE NEXT CARD AS    ENERGY=9.0+1.0*RJK
      ENERGY=12.0+0.5*RJK
C     FIRST TRIP HAS THE NEXT CARD AS       R=(21.0081-ENERGY)/7.401
      R=7.483/2.870-SQRT(7.483*7.483-4.*1.435*(20.2203-ENERGY))/2.870
      ZO=SALF*(R-1.40)
      WRITE(6,901) R,ZO
901   FORMAT(1H1,20X,21HA NEW VALUE OF R, R=,F7.4,20X,3HZO=,F7.4)
C
C     NOW CALCULATE THE K-ALFA MOMENTS OF THE WEIGHTING FUNCTION W(X).
C
      CALL MOMENT(ZO)
      WRITE(6,202) ALFC
202   FORMAT(1H0,50X,4HALFC//(50X,F10.6/))
C
C     FORM THE A,B,C MATRICES
C
      DO 300 J=1,3
      A(J,1)=ALFC(J)
      A(J,2)=ALFC(J+1)
300   A(J,3)=ALFC(J+2)
      WRITE(6,301) ((A(N,M),N=1,3),M=1,3)
301   FORMAT(1H0,50X,29HTHE A MATRIX COMPOSED OF ALFC///(40X,3F15.6//))
      B(1,1)=-ALFC(4)
      B(2,1)=-ALFC(5)
      B(3,1)=-ALFC(6)
      WRITE(6,401) (B(N,1),N=1,3)
401   FORMAT(1H0,65X,8HB MATRIX///(55X,F15.6//))
      CALL MATINV(A,3,B,1,DETERM)
      WRITE(6,501) IT,DETERM,(B(N,1),N=1,3)
501   FORMAT(1H0,25X,3HIT=,I3,10X,7HDETERM=,F7.5//8HC MATRIX///
     33(40X,F15.6//))
C
C     FIND THE ROOTS OF THE POLY--THE AJ VALUES.
C
      COF(1)=1.0
      COE(2)=B(3,1)
      COF(3)=B(2,1)
      COF(4)=B(1,1)
      WRITE(6,502) COE
502   FORMAT(1H0,50X,16HCOEFFICIENTS COE//(55X,F16.5//))
      CALL MULLER(COE,3,ROOTR,ROOTI)
      WRITE(6,503) ROOTR,ROOTI
503   FORMAT(1H0,25X,5HROOTR,75X,5HROOTI///3(10X,F15.6//),3(80X,F15.6/))
      AJ(1)=ROOTR(1)/SALF+1.40
      AJ(2)=ROOTR(2)/SALF+1.40
      AJ(3)=ROOTR(3)/SALF+1.40
      WRITE(6,940) AJ
940   FORMAT(1H0,22HTHE ABCISSA VALUES ARE/(30X,F15.6//))
C
C     DETERMINE THE WEIGHTS HJ
C
```

```
      B(1,1)=ALFC(2)
      B(2,1)=ALFC(3)
      B(3,1)=ALFC(4)
      DO 601 N=1,3
      A(1,N)=ROOTR(N)
      A(2,N)=ROOTR(N)**2
601   A(3,N)=ROOTR(N)**3
      WRITE(6,602) (((A(K,L),K=1,3),L=1,3),(B(N,1),N=1,3))
602   FORMAT(1H0,30X,15HSECOND A MATRIX25X,15HSECOND B MATRIX//
     23(20X,3F15.6///),3(85X,F15.6//))
      CALL MATINV(A,3,B,1,DETERM)
      WRITE(6,603) IT,DETERM,(B(N,1),N=1,3)
603   FORMAT(1H0,3HIT=,I3,30X,7HDETERM=,F7.5//50X,21HWEIGHT COEFFICIENTS
     4 H//3(30X,F15.6//))
      CALCUL=B(1,1)+B(2,1)+B(3,1)
      TRUE=ALFC(1)
      WRITE(6,700) CALCUL,TRUE
700   FORMAT(1H0,20X,7HCALCUL=,F12.7,20X,5HTRUE=,F12.7)
900   CONTINUE
      STOP
      END
$IBFTC MOMENT  DECK
      SUBROUTINE MOMENT(B)
      COMMON/THREE/ALFC(6)
      SPI=SQRT(3.14159265)
      EPP=EXP(-B*B)
      ALFC(1)=SPI/2.*(1.-ERF(B))
      ALFC(3)=0.5*(ALFC(1)+B*EPP)
      ALFC(5)=1.5*ALFC(3)+0.5*(B**3)*EPP
      ALFC(2)=0.5*EPP
      ALFC(4)=ALFC(2)+B*B*EPP/2.
      ALFC(6)=2.*ALFC(4)+(B**4)*EPP/2.
      RETURN
      END
```

Proposition I

In the study of electron molecule collisions the simplest system which can be studied theoretically is the system: electron incident on the hydrogen molecule ion. In the framework of non-relativistic quantum mechanics there are many theoretical methods[1] with which to calculate the relevant scattering parameters, but of these many existing methods, few of them are practical when dealing with the intrinsic non-central force field of molecular systems. As a result of such mathematical difficulties the method used almost entirely for both elastic and inelastic problems has been the Born-Oppenheimer (scattering) approximation.[2]

It is proposed that a rigorous elastic s wave method introduced by A. Temkin,[3] called the Non-Adiabatic Theory, can be extended to cope with the non-central potential of the hydrogen molecule ion. The principle asset of this method is that it enables one to derive a difference relation between the true (s) wave elastic scattering phase shift and the approximate phase shift of this method. This difference can be expressed as a series which rapidly converges and whose terms correspond to multipole distortions of the molecular field by the incoming electron. These multipole distortion terms represent polarizations of the molecular field by the incident electron which are considered by many[4] as one of the most important mechanisms in low energy electron scattering.

Method:

In the case of an electron incident on the hydrogen molecule ion the Schrödinger equation for the system with the nuclei fixed, which will depend on the 6 coordinates of the two electrons and para-

metrically on the internuclear separation, is expanded in terms of relative partial waves.[5] The usefulness of the relative partial wave expansion method is the choice of three Euler angles (θ, Φ, ψ) and three residual coordinates (r_1, r_2, θ_{12}), as the six coordinates describing the position of the two electrons. This choice for description is important because then the angular momentum depends only on the Euler angles. Consequently, the eigenfunctions of the total angular momentum operator (M^2) and the z-component of angular momentum operator (M_z), which are denoted by $\mathfrak{D}_{\ell}^{(m,k)}(\theta, \Phi, \psi)$ [6], play a central role in the description of the electronic wave functions. An added advantage with this basis set is that these functions are also eigenfunctions of the space inversion operator (iE) with eigenvalue $(-1)^k$, and since this operator commutes with the Hamiltonian, the wave function is limited to definite k (even or odd).[7] In diatomic molecules (M^2) is no longer a constant of the motion and this fact is used to expand the molecular wave function in terms of the orbital angular momentum:[7]

$$\psi_m = \sum_{\ell=|m|}^{\infty} \psi_{\ell m} .$$

The basis set $\mathfrak{D}_{\ell}^{(m,k)}$ is chosen so that they are real for m = 0 and are eigenfunctions of the exchange operator ε_{12}

$$\varepsilon_{12}\mathfrak{D}_{\ell}^{(m,k)\pm} = (\pm)(-1)^{\ell+k}\mathfrak{D}_{\ell}^{(m,k)\pm}$$

while maintaining their eigenfunction character with respect to (iE),

(M^2), and (M_z).[7],[8] For the case of interest here, m = 0, the expansion is

$$\psi_o = \sum_{\ell=0}^{\infty} \sum_{k}'' \{f_\ell^{(o,k)+}(r)\, \mathcal{D}_\ell^{(o,k)+} + f_\ell^{(o,k)-} \mathcal{D}_\ell^{(o,k)-}\} \qquad (1)$$

where the double prime on the sum means every second value of k is taken and the argument r of the functions f means (r_1, r_2, θ_{12}). Thus, there are two classes for ψ_o, even and odd (gerade and ungerade). The potential of the system is given by:

$$V_{MOL} + \frac{2}{r_{12}} = -\frac{2}{R_{A1}} - \frac{2}{R_{A2}} - \frac{2}{R_{B1}} - \frac{2}{R_{B2}} + \frac{2}{r_{12}}$$

and V_{MOL} can be expanded[7] as

$$V_{MOL} = -4 \sum_{\lambda \text{ even}}'' \left[g_\lambda\left(\frac{R_{AB}}{2}, r_1\right) P_\lambda(\theta_1) + g_\lambda\left(\frac{R_{AB}}{2}, r_2\right) P_\lambda(\theta_2) \right]$$

where

$$g_\lambda(x, y) = \begin{cases} x^\lambda / y^\lambda + 1 & x < y \\ y^\lambda / x^\lambda + 1 & y < x \end{cases}$$

and similarly the P_λ functions can be expanded in terms of the $\mathcal{D}_\lambda^{(m,k)}$ functions as[8]

$$P_\lambda \begin{Bmatrix} \theta_1 \\ \theta_2 \end{Bmatrix} = \frac{4\pi}{\sqrt{2\lambda+1}} \sum_{\mu \text{ even}}'' \left\{ \alpha_\lambda^{\mu+}(\theta_{12}) \mathcal{D}_\lambda^{(o,\mu)+} \pm \alpha_\lambda^{\mu-}(\theta_{12}) \mathcal{D}_\lambda^{(o,\mu)-} \right\}$$

where

$$\alpha_\ell^{\mu\pm}(\theta_{12}) = P_\ell^k(\pi/2)\left[\frac{(\ell-k)!}{(\ell+k)!}\right]^{1/2} \begin{Bmatrix} \frac{\delta_{ok}}{\sqrt{2}} + (1-\delta_{ok})\cos\left(\frac{k\theta_{12}}{2}\right) \\ \sin\left(\frac{k\theta_{12}}{2}\right) \end{Bmatrix} .$$

The sum of the kinetic energy operator, the derivation of which is long and complicated[8], and the potential, is the Hamiltonian operator of the system and when the wave function[1] is substituted into

$$(H - E)\psi = 0$$

the V_{MOL} part of the potential will couple terms of different ℓ. This coupling is complicated[9], involving integrals over 3 vector spherical harmonics, but for $\sum$ states (m = 0) the coupling simplifies to the connecting radial functions of the same parity only but no intermixing of different ℓ parity. The kinetic energy operator in this case has exchange symmetry and consequently the solution can be restricted to $r_1 > r_2$ with the boundary conditions[3]

$$\left[\frac{\partial}{\partial r} f_\ell^{(m,k)}\right]_{r_1=r_2} = 0 \qquad \text{(singlet)}$$

$$\left[f_{\ell}^{(m,k)} \right]_{r_1=r_2} = 0 \qquad \text{(triplet)} \ . \tag{2}$$

The complete radial equations are similar to those found in reference (7) but have been omitted here since they are very complicated and must be simplified before a solution is attempted. The practical method of solution consists in truncating the coupling terms, which are doubly infinite (involving the potential summation index λ and the angular momentum index ℓ) at some value for angular momentum so that only a finite number of terms enter. The Non-Adiabatic method is to truncate at the lowest possible value of orbital angular momentum (L = 0) and if it is assumed that the hydrogen molecule is in the ground state ($\sum_g^+$) the equation that must be solved is:

$$\left\{ \frac{1}{r_1} \frac{\partial^2}{\partial r_1^2} r_1 + \frac{1}{r_2} \frac{\partial^2}{\partial r_2^2} r_2 + (r_1^{-2} + r_2^{-2}) \frac{1}{\sin\theta_{12}} \frac{\partial}{\partial \theta_{12}} \left(\sin\theta_{12} \frac{\partial}{\partial \theta_{12}}\right) + \right.$$

$$\left. E - \frac{2}{r_{12}} + 4g_o\left(\frac{R_{AB}}{2}, r_1\right) + 4g_o\left(\frac{R_{AB}}{2}, r_2\right) \right\} f(r_1, r_2, \theta_{12}) = 0 \tag{3}$$

along with the boundary conditions equations (2). The solution of (3) would be carried out in the manner of Temkin[3], which involved the expansion of the function f in terms of relative partial waves

$$f(r_1, r_2, \theta_{12}) = \sum_{n=0}^{\infty} \frac{(2\ell+1)^{1/2}}{r_1 r_2} \Phi_n(r_1 r_2) P_n(\theta_{12}) \ . \tag{4}$$

The basis set $P_n(\theta_{12})$ is used because they are eigenfunctions of the derivatives of (3) and because $1/r_{12}$ has an expansion in terms of $P_n(\theta_{12})$.[10] Substitution of (4) into (3) gives an infinite set of 2-dimensional partial differential equations

$$\left\{ \frac{\partial^2}{\partial r_1^2} + \frac{\partial^2}{\partial r_2^2} - \ell(\ell+1)(r_1^{-2} + r_2^{-2}) + E + 4g_o\left(\frac{R_{AB}}{2}, r_1\right) + 4g_o\left(\frac{R_{AB}}{2}, r_2\right) - M_{\ell\ell} \right\} \Phi_\ell(r_1 r_2) = \sum_{m=0}^{\infty}{}' M_{\ell m} \Phi_m(r_1 r_2) \qquad (5)$$

where the prime means parity continuity with the left hand side and where

$$M_{\ell m} = (2\ell+1)^{1/2}(2m+1)^{1/2} \sum_{n=0}^{\ell+m} \frac{r_2^n}{r_1^{n+1}} \int_0^{\pi} P_\ell(\cos\theta) P_m(\cos\theta) P_n(\cos\theta) \sin\theta d\theta$$

with the boundary conditions

$$\begin{aligned} \Phi_\ell(r_1 r_2)\big|_{r_1=r_2} &= 0 \qquad \text{(triplet)} \\ \frac{\partial}{\partial n} \Phi_\ell(r_1 r_2)\big|_{r_1=r_2} &= 0 \qquad \text{(singlet)} \end{aligned} \qquad (6)$$

and

$$\Phi_\ell(r, o) = 0 \ .$$

The overall charge on the hydrogen molecule ion requires the asymptotic boundary conditions to be

$$\lim_{r_1 \to \infty} \Phi_o(r_1 r_2) = \sin(kr_1 + \delta + \frac{1}{ka_o} \ln 2kr_1) R_{1\Sigma}(r_2)$$

$$\lim_{r_1 \to \infty} \Phi_\ell(r_1 r_2) = 0 \qquad \ell > 0$$

(no inelastic scattering)

where k^2 is related to the energy of H_2^+ by

$$E = -\varepsilon + k^2$$

(atomic units)

and $R_{1\Sigma}(r_2)$ is the ground state wave function for H_2^+. Equations (5), along with the boundary conditions (6), are solved in the following systematic manner:

The zeroth order problem is formed by setting $\ell = 0$ in (5), to give the zeroth order equation and

$$\left\{ \frac{\partial^2}{\partial r_1^2} + \frac{\partial^2}{\partial r_2^2} + E + 4g_o(\frac{R_{AB}}{2}, r_1) + 4g_o(\frac{R_{AB}}{2}, r_2) \right\} \Phi(r_1 r_2) =$$

$$\sum_{m=0}^{\infty}{}' \frac{2}{(2m+1)^{1/2}} \frac{r_2^m}{r_1^{m+1}} \Phi_m \cdot \qquad (7)$$

Neglecting the right hand side of (7) gives

$$\left\{ \frac{\partial^2}{\partial r_1^2} + \frac{\partial^2}{\partial r_2^2} + E + 4g_o\left(\frac{R_{AB}}{2}, r_1\right) + 4g_o\left(\frac{R_{AB}}{2}, r_2\right) \right\} \Phi_o^{(o)}(r_1 r_2) = 0 \tag{8}$$

$$\lim_{r_1 \to \infty} \Phi_o^{(o)} = \sin(kr + \delta_o + \frac{1}{ka_o} \ln 2kr_1) R_{1\Sigma}(r_2) .$$

A relation between δ and δ_o is established by following the procedure of A. Temkin[3] and multiplying (7) by $\Phi_o^{(o)}$ and (8) by Φ_o subtracting, and integrating over the half plane $r_1 > r_2$; applying Green's theorem in two dimentions and utilizing the boundary conditions (6) in the resulting line integrals. This leads to an expression for the difference in phases:

$$\sin(\delta - \delta_o) = -\frac{1}{k} \sum_{m=1}^{\infty} \frac{2}{(2m+1)^{1/2}} \int_0^{\infty} dr_1 \int_0^{r_1} dr_2 \, \Phi_o^{(o)} \frac{r_2^m}{r_1^{m+1}} \Phi_m \tag{9}$$

δ = true phase shift

δ_o = zeroth order phase shift

$\Phi_o^{(o)}$ = zeroth order solution

Φ_o = multipole solution corrections

The above equation is the heart of this method because it allows a systematic and physically appealing series of converging approximations to be conducted to determine the best value for δ. In the Non-Adiabatic Theory, the zeroth order problem $\Phi_o^{(o)}$ is solved by expanding $\Phi_o^{(o)}$ in terms of the separable solutions of (8) and applying the boundary conditions to these solutions. The separable solutions are:

$$\Phi_o^{(o)} = \sin(kr_1 + \delta_o + \frac{1}{ka_o} \ln 2k r_1) R_{1\Sigma}(r_2) + (\sum_n + \int dp) C_n e^{-k_n r_1} R_{n\Sigma}(r_2)$$

where the integral is necessary to account (in principle) for the continuum states of the hydrogen molecule ion. The parameters are determined variationally from the condition

$$\delta \int_0^\infty |\Phi_o^{(o)}(r_1 = r_2)|^2 \, dr_1 = 0 \qquad \text{(triplet)}$$

$$\delta \int_0^\infty \left| \frac{\partial}{\partial n} \Phi_o^{(o)} \right|^2_{r_1 = r_2} dr_1 = 0 \qquad \text{(singlet)} \; .$$

The lowest order solution to (9) is obtained by replacing Φ_m by $\Phi_o^{(o)}$. The higher order contributions are obtained by introducing a perturbation theory based on the assumption that the neglect of higher order Φ_ℓ in the equations do not significantly affect the solution for the lower $\Phi_\ell^{(3)}$. With some effort the set of equations (7) and (9) can be replaced by a set of equations in terms of increasing powers of the perturbing parameter. Successive solutions for the perturbed functions and substitution of these functions into (9) gives the higher order corrections to the zeroth order phase shift. As mentioned above, these corrections have the physical significance of multipole distortions of the molecular field by the incident electron.

The method outlined above would undoubtedly be lengthy and require much numerical work. However, it seems that the results obtained stand a good chance of being far better than any existing theoretical results for this system.

References for Proposition I

(1) P. G. Burke and K. Smith, "Reviews Modern Physics", 34, p. 458 (1962).

(2) Craggs and Massey, "Handbuch der Physik" Vol. 37/1. Edited by S. Flugge, p. 333 (1959).

(3) A. Temkin, "Physical Review", 126, p. 130, April (1962).

(4) A. Dalgarno and A. Stewart, "Proceedings Royal Society London", A 238, p. 267 (1956).

(5) A. Temkin, "Journal Chemical Physics", 39, p. 161, July (1963).

(6) L. Pauling and E. B. Wilson, Introduction to Quantum Mechanics, (McGraw-Hill, New York 1935), p. 280.

(7) A. Temkin, "Journal Chemical Physics", 42, p. 644 (1965).

(8) A. Bhatia and A. Temkin, "Reviews Modern Physics", 36, p. 1052 (1964).

(9) A. R. Edmonds, Angular Momentum in Quantum Mechanics, p. 62.

(10) See for example, Jackson, J. D., Classical Electrodynamics, (John Wiley and Sons, New York 1963), p. 63.

Proposition II

When a conducting body moves through a rarefied region containing charged particles (a plasma) the surface of the body acquires a negative charge due to the difference in the mobility of the electrons and ions. This negative potential increases in magnitude until the flux of ions becomes equal to the flux of the electrons. The presence of this charged surface affects the trajectories of the nearby charged particles and in turn these adjacent charged particles modify the potential due to their presence as space charges. This electrodynamical phenomenon is encountered in the attempted measurement of particle density and temperature both in the laboratory and in the upper atmosphere by a satellite probe.

The traditional manner of solution of this problem involves the Boltzman equation which determines the distribution of the particles, and Poisson's equation which governs the potential field. [1] These equations are coupled through the charge density in Poisson's equation and the gradient of the potential in the Boltzman equation. These equations are non-linear in the potential and numerous approximations must be made before the system can be solved. Consequently, the applicability of these equations in the rarefied gas situation is currently controversial and a new approach has been recently formulated to help understand these psuedo-macroscopic interactions. [2]

It is proposed that this new method, which treats only electrostatic interactions and planar geometry can be generalized to include a static magnetic field and cylindrical geometry and therefore

describe more realistically the situation as found in the upper atmosphere or laboratory.

The basis for this new method is the replacement of the Boltzman equation by the Schrödinger equation to represent the motion of the particles. As in the traditional methods, the description of the electrostatic field is given by Poisson's equation. Problems in hydrodynamic stability and wave excitations are removed from consideration by investigating only the steady state of the interaction. It is realistically assumed that the free stream velocity of the particles $\vec{v}_o$ is much larger than the thermal velocity of the ions and much less than the thermal velocity of the electrons and as a result, the electron distribution is almost completely determined by the electric field. (1) On the other hand, the electric field doesn't strongly influence the ions since their relative (to the body) energy greatly exceeds their thermal velocity

$$Mv_o^2 >> kT$$

and consequently exceeds their potential energy in the electric field which is order kT. (1) In addition, assume the characteristic dimension of the body is much less than the mean free path of the particles so that particle-particle interactions can be neglected, and also that the body absorbs and neutralizes all the charged particles which it encounters, (2) (which will lead to the overall negative potential attained by the body).

Assuming that the velocity of the body ($\vec{v}_o$) is uniform it is convenient to consider a coordinate system fixed in the moving body so that the particle distribution is stationary. (3) As a good first approximation to coping with the complicated coupling of the problem,

assume that the electrons close to the body experience only the electrostatic force and are therefore distributed according to the Maxwell-Boltzman law.[4] (see above discussion)

$$n_e(r) = n_{eo} e^{\frac{e\phi(r)}{kT_e}} \tag{1}$$

where e, k, T_e, ϕ and n_{eo} denote the electron charge, Boltzman constant, electron temperature, electrostatic potential and electron density in the absence of the electric field.

The effect of the magnetic field on the motion of the ions is written in the Schrödinger equation as:[5]

$$\frac{1}{2\mu}\left(\frac{\hbar}{i}\nabla - e\vec{A}\right)^2 \psi + e\phi\psi = E\psi$$

which can be expanded to

$$\left\{ -\frac{\hbar^2}{2\mu}\nabla^2 + \frac{ie\hbar}{2\mu}(\nabla \cdot \vec{A}) + \frac{ie\hbar}{\mu}(\vec{A}\cdot\nabla) + \frac{e^2}{2\mu}A^2 + e\phi - E\right\}\psi = 0 . \tag{2}$$

The Coulomb gauge[6] is chosen for the representation of the fields so that

$$\nabla \cdot \vec{A} = 0$$

and equation (2) can be written as

$$\left\{ -\frac{\hbar^2}{2\mu}\nabla^2 + \frac{ei\hbar}{\mu}(\vec{A}\cdot\nabla) + \frac{e^2}{2\mu}A^2 + e\phi - E\right\}\psi = 0 . \tag{3}$$

Equation (3) is coupled to Poisson's equation which governs the variation of ϕ according to:

$$\nabla^2\phi = -\frac{e}{\epsilon_o}(n_i - n_e) = \frac{en_o}{\epsilon_o}\left[|\psi|^2 - e^{\frac{e\phi}{kT_e}}\right] \tag{4}$$

with

$$\phi, \nabla\phi \to 0 \text{ as } |\vec{r}| \to \infty$$

(MKS units used)

where the probability interpretation that $n_o|\psi|^2$ represents the number density of ions at $\vec{r}$ has been used. The simultaneous solution of equations (3) and (4) would yield the structure of the potential shield around the body moving through the plasma.

Method of Solution

The two coupled partial differential equations that must be solved are equations (3) and (4).

In order to make any headway with these equations it is necessary to make some assumptions about the geometry of the object traveling through the plasma and the local region of interest on the body. To illustrate with a simple case, assume cylindrical symmetry for the body and assume that the body is oriented in its travel such that its axis always points in the direction of the magnetic field and perpendicular to the motion of the body.

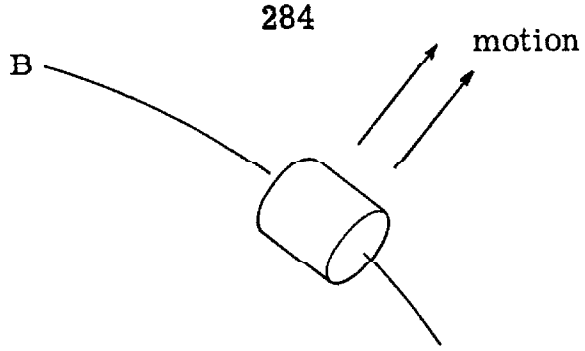

In this case, the cylindrical portion of the body in the direction of motion will become negatively charged. To greatly simplify things for the sake of illustration, neglect edge effects and assume that $\phi(\vec{r}) = \phi(\rho)$, which is the same as assuming the potential distributes itself uniformly over the area of interest. Under these assumptions, equation (3) can be reduced to one ordinary differential equation. With $\vec{B} = B\hat{e}_z$ or $\vec{A} = (0, \frac{B}{2}\rho, 0)$ equation (3) becomes

$$\left\{ -\frac{\hbar^2}{2\mu}\left(\frac{\partial^2}{\partial \rho^2} + \frac{1}{\rho}\frac{\partial}{\partial \rho}\right) + \frac{e^2B^2}{8\mu}\rho^2 + e\phi(\rho) - E \right\}\psi = 0 \qquad (5)$$

where ψ is now a function only of ρ; the above can be rewritten as:[7]

$$[\psi(\rho, \varphi, z) = (2\pi)^{-\frac{1}{2}} R(\rho) e^{2kz}$$

$$\frac{d^2R}{d\rho^2} + \frac{1}{\rho}\frac{dR}{d\rho} + \left(\beta - \gamma^2\rho^2 - \frac{2\mu}{\hbar^2} e\varphi(\rho)\right)R = 0$$

where $\gamma = \frac{eB}{2\hbar}$, $\beta = \frac{2\mu E}{\hbar^2} - k^2$, k^2 = separation constant of dimension ℓ^{-2} = 0 in this case .

To completely solve the problem it is necessary to solve the remaining coupled equations:

$$\frac{d^2R}{d\rho^2} + \frac{1}{\rho}\frac{dR}{d\rho} + (\beta - \rho^2(\gamma^2 + \frac{e\phi}{\rho^2}(\rho)))R = 0$$

$$\frac{d^2\phi}{d\rho^2} + \frac{1}{\rho}\frac{d\phi}{d\rho} = \frac{en_o}{G_o}\left\{e^{\frac{e\phi}{kT_e}} - |\psi|^2\right\} \tag{6}$$

constrained by

$$|\psi|^2 \to 1 \quad \text{as} \quad \phi \to 0$$

$$\phi, \nabla\phi \to 0 \quad \text{as} \quad \rho \to \infty .$$

This is clearly difficult to accomplish as they stand, but an approximation that might be reasonable with the physics of this problem is to solve the first of equations (6) by the WKB approximation.[8] This approximation is justified since in the upper atmosphere, the Debye shielding distance (the distance over which ϕ changes significantly) is order .5 cm[3] while the de Broglie wave length for the ions in that region of space is order 10^{-4}cm.[9] It should be pointed out that if the solution ϕ is obtained in the manner outlined above it can be considered to be the potential as a function of ρ in the frontal zone only since by making the WKB approximation all the "diffraction" effects found in the wake of the moving body are lost.[10]

Since this proposition describes an application of quantum mechanical methods to a physical situation that is adequately described by classical mechanics one may ask the why of it. The main reason for this new approach is that in many cases the mathematics associated with the solution of the Schrödinger equation would be easier than that associated with the Boltzman equation since the classical (WKB) limit would be taken which simplifies some of the mathematics of the Schrödinger equation.[2] This limit in turn returns the formalism to that of the macroscopic process.

References for Proposition II

(1) V. A. L. Al'pert, A. V. Gurevich, and L. P. Pelaevskii, "Soviet Physics Uspekhi", 6, 13 (1963).

(2) V. C. Liu, "Nature", 208, 5013, November 27 (1965).

(3) Ref. 1, p. 17 (tables therein).

(4) P. M. Morse, Thermal Physics, Benjamin, p. 105 (1962).

(5) J. L. Powell, and B. Crasemann, Quantum Mechanics, Addison-Wesley, p. 348 (1961).

(6) J. D. Jackson, Classical Electrodynamics, John Wiley p. 181 (1963).

(7) I. I. Gol'dman, and V. D. Krivchenkov, Problems in Quantum Mechanics, Addison-Wesley, p. 148 (1961).

(8) Ibid. Reference 5, p. 141.

(9) Conservatively estimated for a mass of (20) x $(1.67)10^{-24}$ gm., and velocity given in the tables of reference 3.

(10) D. Halliday, and R. Resnick, Physics, Wiley, p. 943 (1962).

Proposition III

Natural aerosols are defined as those particles of greater than molecular size which can exist in the atmosphere at relative humidities below saturation.[1] This definition includes particle sizes that range from .04μ to 100μ and excludes such phenomenon as fog, rain droplets and clouds. Knowledge of the size, type and altitude distribution are important in studies of visibility, atmospheric physics and chemistry, and radiation processes.

At the present time, there exists no method of determining rapidly the distribution in type and size of aerosols over some given area. This experimental void is due primarily to the size of the particles being investigated and the techniques employed in the past--namely rockets and balloons for the small aerosols and radar for the much larger phenomenon.

It is proposed that the visible portion of the electromagnetic spectrum can be used with the basic methods of radar to probe the atmosphere and determine useful information concerning aerosol size and distribution. It should be pointed out that radar frequencies will not give the kind of information desired. Basically this is because the wave length is much greater than the size of the aerosols, and as a result of the Rayleigh scattering the angular distribution is the same for all particles which satisfy: (radius $<< \lambda$).[2] To "see" the details of the particles one must use a radiation probe whose wave length is the same order of magnitude as the diameter of the particles.

For a single particle, the relative intensity of scattered radiation by particles at point R comparable to or larger than the

wave length of incident radiation is given by:[3]

$$I(\alpha, \varphi, m) = \frac{\lambda^2}{4\pi^2} \left(\frac{i_1 + i_2}{2}\right) \frac{1}{R^2} \quad , \tag{1}$$

where i_1 and i_2 are the Mie scattering coefficients in two mutually perpendicular planes, $\alpha = 2\pi r/\lambda$, r = the radius of the scattering particle, φ is the scattering angle measured from the incident direction and m is the ratio n_2/n_1 of refractive index of scatterer to refractive index of surrounding medium (air in this case). If there is a distribution of particle sizes in the volume of illuminated air which obeys Junge's Law[4], then

$$\frac{dn(r)}{d\log_e^r} = \tilde{c}\, r^{-\gamma} \quad ,$$

where $\tilde{c}$ is a constant dependent on the total number of particles in the volume. The equation (1) is modified to read[5]

$$I(\alpha, \varphi, m) = \frac{\lambda^2}{4\pi^2} \int_{r_1}^{r_2} \left(\frac{i_1 + i_2}{2}\right) \frac{dn(r)}{R^2} \tag{2}$$

where $r_1(r_2)$ is the smallest (largest) diameter of particle appearing in the distribution usually assumed to be $.04\mu(10\mu)$ for aerosols. Equation (2) must be modified again to be useful in the application of pulsed radar techniques. The equation can be written as[6]

$$\frac{\vec{I}_r}{I_t} = \frac{G^2\lambda^2}{(4\pi)^3 R^4}(R^2\theta\phi\frac{\tau c}{2})A_{int}\int_{r_1}^{r_2}(\frac{i_1 + i_2}{2})dn(r) \qquad (3)$$

where I_r is the average returned intensity, I_t is the transmitted intensity, G is the gain of the receiver, θ and ϕ are the beam widths or solid angle of the transmitted pulse; τ is the duration of the pulse in seconds and A_{int} is the area intercepted by the beam at a distance R from the transmitter.

Equation (3) can be rewritten using $G\lambda^2 = 4\pi A_{eff}$ where A_{eff} is the effective area of the receiver, and the fact that $\theta\phi \approx 4\pi/G$[6] to give

$$\frac{\vec{I}_r}{I_t} = \frac{A_{eff}A_{int}}{8\pi R^2}\tau c\int_{r_1}^{r_2}(\frac{i_1 + i_2}{2})dn(r) \quad . \qquad (4)$$

Equation (4) expresses the returned intensity of radiation in terms of the power transmitted, the physical parameters of the transmitting system, and the details of the scattering aerosols, the latter being contained in the integral. The R^2 in the denominator of equation (4) is an expression of the attenuation of the radiation pulse due to all scattering and absorption processes.

In general, atmospheric backscatter will consist of both Rayleigh (molecular) and Mie (aerosol) scattered radiation. However, it has been shown that Rayleigh scattering will contribute to the total returned radiation in the visible spectrum only if the range visibility

is greater than 5 KM (3.1 miles) and in cases where Rayleigh backscatter is not negligible the contribution can be reasonably well accounted for.[7]

For this experiment, the radiation source is visualized as that of a laser because it is possible to obtain very short, high peak power pulses of essentially monochromatic radiation. The high peak power-short pulses are necessary to give the range and still facilitate the separation of the returned signal from the background noise, while the monochromatic radiation serves as a well defined probe.

For a given wave length laser and receiver, the A_{eff}, τc and A_{int} are determined. The experimental technique would consist of pulsing the radiation and measuring both the intensity and degree of polarization of the backscattered radiation. Then the frequency would be changed to some other region of the visible and the experimental procedure repeated.

The important aspects of Mie scattering theory which are utilized are the following. First, the shape of the indicatrix (angular distribution) is strongly dependent on the wave length. For instance, for a ruby laser ($\lambda = .6943\mu$) and assuming perfectly reflecting particles the intensity of backscattered radiation is 80% of the incident intensity for particles .1μ in radius but essentially zero for particles .3μ in radius;[8] while for radiation in the blue ($\lambda \approx .45\mu$) the corresponding upper radius cutoff appears at .2μ. In other words, a certain range of particle size can be searched for by proper choice of the monochromatic radiations employed.

The analysis of data could be conducted as follows: The backscattered signals received will be a function of time (the R

in equation (4)) and must be integrated to give the total back-scattered energy from all the particles in the beam. A form for the aerosol size distribution is chosen (Junge distribution) and the expected degree of polarization is calculated from[9].

$$P_{\phi} = \frac{I_1(\phi) - I_2(\phi)}{I_1(\phi) + I_2(\phi)}$$

where

$$I\left\{\begin{matrix}1\\2\end{matrix}\right\} = I_t \frac{A_{eff} A_{int}}{8\pi R^2} \tau c \left\{ \begin{matrix} \int_{r_1}^{r_2} \frac{i_1}{2} dn(r) \\ \int_{r_1}^{r_2} \frac{i_2}{2} dn(r) \end{matrix} \right\}$$

and ϕ , the observation angle, $= \pi$ in this experiment.

Since the polarization is a more sensitive measure for the aerosol size distribution than the scattering functions themselves,[10] the form of the distribution function is varied until a reasonable agreement with the data is obtained. Then the parameters, α and m, of the Mie functions (i_1 and i_2) are varied until the calculated total backscattered intensity agrees with the data obtained for the various wave lengths employed. In this manner it should be possible to obtain information concerning the type and size distribution as a function of altitude, location, etc.

Because the investigation of aerosols in their environment is complicated by many spurious factors, it is probable that

sophisticated experimental and data processing techniques will be needed for this method to yield accurate information concerning aerosols in the atmosphere.

References for Proposition III

(1) Handbook of Geophysics, U. S. Airforce Cambridge Research Center, p. 8-1 (1960).

(2) H. C. Van de Hulst, Light Scattering by Small Particles, J. Wiley, p. 67 (1957).

(3) K. Ya. Kondral'yev, Actinometry, NASA Translation from the Russian TT F-9712, p. 163 (1965).

(4) C. E. Junge, "Atmospheric Chemistry", Chapter 7, Advances in Geophysics, Vol. IV, Academic Press, New York, (1957).

(5) K. Bullrich, Electromagnetic Scattering, Edited by M. Kerker, (1962), p. 192; and P. Beckman and A. Spizzichino, The Scattering of Electromagnetic Waves, (1963), p. 404.

(6) H. Goldstein, D. E. Kerr, and A. E. Bent, MIT Radiation Lab Series, Vol. 13, p. 591.

(7) See Reference 4, p. 198.

(8) See figures of Reference 3, p. 165.

(9) D. Durmendjian, Electromagnetic Scattering, Edited by M. Kerker, p. 177 (1962).

(10) See Reference 4, p. 200.

Proposition IV

I. Introduction

It has recently become feasible to attempt calculations of cross sections for the excitation and ionization processes in N_2, O_2, N and O. It is suggested that by using these cross sections, one can obtain insight into some of the interesting properties of the aurora.

A good deal of work has been done on the emission of visible, near-UV and infrared radiations from the aurora because these processes can be measured by ground based equipment.[1] However, due to the atmospheric cut-off, the UV portion of the spectrum cannot be seen from the surface of the earth. It has recently been suggested[2] that a major portion of the energy deposited in the emitting states of the atmospheric atoms and molecules must appear in the form of UV radiation. This was concluded because so little ($\sim$ 5%) of the expected radiation appears in the visible and infrared. A recent experiment[3] has verified that indeed this is the case as rocket experiments measured intense radiation in the 1000-1350 Å region. From an analysis of the response of the rocket-borne detection system, it was concluded[3] that most of the radiation comes from atomic oxygen and molecular nitrogen.

It would be very interesting to try and explain these UV emissions for two reasons. The first is because an adequate description of the source of these radiations would represent a step forward in the understanding of the complex aurora processes. The second is, because from a description of the source of aurora

emission, one can perhaps determine the distribution in energy of the primary and secondary charged particles which produce the aurora. A knowledge of these distributions is very important since these particles may be part of an energy-coupling of the earth's polar regions with the magnetosphere.[4]

II. Theory

The basic analysis proceeds from Bethe's expression for the stopping power of a charged particle in matter.[5] To simplify presentation of the method, assume that only one type of particle is present (say N_2) and all of them are in their ground electronic state. One can then define an energy-loss function for a primary particle of energy E as

$$\mathcal{L}(E) = -\frac{1}{N}\frac{dE}{dx} = \sum_n Q_n(E)[E_n - E_o] + \int_0^{K_{max}} [E_k - E_o]Q_k dk, \quad (1)$$

where N is the number density of atoms or molecules; $(E_n - E_o)$ is the excitation energy of state n; Q_n is the total cross section for excitation to state n; Q_k is cross section, differential with respect to energy of the ejected electron, and K_{max} is determined by the energy relation

$$E = \frac{\hbar^2 K_{max}^2}{2m}, \quad (2)$$

where m is the electron mass. One then defines the fractional energy loss to each mode as

$$\text{(excitation)} \qquad f_n(E) = (E_n - E_0)Q_n(E)/\mathcal{L}(E) , \tag{3}$$

$$\text{(ionization)} \qquad f_i(E) = I_i\ \sigma_i(E)/\mathcal{L}(E) , \tag{4}$$

$$\text{(energy of secondaries)} \quad f_s(E) = (\bar{W}_i - I_i)\ \sigma_i(E)/\mathcal{L}(E) , \tag{5}$$

where I_i is the ionization energy of state i, σ_i is the total ionization cross section; and $\bar{W}_i$ is the average energy lost in ionizing state (i) and is defined by

$$\bar{W}_i\ \sigma_i = \int_0^E W_i(k)\ Q_k\ dk . \tag{6}$$

From the above quantities, one can calculate

$$E_\mu(E) = \int_0^E f_\mu(E')\ dE' \tag{7}$$

which represents the energy deposited in the μth mode by the primary particle of energy E as it is slowed down.

III. Discussion

The above equations contain the information necessary to perform the calculations which proceed (qualitatively) as follows. For a given primary incident energy (E) one determines the energy deposited in the emitting states by the primary particle through use of (3) and (7). Also, from (4) and (7) one calculates the energy lost in ionization which, by division with the ionization energy for the state, leads to the number of secondary electrons. From the total secondary energy one then finds the energy per secondary electron. The above process of degradation is then repeated for these secondaries, and then the tertiaries, etc. until all the available energy is dissipated. By this procedure, the total amount of energy emitted in the form of UV radiation is then determined. These results can then be normalized to yield absolute emission rates.[6]

To be realistic, the process outlined above would have to allow for a distribution in energy of the primary and secondary electrons. Different forms for the distributions could be tried until (hopefully) consistent emission rates are obtained. Recently, some measurements of the secondary electron distribution have been made[7] which could guide the theoretical choices. However, little is presently known about the energy distribution of primaries and if this calculation were successful, it would provide information as to the source of these particles.

Of most importance in carrying out such a program is knowledge of the ionization and excitation cross sections of N_2 and O. There are some recent experimental results on the allowed excitations in N_2 but very little is known about the forbidden or ionization cross

sections of the states in N_2 and O.[8] However, a good portion of the important cross sections for which there are no data can be reliably calculated with an extension of a method just recently developed.[9]

References for Proposition IV

(1) a) J. W. Chamberlain, Physics of the Aurora and Airglow, (Academic Press, New York 1961). b) A. Vallance Jones, Optical Measurements of Auroras, in Auroral Phenomena, Experiments and Theory, edited by Martin Walt, Stanford University Press (1965).

(2) Ref. 1a) and J. W. Chamberlain, Mem. Soc. Roy. Sci. Liege, [5] 4, 606 (1961).

(3) W. B. Murcray, J. Geoph. Res. 71, 2739 (1966).

(4) A. E. S. Green and C. A. Barth, J. Geoph, Res. 70, 1083 (1965).

(5) a) H. A. Bethe, Ann. Phys. (Liepzig) 5, 325 (1930) (In German); b) A. Dalgarno, Range and Energy Loss, in Atomic and Molecular Processes, edited by D. R. Bates (Academic Press, New York 1962) p. 622.

(6) The method suggested is to normalize to the 3914 A (0, 0) band of N_2^+ which is defined to have a certain emission rate. See ref. 1a).

(7) W. J. Heikkila and D. L. Matthews, Nature 202, 789 (1964); J. P. Doering and W. G. Fastie (to be published 1967).

(8) Bibliography of Low Energy Electron Collision Cross Section Data, Nat. Bur. Stands. #289, 1967.

(9) D. C. Cartwright and A. K. Kuppermann, Phys. Rev., (to be published, 1967).

Proposition V

I. Introduction

It is proposed that the bound-free absorption coefficients (or photodetachment cross sections) for the negative ions of astrophysical interest can be calculated accurately, and with much less the usual effort, by using the new GF wave functions.

The attenuation of electromagnetic radiation in the visible and infrared (called opacity) by the atmosphere of cooler late-type stars is due predominantly to bound-free transitions of H^- and other systems with Z's ranging from 2 to 30.[1] The H^- system accounts for about 85% of this absorption and O^- about half of that remaining. Knowledge of the absorption coefficients for these photoionization processes is necessary for the development of any detailed steller model for these stars. Because these processes are so difficult to measure experimentally, it is essential to have reliable theoretical values.

There have been many calculations of absorption coefficients since the discovery of their importance in 1939.[2] However, the efforts have been devoted almost entirely to H^- and calculations continue to appear in which people use increasingly more complicated two-electron wave functions for the bound and free states.[3] Even though the calculations are becoming internally consistent, there is no clear cut basis for the best theoretical approach in the general case. In addition, most the methods employed for H^- are not easily extendable to O^- and other negative ions because of the complexities associated with the larger number of electrons in these

ions. Most of the calculations on H^- are performed using Pekeris-type (Hylleraas-type) bound state wave functions[4] which contain explicit electron correlation terms and many (70 to 203) variational parameters. If one hopes to calculate these photoionization cross sections for the more complicated ions, it appears necessary to search for wave functions which will yield reliable results for H^- and still allow solution of the processes involving the other ions. The GF wave functions[5] appear to offer the required flexibility and still possess the quality necessary for accurate results.

II. Theory

For simplicity, the methods used to calculate the absorption coefficient are presented for the case of H^-. The techniques can in principle be extended to any Z-system.

There are three formally equivalent ways of expressing the absorption coefficient which in practice differ because the wave functions used are not exact. These expressions, all descriptions of an oscillating dipole, differ in the matrix elements used[6]:

$$\mu_z = \int \Psi_d^* (z_1 + z_2) \Psi_c \, d\tau \,, \tag{1}$$

$$\mu_z = - \frac{1}{(E_d - E_c)} \int \Psi_d^* \left(\frac{\partial}{\partial z_1} + \frac{\partial}{\partial z_2} \right) \Psi_c \, d\tau \,, \tag{2}$$

$$\mu_z = \frac{1}{(E_d - E_c)^2} \int \Psi_d^* \left(\frac{z_1}{r_1^3} + \frac{z_2}{r_2^3} \right) \Psi_c \, d\tau \,, \tag{3}$$

where Ψ_d, Ψ_c are the bound and free two-electron wave functions of energy E_d and E_c respectively; $d\tau$ is the two-electron volume element and the other symbols have their usual meaning. Only the z-component of the matrices have been written. The absorption coefficients K_ν for incident radiation ν, in which an electron with velocity v is ejected is given by (assuming the ejected electron traveling in z-direction)

$$K_\nu(cm^2) = 6.812 \times 10^{-20} \, k(k^2 + 2I) \left| \int \Psi_d^* (z_1 + z_2) \Psi_c \, d\tau \right|^2 , \tag{4}$$

$$K_\nu(cm^2) = 2.725 \times 10^{-19} \frac{k}{(k^2 + 2I)} \left| \int \Psi_d^* \left(\frac{\partial}{\partial z_1} + \frac{\partial}{\partial z_2} \right) \Psi_c \, d\tau \right|^2 , \tag{5}$$

$$K_\nu(cm^2) = 1.090 \times 10^{-18} \frac{k}{(k^2 + 2I)^3} \left| \int \Psi_d^* \left(\frac{z_1}{r_1^3} + \frac{z_2}{r_2^3} \right) \Psi_c \, d\tau \right|^2 , \tag{6}$$

where all the symbols are in Hartree atomic units but K_ν is expressed in cm^2 by the numerical factors in the equations. The symbol k denotes the wave number of the ejected electron and I the electron affinity. The wave length (in angstroms) of the incident radiation is related to k^2 by

$$\lambda(\mathring{A}) = \frac{911.3}{k^2 + 2I} \,. \tag{7}$$

For the bound state wave functions one uses the GF wave functions, which for H^- and Li^- have already been calculated.[5] The free-state wave function also poses a problem since it is necessary to include exchange and the distortion of the neutral atom by the ejected electron. There are a number of (approximate) ways of doing this. The most frequently employed method is the explicit inclusion of neutral bound excited states in a Hartree-Fock eigenfunction expansion for the continuum waves.[7] An alternate approach, which is less complicated and more physically appealing, is the method of polarized orbitals.[8] For $H + e^-$, the necessary polarized orbitals have been calculated,[8b] but this is not the case for higher z-systems.

III. Discussion

It is almost unnecessary to point out that the calculations which use Pekeris-type bound state wave functions and Hartree-Fock continuum wave functions are very complicated. For this reason it will probably be a few years before the larger Z-systems are done. It is therefore worth while searching for an approach which will work well for H^- and still be applicable to the larger Z-systems. The GF wave functions[5] could represent a practical improvement in the bound state situation. The reasons accurate cross sections might result from using the GF wave functions are as follows.

Equations (4), (5) and (6), because of the form of their matrix elements, are called respectively the dipole length, dipole velocity and dipole acceleration expressions for the absorption coefficients. The following general comments pertain to these equations. The dipole length formulation (4) uses portions of

configuration space which are more distant than those regions important in the evaluation of the energy. On the other hand, the acceleration formulation (6) emphasizes most strongly the regions near the nucleus. The velocity formulation (5) is somewhat intermediate although it weights the inner regions more strongly than the outer regions. By investigating the properties of the GF wave function for H^-, one would expect the dipole velocity and dipole acceleration formulations to give the most accurate results. This statement is based on the fact that the GF wave function for H^- gives a good value for the charge density at the nucleus while giving a somewhat poor value for $\langle \Sigma \vec{r}_i \rangle$. [These conclusions are drawn from Table VIII of ref. (5)]. Because the GF wave function gives almost as good a value as the Pekeris wave function for the charge density at the nucleus, one might hope for a reliable value for the absorption coefficient without having to use correlation explicitly. It is worth noting that from the results of GF calculations[5] one notes that as Z increases the general quality of the GF wave functions for negative ions (relative to H^-) seems to increase. Thus, if the results obtained in the H^- calculation are good, then one can expect equally accurate (or better) results for the higher Z-systems.

As a final comment, note that such a calculation would also be interesting because from a comparison of the absorption coefficient using GF wave functions and that using the Pekeris-type, one could obtain information concerning the importance of correlation in predicting physical processes of this type.

References for Proposition V

(1) a) S. Chandrasekhar, Revs. Mod. Phys. 16, 301 (1944);
b) Hans A. Bethe and E. S. Salpeter, Quantum Mechanics of One- and Two-Electron Atoms (Springer-Verlag, 1957) p. 317.

(2) R. Wildt, Astrophysical Journal 89, 295 (1939).

(3) K. L. Bell and A. E. Kingston, Proc. Phys. Soc. 90, 895 (1967).

(4) C. L. Pekeris, Phys. Rev. 126, 1470 (1962).

(5) W. A. Goddard III, Wave Functions and Correlation Energies for Two-, Three-, and Four-Electron Atoms, to be published (1967).

(6) a) S. Chandrasekhar, Astrophysical J. 16, 224 (1945);
b) ref. 1b), p. 251.

(7) N. A. Doughty, P. A. Fraser, R. P. McEachran, Mon. Nat. R. Astr. Soc. 132, 255 (1966).

(8) a) A. Temkin and J. C. Lamkin, Phys. Rev. 121, 788 (1961);
b) I. H. Sloan, Proc. Roy. Soc. 281, 151(1964);
c) K. L. Bell and A. E. Kingston, Proc. Phys. Soc. 90, 31 (1966).